High Throughput Search for New Noble Metal Free Catalysts for Selective Propane Combustion in the Presence of CO

Dissertation
zur Erlangung des Grades
des Doktors der Ingenieurwissenschaften
der Naturwissenschaftlich- Technischen Fakultät III
Chemie, Pharmazie, Bio- und Werkstoffwissenschaften
der Universität des Saarlandes

von
Prasanna Rajagopalan

Saarbrücken
2009

Tag des Kolloquiums: 05.02.2010
Dekan: Prof. Dr.-Ing. Stefan Diebels
Berichterstatter: Prof. Dr. Wilhelm F. Maier
Prof. Dr. Rolf Hempelmann
Vorsitz: Prof. Dr. Uli Kazmaier
Akademischen Mitarbeiter: Dr. Harald Natter

Dedicated to My Beloved Parents

&

To My Beloved Professor Dr. W. F. Maier

The work had been achieved during the time from October 2005 to December 2008 at Universität des Saarlandes, Saarbrücken, under the guidance of Prof. Dr. W. F. Maier.

I express my sincere gratitude to my Prof. Dr. W. F. Maier for giving me an opportunity to work in his department, expert guidance, suggestions, advices, support and encouragements in all means to complete this work successfully.

I thank Prof. Dr. Rudolf Hempelmann for his acceptance to be an reviewer.

I thank Dr. Uwe Endruschat and Dr. Ansgar Wille for their valuable suggestions to complete the project.

I thank Prof. Dr. K. Stöwe for his advices during the project and for XRD measurements and Dr. F. Müller for XPS measurements. I thank Mr. R. Richter, Mrs. H. Höltzen and Mr. C. Thome for their invaluable technical support.

I thank Heraeus Holding GmbH for their financial support.

I thank all of my colleagues for their support and valuable suggestions.

Last but not the least, I would like to thank my parents and friends for their complete help and support.

Abstract

High throughput synthesis and screening methods were adopted for the search of new noble metal free oxide catalysts for the selective propane combustion in the presence of CO. The $Ce_{20}Ti_{50}Cr_{30}$ catalyst was found as the best performing from ternary composition spreads. Through special optimisation routine, catalysts such as $Ce_{19}Ti_{49}Cr_{29}D_3$ (D = Sc, Si, Tm, Gd) were found highly active. Finally, it was found that $Ce_{19}Ti_{49}Cr_{29}Gd_3Ag_{0,01}$ shows very high propane conversion of about 87% and $Ti_{62,5}Cr_{37,5}$ is found as completely selective propane oxidation catalyst with conversion of 43%.

Hochdurchsatzsynthese und „Screening“-Methoden wurden für die Suche nach neuen edelmetalfreien Oxidkatalysatoren für die selektive Propanverbrennung in Anwesenheit von CO eingesetzt. Der Katalysator $Ce_{20}Ti_{50}Cr_{30}$ wurde als bester Kandidat aus ternären Zusammensetzungsräumen ermittelt. Durch die Optimierungsstrategien wurden hoch aktive Katalysatoren, wie $Ce_{19}Ti_{49}Cr_{29}D_3$ (D = Sc, Si, Tm, Gd), identifiziert. Schließlich wurde entdeckt, dass $Ce_{19}Ti_{49}Cr_{29}Gd_3Ag_{0,01}$ einen sehr hohen Propan Umsatz von ungefähr 87% aufweist und der Katalysator $Ti_{62,5}Cr_{37,5}$ Propan vollständig selektiv mit einem Umsatz von 43% oxidiert.

Table of contents

List of figures

List of tables

1 Introduction

The catalytic combustion of hydrocarbons has received much attention because it is a very important technology for the energy production in gas turbines and in emission control in automotive exhaust catalysts [1]. The emission levels of hydrocarbons, CO and NO_x from automobiles have decreased by more than 90% since the introduction of catalytic converters [2, 3]. Improvement of urban air quality during the last decades is mainly due to the decisive role of catalysis. Presently, exhaust regulations emphasise on reduction of hydrocarbon emissions. Between 50 and 90% of total hydrocarbons from modern cars with three way catalysts are released during the start of the cold engine when the catalyst temperature still is low [2, 4, 5, 6]. The light off occurs typically between 250°C to 300°C [7, 8]. Catalytic oxidation of hydrocarbons has become also the focus of basic and applied catalysis research because of its importance in industrial processes [9, 10, 11]. Total oxidation of lean and near stoichiometric hydrocarbon-air mixtures has received great interest in the contest of catalytically aided combustion for power generation [9]. The majority of automobiles and trucks use spark ignited gasoline engines to provide power. Gasoline blends consist of mixtures of paraffins and aromatic hydrocarbons which combust in air at very high efficiency [4].

$$\text{Gasoline} + \text{air} \longrightarrow CO_2 + H_2O + \text{heat}$$

Due to incomplete combustion, typical exhaust gases of the normal operating engine contain also CO, hydrocarbons and nitrous oxides. Because of the large vehicle population, significant amounts of hydrocarbons, CO and NO_x are emitted to the atmosphere. The formation of ground level ozone occurs due to the interaction of hydrocarbons, NO_x and sunlight. When stagnant air masses linger over urban areas, the pollutants are held in place for longer periods of time. Sunlight interacts with those pollutants and forms ground level ozone. Thus to meet current emission standards, catalytic converters for complete oxidation of hydrocarbons are required [12].

1.1 Emission standards

Class	**Engine size (cc)**	**Implementation date**	**HC (g/km)**	**HC + NOx (g/km)**	**CO (g/km)**
Class I	less than 170	2006	1	-	12
Class II	170 – 279	2006	1	-	12
Class III	280 and above	2006	-	1,4	12
		2010	-	0,8	12

Table 1-1 Emission standards of highway motorcycles adopted by EPA

Tier	**Year**	**CO (g/km)**	**HC (g/km)**	**NO_x (g/km)**	**HC + NO_x (g/km)**	**PM (g/km)**
Euro 1	July 1992	2,72	-	-	0,97	0,14
Euro 2	Jan 1996	2,2	-	-	0,5	-
Euro 3	Jan 2000	2,3	0,2	0,15	-	-
Euro 4	Jan 2005	1,0	0,1	0,08	-	-
Euro 5	Sep 2009	1,0	0,1	0,06	-	0,005
Euro 6	Sep 2014	1,0	0,1	0,06	-	0,005

Table 1-2 European emission standards of gasoline driven passenger cars

Tier	**Year**	**CO (g/km)**	**HC (g/km)**	**NO_x (g/km)**	**HC + NO_x (g/km)**	**PM (g/km)**
Euro 1	Oct 1994	2,72	-	-	0,97	-
Euro 2	Jan 1998	2,2	-	-	0,5	-
Euro 3	Jan 2000	2,3	0,2	0,15	-	-
Euro 4	Jan 2005	1,0	0,1	0,08	-	-
Euro 5	Sep 2009	1,0	0,1	0,06	-	0,005
Euro 6	Sep 2014	1,0	0,1	0,06	-	0,005

Table 1-3 European emission standards of gasoline driven light commercial vehicles (Category N1 – I)

The U. S. Environmental protection agency is adopting more stringent emission standards for gasoline engines. The standards are based on comparable requirements adopted in California.

The tables 1-1 to 1-3 show new exhaust standards of high way motorcycles and automobiles [13].

These standards are expected to be met through increased use of technology. These standards will help to reduce the public exposure to emissions and help to avoid adverse health effects associated with ozone and particulate matter levels in terms of respiratory illness. Also, it is very clear from the tables that the allowable limits of hydrocarbons are far below than CO limits. This may be due to the high odour of hydrocarbons and CO get diluted due to the engine operation in the open atmosphere. It is well known that CO oxidation is rather facile at low temperatures when compared to hydrocarbon oxidation and it is challenging to reach this low hydrocarbon limits with excess of CO in the exhaust.

1.2 Propane combustion

Based on stringent emission regulation for hydrocarbons emissions, here we try to focus on propane combustion as model hydrocarbon. Intensive research is going on to find better catalysts for propane combustion. This section deals with the same to get an overview of propane combustion catalysts. Numerous studies have been reported on catalytic combustion of propane as model for volatile hydrocarbons over different precious metals. Platinum is the most widely used catalyst for the combustion of propane [14-28]. Supported noble metal catalysts, especially supported palladium and platinum catalysts, are regarded as promising catalysts [1]. The catalytic performance of supported catalysts is significantly modified by support materials. The support effects on catalytic performance of platinum catalysts for low temperature propane combustion have been investigated [1, 29-31]. Besides platinum, transition metal oxides [32-35], perovskite type oxides [33, 34, 36], metal doped zeolites [37], metal doped solid super acids [23] and highly dispersed Au catalysts [38] are active in total oxidation. Yu Yao investigated propane oxidation in the temperature range from 200 to 250°C and found Pt to be better catalyst than Pd and Rh [39]. Similar results were obtained by Morooka et.al. [35] and by Hodnett and co-workers [40], who found that the reaction starts at 150°C over a Pt/β-zeolite catalyst. Maier and co-workers [41], however, found that Pd is more active in comparison whereas for oxidation of higher hydrocarbons Pt is the most active catalyst. Transition metals oxidise propane at 250°C or higher temperatures [42].

Partially oxidised palladium catalysts were effective for propane combustion [43] and it is observed that catalyst performance of supported palladium catalysts can be improved by the selection of acid strength of support materials to obtain the proper oxidation state of palladium for the desired reaction conditions [44, 45]. Ishikawa et.al. [23] showed that SO_4^{2-} - ZrO_2, a solid super acid is superior as support material and suggested that the acid strength of support materials has an effect on the catalytic performance of supported platinum catalysts [23].

The most active single metal oxide catalysts for complete oxidation of variety of volatile organic compounds are the oxides of Cr, Mn, Fe, Co, Ni and Cu [46-49]. They were deposited on metal grid supports by wet impregnation methods. These are p-type semiconductor oxides and are able to adsorb oxygen by donating an electron from the metal cation. This process leads to a formation of electrophilic oxygen species (O_2^-, O^-) known to be active in deep oxidation. For these reasons these p-type oxides were used as active components deposited on metal grids supports and tested for catalytic activity of total propane oxidation. Here cobalt oxide was found to be most active catalyst for propane oxidation. This agrees with results reported by different authors [34, 50, 51, 52] The activity order was $Co_3O_4 > Mn_3O_4 > Cr_2O_3 > CuO$. Cobalt oxide supported on modified Ni grids was found be to best active catalyst for propane oxidation and its activity enhanced by reduction with H_2 prior to reaction [49].

Kiwi Minisker et.al. [17] found that platinum and palladium supported on different glass fiber (Ti, Zr and Al) optimised with improved porosity and specific surface areas are effective combustion catalysts. Compared to Pd, Pt was found the better catalyst with ignition temperatures in the range of 200 – 220°C. Modification of glass fiber supports by titania or zirconia lead to very high propane conversion of nearly 100% with a short residence time of 10^{-1} seconds. Further Garetto et. al. [20] report that zeolite supported platinum catalysts are more active than alumina supported catalysts. The Pt/zeolites superiority was attributed to their ability to maintain higher concentration of propane at the metal support interface.

Yazawa et.al. [21, 27] investigated the variation in reaction rate with large number of metal additives on Pt/Al_2O_3 and found that intrinsic catalytic activity increases with electronegativity of the additive. Further several authors have proposed that small amounts of SO_2 over Pt/Al_2O_3 can promote the catalytic combustion of propane [16, 24, 25]. The effect of SO_2 is support specific and not confined to the catalyst itself, because it facilitates dissociative chemisorption of propane at the Pt/Al_2O_3 interface [16]. Burch et. al. [24] found that SO_2 enhances the catalytic activity of propane over alumina supported Pt catalysts but no influence over silica supported Pt catalyst.

Generally, noble metal based catalysts have high combustion activity, but they are more expensive and prone to deactivation by poisoning [34]. Choudhary et.al. found that a Mn doped zirconia catalyst is the most promising catalyst for combustion of dilute propane. Propane combustion activity of this catalyst is strongly influenced by the precipitating agent (tetramethyl ammonium hydroxide) used in the catalyst synthesis, Mn/Zr ratios of the catalyst, calcination temperature of the catalyst and the crystalline phase of ZrO_2 (monoclinic or cubic phase) [19].

Propane combustion activity reaches maximum with excellent long term stability with a Mo promoted Pt/Al_2O_3 catalyst with inverse opal structure in micro channel reactors [53]. The temperature to reach maximum conversion was about 100°C lower than the catalyst prepared without inverse opal structure in the fixed catalyst bed [21].

1.3 Carbon monoxide combustion

This section deals with catalysts of high CO combustion activity. Low temperature CO oxidation catalysts have received attention in recent years due to stringent emission regulations such as super low emission vehicles (SULEV) and zero emission vehicles (ZEV). Nano structured gold catalysts possess unique low temperature oxidation activity and are resistant to moisture. The major drawback of this gold catalyst is very low temperature stability and practical applications in exhaust purifications are limited due to cost [54-56]. In last several years, CuO and Co_3O_4 in particular have been the focus of many researches due to high CO oxidation activity and also low costs. It has been reported that $CuO\text{-}CeO_2$ catalysts are comparable with noble metal catalysts for CO oxidation, and that some Co based catalysts exhibits ultra low light off temperature of -63°C for CO oxidation [57, 58]. Luo et.al. found that nano structured $CuO\text{-}CeO_2$ exhibits high activity for CO oxidation and CO adsorbs as carbonyl and bidentate carbonate species on the surface of the catalyst [54].

Hopcalite ($CuMn_2O_4$) is a commercial catalyst used for low temperature CO oxidation though it deactivates at room temperature in moist air [59]. Saalfrank et.al. [59] found that $Al_1Mn_{6,7}Co_{92,3}$ is the best promising catalyst for low temperature CO activity at low temperature of 25°C with a conversion of about 95%. Further Kraemer et.al. [60] showed that $Cu_{20}Mn_{80}$ catalyst prepared by an ethylene glycol method is the best candidate for CO oxidation at 25°C and comparable to that of commercial hopcalite catalyst. Recently, $La_{0,8}Ce_{0,2}MnO_3$ can catalyse selective combustion of methane, CO and synthetic soot to give CO_2 using microwave irradiation [61-63].

1.4 Propane and carbon monoxide combustion

Exhaust gases from the combustion engines contain smaller hydrocarbons and CO. Jurriaan et.al. [64] screened twelve perovskite catalysts for simultaneous oxidation of propane and CO. It is interesting to note that surprisingly $La_{0,8}Ca_{0,2}Cr_{0,3}$ burned propane much faster than CO, which is in contrast to general knowledge [65, 66]. Castillo et.al [67] reported, structural refinements and catalytic evaluation of series of palladium supported ceria-zirconia catalysts through surfactant assisted techniques. It was found that zirconium addition to ceria leads to crystalline structure distortion and inhibits crystal growth at high temperature. Rietveld refinements confirmed that all ceria-zirconia samples have nanocrystals with cationic defects in their structures. The Pd supported catalysts were very active for complete oxidation of CO and propane. The best catalyst (3wt% $Pd/Ce_{0,8}Zr_{0,2}O_2$) has a light off temperature (T_{50}) as low as 120°C for CO oxidation and 180°C for propane combustion [67].

1.5 Sol-gel synthesis

Sol-gel chemistry is a versatile tool for both preparation and understanding of catalytic materials. [68]. Interest in sol gel processing of inorganic ceramic and glass materials began as early as the mid 1800s with the Ebelmann and Grahams studies on silica gels [69]. These early investigators observed that the hydrolysis of tetra ethyl orthosilicate ((TEOS), $Si(OC_2H_5)_4$), under acidic conditions yielded SiO_2. However extremely long drying times of 1 year or even more is necessary to avoid fracturing of silica gels into a fine powder. Sol-gel methods represent an attractive and easy to tailor alternative to conventional synthesis methods such as impregnation, precipitation/peptisation or ion exchange on supported mixed oxides [70]. A broad range of porous materials such as metal oxides, crack free or non-shrinking monoliths, fibers, membranes and highly ordered crystalline materials with pores of uniform size- is accessible through sol-gel processes [71]. For the preparation of polynary mixed oxides [72-77] or glasses [78], the sol-gel process represents an attractive alternative to conventional synthesis methods. Potential advantages of sol-gel processing include purity, homogeneity and controlled porosity combined with the ability to form large surface area materials at low temperatures. Important variables which must be considered in the synthesis of supported metals by the sol-gel method include: pH, reactant stoichiometries, gelation temperature, metal loading, solvent removal and pre treatment conditions [79]. Compared to solid state reactions, this mild synthesis method usually results in the formation of mixed oxides of improved homogeneity. The sol-gel process itself is low cost, requires mild reaction conditions and provides homogeneous gels of most of elements in the periodic table which form solid mixed oxides [70]. Also, it leads to very high surface areas, uniform pore size distribution, readily controlled composition, improved thermal stability of supported metals and simple preparation conditions without extra steps such as filtration, reflux and distillation [79-83].

The sol-gel process [84] leads to the evolution of inorganic networks through the formation of a colloidal suspension (sol) and gelation of the sol to form a network in a continuous liquid phase (gel). The precursors for synthesising these colloids consist of a metal or metalloid element surrounded by various reactive ligands. Metal alkoxides are most popular because they react readily with water. The most widely used metal alkoxides are the alkoxysilanes, such as tetramethoxysilane (TMOS) and tetraethoxysilane (TEOS). However, other alkoxides such as aluminates, titanates, and borates are also commonly used in the sol-gel process, often mixed with TEOS. At functional group levels, three main reactions are occurring in the sol-gel process. They are hydrolysis and condensation. The reaction scheme shown in figure 1-1.

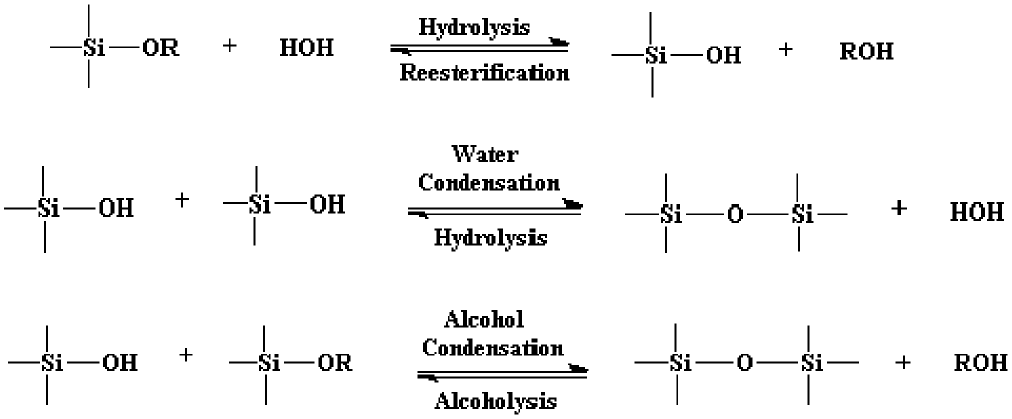

Figure 1-1: **Reaction schemes for sol-gel process [83].**

Generally, hydrolysis reaction takes place by the addition of water which replaces alkoxide groups with hydroxyl groups. Condensation followed by formation of siloxane bonds by involvement of silanol groups with the by-products water and alcohol.

The sol-gel process involves several steps such as hydrolysis, condensation (acid and basic conditions), gelation and aging. Each step can be controlled to improve the microstructure of the catalyst. When the pore liquid is removed as gas phase from the inter-connected solid gel network under hypercritical conditions, the network does not collapse resulting in large volume of aerogel of low densities. On the other hand, when the pore liquid is removed at ambient pressure by thermal evaporation, it leads to the formation of a xerogel with high surface areas of 400m^2/g [69]. Catalyst synthesis by sol-gel processes depend on a number of factors. Major important factors are pH, nature and concentration of catalyst, H_2O/Si molar ratios and temperatures. By varying these factors one can vary the structure and can thus influence or tailor the inorganic network, especially porosity and pore size distribution.

Sol-gel synthesis can be carried out under acidic conditions (pH < 7), basic conditions (pH > 7) and under neutral conditions (pH = 7). General acid and base catalysed hydrolysis are explained below.

1.5.1 Acid catalysed hydrolysis

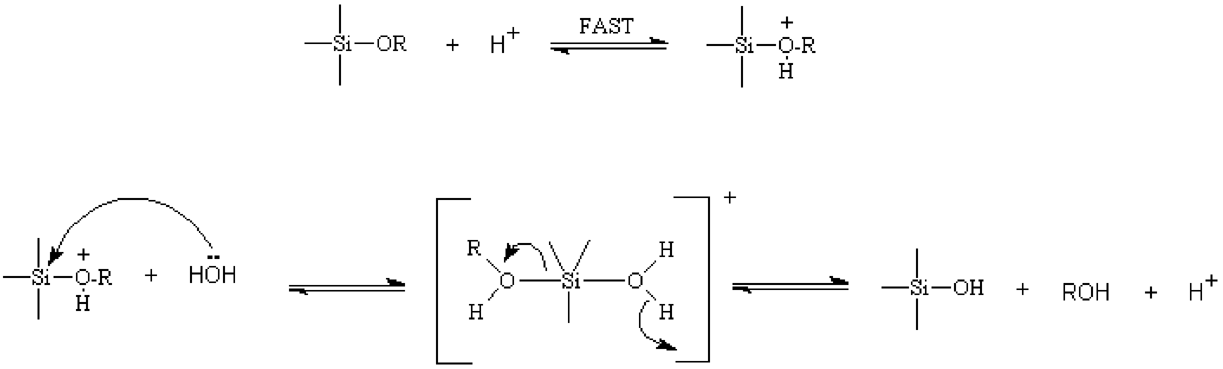

Figure 1-2: **Acid catalysed hydrolysis.**

Under acidic conditions, it is likely that an alkoxide group is protonated in a rapid first step. Electron density is withdrawn from the silicon atom, making it more electrophilic and thus more susceptible to attack from water. This results in the formation of a penta coordinates transition state which decays by displacement of alcohol and inversion of silicon tetrahedron [85, 86]. When an acid catalyst used for mixed oxides preparation, uniform mixed oxides were formed without discrimination by electronegativity since hydrolysis and condensation are controlled by the loan pairs on oxygen atoms.

1.5.2 Base catalysed hydrolysis

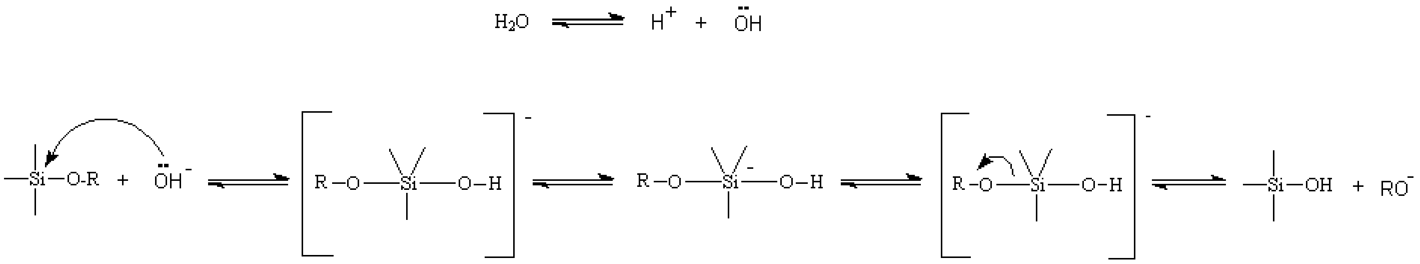

Figure 1-3: Base catalysed hydrolysis.

Under basic conditions, it is likely that water dissociates to produce hydroxyl anions in a rapid first step. The hydroxyl anions then attacks the silicon atom and hydroxyl groups displace the alkoxide groups with the inversion of silicon tetrahedron. Under basic conditions, phase separations can be formed because hydrolysis and condensation are controlled by electronegativity of the central atoms.

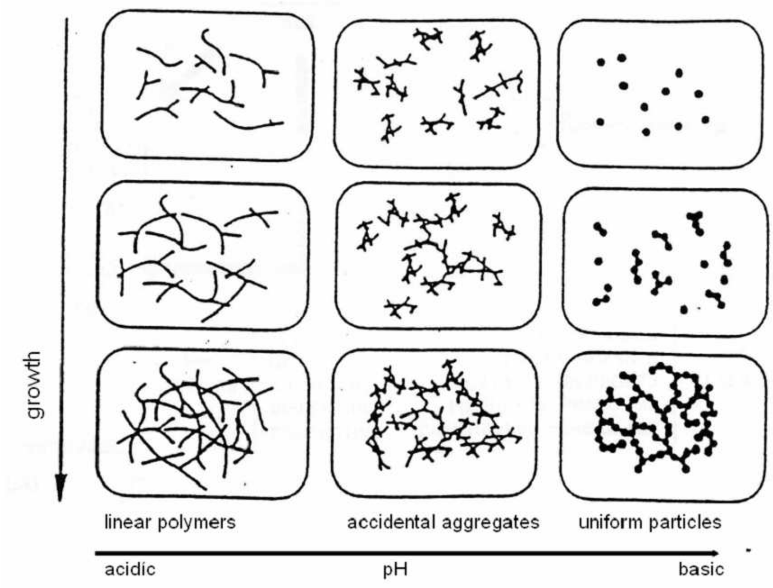

Figure 1-4: Influence of pH on sol-gel network formation [86].

1.6 Combinatorial chemistry

The combinatorial method and high throughput experimentation have been applied to catalysis development in the last decade. This methodology was first introduced by Hanak in 1970 in search of semi-conductors, super-conductors and magnetic materials and named as Multiple sample concept (msc) [87, 88]. Combinatorial catalysis is the systematic preparation, processing and testing of large diversities of chemically and physically different materials libraries in high throughput fashion. The major application of combinatorial chemistry remains the search for biologically active molecules. Diversity based strategies however might be effective in the identification of compounds that have attractive properties. Combinatorial and related strategies have indeed been utilised in investigations in material science, molecular recognition, polymer chemistry and asymmetric catalysis. Figure 1-5 represents the general overview of classical and high throughput catalysis approach.

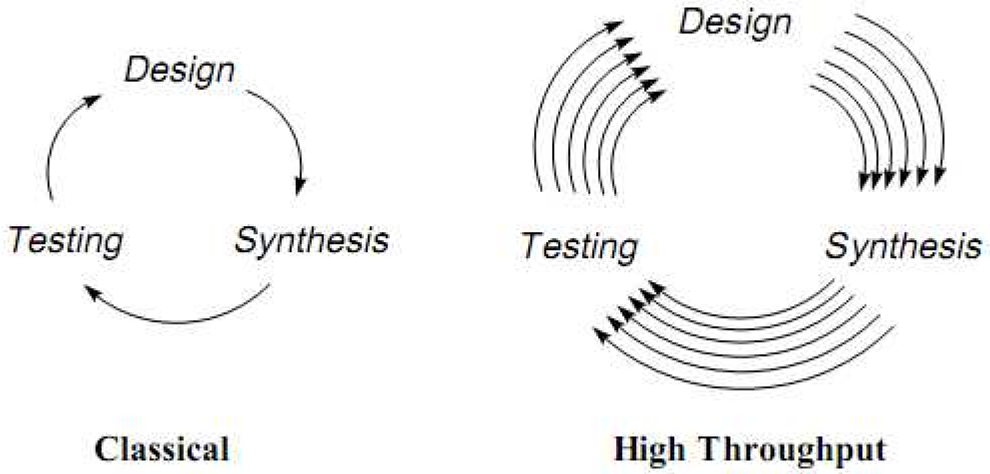

Figure 1-5: Comparison of classical and high throughput approach [89].

The discovery and development of new materials and catalysts used to be time consuming and rather unpredictable trial and error processes. However combinatorial and high throughput approaches are changing this perception. This technology is aimed to speed up the pace of research leading to increase the chances of discovery of totally new and unexpected catalysts and their optimisation [90].

The developed high throughput techniques allow to significantly enhance the number of experiments carried out during a given time [91-93]. Compared with the classical approach, where experiments are designed one at time, combinatorial chemistry makes use of materials libraries, prepared and tested in parallel or rapid sequential manner. Results obtained from the combinatorial approach under the same reaction conditions are comparable and more meaningful than single batch experiments, automation and measurement under defined conditions are highly reproducible, a reference standard can be measured under the same conditions and used for calibration [90, 94, 95]. Due to an enormous industrial impact of the development of better materials and catalysts, a number of companies are already active in this field namely Symyx technologies, hte Aktiengesellschaft, Avantium, AMTEC, INM, SINTEF, and combinatorial chemistry is now a core technology in many major chemical and material companies such as BASF, Bosch, Degussa, UOP, P&G, GE, Bayer, DuPont, DOW and many others.

The schematic catalyst discovery and optimisation process is represented in figure 1-6.

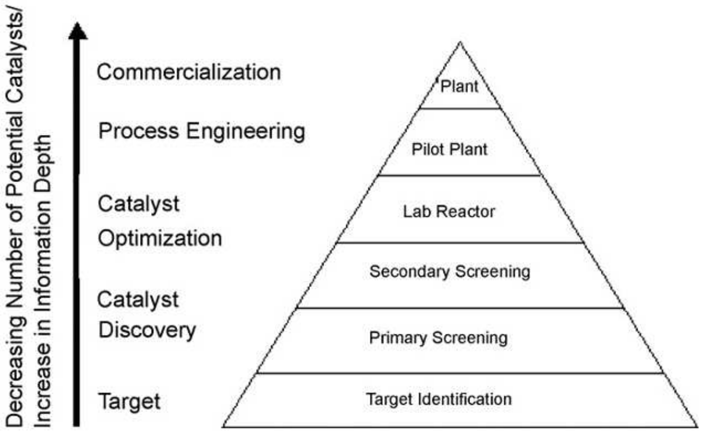

Figure 1-6: Catalyst discovery and optimisation process [95].

It has to be pointed out that commonly used screening strategies are limited and do not answer which reactions can be catalysed by the particular catalyst, catalysts identified are from the primary screening stage, and activity towards particular reaction. Therefore the screening strategy [95] should allow (i) to continuously analyse the samples in real time to determine reaction rates, (ii) to monitor not only the major product and educt, but also side reactions, to be scaleable to reaction monitoring in parallel reactors, and (iv) be applicable to combinatorial libraries. The challenges are very similar to those in synthetic combinatorial approaches of materials and catalysts, as addressed in review article by Jandeleit et. al [96].

Thus combinatorial catalysis is a methodology or set of tools where large diversities of solid state materials libraries are prepared, processed and tested for activity and selectivity in a high throughput fashion [97]. Since the data and information are vast, the development and use of sophisticated high capacity information management systems is also essential component of this methodology. Infact the successful implementation of combinatorial approaches will require that all of the components shown in figure 1-7 must be in place and function smoothly, otherwise bottlenecks will limit the throughput [97].

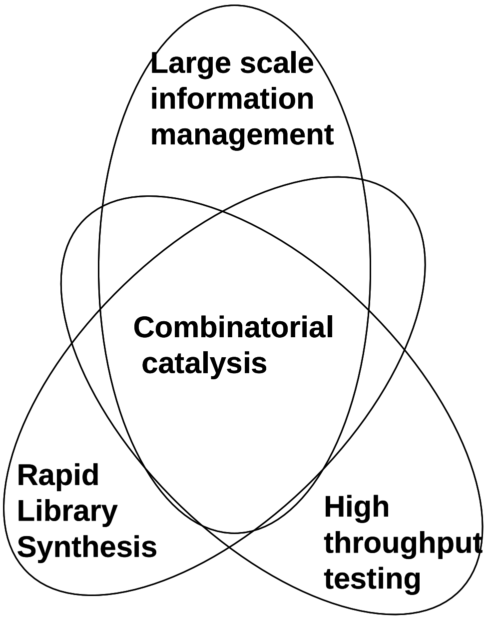

Figure 1-7: Essential components of combinatorial catalysis [97].

The integration of all the components of combinatorial catalysis is the ultimate goal of this field, enabling the intelligent planning and execution of highly parallel experiments with minimal human intervention. Initial integration of library synthesis and high throughput screening is nearly realised as evidenced by numerous publications in these fields.

New discoveries should lead to quantum leap in our understanding of catalysis, analogous to the impact that the discovery of high temperature superconductors had in physics. Interestingly, the idea of applying combinatorial approaches to heterogeneous catalysts is not new. In the early part of the 20th century Alwin Mittasch implemented an impressive program preparing and testing a large number of combinations of metals to catalyse the synthesis of NH_3 from H_2 and N_2. However, the Mittasch approach for the catalyst discovery and optimisation was not pursued much further due to higher labour costs [98].

The implementation of combinatorial techniques to heterogeneous catalysis is a significantly more challenging problem than in other application areas of material science [97] and additional challenges arise from the complex and dynamic nature of the catalysts. First, real heterogeneous catalysts generally are extended solids with multiple discontinuities in structure and composition allowing very limited systematic variation in these properties with the overall composition. In addition, structures are strongly dependent on the methods of preparation and change with time under reaction, with better catalysts being more resilient to change. All of these issues render heterogeneous catalysis research a difficult subject.

Second, heterogeneous catalysts must bind the reactants to induce them to bonding interactions and allow the products to depart so that the catalytic cycle progresses. These requirements demand that no catalyst intermediate be too stable or the product too strongly adsorbed, otherwise the turnover number cannot be high enough to be practically useful. In other words, heterogeneous catalysts must expedite the formation of a suitable and energetically favourable transition state. Transition states are induced by three dimensional active sites on catalyst surfaces, both of which are poorly understood. It is likely that multitude of active sites exists on solid surfaces and their distribution changes with time. The rates of change or shift of these sites influenced by temperature and local composition. Typically, catalysts deactivate with time as consequence of events such as surface reconstruction, sintering, poisoning, coke formation and volatilisation [97]. Conversely the activities of some catalysts peak only after a period “on stream” again suggesting the involvement of events such as reconstruction. These considerations clearly call for the development of methodologies that will allow the undertaking of a large number of systematic, parallel experiments to unravel the underlying elementary events.

The preparation of solid state libraries of catalytic materials can be accomplished by thin film deposition methods and solution based methods. Sputtering with physical masking has been used to deposit solid state libraries for the discovery and optimisation of CO oxidation catalysts [99]. Cong et.al. [99] prepared thin film library containing 120 ternary combinations of Rh-Pd-Pt, and was prepared by sequentially depositing films of the individual elements on to quartz substrate using masks. The total library synthesis took about 1h and followed by annealing at 773K under H_2/Ar atmosphere for two hours. Even greater speeds of synthesis of solid state material libraries can be accomplished by simultaneous or co sputtering of multiple target materials which is originally proposed by Hanak [87]. With sputtering large number of sites can be prepared simultaneously with very high speed and is a useful tool for the creation of very large discovery of libraries. Other thin film deposition methods, such as thermal [100, 101] and plasma chemical vapour deposition [102, 103], molecular beam epitaxy [104] and pulsed laser deposition [105, 106] can be used to create solid state libraries. Thin film deposition based catalyst preparation techniques are particularly promising for use in conjuction with micro-electro-mechanical systems (MEMS) that are created by using semiconductor device manufacturing techniques [107]. Solution based methods involve sol-gel, impregnation, co-precipitation and polymerisation. Solution based ink-jet print head technology has successfully been used to prepare a 645 combinations of Pt-Ru-Os-Ir library for the reforming of methanol [108]. A large scale automation of co-precipitation technique was developed and used for the synthesis of 16 combination library of Au-Co_3O_4 and Au-TiO_2 for the oxidation of CO [109]. The application of sol-gel synthesis has been introduced by Maier and co-workers for synthesis of amorphous mixed oxides [110].

In an efficient high throughput process you should analyse in a day what you make in a day [111] and it is the most important technology of combinatorial catalysis. High throughput testing of heterogeneous catalysts is one of the difficult tasks of combinatorial chemistry to get reliable results. It consist of two steps, primary and secondary screening. Primary screening deals with numerous compounds with high diversities and qualitatively evaluated based on their activity rankings. Secondary screening is followed based on the results of primary screening in the conventional reactor to confirm trends. High throughput includes optical methods, gas chromatography (GC) and mass spectrometry (MS) were used. Optical screening is based on colour indicator method, which is applicable to liquid phase reactions and first applied to determine relative catalytic activity of series of conventional hydrosilation catalysts [112]. Other optical methods includes infrared thermography [113, 114], laser induced fluorescence imaging (LIFI)[115], resonance enhanced multiphoton ionisation [116], photothermal deflection (PTD) [117] and fourier transform infrared [118, 119] and gas sensors [120]. Also, use of thermistor arrays were also proposed to screen libraries of catalyst materials [121]

LIFI exploits the alteration of fluorescence properties of molecules as a consequence of the breakage and formation of chemical bonds. However this technique is limited due to the detection of only fluorescent species. REMPI is based on in situ ionisation of reaction products by UV lasers, followed by the detection of protons or electrons by spatially addressable microelectrodes placed in the vicinity of the laser beam. Unfortunately REMPI features of many molecules are unknown and it must be determined before the technique applied for catalyst screening.

Mass spectrometry is widely used detection technology for high throughput testing of heterogeneous catalysts. Cong et.al. [99] reported a quadrupole mass spectrometer for sequential screening of heterogeneous catalyst libraries. Each catalyst site of the library was sequentially heated to desired reaction temperature by CO_2 laser beam. The reactant products withdrawn from the probe were analysed by on-line quadrupole mass spectrometry. The total time to heat and screen one catalyst site was about 1 minute. Maier and co-workers reported a system based on the use of plate libraries, where individual catalyst placed in open wells monitored by capillary which is connected to mass spectrometry and gas chromatography [122]. Claus and co-workers reported the use of monolith reactor system with up to 250 catalysts in parallel in combination with quadrupole mass spectrometer [123, 124].

Parallel catalyst screening techniques close to conventional catalysis research are mostly accompanied with parallel conventional reactors such as fixed bed reactors [125, 126] or continuous stirred tank reactors [127, 128]. Yamada et.al. developed a parallelised conventional methods for conventional materials [120, 129]. Similarly, development of an automated high pressure system containing 16 parallel multi tube reactors was recently reported by Schüth and co-workers [109]. Also, Baerns group [32, 130] developed a similar block reactor system containing 15 packed bed reactors and in related study consisting of 6 parallel reactors was also reported [97].

One of the optical techniques, emissivity corrected infrared thermography (ec-IRT) is used as a primary screening tool in this project to identify the potential hits. Wilson and co-workers were the first to demonstrate the utility of IR thermography as a heterogeneous catalyst screening tool using hydrogen oxidation as a model tool [113]. Subsequently Maier and co-workers refined IR thermography method by taking into account the different emissivities of catalyst clusters and make it a more quantitative tool [114]. In IR thermography, radiation energy is emitted from surfaces according to modified Stefan-Boltzmann law. As evidence from Stefan-Boltzmann equation, radiation is extremely sensitive to surface temperature by IR technique. IR radiation is actively emitted by all objects and no external light source is required for imaging. However IR thermography is an extremely fast and nonintrusive screening technique, it does not provide information on the chemical identity of the products formed in a reaction. Nevertheless, IR thermography is a useful preliminary activity screening tool to explore very large library discoveries. Detailed experimental work flow of high throughput testing of catalyst libraries using emissivity corrected infrared thermography (ec-IRT) is explained elsewhere in section 3.2.

Although large number of samples can be synthesised and tested by high throughput technology, possible number of compositions is almost infinite. An important issue in combinatorial catalysis is the design of experiment (DOE) is required to organise the experimental work into minimum work input and maximum output with optimised solutions. Techniques used for design of experiments are parametric space, stochastic methods such as genetic algorithms (GA) and simulated annealing (Monte Carlo methods), holographic search [131] and split and pool methods [132]. Genetic algorithms is an effective tool which has been applied for synthesis of combinatorial chemical libraries [133, 134] for the design of heterogeneous catalysts [97] and in the preparation, optimisation of combinatorial libraries of heterogeneous catalysts [135], low temperature oxidation of propane [85], low temperature light paraffin isomerisation [136] and selective oxidation of propane [137]. Maier and co-workers applied an evolutionary strategy in conjunction with CO oxidation catalyst [90]. Corma and co-workers used artificial neural networks (ANN) prediction model with genetic algorithms in the optimisation of epoxidation catalysts [128].

1.7 Research objective and goal of the project

Hydrocarbon combustion is of fundamental importance for many types of exhaust gas cleaning. Especially for combustion engines, HC are combusted together with CO. State-of-the-art catalysts do show high selectivity for CO or n-propane based on reaction conditions. It is well known, that CO combustion is rather facile and occurs readily at temperatures below 100°C, while the combustion of alkanes requires temperatures above 200°C. Therefore under lean conditions the oxygen is preferentially consumed by CO and HC combustion remains incomplete. The reason for the preferred CO-combustion lays essentially in the polar and reactive nature of CO (low activation barriers) relative to the high activation barriers for C-H-bond cleavage of alkanes. It is therefore of fundamental interest, if it is possible to find catalysts capable of selectively activating alkanes in the presence of CO. To us such a search appeared to be an interesting challenge to test the power and capabilities of high throughput technologies, especially since there is no rational theoretical approach to solve such a problem. The typical performance of a typical combustion catalyst is shown in Figure 1-8, documenting the selective conversion of CO at much lower temperature, propane conversion starts only at temperatures, where most of the CO is already converted. The quest was, to find catalyst with the inverse catalytic behaviour.

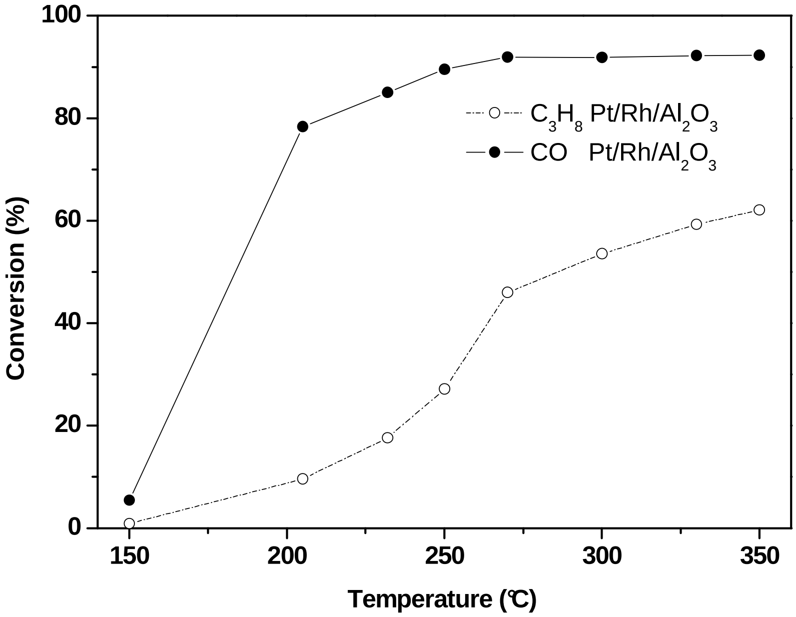

Figure 1-8: **Temperature dependence of the conversion of CO and propane on Pt/Rh/Al_2O_3 in a gas phase low reactor with reaction in increment order of temperatures from 150°C to 350°C. Reaction conditions: 20mg of catalyst diluted with 100mg of γ-alumina with particle size of 100–200 µm (both). Total flow rate: 50ml/min ($C_3H_8/CO/CO_2/O_2/N_2$ = 2/10,9/15,8/10/61,3). Catalyst pre-treatment: synthetic air with 50ml/min at 350°C for1h.**

Our intention is to find new noble metal free catalysts for the combustion of n-propane in the presence of CO. The work implemented for a catalyst search is done to reduce the scavenging fuel loss and also to prevent pungent smelling due to unconverted hydrocarbons which in turn results in respiratory diseases. CO oxidation is not desired and can be diluted to the atmosphere or partial oxidation of n-propane to CO is also welcome. Therefore an increase in CO content released from the system to the atmosphere would still be tolerated by emission standards.

2 Results and discussion

2.1 Combinatorial approach for selective combustion of propane in the presence of CO

The ever increasing need for more selective heterogeneous catalysts in chemical processing cannot be satisfied by conventional catalyst development and therefore combinatorial approaches should be considered [114]. High throughput screening leads to the automated synthesis and testing of several many catalysts per run in parallel and thus a catalyst search process is accelerated. This may save cost and time compared to conventional methods. A high throughput work flow for catalyst development could be based on two routes [88, 138]. They are

1) Screening based on prior information using catalytic systems that show activity for the desired reaction.

2) Catalytic systems chosen without any precedence to the desired reaction of high diversities.

The first approach involves well known materials in that particular areas were chosen and designed in a systematic way which increases the chances to find better or novel active materials relatively in the parametric space. But the main drawback is the discovery of new catalysts was limited. Hence two strategies were employed in this present study.

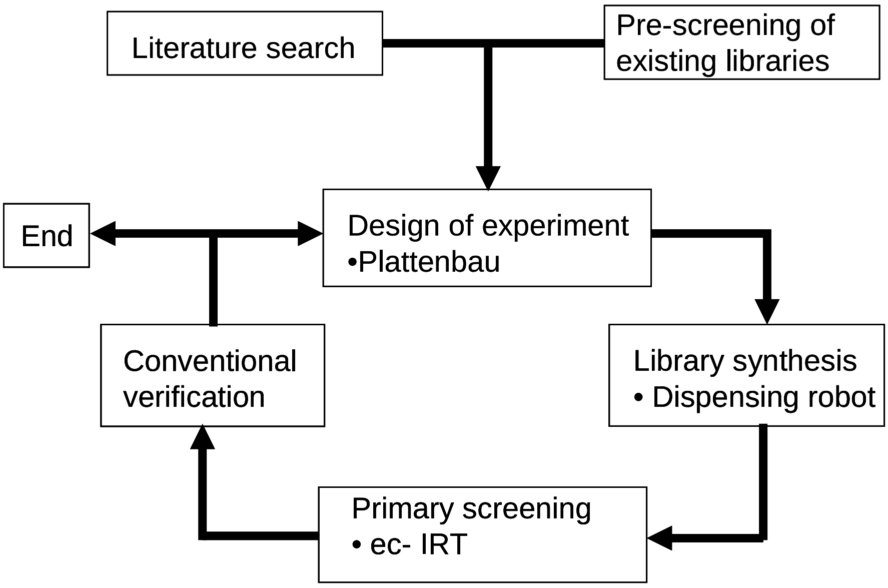

Figure 2-1 High throughput work flow.

Figure 2-1 represents the high throughput work flow of selective propane combustion catalyst search in presence of CO. The project is initiated with an existing library of other projects synthesised by different co-workers in our group by my formal colleague Dahu Dapheng. The library was tested in iso-octane oxidation and elements such as Ce, Co, Cu, Fe and Ni were found active. Based on those five elements binary and ternary composition were proposed and three libraries were planned to be prepared for high throughput screening.

2.2 High throughput library synthesis

The activity of heterogeneous catalysts was sensitive towards preparation methods. Differences in sequencing of the addition of precursors, drying and calcination temperatures result in variety of different materials with different catalytic activities and selectivities of identical catalyst composition. Thus composition tolerant sol-gel recipes were employed for catalyst preparation techniques. The sol-gel process represents an attractive alternative to conventional synthesis methods. It results in the formation of mixed oxides of improved homogeneity, facile tailoring of morphology of mixed oxides and requires mild reaction conditions such as room temperature and atmospheric pressures [70]. The software “Plattenbau” [139] developed in our group is used for high throughput experimental design. The software calculates the optimised pipetting list based on dopants and matrix solution and catalysts syntheses were automated with the help of a commercial pipetting robot (Lissy, Zinsser Analytic). The robot work space is shown in figure 2-2.

Figure 2-2: Roboter work space.

The robot work space consists of 2 needles which transfer the stock solutions from the corresponding dopant and reagent racks into the GC rack containing 50 2 ml HPLC vials positioned in an array (10 x 5). After all pipetting steps finished, the entire rack is stirred in an orbital shaker to obtain a homogenous solution followed by drying and calcination. Then the calcined catalyst were ground with spatula and filled manually into the 206 catalyst wells of hexagonal slate plate libraries. Also, each library is filled with reference catalyst (2,6 wt% $Pt/Rh/Al_2O_3$) for activity comparison.

2.3 Primary screening of catalysts (ec-IRT)

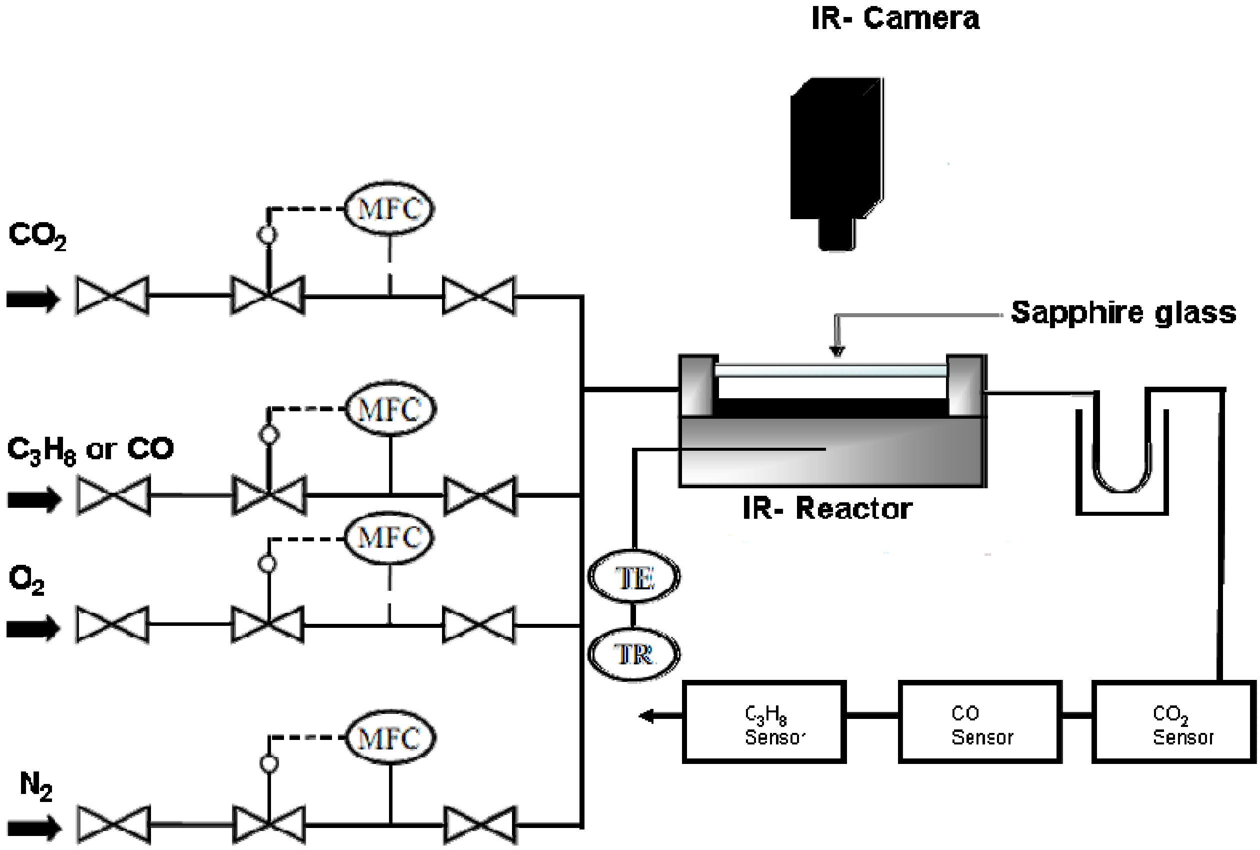

Figure 2-3: **Schematic flow diagram of ec-IRT experiment set up. MFC: Mass flow controller; TE: thermoelement; TR: temperature controller: PC: Personal computer**

The emissivity corrected infrared thermography was used for parallel screening of catalyst libraries to identify potential catalysts for selective propane combustion reaction. The schematic flow diagram of ec-IRT measurement is shown in figure 2-3. The required feed gas for the reaction was supplied to the IR reactor unit with a help of mass flow controllers [MKS]. The IR camera equipped with 640 x 480 pixel PtSi-FPA detector and mounted over the top of the IR reactor. The infrared reactor is made of steel housing and has a large opening where the library is placed for the measurement. The heating plate is mounted under the bottom of the reactor and the temperature is controlled by a thermoelement. The sapphire glass is used to cover the top of the reactor which allow us to monitor the infrared radiation of the plate by an infrared camera. The reaction gas enters through the upper part of eight drilled holes into the reaction chamber and leaves the reactor from the centre hole of the reactor unit to the steam trap to condense the water before entering the C_3H_8, CO and CO_2 infrared sensors [GfG].

The ec-IRT allows the detection of heat of reaction of the particular reaction on the catalyst surface, which can be interpreted as catalytic activity. Measurement and detailed working principles were explained elsewhere previously [140-142]. Different catalyst materials have different reflectivities and emissivities. Reflectivity and emissivity are material specific properties and differs from sample to sample. Local differences in emissivity and reflectivity on the library surface and its individual catalyst spots do appear as different photon intensities, which can be misinterpreted as different temperatures, though true surface temperatures are identical. Hence emissivity correction by six point calibration is obligatory prior to the measurement. It is done by measuring the emissivity of the library at 6 different temperatures in between -4°C and +6°C of the desired reaction temperature in steps of 2°C. For example, if the desired reaction temperature was 250°C, calibration is done at 246, 248, 250, 252, 254 and 256°C. The measured detector sensitivity and samples emissivity are used to correct the detector sensitivity and sample emissivity at the desired reaction temperature. The whole high throughput screening process is completely automated and controlled by the IR Testrig software [142].

A typical IR thermography experiment was carried out in the following sequence.

- Six point temperature calibration of the library using calibration gas (O_2, N_2 and CO_2).
- Testing of propane combustion reaction.
- Reactor flushing using calibration gas.
- Testing of CO combustion reaction.
- Purging the reactor using N_2.

The selection of new leads in all catalyst generations is based on the relative activities of propane oxidation and also compared with CO oxidation. Initially IR image of the library under propane and CO oxidation is compared. Detailed explanation of primary screening hits were illustrated in the forthcoming sections. The selected hits from different generations were upscaled from 300 µmoles to 8 Mmoles and tested in the conventional fixed bed reactor with a total feed flow rate of 50 ml/min, operating temperature window (150-350°C) and feed gas concentration as ($C_3H_8/CO/CO_2/O_2/N_2$ = 2/10,9/15,8/10/61,3). The best performing catalysts of each generation were continued for further catalyst development of the next generation.

2.4 High throughput experimentation of generation 1

The search of catalysts for propane oxidation in the presence of CO was started by testing a highly diverse library (library 1) prepared by a co worker (G. Frenzer) from our group. The table 2-1 represented with block letters are the elements used as matrices and dopants corresponding to their respective generations.

H																	He
Li	Be											**B**	C	N	O	F	Ne
Na	**Mg**											**Al**	Si	P	S	Cl	Ar
K	**Ca**	**Sc**	**Ti**	**V**	**Cr**	**Mn**	**Fe**	**Co**	**Ni**	**Cu**	**Zn**	**Ga**	**Ge**	As	**Se**	Br	Kr
Rb	**Sr**	**Y**	**Zr**	**Nb**	**Mo**	**Tc**	**Ru**	**Rh**	**Pd**	**Ag**	**Cd**	**In**	**Sn**	**Sb**	**Te**	I	Xe
Cs	**Ba**		**Hf**	**Ta**	**W**	**Re**	**Os**	**Ir**	**Pt**	**Au**	Hg	Tl	**Pb**	**Bi**	Po	At	Rn
Fr	Ra		Db	Jl	Rf	Bh	Hn	Mt	Uun	Uuu							

La	**Ce**	**Pr**	**Nd**	Pm	**Sm**	**Eu**	**Gd**	**Tb**	**Dy**	**Ho**	**Er**	**Tm**	**Yb**	**Lu**
Ac	Th	Pa	U	Np	Pu	Am	Cm	Bk	Cf	Es	Fm	Md	No	Lr

Table 2-1 **Elements used as matrices and dopants for catalyst development strategies mentioned in block letters**

Initially, library 1 was tested for iso-octane oxidation as a test case. It was found that Ce, Co, Cu, Fe and Ni were active elements. These five elements led to binary and ternary composition spreads with a step variation of 10 mol%. Detailed catalyst compositions used in each library of generation 1 is mentioned in the table 2-2. The catalyst development phenomena introduce the concept of variation and selection. Variation was obtained by doping and composition spreads. Potential hits selections were based on the relative catalyst activities of C_3H_8 oxidation in comparison with CO oxidation. It should be noted that catalysts were described in terms of metal ions with mol% as subscripts which represent the expected concentration of catalyst sols. An example shown states clearly; $Ni_{60}Co_{40}O_x$ means 60 mol% of Ni and 40 mol% of Co with O_x

corresponding to the unknown oxidation states of the mixed metal oxides. Feed gas conditions for ec-TRT screening in first generation libraries are mentioned in the table 2-3.

Library	Catalyst composition
1	Highly diverse[HD] [HD] = Al, Ce, Cr, Fe, Hf, La, Mn, Na, Ni, Pt, Re, Rh, Si, Sm, Ti, V, W, Y and Zr
2	A_xB_{100-x}, with A and B = Ce, Co, Cu, Fe and Ni; x varies from 0 to 100 mol% in steps of 5 mol%
3 & 4	$A_xB_yC_{100-x-y}$ with A, B and C = Ce, Co, Cu, Fe and Ni; x and y varies from 0 to 100 mol% in steps of 10 mol%

Table 2-2 Catalysts prepared for HT screening in the first generation

Gas atmosphere	C_3H_8 (Vol%)	CO (Vol%)	CO_2 (Vol%)	O_2 (Vol%)	N_2 (Vol%)
Propane	2	0	15,8	10	72,2
CO	0	10,9	15,8	10	63,3
Exhaust	2	10,9	15,8	10	61,3

Table 2-3 Feed conditions of ec-IRT screening of first generation libraries

High throughput screening of a library in first generation flows was done on as shown below.

1) Pre treatment of catalyst library at 250°C using synthetic air.
2) Six point temperature calibration at desired reaction temperature using calibration gas atmosphere ($CO_2/N_2/O_2$ = 15,8/10/74,2 vol%).
3) Reaction over catalysts library using feed gas consisting of $C_3H_8/CO/CO_2/O_2/N_2$ and about 2/10,9/15,8/10/61,3 vol%.
4) Purging with N_2 over the library.

Based on above said four points, primary screening is carried out and the ec-IRT image of a library 2 is shown in figure 2-4. It can be inferred that several catalysts were found active. But it could not be differentiated which catalysts are responsible for CO and C_3H_8 oxidation.

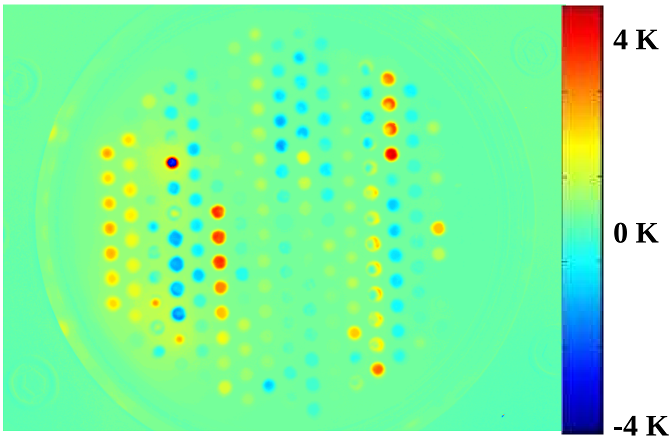

Figure 2-4: **EC-IRT image of library 2 in exhaust gas (C_3H_8 and CO atmosphere) feed at 150°C; Total flow rate 50ml/min; $C_3H_8/CO/CO_2/O_2/N_2$ = 2/10,9/15,8/10/61,3.**

Hence high throughput screening has to be repeated keeping the first and second points same and further steps (steps 5-8) are explained below.

5) Reaction over the library under propane atmosphere consisting of $C_3H_8/CO_2/O_2/N_2$ with 2/15,8/10/72,2 vol% in the feed.
6) Flushing of the reactor using calibration gas.
7) Reaction over library under CO atmosphere consisting of $CO/CO_2/O_2/N_2$ with 10,9/15,8/10/63,3 vol% in the feed.
8) Repeat step 4.

High throughput screening of libraries (2 to 4) were measured by my formal colleague Dahu Dapheng. Repetitions of IR thermography measurements of same libraries by me in order to confirm the trends and shown in figure 2-5 (library 2).

a) C_3H_8 oxidation

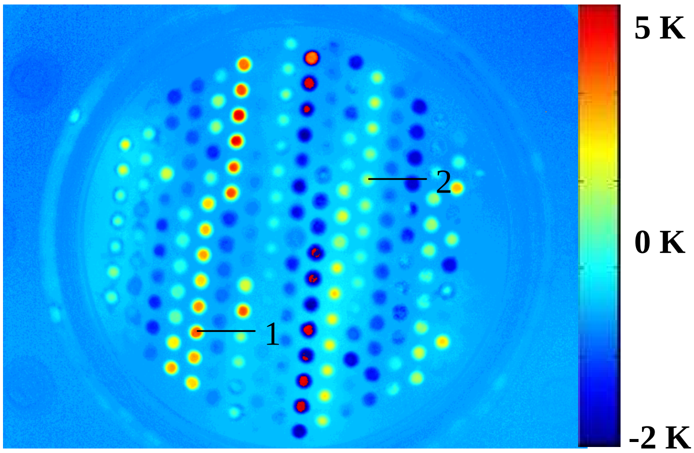

b) CO oxidation

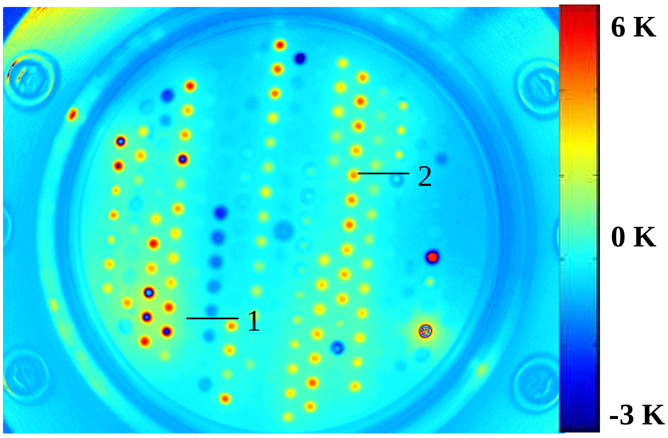

c) Background image after C_3H_8 oxidation at 250°C

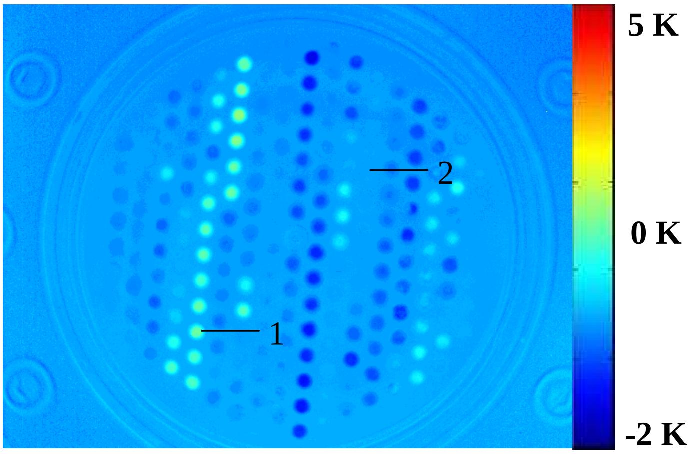

Figure 2-5: **Emissivity corrected infrared thermography image of library 2 at 250°C Reaction conditions (a): $C_3H_8/CO_2/O_2/N_2$ = 2/15,8/10/72,2 vol%. (b) $CO/CO_2/O_2/N_2$ = 10,9/15,8/10/63,3 vol%. (c) $CO_2/O_2/N_2$ = 15,8/10/74,2vol%. 1: $Ce_{55}Fe_{45}$; 2: $Ni_{60}Co_{40}$.**

It is observed that catalysts which are found active with the used libraries were not the same when compared to that of fresh libraries. Hence potential hits selected based on highest relative activities of individual catalysts from both works of primary screening have been selected for conventional verification and mentioned in table 2-4.

From figure 2-5, $Ce_{55}Fe_{45}$ and $Ni_{60}Co_{40}$ were selected as potential hits of library 2. $Ce_{55}Fe_{45}$ catalyst shows very high activity towards propane oxidation but suffers emissivity changes after the reaction and shows little activity towards CO oxidation. $Ni_{60}Co_{40}$ is less active and suffers lesser emissivity changes when compared to the former one. One more drawback is that $Ni_{60}Co_{40}$

catalyst is comparably active for CO oxidation. Hence it is necessary to validate the performance of both catalysts conventionally.

No	Catalysts	No	Catalysts
1	$Ce_{55}Fe_{45}$	8	$Ce_{33,3}Fe_{33,3}Cu_{33,3}$
2	$Ni_{60}Co_{40}$	9	$Ce_{55}Cu_{45}$
3	$Ce_{70}Cu_{20}Fe_{10}$	10	Ce_5Co_{95}
4	$Ce_{10}Co_{80}Ni_{10}$	11	$Fe_{20}Co_{80}$
5	$Ce_{20}Fe_{70}Ni_{10}$	12	Fe_5Ni_{95}
6	$Cu_{20}Co_{70}Ni_{10}$	13	$Pt/Rh/Al_2O_3$ (reference)
7	$Ce_{30}Co_{60}Fe_{10}$		

Table 2-4 Selected potential hits of first generation for conventional testing

Table 2-4 shows the selected catalysts for conventional verification of libraries from 2 to 4 based on ec-IRT image carried out by my colleague (Dahu Dapheng) and by me. Those catalysts were selected based on criteria as explained in the above example ($Ni_{60}Co_{40}$ and $Ce_{55}Fe_{45}$ catalyst selection). Catalysts (1 to 6) are selected based on IR screening by me and catalysts (7 to 12) are selected based on Dahu Dapheng screening.

2.5 Conventional testing of first generation hits

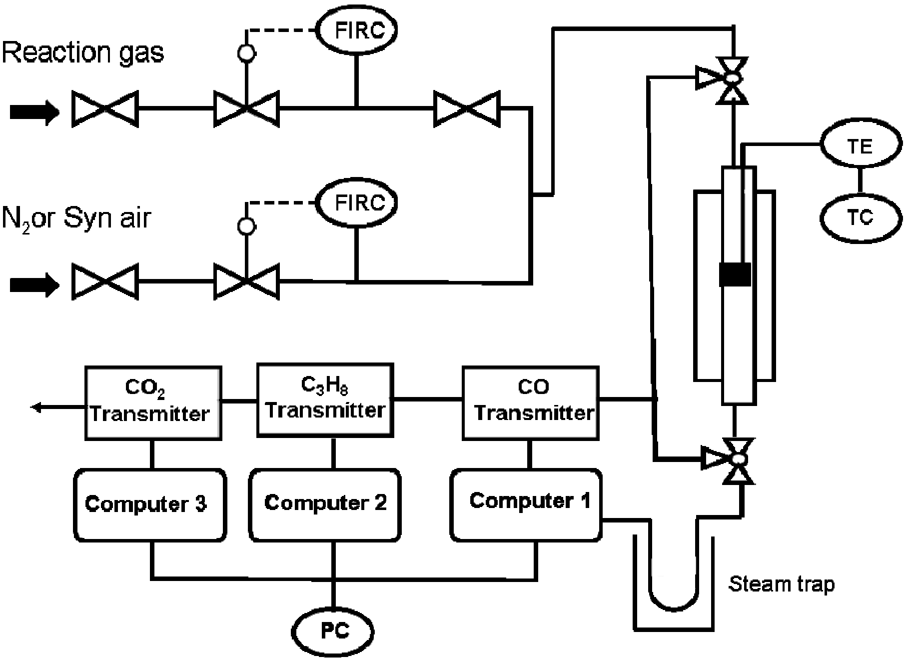

Figure 2-6: Schematic flow diagram of conventional experiment set up. TE: Thermoelement; TC: temperature controller: PC: Personal computer

To validate the performance of high throughput screening results, active hits were upscaled from 300 µmoles to 8 Mmoles and tested in the conventional fixed bed reactor. Detailed description of conventional synthesis and experiments were explained in the section 3.3 to 3.5.

The schematic representation of the conventional test set up is shown in figure 2-6. The premixed reaction gas and synthetic air in the ratio of 1:1 enters the conventional gas flow reactor. About 100 mg of catalyst of particle size 100-200 µm with a total feed flow rate of 50 ml/min and feed gas concentration of $C_3H_8/CO/CO_2/O_2/N_2$ = 2/10,9/15,8/10/61,3 vol% is used. The product gas leaving the reactor enters the steam trap by preventing the water molecules entering the infrared sensors. The product gas is analysed for the exit concentrations using C_3H_8, CO and CO_2 sensors [GfG]. The sensor signals were monitored by mini computer and transferred to the main computer. The temperature of the catalyst is controlled by a thermoelement. The operating temperature window for the reaction is 150-350°C (150-250°C for first generation). The best performing catalysts of each generation were continued for further catalyst development of the next generation.

Conventional experiments were started by testing the reference catalyst (2,6 wt% $Pt/Rh/Al_2O_3$) which was supplied by the industrial partner. About 100mg of catalyst were placed in the reactor with the total feed flow rate of 50 ml/min and tested. It is observed that there was a steep increase of temperature in the catalyst bed due to the high heat evolution of both exothermic reactions (C_3H_8 and CO) and found very difficult to maintain the desired temperature. Therefore it was decided to mix the catalyst with the inert (γ-alumina) in the weight ratio of 1:5 (100mg/500mg).

Conventional test results of first generation hits with two catalysts along with reference catalyst were shown in figure 2-7 (C_3H_8 and CO conversion). The activity of the reference catalyst towards propane oxidation is higher around 50% at 250°C and completely active for CO oxidation. The $Ce_{55}Fe_{45}$ catalyst shows no activity for propane, but it is active for CO oxidation, although it was one of the most active materials of library 2 in the high throughput screening. The poor performance in the conventional tests indicates that the catalyst material undergoes emissivity changes in the presence of CO. The catalyst $Ni_{60}Co_{40}$ showed comparable activity to reference catalyst in the conventional testing though it was less active in the high throughput screening. At this point it became clear that a detailed consideration of emissivity changes of materials need to be implemented for hits selection from high throughput screening to avoid false positives and false negatives.

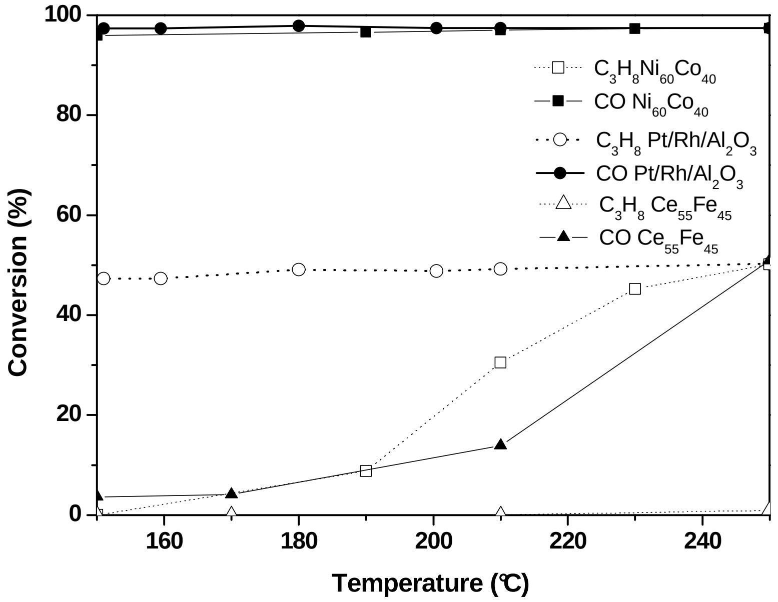

Figure 2-7: **Conventional test results of active hits of generation 1. Reaction conditions: 100mg of catalyst diluted with 500mg of γ-alumina with particle size of 100 – 200 µm (both). Total flow rate: 50ml/min ($C_3H_8/CO/CO_2/O_2/N_2$ = 2/10,9/15,8/10/61,3). Catalyst pre-treatment: synthetic air with 50ml/min at 250°C for 1h.**

Catalyst	**X_{C3H8} (%) at 250°C**	**X_{CO} (%) at 250°C**
$Pt/Rh/Al_2O_3$	50	97
Ce_5Co_{95}	49	97
$Ce_{55}Cu_{45}$	5	97
$Ce_{55}Fe_{45}$	1	51
$Fe_{20}Co_{80}$	39	97
Fe_5Ni_{95}	2	96
$Ni_{60}Co_{40}$	50	97
$Ce_{20}Fe_{70}Ni_{10}$	3	93
$Ce_{10}Co_{80}Ni_{10}$	48	97
$Cu_{20}Co_{70}Ni_{10}$	28	96
$Ce_{30}Co_{60}Fe_{10}$	19	95
$Ce_{70}Cu_{20}Fe_{10}$	12	96
$Ce_{33,3}Fe_{33,3}Cu_{33,3}$	5	96

Table 2-5 **Competitive conversion of C_3H_8 and CO oxidation at 250°C of active hits of first generation**

2.6 Prerequisites for second generation catalyst development

1) Since performance of the catalytic activity and selectivity is based on gas mixture compositions, C_3H_8 concentration was increased from 2 vol% to 4 vol% and CO concentration is reduced from 10,9 vol% to 5,45 vol%.
2) Since the weight hourly space velocity is quite low in conventional tests, the catalyst mass was reduced by a factor of 5 with a constant total flow rate of 50 ml/min.

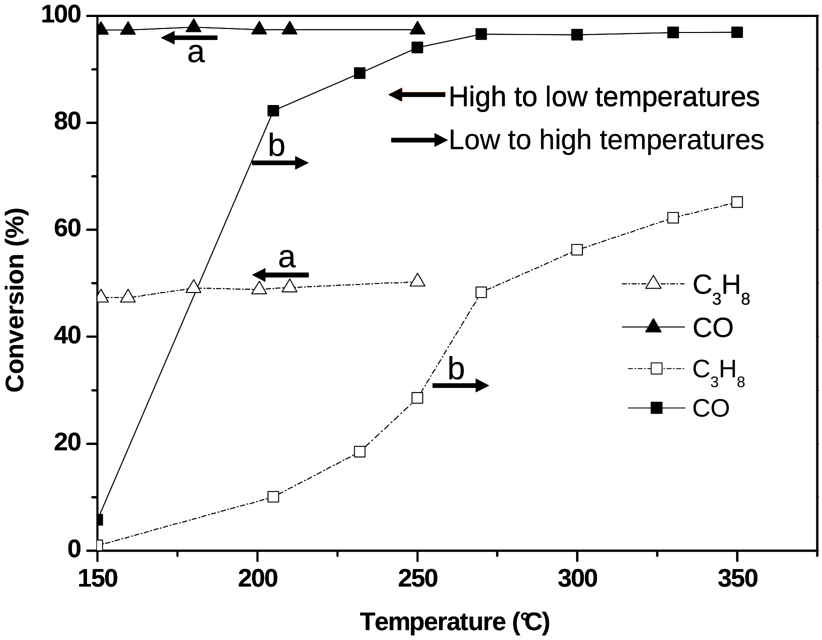

Figure 2-8: **Conventional test results of Pt/Rh/Al_2O_3 catalyst. a: reaction in decrement order of temperatures from 250°C to 150°C. b: reaction in increment order of temperatures from 150°C to 250°C. Reaction conditions: a) 100mg of catalyst diluted with 500mg of γ-alumina with particle size of 100-200 µm (both). b) 20mg of catalyst diluted with 100mg of γ-alumina with particle size of 100-200 µm (both). Total flow rate: 50ml/min (C_3H_8/CO/CO_2/O_2/N_2 = 2/10,9/15,8/10/61,3). Catalyst pre-treatment: synthetic air with 50ml/min at 250°C for 1h.**

3) The reaction has to be carried out in increasing order of temperature. Figure 2-8 shows that the catalyst activity is a function of temperature, i.e. as the reaction proceeds from higher to lower temperatures; the catalyst remains active with respect to higher temperatures. But when it proceeds from low to higher temperatures, it follows the expected steady increase in activity as a function of temperatures with higher propane selectivity. For example propane conversion at 200°C reproduces the same as 250°C when the reaction is carried out from higher to lower temperatures showing that the

reaction is temperature independent. The reason could be the catalyst is highly reactive and active at higher temperatures and posses the same though the temperature is lowered. Another possibility could be the amount of catalyst mass is higher (5 times; 100mg) when compared to the reaction from low to higher temperatures (20mg). This leads to high residence time with a low space velocity (0,5 mlg^{-1}min^{-1}) and higher activities.

4) The temperature operating window varied from 150°C to 350°C.

a)

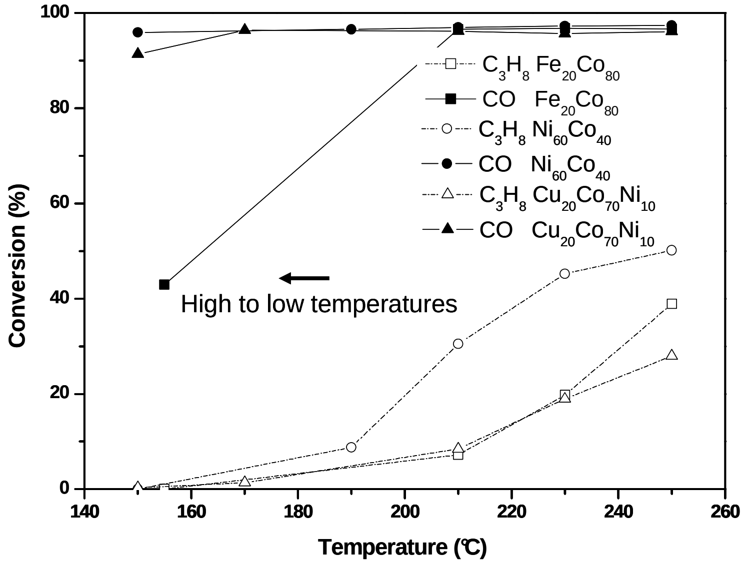

b)

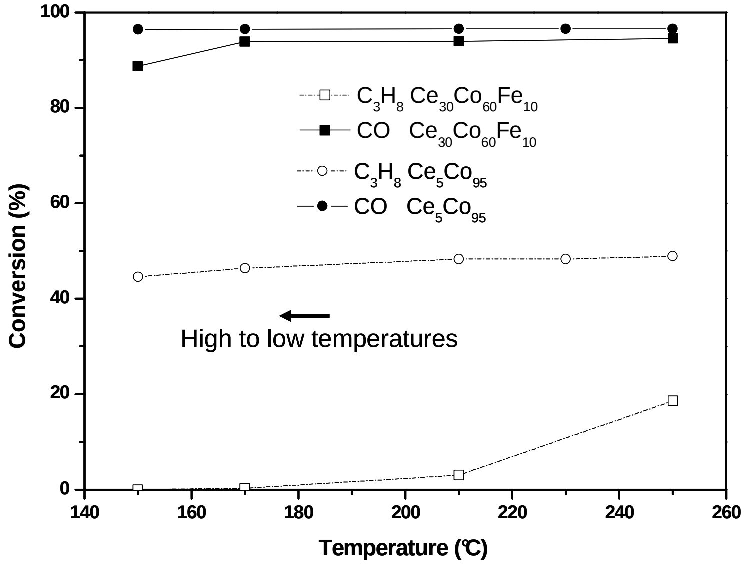

Figure 2-9: a & b Conventional test results of first generation catalysts with reaction in decrement order of temperatures from 250°C to 150°C. Reaction conditions: 100mg of catalyst diluted with 500mg of γ-alumina with particle size of 100-200 µm (both). Total flow rate: 50ml/min ($C_3H_8/CO/CO_2/O_2/N_2$ = 2/10,9/15,8/10/61,3). Catalyst pre-treatment: synthetic air with 50ml/min at 250°C for 1h.

5) $Fe_{20}Co_{80}$, $Ni_{60}Co_{40}$, $Cu_{20}Co_{70}Ni_{10}$, $Ce_{30}Co_{60}Fe_{10}$ and Ce_5Co_{95} were selected for second generation catalyst development by doping. Prior to second generation it is envisaged that increase of temperature there is slow and steady increase of propane combustion though there is a constant maximum conversion of CO for the first four selected candidates (see figure 2-9a & 2-9b) and Ce_5Co_{95} is not varying much with increase of temperature.
6) From figure 2-9a & 2-9b, it is indicative that there is a chance of increasing propane combustion activity with increase of temperature thereby reduction in CO activity. Thus conventional experiments were repeated from 250°C to 350°C for first four candidates to see the effect of propane combustion (figure 2-10).

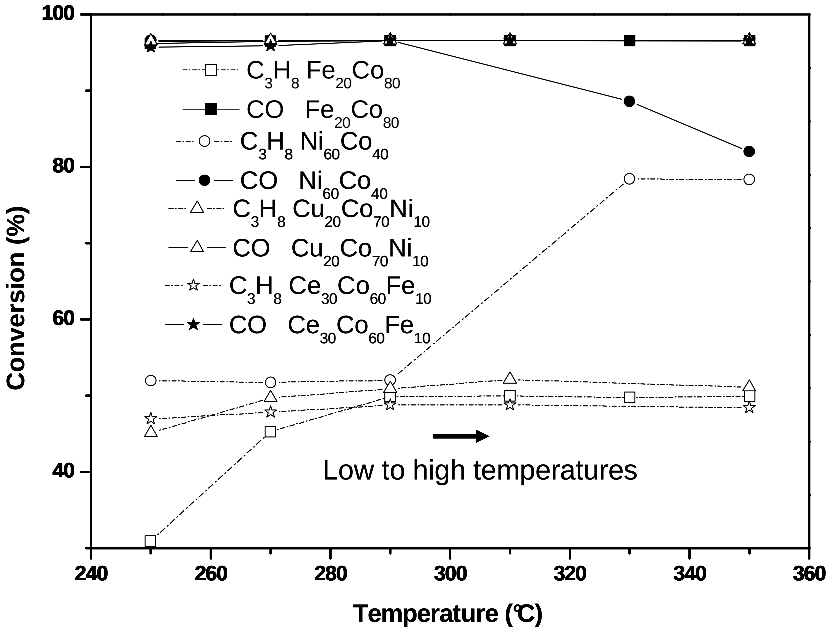

Figure 2-10: Conventional test results of 4 selected first generation catalysts with reaction in increment order of temperatures from 250°c to 350°C. Reaction conditions: 100mg of catalyst diluted with 500mg of γ-alumina with particle size of 100-200 µm (both). Total flow rate: 50ml/min ($C_3H_8/CO/CO_2/O_2/N_2$ = 2/10,9/15,8/10/61,3). Catalyst pre-treatment: synthetic air with 50ml/min at 250°C for 1h.

Figure 2-10 indicates that the activity of $Ni_{60}Co_{40}$ is very dependent on temperature. C_3H_8 combustion increases with decrease in CO reactivity whereas other catalysts have minimum influence but achieves around conversion of about 50% for propane and with a constant maximum conversion of about 96% for CO. Nevertheless all five catalysts were considered for further doping in the second generation catalysts search.

2.7 High throughput experimentation of generation 2

So far in the first generation, none of the catalysts were found selective for propane combustion. The best five active hits were doped with 3% ca. of 48 different transition elements and filled in two libraries (library 5 & 6). Also two more highly diverse libraries (library 7 & 8) from another project prepared by G. Frenzer are also investigated. Elements which are found active in those highly diverse libraries were considered for composition spreads with varying concentration of 10, 50 and 90 mol% and developed as in library 9. All these five libraries together are considered as second generation of our catalyst search and compositions are mentioned in table 2-6. Catalytic testing of these libraries in propane and CO atmospheres were carried out at temperatures of 150°C, 250°C and 350°C. The operating temperature window set as 150 to 350°C because propane light off starts at a temperature range of 200 to 250°C.

Library	Catalyst composition
5	$D_3Ce_5Co_{92}$, $D_3Fe_{20}Co_{77}$, $D_3Ni_{60}Co_{37}$ with D = Al, B, Ba, Bi, Ca, Cd, Cr, Cs, Cu, Dy, Er, Eu, Fe, Ga, Gd, Ge, Hf, Ho, In, K, La, Li, Lu, Mg, Mn, Mo, Na, Nb, Nd, Rb, Sb, Sc, Se, Si, Sm, Sn, Sr, Ta, Tb, Te, Ti, Tm, V,W, Y, Yb, Zn, Zr
6	$D_3Cu_{20}Co_{67}Ni_{10}$, $D_3Ce_{30}Co_{57}Fe_{10}$ with D as same like library 5
7	$Ce_xCu_yFe_{100-x-y}$, $Ce_xCo_yMn_{100-x-y}$, Ni_fY_{100-f}, $Ni_fLa_gRe_h$ with x and y varies from 0 to 100 mol% in steps of 10 mol%; f varies from 90 to 100 mol% in steps of 1 mol%; g varies from 1 to 9 mol% in steps of 1 mol%; h = 0 and 0,01 mol%.
8	$A_{50}B_{50}$, $A_{33,3}B_{33,3}C_{33,3}$, $Co_{20}Cu_{50}Mn_{30}$, $Co_{20}Mn_{80}$, with A, B and C = Ce, Co, Cr, Cu, Fe, La, Mn, Mo, Ti and V
9	A_xB_{100-x} with A and B = Ce, Co, Cr, Cu, Fe, Mn, Mo and Ti; x = 10, 50 and 90 mol%

Table 2-6 Catalyst compositions of libraries prepared for HT screening in second generation

Hence it is notified to observe the effect of transition metal oxide libraries by closely looking at one temperature as lower limit of 150°C and upper limit as 350°C. The catalyst activity of a library was measured as an average heat of evolution at each catalyst wells during reaction and recorded as per pixel values with a help of IR Testrig software. The absolute temperature increase at each catalyst spot were calculated from per pixel values. The IR image of the library 8 is shown in figure 2-11. Several candidates were found active and drastic change in the emissivity of the materials was observed after C_3H_8 oxidation which is major indicator of identifying the hits. Though several candidates show activity, it was very difficult to identify “reliable” hits. The IR images allow detailed analysis of temperature changes in each catalyst well and ranking analysis based on highest activity in C_3H_8 and CO oxidation were analysed to find potential hits of second generation for conventional verification.

Temperature differences (table 2-7) were selected on per pixel values of each catalyst well, which are recorded by the IR Testrig software in Excel format during measurements. Both C_3H_8 and CO oxidation were considered. The sorting of catalyst activity of a library is based on these absolute temperature changes at each catalyst well is as followed. The first 30 candidates which show highest temperature increase for C_3H_8 oxidation is compared with first 30 most active materials of CO oxidation. Candidates for C_3H_8 oxidation which are not present in the list of first 30 materials for CO oxidation are selected as hits for further studies. i.e. hits selected were compared with the temperature changes after the reaction for C_3H_8 oxidation. For example in $Mo_{50}Fe_{50}$ catalyst (table 2-7), it was found that temperature rise at this catalyst was about 5,94°C during C_3H_8 oxidation. After the reaction (background image) was about 1,37°C which is an indication of high emissivity change of the catalyst. Similarly with $Ce_{33,3}Ti_{33,3}Cr_{33,3}$ catalyst it was 5,04°C during C_3H_8 oxidation and -0,1°C after the reaction respectively.

a) C_3H_8 oxidation

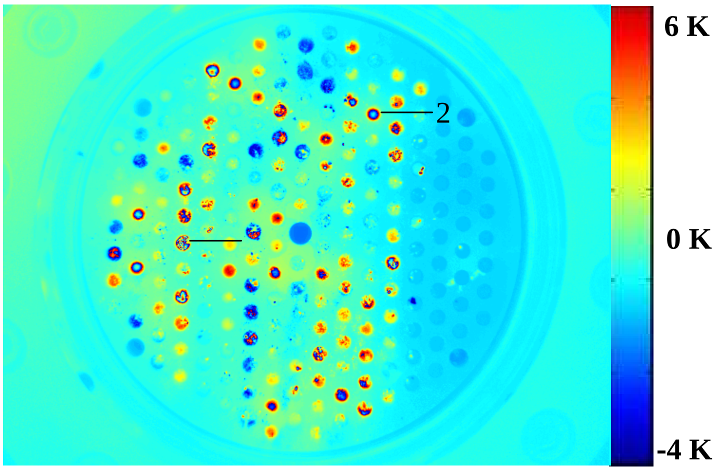

b) CO oxidation

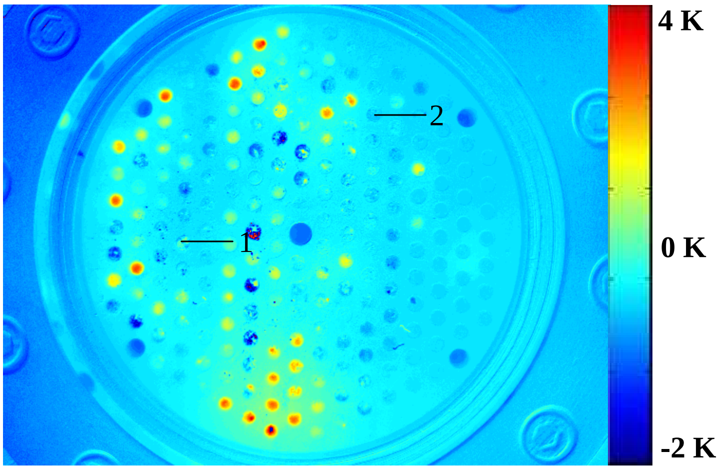

c) Background image after C_3H_8 oxidation

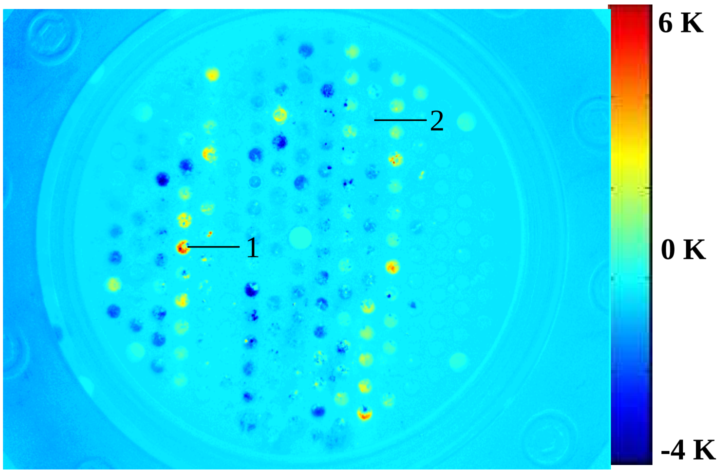

Figure 2-11: Emissivity corrected infrared thermography image of library 8 at 350°C. Reaction conditions (a): $C_3H_8/CO_2/O_2/N_2$ = 4/15,8/10/70,2 vol%. (b) $CO/CO_2/O_2/N_2$ = 5,45/15,8/10/68,75 vol%. (c) $CO_2/O_2/N_2$ = 15,8/10/74,2vol%. 1: $Mo_{50}Fe_{50}$; 2: $Ce_{33,3}Ti_{33,3}Cr_{33,3}$.

From the two catalysts it is clear from $Mo_{50}Fe_{50}$ have high heat of evolution during reaction with high emissivity change of the catalyst and $Ce_{33,3}Ti_{33,3}Cr_{33,3}$ have high heat of evolution with lesser emissivity change. This two extreme ends of emissivity change of materials with high relative activity were selected as potential hits for conventional verification to avoid false positives and false negatives.

Composition	**ΔT_{C3H8}°C (Reaction)**	**ΔT_{C3H8}°C (Background)**	**Difference °C**	**ΔT_{CO}°C (Reaction)**
$Ce_{33,3}Ti_{33,3}Cr_{33,3}$	5,04	-0,1	5,14	-0,14
$Mo_{50}Fe_{50}$	5,94	1,37	4,57	0,12
$Co_{50}Cr_{50}$	4,28	-0,28	4,56	0,42
$Ce_{50}Ti_{50}$	6,12	1,62	4,51	-0,48
$Mn_{33,3}Ce_{33,3}Co_{33,3}$	2,75	0,02	2,73	0,45
$Mn_{33,3}Cu_{33,3}Cr_{33,3}$	2,68	-0,007	2,69	0,57
$Mn_{33,3}Cr_{33,3}Co_{33,3}$	2,45	-0,03	2,48	0,29
$Ti_{33,3}Cu_{33,3}Cr_{33,3}$	2,24	-0,14	2,38	0,16

Table 2-7 Selected catalysts of library 8 for conventional verification based on temperature evaluation technique at 350°C

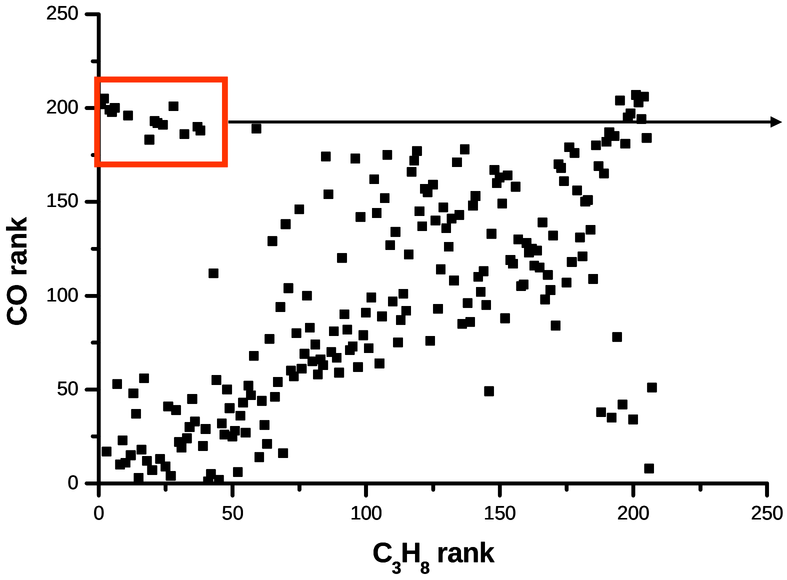

No.	**Catalyst**	**No.**	**Catalyst**
1	$Ce_{90}Ti_{10}$	8	$Cr_{10}Mo_{90}$
2	$Ce_{50}Ti_{50}$	9	$Mn_{10}Mo_{90}$
3	$Ce_{90}Mo_{10}$	10	$Cu_{10}Ti_{90}$
4	$Ti_{90}Mo_{10}$	11	$Ce_{10}Ti_{90}$
5	$Fe_{10}Ti_{90}$	12	$Mo_{90}Ti_{10}$
6	$Co_{10}Mo_{90}$	13	$Ce_{50}Mo_{50}$
7	$Ce_{10}Mo_{90}$		

Figure 2-12: Ranking analysis of library 9 at 350°C.

Further ranking analysis of library 9 at 350°C is shown in figure 2-12. This is done in order to get active hits and also some missed active catalysts in temperature evaluation technique. The catalysts are ranked as C_3H_8 and CO rankings (say 1, 2, 3……….etc.) based on temperature increment at each catalyst wells in incremental order i.e. maximum temperature increment due to reaction ranks 1 and minimum temperature increment ranks 206. Ranking of C_3H_8 is plotted against ranking of CO. Catalysts falls in the box of the ranking profile were selected for emissivity comparison and screened. Thus, all the above three procedures (IR image, temperature evaluation techniques and ranking analysis) were followed throughout the second generation libraries and catalysts were selected for conventional testing to find the best performance of catalysts in a fixed bed reactor.

2.8 Conventional testing of second generation hits

Around 26 catalysts selected by high throughput screening were tested conventionally. Performances of the four catalysts are represented in figure 2-13 (a & b). Activities of the remaining candidates were tabulated in the table 2-8 at 350°C. It was quiet surprising that $Ce_{33,3}Ti_{33,3}Cr_{33,3}$ was the only catalyst found more active and selective for propane combustion in the presence of CO. The catalysts from the doping of first generation hits were highly active, but exhibited poor selectivity. Thus at the end of second generation catalyst development the best hit is based on CeTiCr. This catalyst shows very high relative activity towards propane, no reactivity for CO oxidation and negligible emissivity changes.

a)

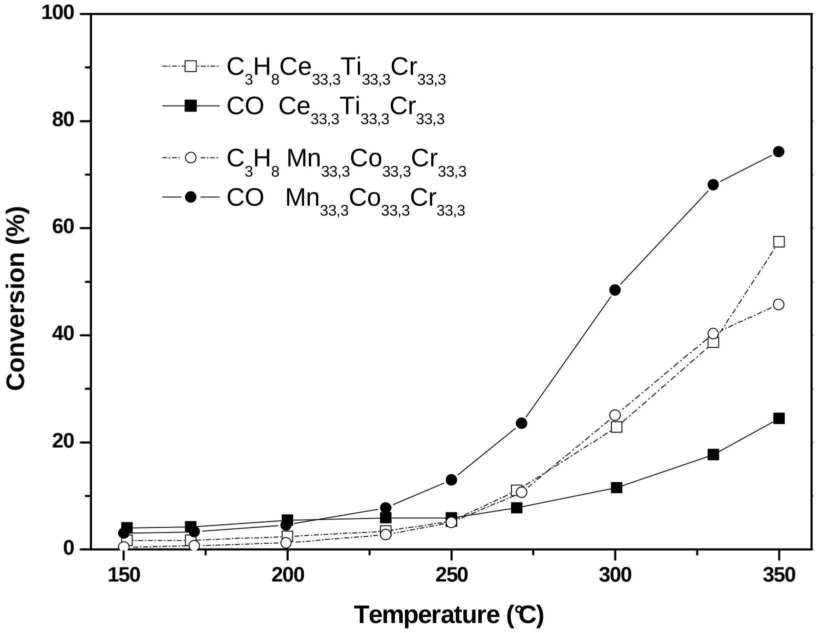

b)

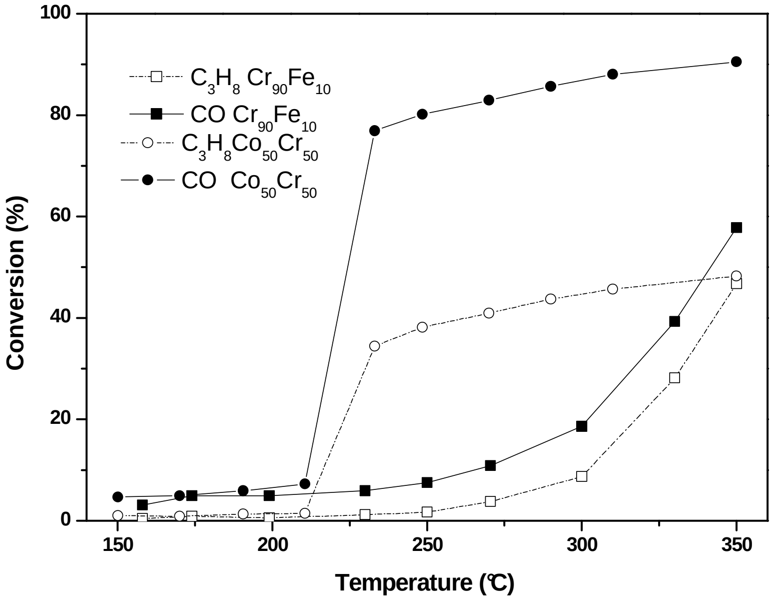

Figure 2-13: **a & b Conventional test results of 4 selected second generation catalysts with reaction in increment order of temperatures from 150°c to 350°C. Reaction conditions: 20mg of catalyst diluted with 100mg of γ-alumina with particle size of 100-200 µm (both). Total flow rate: 50ml/min ($C_3H_8/CO/CO_2/O_2/N_2$ = 2/10,9/15,8/10/61,3). Catalyst pre-treatment: synthetic air with 50ml/min at 350°C for 1h.**

Catalyst	**X_{C3H8} (%) at 350°C**	**X_{CO} (%) at 350°C**	**Catalyst**	**X_{C3H8} (%) at 350°C**	**X_{CO} (%) at 350°C**
$Ni_{60}Co_{37}Fe_3$	31	95	$Mo_{50}Fe_{50}$	2	5
$Ni_{60}Co_{37}Cd_3$	44	95	$Co_{50}Cr_{50}$	48	91
$Ni_{60}Co_{37}Sc_3$	48	100	$Ce_{50}Ti_{50}$	3	12
$Ni_{60}Co_{37}Mg_3$	47	100	$Mn_{33,3}Ce_{33,3}Co_{33,3}$	24	86
$Ni_{60}Co_{37}Sr_3$	34	100	$Mn_{33,3}Cu_{33,3}Cr_{33,3}$	44	97
$Ni_{60}Co_{37}Cr_3$	51	100	$Mn_{33,3}Co_{33,3}Cr_{33,3}$	46	74
$Cu_{20}Co_{67}Ni_{10}Hf_3$	46	100	$Cu_{33,3}Cr_{33,3}Ti_{33,3}$	30	96
$Ce_{90}Fe_{10}$	3	24	$Mn_{10}Mo_{90}$	2	7
$Ce_{10}Fe_{90}$	14	77	$Ce_{10}Mo_{90}$	2	7
$Ce_{30}Mn_{70}$	14	68	$Ce_{10}Mn_{90}$	43	93
$Ce_{50}Mn_{50}$	25	92	$Cr_{90}Fe_{10}$	47	58
$Ce_{10}Co_{90}$	47	97	$Cr_{10}Mn_{90}$	56	89
$Ce_{33,3}Ti_{33,3}Cr_{33,3}$	58	25	$Cr_{10}Fe_{90}$	37	80

Table 2-8 **Conversion of C_3H_8 and CO oxidation at 350°C of active hits of second generation**

2.9 High throughput experimentation of generation 3

Third generation catalyst development were followed by doping of the highly selective and active candidate $Ce_{33,3}Ti_{33,3}Cr_{33,3}$ of the second generation with 48 transition metal oxides, binary and ternary composition spreads of Ce, Ti and Cr elements were also carried out. Additionally binary and ternary spreads of Co, Cr and Mn elements is included in this generation with concentration steps of 10%. All catalysts tested in this generation are summarised in the table 2-9 below.

Library	Catalyst composition
10	$D_3Ce_{33,3}Ti_{33,3}Cr_{33,3}$, with D = Al, B, Ba, Bi, Ca, Cd, Cr, Cs, Cu, Dy, Er, Eu, Fe, Ga, Gd, Ge, Hf, Ho, In, K, La, Li, Lu, Mg, Mn, Mo, Na, Nb, Nd, Rb, Sb, Sc, Se, Si, Sm, Sn, Sr, Ta, Tb, Te, Ti, Tm, V,W, Y, Yb, Zn, Zr A_xB_{100-x}, $A_xB_yC_{100-x-y}$, D_xE_{100-x}, $D_xE_yF_{100-x-y}$; A, B and C refers to Ce, Cr and Ti ; D, E and F refers to Co, Cr and Mn

Table 2-9 Catalyst compositions of libraries prepared for HT screening in third generation

As per the library plan, library 10 had undergone IR thermography screening to identify the possible active hits. The IR image at 350°C is shown in figure 2-14. At 150°C, no catalyst activity is observed in any of the catalyst wells (not shown).

Best candidates based on transition metal oxides were identified based on IR image comparison during reaction and background image after reaction, temperature evaluation techniques and ranking analysis. 8 best candidates shown in table 2-10 were selected for conventional verifications based on the doping of $Ce_{33,3}Ti_{33,3}Cr_{33,3}$ catalyst. The same procedure was also repeated for catalyst selection of composition spreads of CeTiCr elements. Additionally, IR thermography experimental data of CeTiCr composition spreads were investigated through *Mat-Lab* modelling with the help of my colleague Simone Sieg and the computer programs developed by her [143] to identify the trends and to optimise the best compositions for conventional testing (figure 2-15). Composition spreads of CoCrMn spreads were not selective and are not considered in forthcoming generations.

a) C_3H_8 oxidation

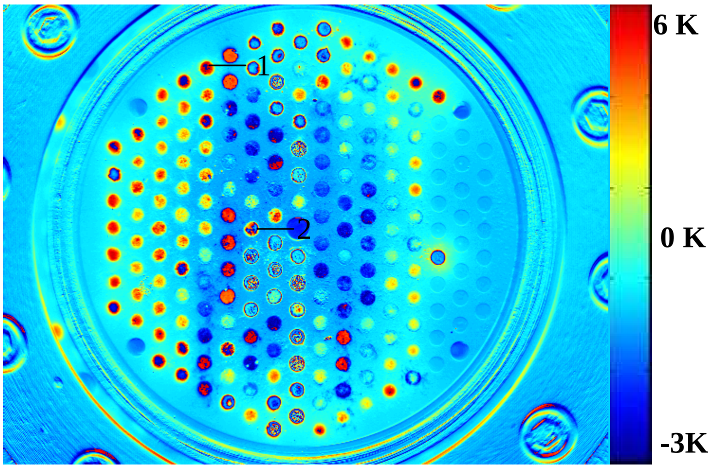

b) CO oxidation

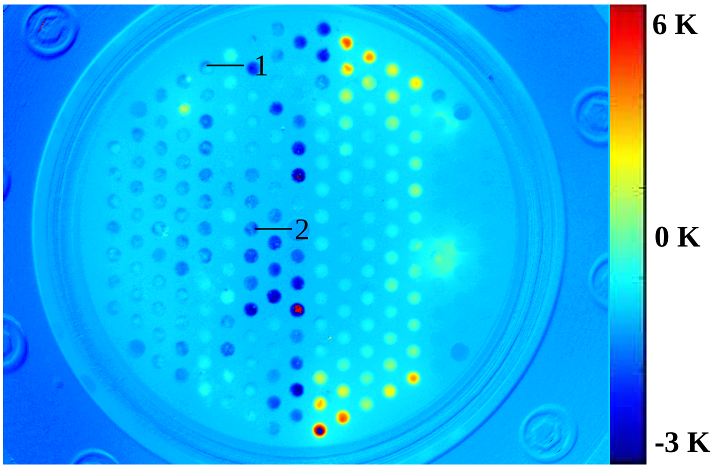

c) Background image after C_3H_8 oxidation

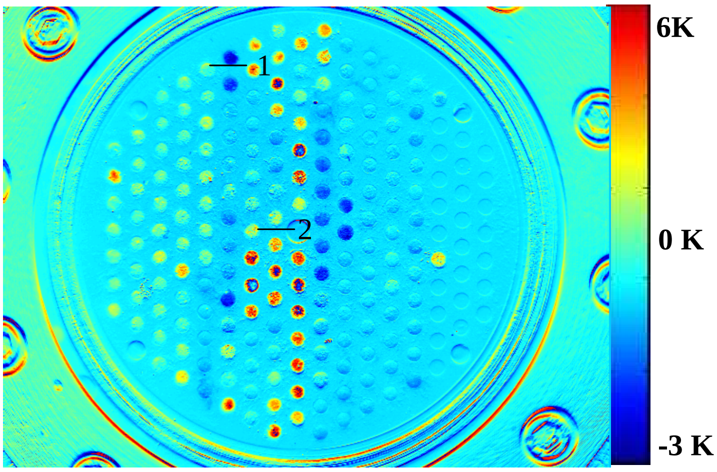

Figure 2-14: Emissivity corrected infrared thermography image of library 10 at 350°C. Reaction conditions (a): $C_3H_8/CO_2/O_2/N_2$ = 4/15,8/10/70,2 vol%. (b) $CO/CO_2/O_2/N_2$ = 5,45/15,8/10/68,75 vol%. (c) $CO_2/O_2/N_2$ = 15,8/10/74,2vol%. 1:$Ce_{32,3}Ti_{32,3}Cr_{32,3}Sc_3$; 2 :$Ce_{20}Ti_{50}Cr_{30}$.

Composition	**ΔT_{C3H8}°C (Reaction)**	**ΔT_{C3H8}°C (Background)**	**Difference °C**	**ΔT_{CO}°C (Reaction)**
$Ce_{32,3}Ti_{32,3}Cr_{32,3}V_3$	4,84	1,55	3,29	-0,77
$Ce_{32,3}Ti_{32,3}Cr_{32,3}In_3$	4,19	0,84	3,35	-0,18
$Ce_{32,3}Ti_{32,3}Cr_{32,3}Sc_3$	4,15	0,78	3,37	-0,19
$Ce_{32,3}Ti_{32,3}Cr_{32,3}Al_3$	3,76	0,5	3,25	-0,06
$Ce_{32,3}Ti_{32,3}Cr_{32,3}Dy_3$	3,06	0,67	2,39	-0,09
$Ce_{32,3}Ti_{32,3}Cr_{32,3}Sr_3$	3,58	0,95	2,63	-0,34
$Ce_{32,3}Ti_{32,3}Cr_{32,3}Hf_3$	3,60	0,60	3,00	-0,08
$Ce_{32,3}Ti_{32,3}Cr_{32,3}Se_3$	2,61	0,46	2,15	-0,26

Table 2-10 **Selected doped catalysts of $Ce_{33,3}Ti_{33,3}Cr_{33,3}$ from library 10 at 350°C for conventional verification based on temperature evaluation technique**

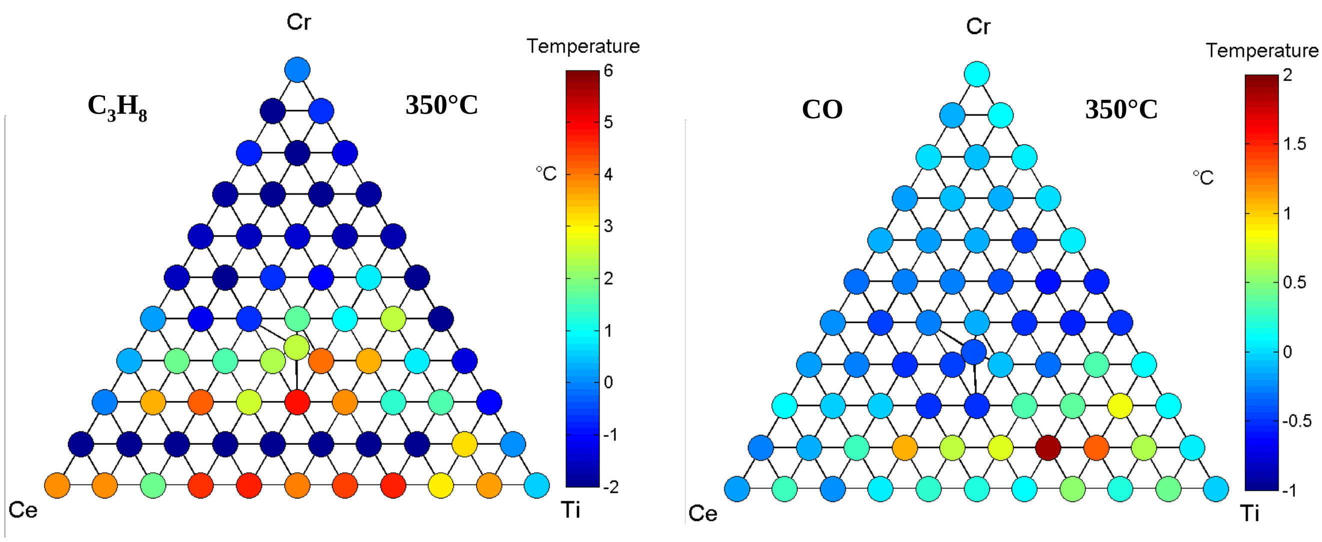

a) C_3H_8 oxidation **b) CO oxidation**

Figure 2-15: **Matlab modelling of infrared thermography experimental data's of CeTiCr composition spreads at 350°C. Reaction conditions (a): $C_3H_8/CO_2/O_2/N_2$ = 4/15,8/10/70,2 vol%. (b) $CO/CO_2/O_2/N_2$ = 5,45/15,8/10/68,75 vol%.**

The temperature change in each catalyst wells of CeTiCr composition spreads for propane and CO oxidation techniques were used in the Mat-Lab modelling. 10 catalysts were selected for conventional testing of CeTiCr composition spreads and listed in table 2-11 below. Red spots on the diagram suggest that catalyst are highly active. Those red spots of propane oxidation were compared with CO oxidation and selected for conventional testing.

No.	Catalysts	No.	Catalysts
1	$Ce_{10}Ti_{80}Cr_{10}$	6	$Ce_{40}Ti_{40}Cr_{20}$
2	$Ce_{20}Ti_{50}Cr_{30}$	7	$Ce_{60}Ti_{20}Cr_{20}$
3	$Ce_{30}Ti_{40}Cr_{30}$	8	$Ce_{60}Ti_{40}$
4	$Ce_{30}Ti_{70}$	9	$Ce_{70}Ti_{10}Cr_{20}$
5	$Ce_{40}Ti_{30}Cr_{30}$	10	$Ce_{70}Ti_{20}Cr_{10}$

Table 2-11 Selected catalysts of CeTiCr composition spreads of library 10 at 350°C

2.10 Conventional testing of third generation hits

The best catalysts selected out of library 10 were put to conventional testing to validate the performance towards propane oxidation. Hf, In, Sc and V doped catalysts resulted out of doping with $Ce_{33,3}Ti_{33,3}Cr_{33,3}$ catalyst were best performing. Similarly, $Ce_{20}Ti_{50}Cr_{30}$ and $Ce_{40}Ti_{40}Cr_{20}$ were found very active and selective, $Ce_{10}Ti_{80}Cr_{10}$ shows high selectivity but poor activity. The performance of 7 candidates are shown in figure 2-16 (a & b).

From the performance profile 2-16a, it can be inferred the activity towards propane combustion are in the order of $V_3 > In_3 > Hf_3 > Sc_3$. Especially vanadium and indium as dopants enhance the propane activity significantly. Comparing high throughput and conventional test results of vanadium doped catalyst (table 2-7) with figure 2-16a shows that high heat of reaction shown by vanadium candidate in IR thermography is also the best active catalyst proven conventionally inspite of its higher emissivity changes. Thus this proves our selection criteria by temperature evaluation techniques is the right way based on high and low emissivity changes. On the other hand, selectivity of these four catalysts were in the order of $Sc_3 > V_3 > In_3 > Hf_3$ at 350°C. Highest selectivity of scandium doped catalyst was about 76,2%.

The composition spread of CeTiCr elements shown in figure 2-16b indicates that both $Ce_{20}Ti_{50}Cr_{30}$ and $Ce_{40}Ti_{40}Cr_{20}$ posses comparatively higher activity and that the former one is the best with a conversion of about 65%. $Ce_{10}Ti_{80}Cr_{10}$ is much less active and highly selective with a conversion of about 21,5%and selectivity of 90,8%. If this selectivity increase is an effect of increased titanium content, or of conversion is not clear yet. A detailed study of the effect of the Ce, Ti, and Cr elements on performance will be discussed in a later section. Therefore two possible hits of the CeTiCr composition spreads were taken into consideration for the next generation catalyst developments. One is highly active ($Ce_{20}Ti_{50}Cr_{30}$) and the other highly selective ($Ce_{10}Ti_{80}Cr_{10}$) catalysts.

a) Doped catalysts

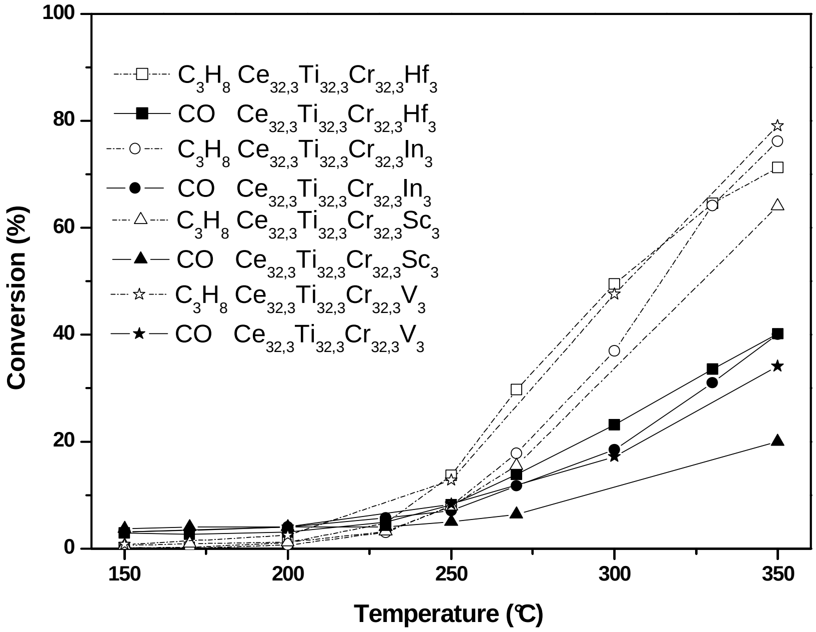

b) Ternary composition spreads catalysts

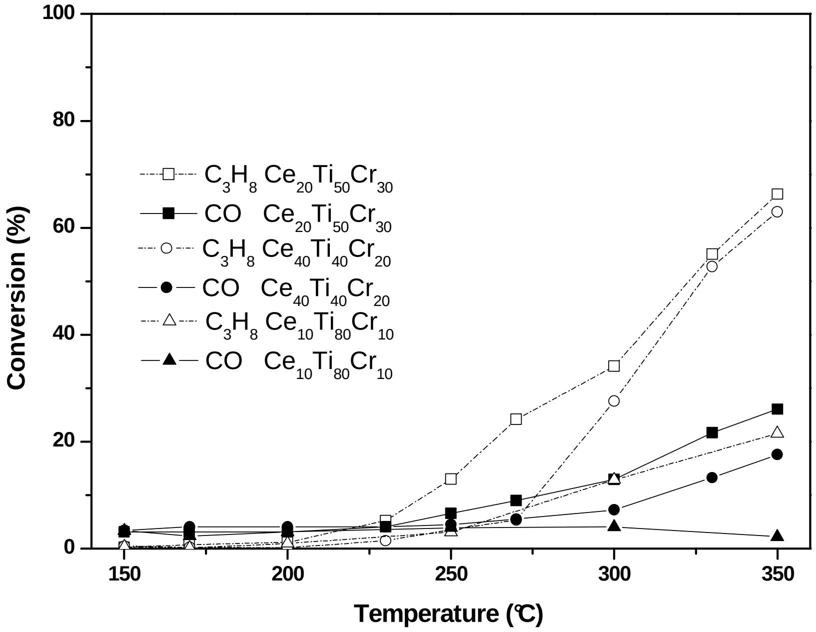

Figure 2-16: Conventional test results of selected doped and composition spreads of CeTiCr candidates of third generation with reaction in increment order of temperatures from 150°C to 350°C. Reaction conditions: 20mg of catalyst diluted with 100mg of γ-alumina with particle size of 100-200 µm (both). Total flow rate: 50ml/min ($C_3H_8/CO/CO_2/O_2/N_2$ = 2/10,9/15,8/10/61,3). Catalyst pre-treatment: synthetic air with 50ml/min at 350°C for 1h.

2.11 Kriging

Kriging is a mathematical modelling technique which covers forecasting and prediction of non observed outcomes of random variables [143, 144]. Based on the conventional test results of composition spreads of CeTiCr elements from generation 3, kriging plots have been drawn to identify the highly active and selective composition space of catalysts for propane combustion and shown in figure 2-17.

a) C_3H_8 conversion

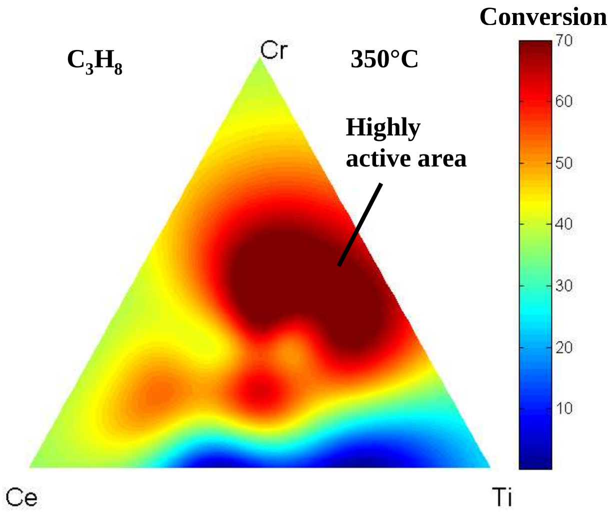

b) C_3H_8 selectivity

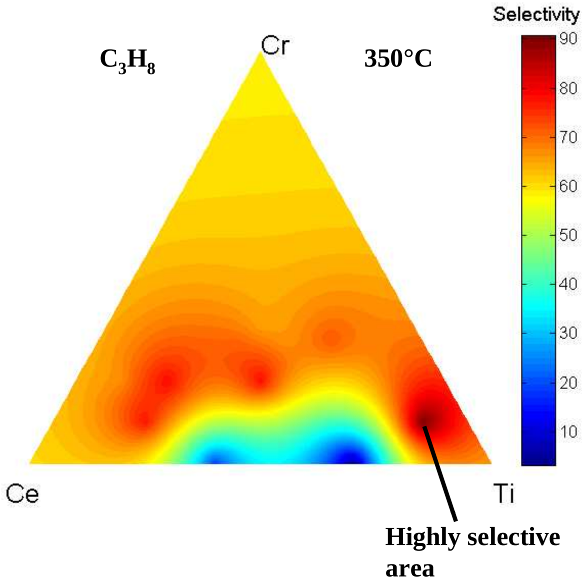

Figure 2-17: Kriging plots of composition spreads of CeTiCr elements during conventional tests at 350°C. Reaction conditions: 20mg of catalyst diluted with 100mg of γ-alumina with particle size of 100-200 µm (both). Total flow rate: 50ml/min ($C_3H_8/CO/CO_2/O_2/N_2$ = 2/10,9/15,8/10/61,3). Catalyst pre-treatment: synthetic air with 50ml/min at 350°C for 1h.

2.12 High throughput experimentation of generation 4

$Ce_{20}Ti_{50}Cr_{30}$ and $Ce_{10}Ti_{80}Cr_{10}$ catalysts along with four doped catalysts have been selected for further improvements in generation 4. Now the research strategy in the present generation was divided in two ways. One was based on highly active catalyst and the other one on highly selectivities. Library 11 covers doping $Ce_{20}Ti_{50}Cr_{30}$ catalyst with dopants which were found best in the last generation, i.e. Hf, In, Sc and V elements. Doping is carried out at four different levels of about 3, 5, 7 and 9 mol% of each dopant. Also precious metal doping of 8 metals at 0,5 and 1 mol% was studied for the $Ce_{20}Ti_{50}Cr_{30}$ catalyst.

Library	Catalyst composition
11	$E_{100-x-y-z}Ce_xTi_yCr_z$ with x = 19, 18,33, 17,67, 17; y = 49, 48,33, 47,67, 47 ; z = 29, 28,33, 27,67, 27 ; E = Hf, In, Sc and V $D_3Cr_{87}Fe_{10}$, $D_3Ce_9Ti_{79}Cr_9$ with D = Al, B, Ba, Bi, Ca, Cd, Cr, Cs, Cu, Dy, Er, Eu, Fe, Ga, Gd, Ge, Hf, Ho, In, K, La, Li, Lu, Mg, Mn, Mo, Na, Nb, Nd, Rb, Sb, Sc, Se, Si, Sm, Sn, Sr, Ta, Tb, Te, Ti, Tm, V,W, Y, Yb, Zn, Zr Cr_xFe_{100-x} with x varies from 0 to 100 mol% in steps of 10mol% $NM_{0,5}Ce_{19,8}Ti_{49,8}Cr_{29,8}$, $NM_{0,5}Ce_{20}Ti_{49,5}Cr_{30}$, with NM = Ag, Au, Ir, Pd, Pt, Re, Rh, Ru
12	Library 11 is synthesised again and named as library 12
13	$E_{100-x-y-z}Ce_xTi_yCr_z$ with x = 32,3, 31,6, 31, 31,3; y = 32,3, 31,6, 31, 31,3; z = 32,3, 31,6, 31, 31,3; E = Hf, In, Sc and V $NM_1Ce_{19,7}Ti_{49,7}Cr_{29,7}$, $NM_1Ce_{20}Ti_{49}Cr_{30}$, $NM_{0,5}Ce_{33,13}Ti_{33,13}Cr_{33,13}$, $NM_1Ce_{33}Ti_{33}Cr_{33}$, with NM = Ag, Au, Ir, Pd, Pt, Re, Rh, Ru $D_3Ce_{19}Ti_{49}Cr_{29}$ with D = Al, B, Ba, Bi, Ca, Cd, Cr, Cs, Cu, Dy, Er, Eu, Fe, Ga, Gd, Ge, Hf, Ho, In, K, La, Li, Lu, Mg, Mn, Mo, Na, Nb, Nd, Rb, Sb, Sc, Se, Si, Sm, Sn, Sr, Ta, Tb, Te, Ti, Tm, V,W, Y, Yb, Zn, Zr $Ce_{50}Cr_{50}$, K_3Ce_{97}, Al_3Ce_{97}, $Ce_{10}La_5Co_{85}$, La_3Co_{97}, $Cu_3Cs_{20}Co_{77}$, $Ce_{40}Ag_{60}$, $K_{25}Ce_{75}$ and $Cs_{20}Co_{80}$

Table 2-12 Catalyst compositions of libraries prepared for HT screening in fourth generation

a) C_3H_8 oxidation

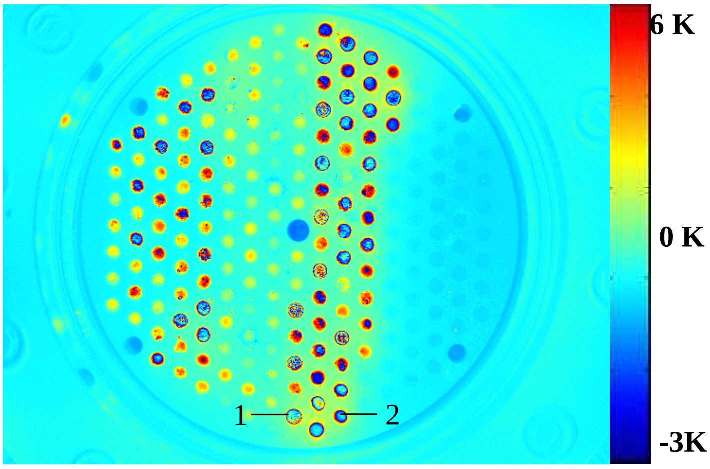

b) CO oxidation

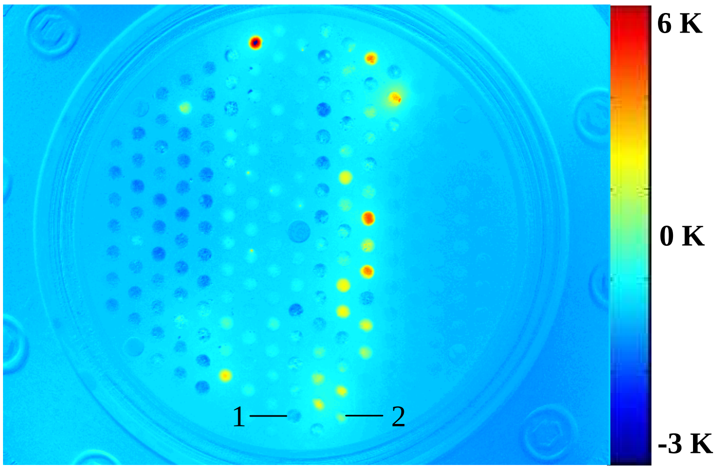

c) Background image after C_3H_8 oxidation

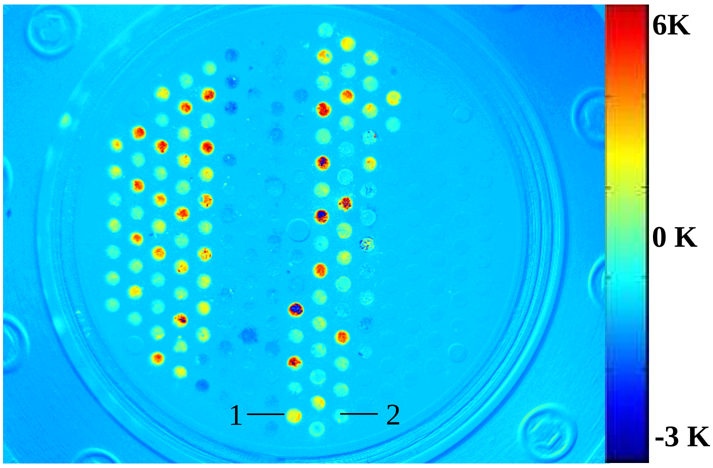

Figure 2-18: Emissivity corrected infrared thermography image of library 11 at 350°C. Reaction conditions (a): $C_3H_8/CO_2/O_2/N_2$ = 4/15,8/10/70,2 vol%. (b) $CO/CO_2/O_2/N_2$ = 5,45/15,8/10/68,75 vol%. (c) $CO_2/O_2/N_2$ = 15,8/10/74,2vol%. 1:$Ce_{19}Ti_{49}Cr_{29}Sc_3$; 2 :$Ce_{20}$ $Ti_{49,5}Cr_{30}Pd_{0,5}$.

Further doping of about 3 mol% of 47 transition elements with $Ce_{10}Ti_{80}Cr_{10}$ and $Cr_{90}Fe_{10}$ were considered followed by binary composition spreads of the CrFe catalyst and named library 11. This library 11 was prepared twice and named as library 12 due to the wrong calcination programming of 32 hours instead of 5 hours. This generation also includes $Ce_{33,3}Ti_{33,3}Cr_{33,3}$ catalysts doped with precious metals of about 0,5 and 1 mol% and 8 metals along with 9 different catalysts from another project. Thus three libraries 11, 12 and 13 are considered as fourth generation. Libraries and compositions are mentioned in the corresponding table 2-12.

All three libraries prepared have undergone primary screening using IR camera. IR image of library 11 is shown in figure 2-18.

Best catalysts from library 11-13 are summarised in tables 2-13 to 2-15. Conventional testing was performed on the 33 best materials. Figure 2.15 illustrates the performance of the best catalyst found on these libraries.

a) Library 11

Composition	**Temp °C (Reaction)**	**ΔT_{C3H8}°C (Reaction)**	**ΔT_{C3H8}°C (Background)**	**Difference °C**	**ΔT_{CO}°C (Reaction)**
$Ce_{20}Ti_{49,5}Cr_{30}Ag_{0,5}$	250	7,15	4,54	2,61	0,26
Fe_{100}	250	6,91	3,23	3,68	-0,42
$Ce_{19}Ti_{49}Cr_{29}Sc_3$	250	6,52	3,57	2,95	0,07
$Ce_{17}Ti_{47}Cr_{27}Hf_9$	250	4,44	1,91	2,53	0,13
$Ce_{18,3}Ti_{48,3}Cr_{28,3}Hf_5$	250	4,28	1,70	2,68	0,29
$Ce_{19}Ti_{49}Cr_{29}V_3$	350	14,44	4,89	9,54	-0,61
$Ce_{17,7}Ti_{47,7}Cr_{27,7}V_7$	350	10,36	3,25	7,10	0,01
$Ce_{19,8}Ti_{49,8}Cr_{29,8}Pt_{0,5}$	350	6,41	0,49	5,92	-0,09
$Cr_{10}Fe_{90}$	350	6,34	1,26	5,08	-0,25
$Ce_{20}Ti_{49,5}Cr_{30}Pd_{0,5}$	350	5,01	0,5	4,51	0,38

Table 2-13 **Selected catalysts for conventional verification based on temperature evaluation techniques of library 11**

b) Library 12

Composition	**Temp °C (Reaction)**	**ΔT_{C3H8}°C (Reaction)**	**ΔT_{C3H8}°C (Background)**	**Difference °C**	**ΔT_{CO}°C (Reaction)**
$Ce_9Ti_{79}Cr_9Bi_3$	350	11,41	4,86	6,54	-0,12
$Ce_9Ti_{79}Cr_9Mo_3$	350	10,67	4,45	6,22	0,19
$Ce_9Ti_{79}Cr_9Ca_3$	350	9,55	3,40	6,16	0,17
$Ce_9Ti_{79}Cr_9Al_3$	350	8,94	3,23	5,71	0,40
$Ce_9Ti_{79}Cr_9Mg_3$	350	8,77	3,64	5,12	0,13
$Ce_{19}Ti_{49}Cr_{29}W_3$	250	5,86	1,52	4,34	-0,27
$Ce_{19,8}Ti_{49,8}Cr_{29,8}Ru_{0,05}$	350	6,09	0,97	5,12	1,82
$Ce_{20}Ti_{49,5}Cr_{30}Pt_{0,5}$	350	6,84	5,21	1,62	-8,35
$Ce_{18,3}Ti_{48,3}Cr_{28,3}Sc_5$	250	5,55	2,68	2,87	0,66
$Ce_{17,7}Ti_{47,7}Cr_{27,7}Sc_7$	250	5,24	2,50	2,75	0,43

Table 2-14 **Selected catalysts for conventional verification based on temperature evaluation techniques of library 12**

c) Library 13

Composition	**Temp °C (Reaction)**	**ΔT_{C3H8}°C (Reaction)**	**ΔT_{C3H8}°C (Background)**	**Difference °C**	**ΔT_{CO}°C (Reaction)**
$Ce_{19}Ti_{49}Cr_{29}Si_3$	350	18,5	8,70	9,80	-1,22
$Ce_{19}Ti_{49}Cr_{29}Tm_3$	350	9,57	4,11	5,46	-0,68
$Ce_{19}Ti_{49}Cr_{29}Hf_3$	250	7,19	5,12	2,08	0,05
$Ce_{31}Ti_{31}Cr_{31}Hf_7$	250	6,44	3,56	2,88	-0,14
$Ce_{19}Ti_{49}Cr_{29}Gd_3$	250	6,37	3,77	2,60	0,06
$Ce_{19}Ti_{49}Cr_{29}Zn_3$	250	6,10	3,48	2,61	0,01
$Ce_{31,6}Ti_{31,6}Cr_{31,6}V_5$	350	7,30	2,01	5,29	-0,05
$Ce_{31,6}Ti_{31,6}Cr_{31,6}In_5$	350	4,14	1,50	2,64	0,22
$Ce_{31}Ti_{31}Cr_{31}Sc_7$	350	6,48	2,04	4,44	-0,01
$Ce_{50}Cr_{50}$	350	6,58	0,79	5,78	0,11
K_3Ce_{97}	350	7,69	1,52	6,17	-1,33
$K_{25}Ce_{75}$	350	3,96	0,66	3,30	-0,69

Table 2-15 **Selected catalysts for conventional verification based on temperature evaluation techniques of library 13**

2.13 Conventional testing of fourth generation hits

a) Library 11 hits

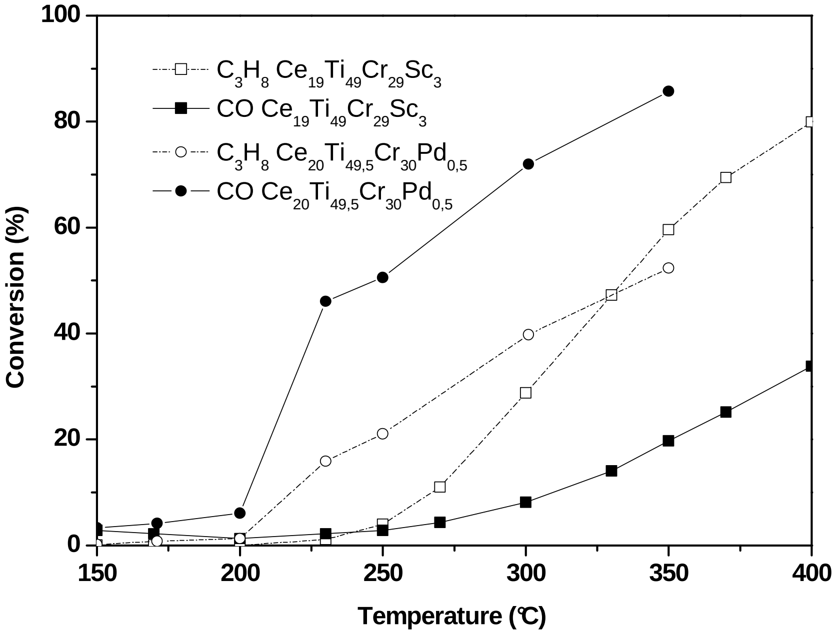

b) Library 12 hits

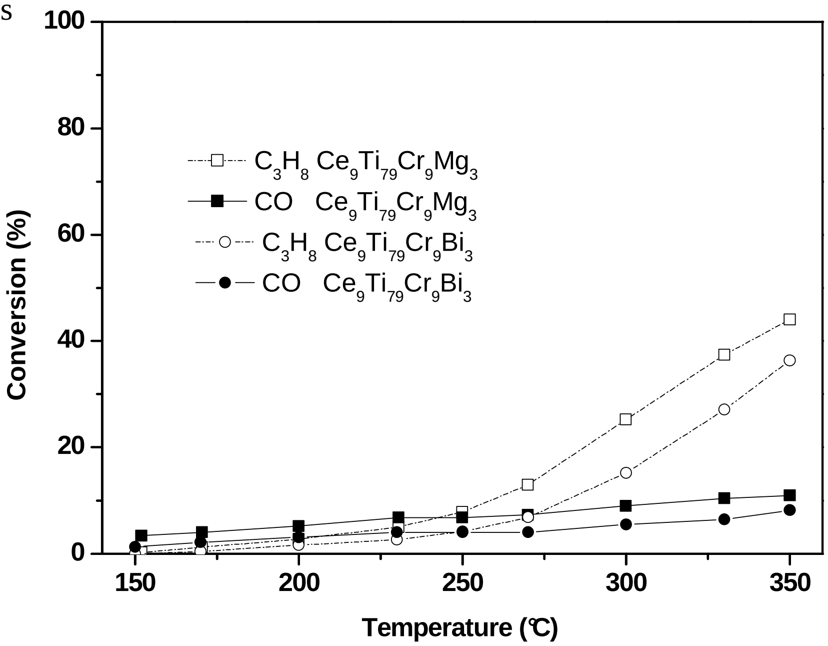

c) Library 13 hits

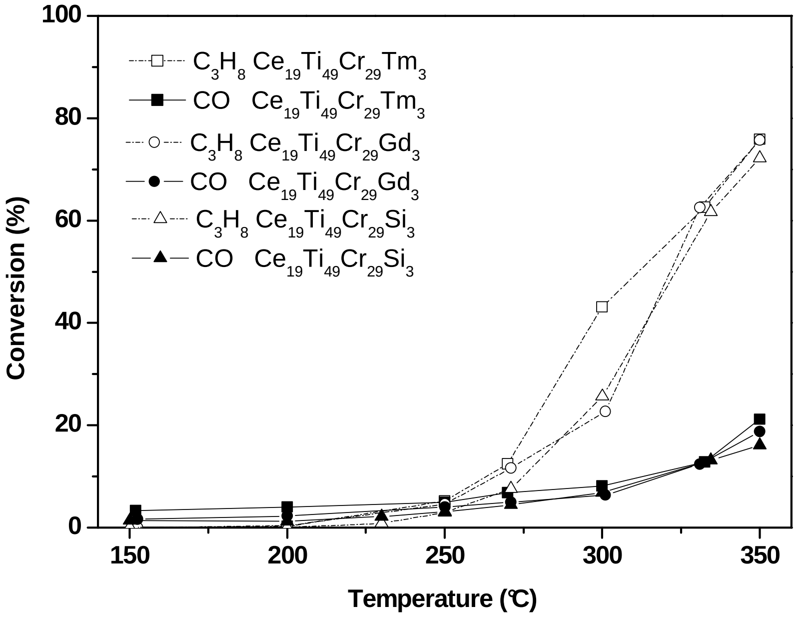

Figure 2-19: **Conventional test results of selected catalysts of 4th generation hits with reaction in increment order of temperatures from 150°c to 350°C. Reaction conditions: 20mg of catalyst diluted with 100mg of γ-alumina with particle size of 100 – 200 µm (both). Total flow rate: 50ml/min ($C_3H_8/CO/CO_2/O_2/N_2$ = 2/10,9/15,8/10/61,3). Catalyst pre-treatment: synthetic air with 50ml/min at 350°C for 1h.**

From figure 2-19a, it can be seen, that the presence of noble metal (Pd) of about 0,5% drastically reduces the selectivity of C_3H_8 oxidation favouring CO oxidation. This was actually the case with all noble metal containing catalysts. It was found that $Ce_{19}Ti_{49}Cr_{29}Sc_3$ is the best catalyst of this library which shows propane conversion of about 80% but only at 400°C. Even though high heat of reaction measured in IR screening of libraries 12 and 13 with noble metal filled catalysts, they were not selected as potential hits for conventional verification due to high CO oxidation activities. From figure 2.19b, it can be seen Mg and Bi doped catalysts of library 12 show high selectivities but activities are still lower when compared to $Ce_{20}Ti_{50}Cr_{30}$ or $Ce_{19}Ti_{49}Cr_{29}Sc_3$ catalysts. Tm, Gd and Si doped CeTiCr catalyst of library 13 were the best performing catalysts of this generation. Activities are in the order of Tm > Gd > Si as shown in figure 2.19c. This data show that there is a tremendous improvement especially in the selectivity of the 4th generation catalysts. It proves that high throughput technology and combinatorial techniques are valuable tool, for catalyst fine tuning. Catalysts developed during the fourth generation can be further finely optimised by fifth generation screening. But prior to this last generation development some detailed studies on the effect of feed gases, calcination temperatures, surface areas, XRD and the effect of individual elements on propane activity were conducted. It was essential to get a broader understanding of the data before the final optimisation.

2.14 Effect of $Ce_{19}Ti_{49}Cr_{29}Sc_3$ catalyst

2.14.1 Reproducibility of the catalyst

Reproducibility is one of the important factors to re-check the activity of the same catalyst and also act as a step stone to upscale the catalyst in larger amounts followed by characterisation and mechanistic studies. Initially $Ce_{19}Ti_{49}Cr_{29}Sc_3$ was checked once again with the conventional set up and results are compared. It was found that the results were reproducible shown in figure 2-20. The CO conversion was even lower indicating that there may be further improvements by optimisation of the catalyst synthesis.

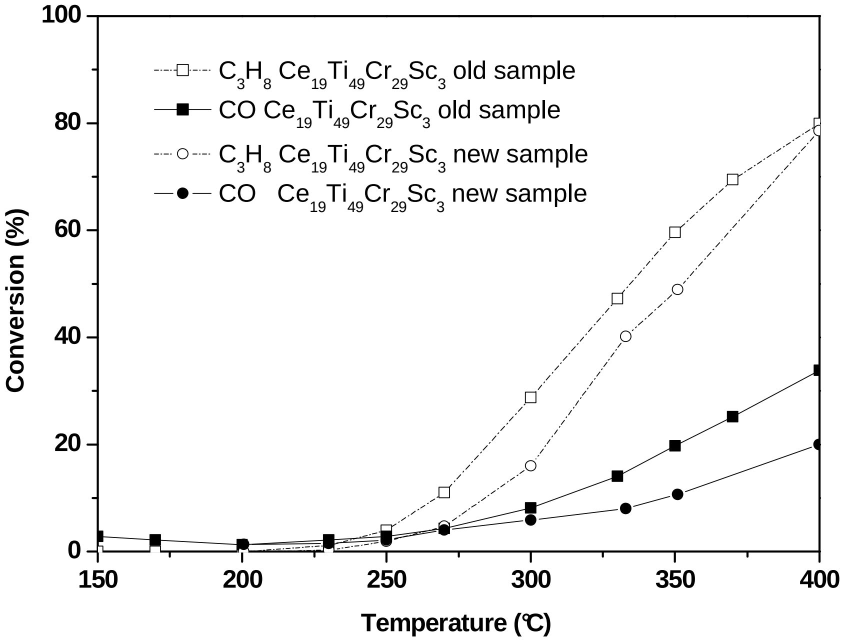

Figure 2-20: Reproducibility of $Ce_{19}Ti_{49}Cr_{29}Sc_3$ catalysts with reaction in increment order of temperatures from 150°C to 350°C. Reaction conditions: 20mg of catalyst diluted with 100mg of γ-alumina with particle size of 100-200 µm (both). Total flow rate: 50ml/min ($C_3H_8/CO/CO_2/O_2/N_2$ = 2/10,9/15,8/10/61,3). Catalyst pre-treatment: synthetic air with 50ml/min at 350°C for 1h.

2.14.2 Up scaling of the $Ce_{19}Ti_{49}Cr_{29}Sc_3$ catalyst

The reproducible catalyst $Ce_{19}Ti_{49}Cr_{29}Sc_3$ was upscaled from 8 Mmoles to 130 Mmoles twice to get approximately 20g catalyst. The two set of catalysts were prepared based on the propionic acid route method [147]. The preparation method is explained in section 3.3. The two samples prepared are named sample 1 and sample 2, performance of both samples are shown in figure 2-21.

It can be seen that the bulk samples 1 and 2 are performing well when compared to that of original catalyst (see figure 2-20). The performance of sample 1 is slightly better than that of sample 2, but both samples are less active than the original catalyst. Thus it can be concluded that the catalyst can be upscaled, but the variation in performance is an indication of high sensitivity on preparation conditions. This also indicates that there might be potential for further improvements by variation of synthesis.

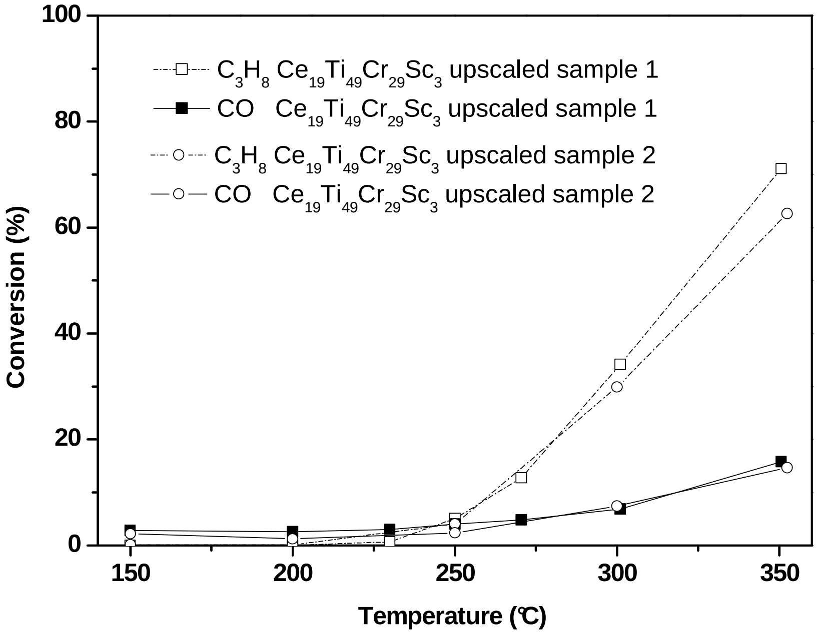

Figure 2-21: Up scaling of $Ce_{19}Ti_{49}Cr_{29}Sc_3$ catalysts with reaction in increment order of temperatures from 150°C to 350°C. Reaction conditions: 20mg of catalyst diluted with 100mg of γ-alumina with particle size of 100-200 µm (both). Total flow rate: 50ml/min ($C_3H_8/CO/CO_2/O_2/N_2$ = 2/10,9/15,8/10/61,3). Catalyst pre-treatment: synthetic air with 50ml/min at 350°C for 1h.

2.15 Performance of the effect of feed gas compositions on the $Ce_{19}Ti_{49}Cr_{29}Sc_3$ catalyst (upscaled sample 1)

2.15.1 Absence of CO_2 in the feed

The first study considered is the effect of CO_2 in the feed. For this feed gases flow through the conventional flow reactor in the absence of CO_2 balanced by N_2. It was found that the conversion is more or less the same at the highest operating temperature of about 350°C. At 300°C, conversion of propane in the presence and absence of CO_2 were about 34,2% and 19,9% as illustrated in figure 2-22. Thus the presence of CO_2 in the feed reduces the active temperature of C_3H_8 oxidation.

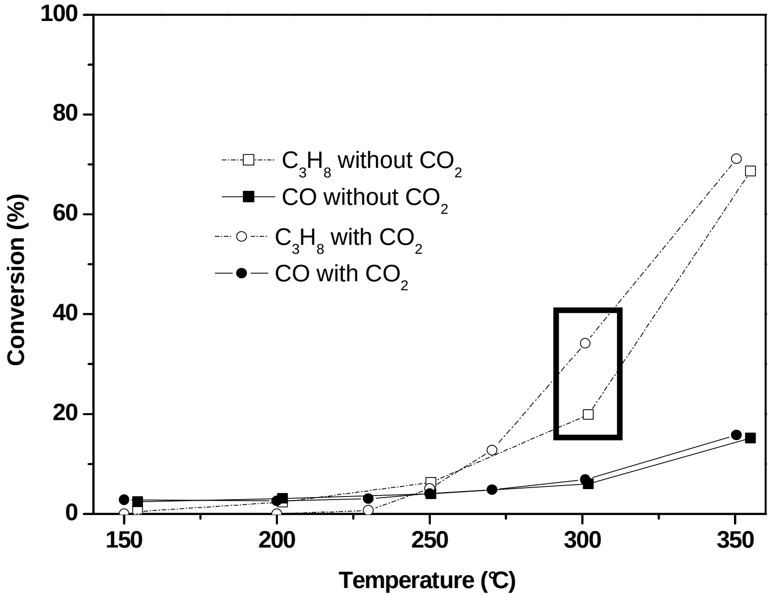

Figure 2-22: Effect of CO_2 in the feed over $Ce_{19}Ti_{49}Cr_{29}Sc_3$ catalyst (upscaled sample 1) with reaction in increment order of temperatures from 150°C to 350°C. Reaction conditions: 20mg of catalyst diluted with 100mg of γ-alumina with particle size of 100 – 200 µm (both). Total flow rate: 50ml/min ($C_3H_8/CO/O_2/N_2$ = 2/10,9/10/77,1). Catalyst pre-treatment: synthetic air with 50ml/min at 350°C for 1h.

2.15.2 Absence of CO in the feed

It is interesting to see the effect, if the feed is fed in the absence of CO as shown in figure 2-23. It is inferred that C_3H_8 conversion is achieved about 72% in the absence of CO in feed and was about 71% in the presence of CO at 350°C indicating that CO does not affect C_3H_8 conversion. It was found that there is CO formation in the product about 0,7 vol% at 350°C. But it is not known, if the CO formed in the product is due to the partial oxidation of C_3H_8 or CO_2 reduction with C_3H_8.

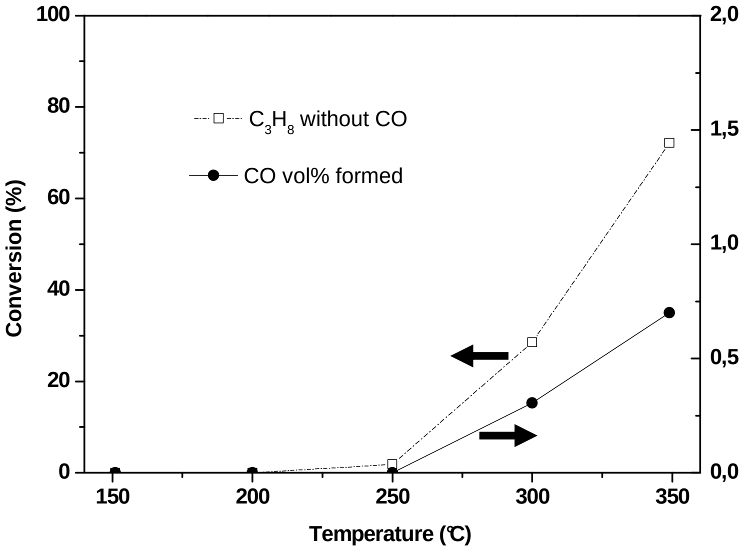

Figure 2-23: **Effect of the absence of CO in the feed over $Ce_{19}Ti_{49}Cr_{29}Sc_3$ catalyst with reaction in increment order of temperatures from 150°C to 350°C. Reaction conditions: 20mg of catalyst diluted with 100mg of γ-alumina with particle size of 100-200 µm (both). Total flow rate: 50ml/min ($C_3H_8/CO_2/O_2/N_2$ = 2/15,8/10/72,2). Catalyst pre-treatment: synthetic air with 50ml/min at 350°C for 1h.**

2.15.3 Absence of C_3H_8 in the feed

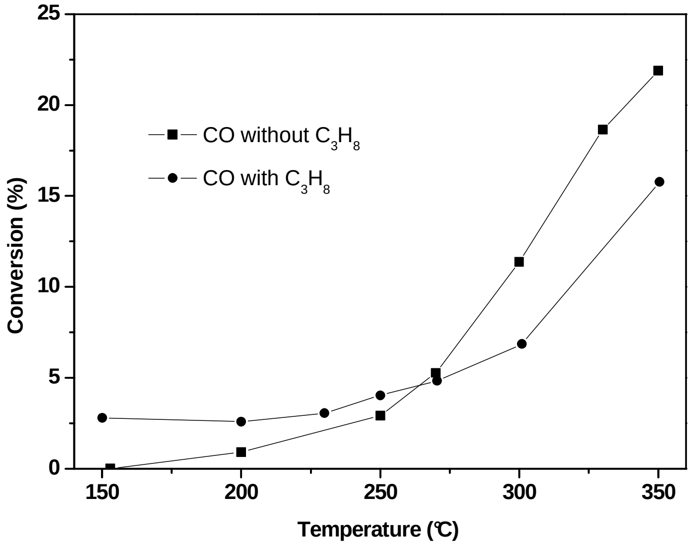

Figure 2-24: **Effect of the absence of C_3H_8 in the feed over $Ce_{19}Ti_{49}Cr_{29}Sc_3$ catalyst with reaction in increment order of temperatures from 150°C to 350°C. Reaction conditions: 20mg of catalyst diluted with 100mg of γ-alumina with particle size of 100-200 µm (both). Total flow rate: 50ml/min ($C_3H_8/CO_2/O_2/N_2$ = 2/15,8/10/72,2). Catalyst pre-treatment: synthetic air with 50ml/min at 350°C for 1h.**

Another experiment is carried out in the absence of C_3H_8 in the feed to see the effect of CO oxidation over the catalyst as plotted in figure 2-24. It is envisaged that CO conversion was 21,9% in the absence of C_3H_8 and 15,8% in presence of C_3H_8 in feed at 350°C. The presence of propane in the feed blocks the active sites for CO and preferentially oxidised by the catalyst. Thus the catalyst is not a solo oxidation catalyst and acts as a preferential oxidation catalyst.

2.15.4 Effect of O_2 concentration in the feed

Another important experimental study considered is the effect of O_2 content in the feed. Two set of oxygen concentrations have been chosen in comparison with our standard concentration of 10 vol% in the feed gas. One is of low feed O_2 concentration with 5 vol% and another with higher concentration of about 15 vol%. Results are plotted in figure 2-25. When the O_2 concentration is reduced to half, then C_3H_8 conversion is also reduced to half from 71,1% to 35,1%. Similarly, increase in O_2 content to 15% increases the propane conversion and reaches a maximum conversion of about 97% with the expense of selectivity at 350°C. Thus there is a first order dependence of C_3H_8 conversion on oxygen concentration, while there is no clear dependence of CO oxidation on conversion.

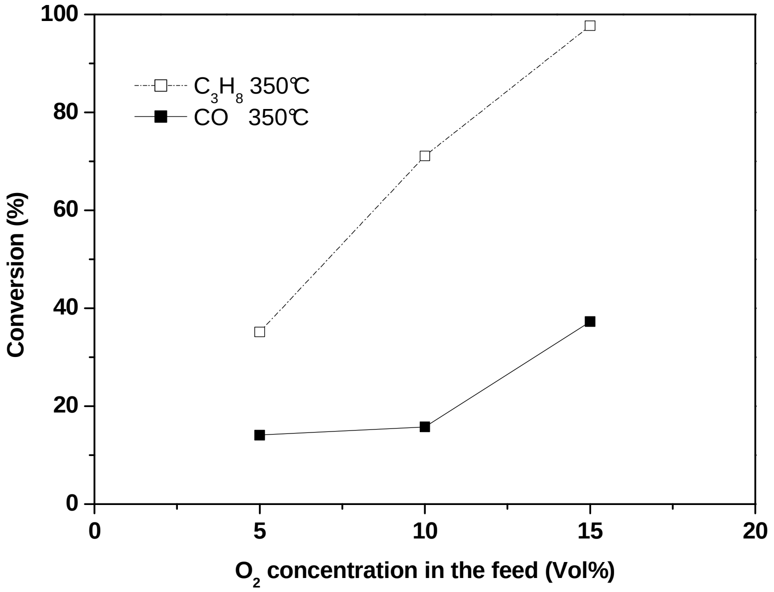

Figure 2-25: Effect of O_2 concentration in feed over $Ce_{19}Ti_{49}Cr_{29}Sc_3$ catalyst with 5, 10 and 15 vol% O_2 concentration in the feed with reaction in increment order of temperatures from 150°C to 350°C. Reaction conditions: 20mg of catalyst diluted with 100mg of γ-alumina with particle size of 100 – 200 µm (both). Total flow rate: 50ml/min. Catalyst pre-treatment: synthetic air with 50ml/min at 350°C for 1h.

2.16 Effect of Ce, Ti and Cr elements on the catalytic activity of $Ce_{20}Ti_{50}Cr_{30}$ catalyst

In order to gain insight into the nature of the catalytic contributions of the three metal ions in $Ce_{20}Ti_{50}Cr_{30}$, the individual oxides Ce_{100}, Ti_{100} and Cr_{100} and binary spreads of all combinations based on the ratios of ternary material prepared as $Ce_{28,6}Ti_{71,4}$, $Ce_{40}Cr_{60}$ and $Ti_{62,5}Cr_{37,5}$ were also investigated. All six catalyst preparations follow the same sol-gel recipe used for the $Ce_{20}Ti_{50}Cr_{30}$ catalyst. The surface areas and activity at 350°C of all 6 catalysts were tabulated in table 2-16.

No.	**Catalysts**	**Conversion at 350°C (%)**		**Surface area (m^2/g)**
		C_3H_8	**CO**	
1	Ce_{100}	27	22	153
2	Ti_{100}	2	8	14
3	Cr_{100}	9	4	17
4	Ti^{IP}_{100}	0	4	33
5	Ti^{*}_{100}	0,6	5	5
6	Cr^{*}_{100}	60	61	255
7	$Ce_{28,6}Ti_{71,4}$	0,2	4	165
8	$Ce_{40}Cr_{60}$	43	20	101
9	$Ti_{62,5}Cr_{37,5}$	42	0	233
10	$Ce_{20}Ti_{50}Cr_{30}$	66	26	238

Table 2-16 Surface areas and activity at 350°C of monoxides and binary oxides of $Ce_{20}Ti_{50}Cr_{30}$ catalyst

* – catalysts calcined at 250°C instead of 400°C and Ti dissolved in iso-propanol.

IP – Ti dissolved in iso-propanol instead of methanol and nitric acid.

2.16.1 Effect of pure Ce, Ti and Cr elements

Initially effect of Ce_{100}, Ti_{100} and Cr_{100} were studied in the conventional flow reactor. The effects are plotted in figure 2-26. Ce_{100} is slightly active and unselective with propane and CO conversions of 28% and 22%. At low temperature there is a slight preference to CO oxidation and at 350°C propane conversion is slightly higher. Ti_{100} is inactive for propane oxidation even

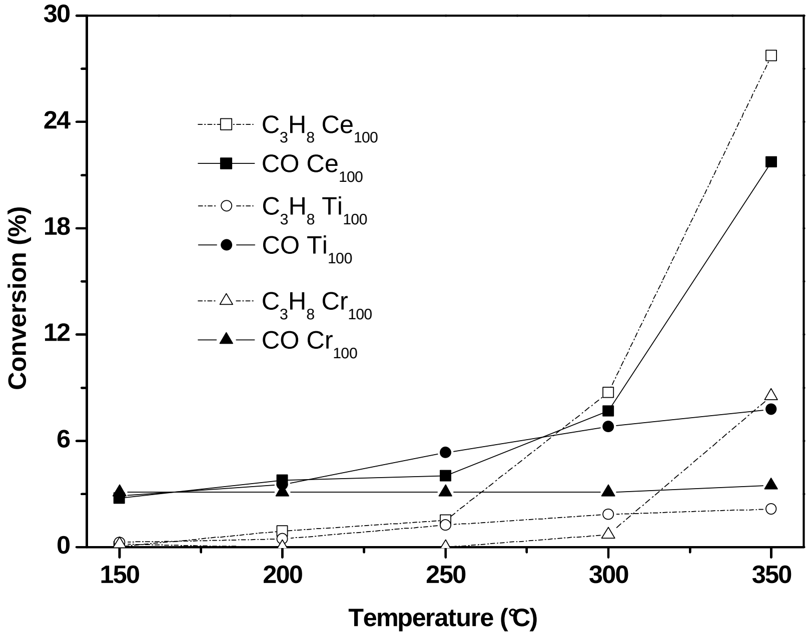

Figure 2-26: **Effect of Ce_{100}, Ti_{100} and Cr_{100} catalysts with reaction in increment order of temperatures from 150°C to 350°C. Reaction conditions: 20mg of catalyst diluted with 100mg of γ-alumina with particle size of 100-200 µm (both). Total flow rate: 50ml/min ($C_3H_8/CO/CO_2/O_2/N_2$ = 2/10,9/15,8/10/61,3). Catalyst pre-treatment: synthetic air with 50ml/min at 350°C for 1h.**

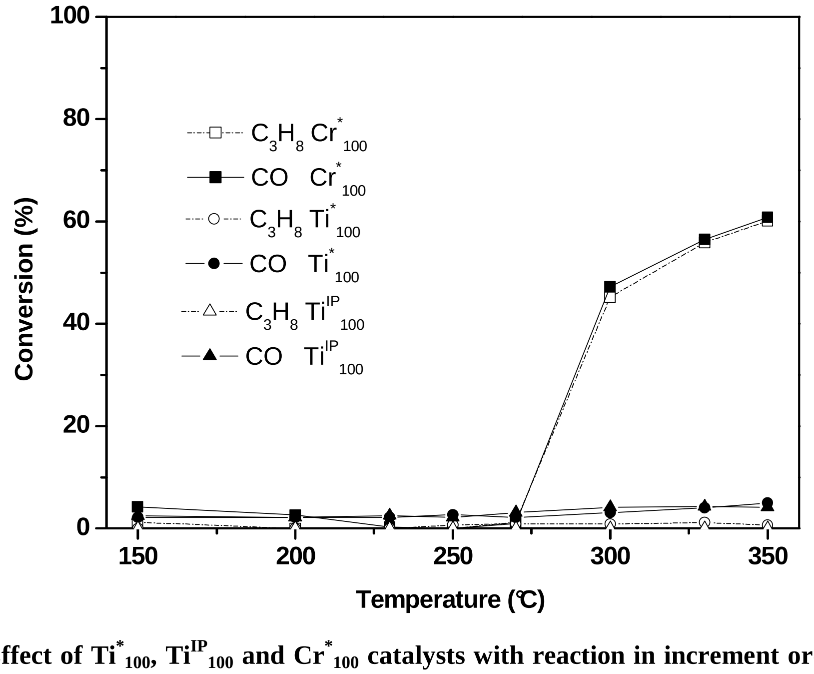

Figure 2-27: **Effect of Ti^*_{100}, Ti^{IP}_{100} and Cr^*_{100} catalysts with reaction in increment order of temperatures from 150°C to 350°C. Reaction conditions: 20mg of catalyst diluted with 100mg of γ-alumina with particle size of 100-200 µm (catalyst) and 200-500 µm (γ-alumina). Total flow rate: 50ml/min ($C_3H_8/CO/CO_2/O_2/N_2$ = 2/10,9/15,8/10/61,3). Catalyst pre-treatment: synthetic air with 50ml/min at 350°C for 1h.**

at higher temperatures, but it only converts CO. Cr_{100} is slightly active showing propane conversion of 10% at 350°C and indicating the origin of the hydrocarbon selectivity. On the other hand, the surface areas of Ti_{100} and Cr_{100} are very small and not comparable with the other oxides. Hence it is worthwhile to improve the surface areas of both Cr and Ti monoxides. One alternative for Ti_{100} preparation was dissolving the titanium precursors in iso-propanol instead of methanol and nitric acid. The surface area increased but it is still smaller compared to the other oxides and it remained completely inactive towards propane oxidation as shown in figure 2-27. Another possibility could be the reduction of calcination temperatures from 400°C to 250°C. Again Cr_{100} and Ti_{100} were prepared by dissolving Ti precursor in iso-propanol and Cr as like conventional method (methanol as solvent), dried and calcined at 250°C. The surface areas are tabulated in table 2-16 and conventional test results of these catalysts are shown in figure 2-27.

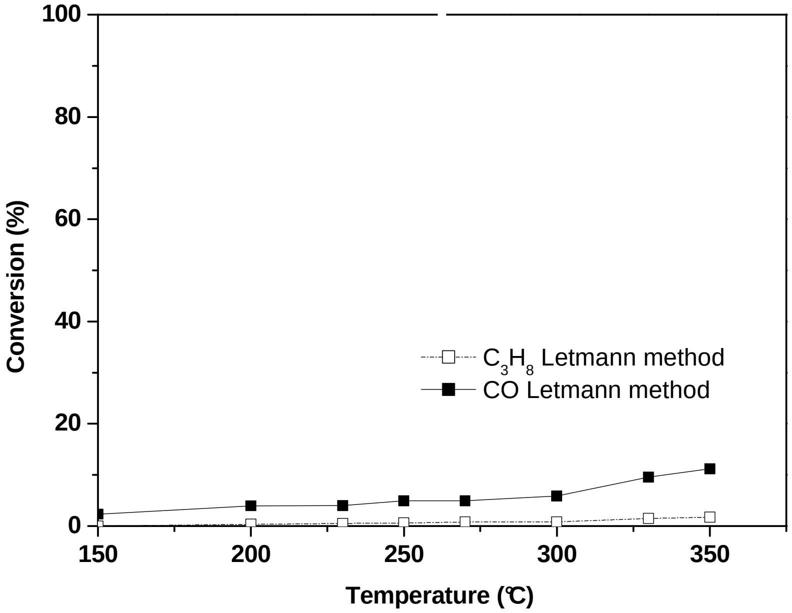

Figure 2-28: **Effect of Ti_{100} catalyst (Letmann method) with reaction in increment order of temperatures from 150°C to 350°C. Reaction conditions: 20mg of catalyst diluted with 100mg of γ-alumina with particle size of 100-200 µm (catalyst) and 200-500 µm (γ-alumina). Total flow rate: 50ml/min ($C_3H_8/CO/CO_2/O_2/N_2$ = 2/10,9/15,8/10/61,3). Catalyst pre-treatment: synthetic air with 50ml/min at 350°C for 1h.**

The performance of the Cr^*_{100} with a very high surface area provides that both reactions are competing each other and achieves conversion of 60% both and leads the catalyst is completely unselective. Similarly both Ti^*_{100} and Ti^{IP}_{100} were completely inactive for propane oxidation. While looking for the surface areas of all three samples, still Ti^*_{100}, Ti^{IP}_{100} is not comparable and

Cr^*_{100} is comparatively higher. Hence it is advisable to adopt new methods for Ti_{100} catalyst preparation. Additional two methods were selected, from Jens Klein et.al. [145] and Letmann et.al. [146]. The method of synthesis is explained in section 3.4. The performance of Ti_{100} (Letmann method) is shown in figure 2-28. The surface areas of Ti prepared by Letmann et.al was found to be 62,5 m^2/g and the sample prepared by the method of Jens Klein et. al cannot be determined. Though surface areas were not identical with the Cr_{100} sample but there is the desired increase in surface area. Conventional verification shows that the Ti_{100} prepared by the Letmann method is completely selective towards CO oxidation and achieves an activity of about 11%, while the other material was completely inactive for both oxidations.

2.16.2 Effect of the binary oxides of the $Ce_{20}Ti_{50}Cr_{30}$ catalyst

The associated binary oxides $Ce_{28,6}Ti_{71,4}$, $Ce_{40}Cr_{60}$ and $Ti_{62,5}Cr_{37,5}$ of $Ce_{20}Ti_{50}Cr_{30}$ have been prepared and studied. The effects are shown in figure 2-29. It seems that CeTi is completely inactive. CeCr is active and reaches conversion of 43% with a selectivity of 68%. The best one is TiCr which is active with a propane conversion of 43% and completely selective. The surface areas of binary oxides are mentioned in the table 2-16.

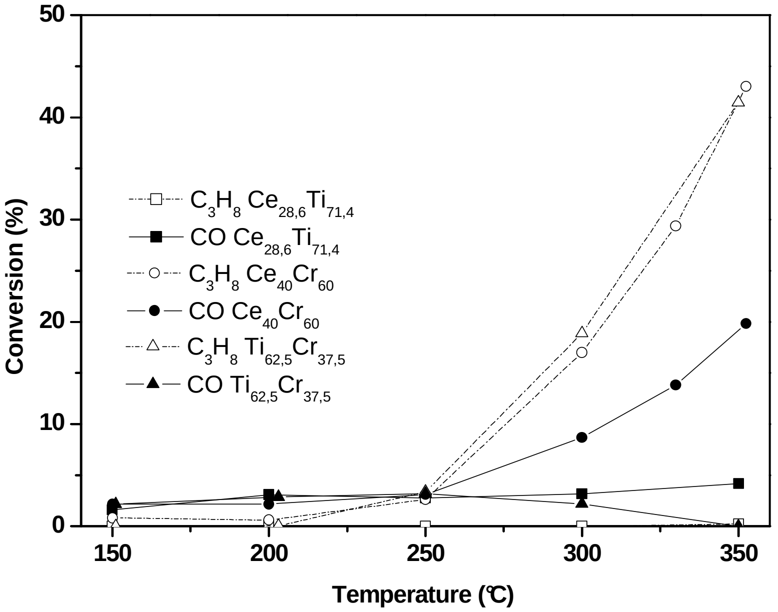

Figure 2-29: Effect of $Ce_{28,6}Ti_{71,4}$, $Ce_{40}Cr_{60}$ and $Ti_{62,5}Cr_{37,5}$ catalysts with reaction in increment order of temperatures from 150°C to 350°C. Reaction conditions: 20mg of catalyst diluted with 100mg of γ-alumina with particle size of 100-200 µm (both). Total flow rate: 50ml/min ($C_3H_8/CO/CO_2/O_2/N_2$ = 2/10,9/15,8/10/61,3). Catalyst pre-treatment: synthetic air with 50ml/min at 350°C for 1h.

Therefore the addition of Ce in the TiCr catalyst increases the catalytic oxidation of propane, apparently at the expense of selectivity. The activity increase by the addition of Ce attributes probably to its oxygen storage capacity [147]. Since Ce_{100} is not selective, there must be some unknown cooperative effect of Ti and Ce to reach this high selectivity. Hence at this stage it can be concluded that Ti and Cr are important elements for selective propane oxidation.

2.17 Improvement of the $Ce_{20}Ti_{50}Cr_{30}$ catalyst

Before entering into the optimisation routine for next generation catalyst development, $Ce_{20}Ti_{50}Cr_{30}$ catalyst was studied in detail for further improvements by the effect of pre-treatment, long term stability, effect of higher temperature calcination, optimum calcination temperatures, best synthesis methods and external mass transport limitations.

2.17.1 Effect of pre-treatment

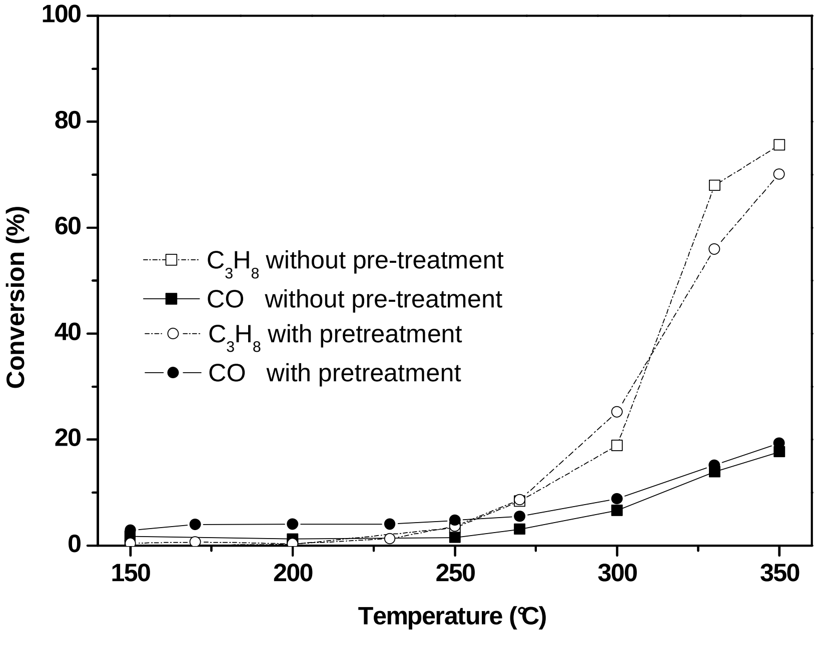

Figure 2-30: Effect of pre-treatment on $Ce_{20}Ti_{50}Cr_{30}$ catalyst with reaction in increment order of temperatures from 150°C to 350°C. Reaction conditions: 20mg of catalyst diluted with 100mg of γ-alumina with particle size of 100-200 µm (both). Total flow rate: 50ml/min ($C_3H_8/CO/CO_2/O_2/N_2$ = 2/10,9/15,8/10/61,3). Catalyst pre-treatment: synthetic air with 50ml/min at 350°C for 1h.

The pre-treatment is a technique to activate the catalyst before the reaction starts. This is done for all experiments by passing synthetic air at a flow rate of 50 ml/min for 1h through the reactor filled with the catalyst. The temperature at the catalyst bed was maintained at 350°C. This study is investigated for the importance of pre-treatment techniques using synthetic air. Comparison of performances with and without pre-treatment is presented in figure 2-30. It shows that there is no drastic improvement in activity and selectivity of the catalyst by pre treatment.

2.17.2 Effect of long term stability measurement

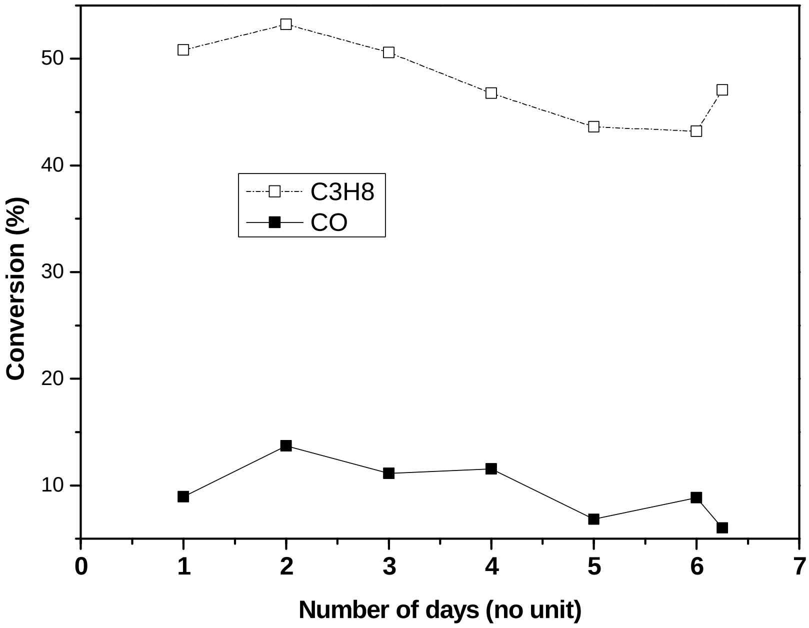

Figure 2-31: Effect of long term stability measurement on the $Ce_{20}Ti_{50}Cr_{30}$ catalyst at 350°C. Reaction conditions: 20mg of catalyst diluted with 100mg of γ-alumina with particle size of 100-200 µm (both). Total flow rate: 50ml/min ($C_3H_8/CO/CO_2/O_2/N_2$ = 2/10,9/15,8/10/61,3). Catalyst pre-treatment: synthetic air with 50ml/min at 350°C for 1h.

The life time of the catalyst is one of the important factors. The catalyst performance profile is shown in figure 2-31. The catalyst stability was tested under reaction conditions at 350°C for about 6,5 days. It shows that the catalyst is completely stable at an average propane conversion of approximately 45% throughout the complete week.

2.17.3 Effect of higher calcination temperature

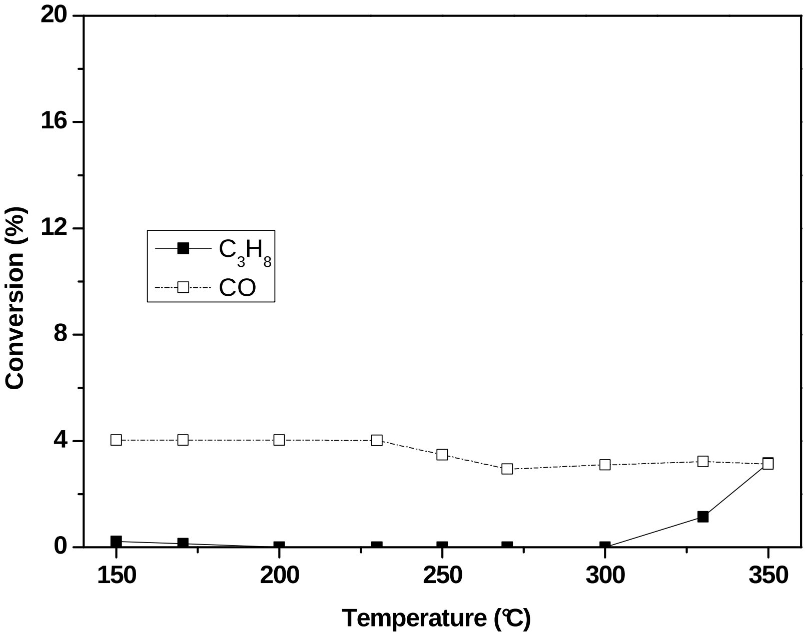

Figure 2-32: **Effect of higher calcination temperature (700°C) over $Ce_{20}Ti_{50}Cr_{30}$ catalyst on the reactivity with reaction in increment order of temperatures from 150°C to 350°C. Reaction conditions: 20mg of catalyst diluted with 100mg of γ-alumina with particle size of 100-200 µm (both). Total flow rate: 50ml/min ($C_3H_8/CO/CO_2/O_2/N_2$ = 2/10,9/15,8/10/61,3). Catalyst pre-treatment: synthetic air with 50ml/min at 350°C for 1h.**

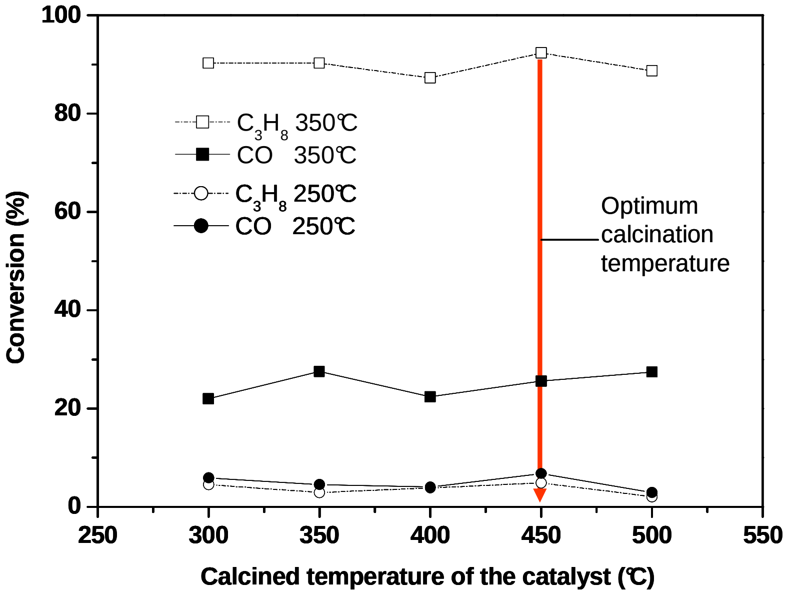

Figure 2-33: **Effect of calcination temperatures over $Ce_{20}Ti_{50}Cr_{30}$ catalyst on the reactivity with reaction at 250°C and 350°C. Reaction conditions: 20mg of catalyst diluted with 100mg of γ-alumina with particle size of 100-200 µm (both). Total flow rate: 50ml/min ($C_3H_8/CO/CO_2/O_2/N_2$ = 2/10,9/15,8/10/61,3). Catalyst pre-treatment: synthetic air with 50ml/min at 350°C for 1h.**

The purpose of this study is to identify the effect of calcination temperature and to find an optimum calcination temperature for catalyst synthesis. $Ce_{20}Ti_{50}Cr_{30}$ catalyst is prepared in the same traditional way, but the calcination temperature was increased to 700°C from 400°C. Conversion profiles are shown in figure 2-32 and inferred that there is complete loss in activity of the catalyst for both oxidation reactions which could be due to increase in particle growth with increased calcination temperature.

Thus from the performance of high temperature calcined catalyst, work flows to find the optimum calcination temperature for catalyst synthesis. For this, 300, 350, 400, 450 and 500°C were chosen as calcination temperatures of $Ce_{20}Ti_{50}Cr_{30}$ catalyst and all 5 different catalysts were tested conventionally. The conventional behaviour shows there is least dependence of calcination temperature window from 300 to 500°C and suggests that catalyst calcined at 450°C is optimum with a slight improvement in activity and selectivity shown as in figure 2-33.

2.17.4 Optimisation of synthesis methods

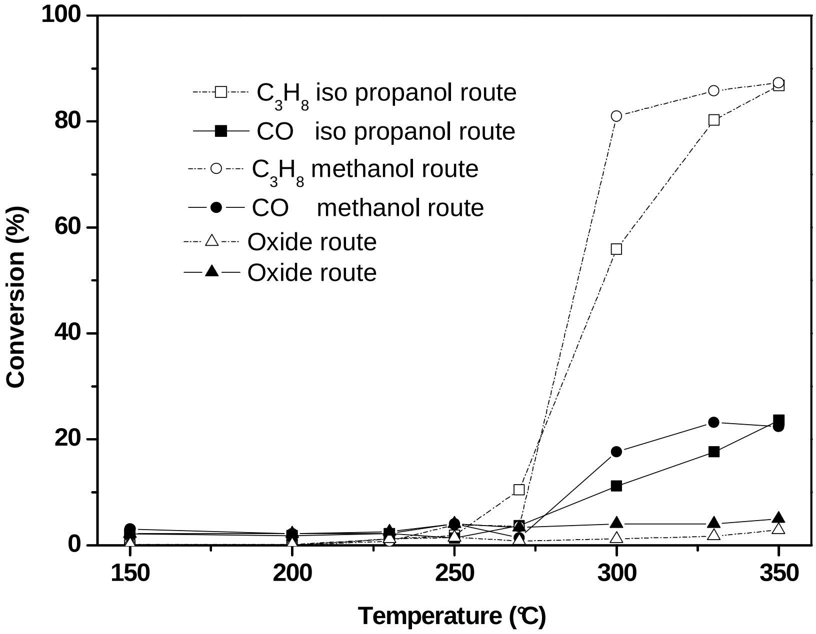

Figure 2-34: Optimisation of new synthesis methods on $Ce_{20}Ti_{50}Cr_{30}$ catalyst with reaction in increment order of temperatures from 150°C to 350°C. Reaction conditions: 20mg of catalyst diluted with 100mg of γ-alumina with particle size of 100-200 µm (both). Total flow rate: 50ml/min ($C_3H_8/CO/CO_2/O_2/N_2$ = 2/10,9/15,8/10/61,3). Catalyst pre-treatment: synthetic air with 50ml/min at 350°C for 1h.

The study focuses to improve the catalyst synthesis methods and also to find whether the synthesis can be simplified and activity can be improved. First, several commercial samples of CeO_2, TiO_2 and Cr_2O_3 were ground together in appropriate proportions in a ball mill for about 1h (oxide route). The macroscopically mixed oxides were calcined at 450°C and verified conventionally and shown in figure 2-34. It shows there is no activity at all and confirms the importance of the sol-gel approach to get mixed metal oxides. As a other method $Ce_{20}Ti_{50}Cr_{30}$ was prepared dissolving titanium iso-propoxide in iso-propanol. This method is very simple and also reduces time. The performance is comparable to that of the conventional method.

2.17.5 Effect of external film transport limitations

In other study the effect of film transport limitations of the $Ce_{20}Ti_{50}Cr_{30}$ catalyst was investigated. In this study 5 different types of flow rates were chosen as listed in the table 2-17. Each flow rate is studied as separate experiment and is plotted in the profile shown in figure 2-35 for the reaction at the temperature of 350°C. In each experiment the ratio of catalyst mass to total flow rate is kept constant to about 0,4 to have constant residence time.

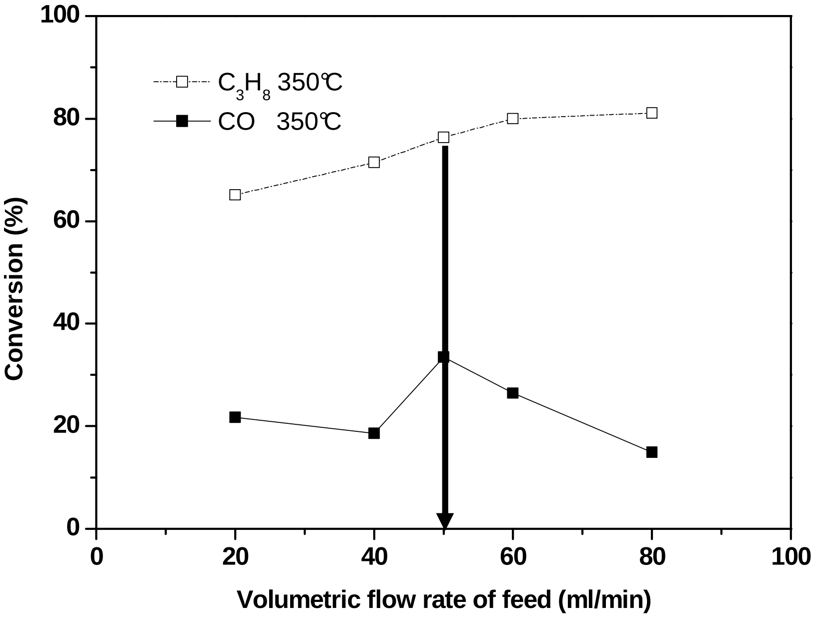

Figure 2-35: Effect of external film transport limitations on $Ce_{20}Ti_{50}Cr_{30}$ catalyst at 350°C. Feed concentration ($C_3H_8/CO/CO_2/O_2/N_2$ = 2/10,9/15,8/10/61,3). Catalyst pre-treatment: synthetic air with 50ml/min at 350°C for 1h.

Total flow rate (ml/min)	**Synthetic air flow rate (ml/min)**	**Reaction gas flow rate (ml/min)**	**Catalyst mass (mg) 100 – 200 µm**	**γ-Alumina mass (mg) 200 – 500 µm**	**Total mass (mg)**
20	10	10	8	40	48
40	20	20	16	80	96
50	25	25	20	100	120
60	30	30	24	120	144
80	40	40	32	160	192

Table 2-17 Feed flow rates, amount of catalyst and inert required for external film transport limitation study with $Ce_{20}Ti_{50}Cr_{30}$ catalyst

From the profile it is clear that, for low flow rate the conversion of propane is smaller and with increasing flow rate there is a steady, although small increase in the conversion of propane. At the flow rate of 50ml/min and higher this mass transport limitation start to disappear.

So far, a detailed study on the effect of feed gases and the effect of the elements of $Ce_{20}Ti_{50}Cr_{30}$ catalyst followed by thermal, long term stability, mass transport limitations and pre-treatment study have been studied. From this it is envisaged that Ti and Cr elements are the important elements of selective propane combustion. In the next generation we search for very high propane activity and complete selectivity.

2.18 High throughput experimentation of catalyst generation 5

Based on the results of the fourth generation, another set of libraries were designed, prepared and named 5th generation libraries. This generation was prepared in order to fine tune the optimum catalyst compositions for propane combustion and also to reduce the light off temperature of propane. Based on the knowledge gained with the 4th generation, precious metal doping is rather selective for CO oxidation. Hence precious metal content was reduced from 1 mol% and 0,5 mol% to 0,05 mol% and 0,01mol%. All libraries prepared in this generation are mentioned in the table 2-18 below.

Library	Catalyst composition
14	Doping of noble metals [NM] in 0,05mol% and 0,01mol% with the candidates mentioned in table 2-19
15	$Ce_{40}Cr_{59,95}NM_{0,05}$, $Ce_{40}Cr_{59,99}NM_{0,01}$, $Ti_{62,45}Cr_{37,5}NM_{0,05}$, $Ti_{62,49}Cr_{37,5}NM_{0,01}$ with NM = Ag, Au, Ir, Pd, Pt, Re, Rh, Ru
16	$Ti_{59,5}Cr_{37,5}D_3$, $Ti_{42,5}Cr_{37,5}D_{20}$, $Ti_{62,5}Cr_{34,5}D_3$, $Ti_{62,5}Cr_{17,5}D_{20}$, $Ti_{52,5}Cr_{27,5}D_{20}$; D= Al, Bi, Dy, Gd, Hf, Sc, Si, Sm, Tm Ti_xCr_y with x and y varies from 0 to 100 mol% in steps of 10 mol%

Table 2-18 Catalyst compositions of libraries prepared for HT screening in fifth generation

No	Catalysts	No	Catalysts
1	$Ce_{32,3}Ti_{32,3}Cr_{32,3}V_3$	7	$Ce_{32,3}Ti_{32,3}Cr_{32,3}Hf_3$
2	$Ce_{32,3}Ti_{32,3}Cr_{32,3}In_3$	8	$Ce_{32,3}Ti_{32,3}$Cr32,3Sc_3
3	$Ce_{19}Ti_{49}Cr_{29}Tm_3$	9	$Ce_{20}Ti_{50}Cr_{30}$
4	$Ce_{19}Ti_{49}Cr_{29}Gd_3$	10	$Ce_{33,3}Ti_{33,3}Cr_{33,3}$
5	$Ce_{19}Ti_{49}Cr_{29}Sc_3$	11	$Ce_9Ti_{79}Cr_9Bi_3$
6	$Ce_{19}Ti_{49}Cr_{29}Si_3$	12	$Ce_9Ti_{79}Cr_9Mg_3$

Table 2-19 Catalysts to be doped for synthesis of library 14

a) C_3H_8 oxidation

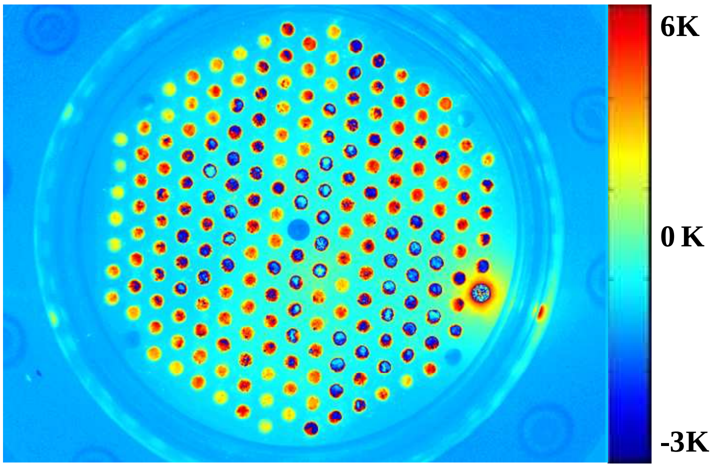

b) CO oxidation

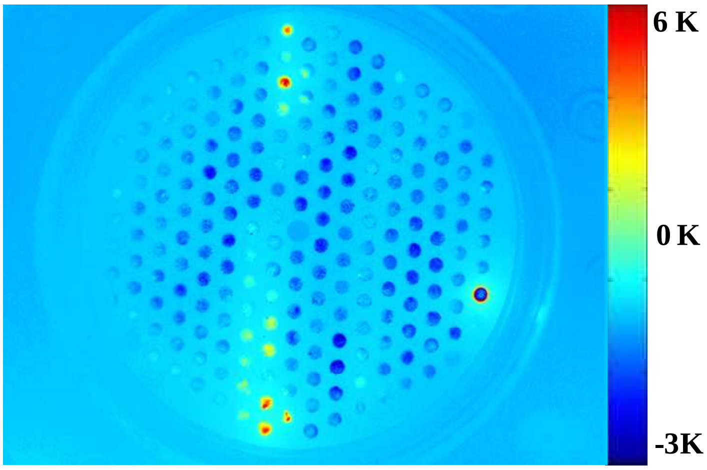

c) Background image after C_3H_8 oxidation

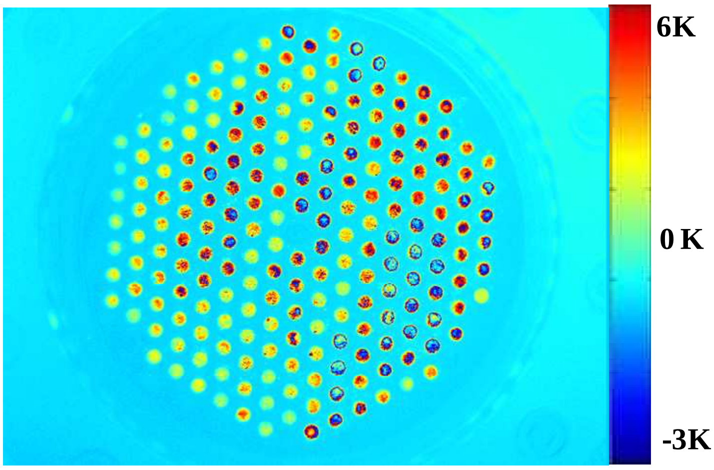

Figure 2-36: Emissivity corrected infrared thermography image of library 14 at 250°C. Reaction conditions (a): $C_3H_8/CO_2/O_2/N_2$ = 4/15,8/10/70,2 vol%. (b) $CO/CO_2/O_2/N_2$ = 5,45/15,8/10/68,75 vol%. (c) $CO_2/O_2/N_2$ = 15,8/10/74,2 vol%.

The IR images shown in figure 2.36 indicate clearly that catalysts suffer a very high emissivity changes after propane oxidation (figure 2-36c). It would be better for a reliable interpretation if the emissivity changes could be minimised. Hence library 14 had been tested with some more experiments to see whether this effect could be reduced significantly. Three more experiments were carried out of library 14.

1] Reduction of integration time of the IR camera from 0,05s to 0,01s at 350°C

2] Increase of the temperature calibration window from -4 to +6°C to -8 to +12°C.

2.18.1 Reduction of integration time

a) C_3H_8 oxidation

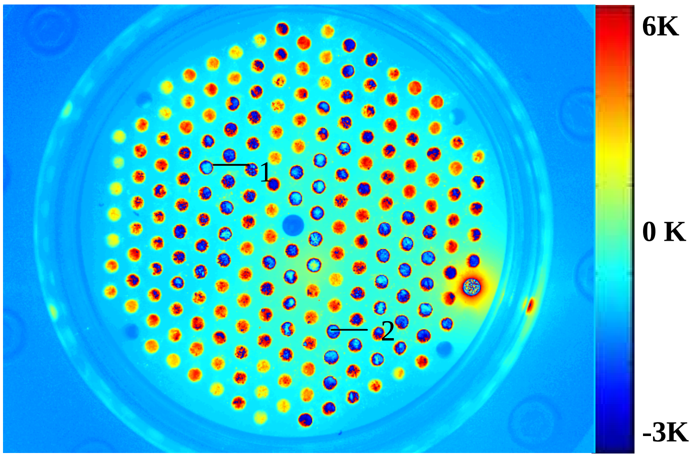

b) Background image after C_3H_8 oxidation

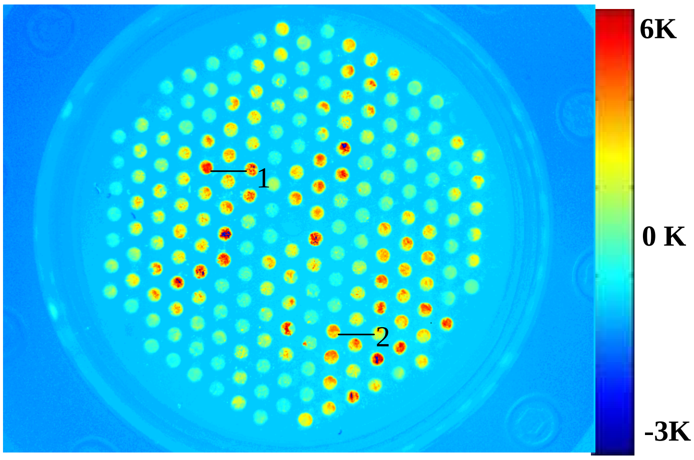

Figure 2-37: Influence of integration time in infrared thermography image of library 14 at 250°C. Reaction conditions (a): $C_3H_8/CO_2/O_2/N_2$ = 4/15,8/10/70,2 vol%. 1:$Ce_{19}Ti_{48,99}Cr_{29}Gd_3Ag_{0,01}$; 2: $Ce_{19}Ti_{48,99}Cr_{29}Tm_3Re_{0,01}$.

Integration time is the time that the IR camera opened to capture pictures of the library plate at the corresponding reaction temperatures and it is an inverse function of temperature. For example at 350°C the integration time was reduced from 0,05s to 0,01s (figure 2-37) which enable us to capture the picture of the library with lesser emissivity changes of the catalyst materials. Since high heat of reaction produced at high temperatures, lesser the integration time could facile the hits selection with reduced complexities such as false positives and negatives.

2.18.2 Increase of temperature calibration window

a) C_3H_8 oxidation

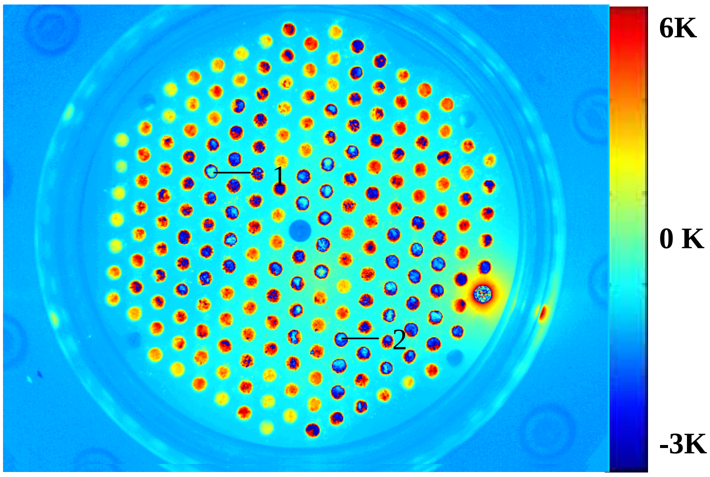

b) Background image after C_3H_8 oxidation

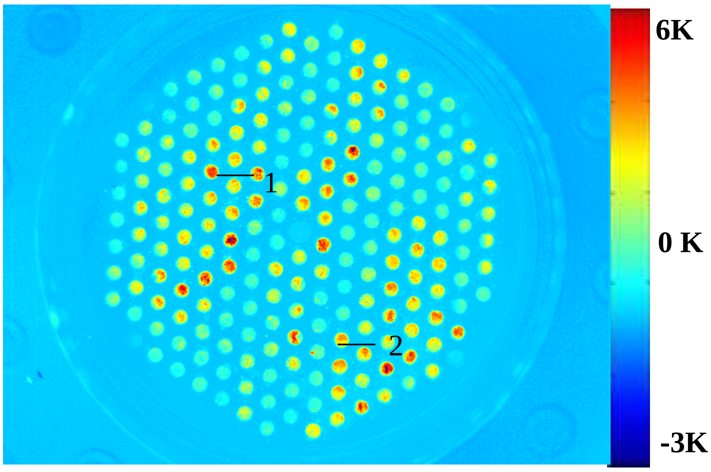

Figure 2-38: Influence of temperature calibration in infrared thermography image of library 14 at 250°C. Reaction conditions(a): $C_3H_8/CO_2/O_2/N_2$ = 4/15,8/10/70,2 vol%. 1:$Ce_{19}Ti_{48,99}Cr_{29}Gd_3Ag_{0,01}$; 2: $Ce_{19}Ti_{48,99}Cr_{29}Tm_3Re_{0,01}$.

Prior to the measurement, library emissivity is measured at 6 different temperatures from -4 to +6°C around the desired reaction temperature under the calibration gas ($CO_2/CO/O_2/N_2$) flow to correct the emissivity differences across the library plate. An attempt has been made by broadening this temperature calibration window from -8 to +12°C instead of -4 to +6°C as shown in figure 2-38 and has no influence on the emissivity changes reduction and rather looks similar to that figure 2-37 which indicates that integration time selection of the IR camera is essential to reduce these effects, selected hits for conventional testing of this library would now be chosen. They are listed in the table 2-20.

2.18.3 IR thermography of library 15

As we discussed in the last generation (Sec 2.16.2), the $Ce_{40}Cr_{60}$ catalyst was found to be an active catalyst in the binary spreads of $Ce_{20}Ti_{50}Cr_{30}$ catalyst. Doping of this $Ce_{40}Cr_{60}$ catalyst with 8 precious metals of 0,05 mol% and 0,01 mol% was carried out and named as library 15. The library synthesised was tested with a new IR camera with 256 x 256 pixel is used. The camera used in all previous libraries could not be used at this moment. Testing conditions were the same except that the maximum temperature limit of the reaction operation was about 300°C. The IR image of this library 15 is shown below in figure 2-39.

a) C_3H_8 oxidation

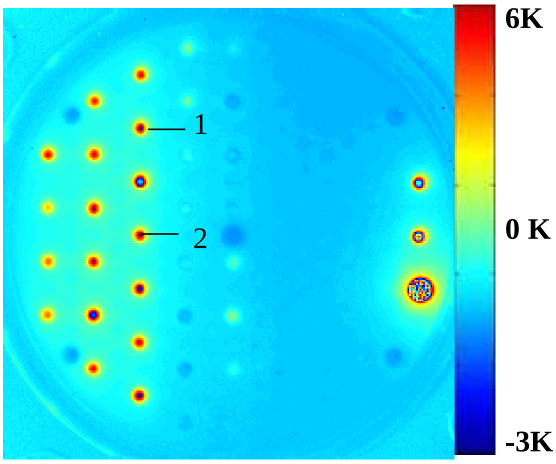

b) CO oxidation

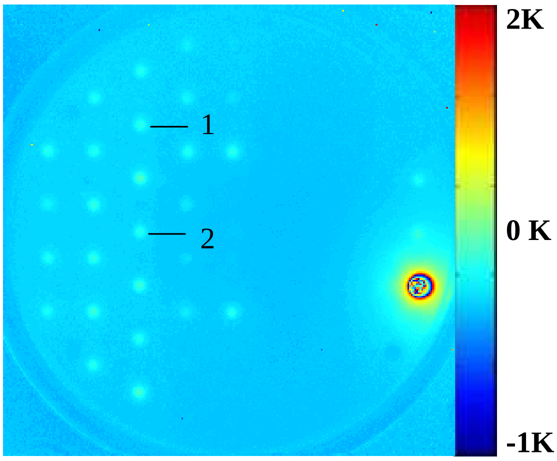

c) Background image after C_3H_8 oxidation

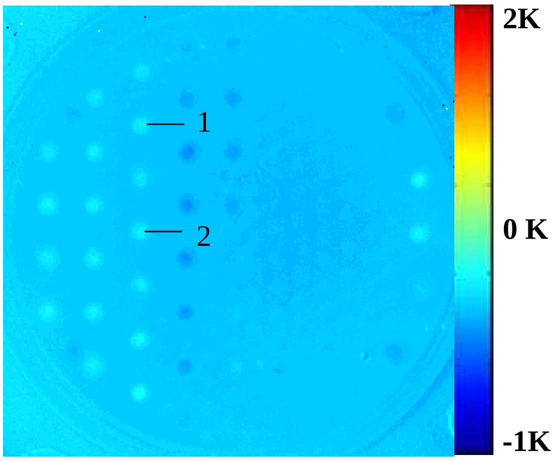

Figure 2-39: **Emissivity corrected infrared thermography image of library 15 at 300°C. Reaction conditions (a): $C_3H_8/CO_2/O_2/N_2$ = 4/15,8/10/70,2 vol%. (b) $CO/CO_2/O_2/N_2$ = 5,45/15,8/10/68,75 vol%. (c) $CO_2/O_2/N_2$ = 15,8/10/74,2vol%. 1:$Ce_{40}Cr_{59,95}Pd_{0,05}$; 2 :$Ce_{40}Cr_{59,95}Re_{0,05}$.**

The results of library 15 meant that there are no emissivity changes of the catalyst after propane oxidation. The reason could be due to the use of thicker sapphire glass which transmits the IR radiations than the old one (thinner) in previous libraries. The hits found from this library are listed in table 2-21.

Finally library 16 was prepared by doping of $Ti_{62,5}Cr_{37,5}$ catalyst with the 9 best elements of previous generations and tested in IR camera. The hits were selected and tabulated in table 2-22.

All potential hits listed in the tables below were conventionally tested and the conventional profiles of best candidates are plotted in figure 2-40 and of the remaining catalysts activities are tabulated in table 2-23.

a) Library 14

Composition	**Temp °C (Reaction)**	**ΔT_{C3H8}°C (Reaction)**	**ΔT_{C3H8}°C (Background)**	**Difference °C**	**ΔT_{CO}°C (Reaction)**
$Ce_{19}Ti_{48,99}Cr_{29}Gd_{3}Ru_{0,01}$	210	3,66	2,17	1,48	-0,24
$Ce_{19}Ti_{48,99}Cr_{29}Sc_{3}Rh_{0,01}$	210	3,58	2,21	1,38	-0,20
$Ce_{32,3}Ti_{32,25}Cr_{32,3}Hf_{3}Rh_{0,05}$	210	3,03	1,66	1,37	-0,06
$Ce_{19}Ti_{48,99}Cr_{29}Gd_{3}Re_{0,01}$	210	3,56	2,20	1,36	-0,30
$Ce_{19}Ti_{48,99}Cr_{29}Gd_{3}Ag_{0,01}$	210	3,48	2,16	1,32	-0,18
$Ce_{19}Ti_{48,99}Cr_{29}Si_{3}Ru_{0,01}$	210	3,24	1,93	1,31	-0,17
$Ce_{19}Ti_{48,99}Cr_{29}Tm_{3}Re_{0,01}$	210	3,45	2,15	1,30	-0,30
$Ce_{32,3}Ti_{32,29}Cr_{32,3}Hf_{3}Pd_{0,01}$	210	3,04	1,75	1,29	-0,12
$Ce_{32,3}Ti_{32,29}Cr_{32,3}Hf_{3}Ru_{0,01}$	210	2,94	1,67	1,28	-0,17
$Ce_{19}Ti_{48,99}Cr_{29}Gd_{3}Rh_{0,01}$	210	3,32	2,05	1,27	-0,19
$Ce_{20}Ti_{49,95}Cr_{30}Ru_{0,05}$	210	3,20	1,94	1,26	-0,18
$Ce_{20}Ti_{49,99}Cr_{30}Ru_{0,01}$	210	3,09	1,84	1,25	-0,14
$Ce_{20}Ti_{49,95}Cr_{30}Ir_{0,05}$	210	3	1,85	1,16	-0,14

Table 2-20 **Selected catalysts for conventional verification based on temperature evaluation techniques of library 14**

b) Library 15

Composition	**ΔT_{C3H8}°C (Reaction)**	**ΔT_{C3H8}°C (Background)**	**Difference °C**	**ΔT_{CO}°C (Reaction)**
$Ce_{40}Cr_{59,95}Pt_{0,05}$	2,48	0,13	2,35	0,85
$Ce_{40}Cr_{59,95}Pd_{0,05}$	2,00	0,22	1,78	0,72
$Ce_{40}Cr_{59,99}Re_{0,01}$	1,58	0,18	1,40	0,59
$Ce_{40}Cr_{59,95}Re_{0,05}$	1,52	0,17	1,35	0,5
$Ce_{40}Cr_{59,95}Rh_{0,05}$	1,51	0,15	1,36	0,55

Table 2-21 **Selected catalysts for conventional verification based on temperature evaluation techniques of library 15 at 300°C**

c) Library 16

Composition	**ΔT_{C3H8}°C (Reaction)**	**ΔT_{C3H8}°C (Background)**	**Difference °C**	**ΔT_{CO}°C (Reaction)**
$Ti_{52,5}Cr_{27,5}Tm_{20}$	12,64	4,38	8,26	0,18
$Ti_{52,5}Cr_{27,5}Mg_{20}$	11,51	5,79	5,73	-0,53
$Ti_{52,5}Cr_{27,5}Hf_{20}$	11,39	4,40	6,99	0,47
$Ti_{52,5}Cr_{27,5}Sr_{20}$	9,92	4,24	5,67	-0,72
$Ti_{52,5}Cr_{27,5}Ce_{20}$	9,53	3,77	5,76	0,03
$Ti_{52,5}Cr_{27,5}Mn_{20}$	5,81	1,40	4,41	0,39
$Ti_{59,5}Cr_{37,5}Dy_{3}$	6,35	2,19	4,16	0,30

Table 2-22 Selected catalysts for conventional verification based on temperature evaluation techniques of library 16 at 350°C

2.19 Conventional testing of fifth generation hits

a) Library 14

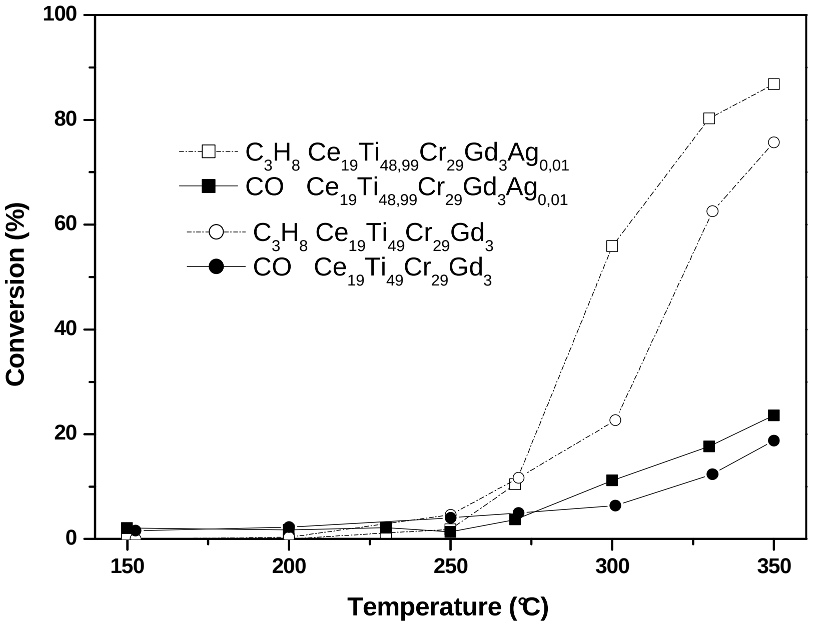

b) Library 15

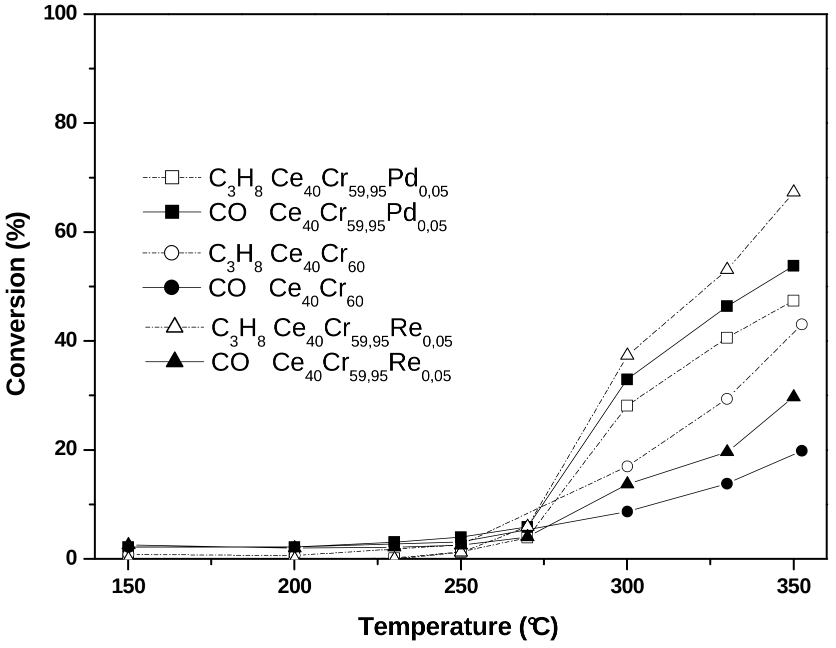

c) Library 16

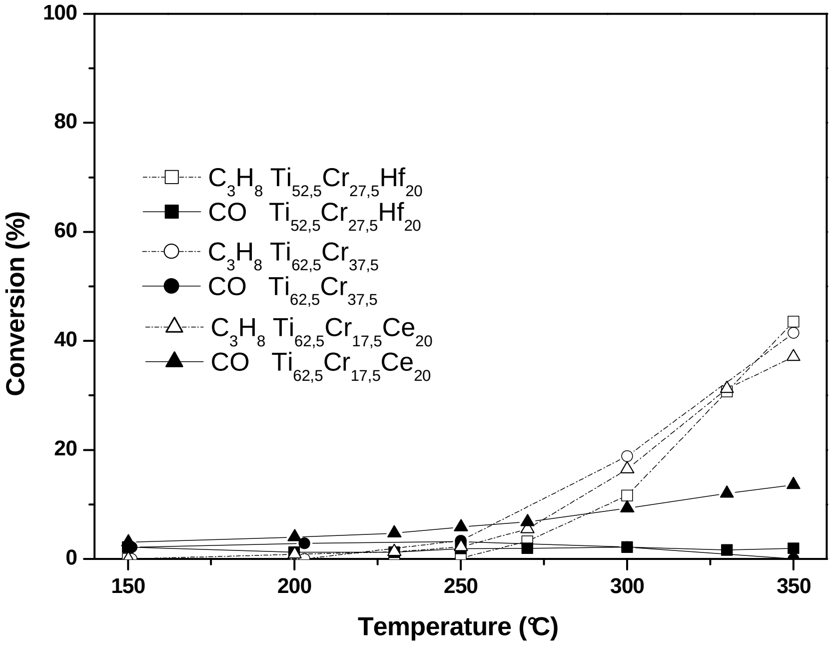

Figure 2-40: Conventional test results of selected catalysts of 5th generation (a) library 14 (b) library 15 (c) library 16 with reaction in increment order of temperatures from 150°c to 350°C. Reaction conditions: 20mg of catalyst diluted with 100mg of γ-alumina* with particle size of 100-200 µm (both). Total flow rate: 50ml/min ($C_3H_8/CO/CO_2/O_2/N_2$ =2/10,9/15,8/10/61,3). Catalyst pre-treatment: synthetic air with 50ml/min at 350°C for 1h.

γ-alumina with particle size of 200 – 500 µm is used in conventional testing of library 16.

Figure 2-40 indicates the best conventional test hit profiles of 3 libraries of generation 5. It is inferred (figure 2-40a) that the reduction of noble content from 1 and 0,5 mol% to 0,05 and 0,01 mol% has a good impact on activity and selectivity of propane oxidation. It shows about 7% increase in propane conversion when the Gd doped catalyst is doped further with a small amount of Ag. The Pd catalyst has still a strong negative influence on propane selectivity, it increases the CO oxidation when the $Ce_{40}Cr_{60}$ catalyst is doped with 0,05 mol% Pd, which is shown in figure 2-40b, but Re increases the propane activity with some loss in selectivity when compared to the undoped CeCr catalyst. Additionally $Ti_{62,45}Cr_{37,5}Pt_{0,05}$ catalyst is tested conventionally though it does not show any activity in high throughput screening. It also shows increase in propane conversion with some loss in selectivity.

Catalyst	**X_{C3H8} (%) at 350°C**	**X_{CO} (%) at 350°C**	**Catalyst**	**X_{C3H8} (%) at 350°C**	**X_{CO} (%) at 350°C**
$Ce_{19}Ti_{48,99}Cr_{29}Gd_3Ru_{0,01}$	79	22	$Ce_{40}Cr_{59,95}Pt_{0,05}$	57	27
$Ce_{19}Ti_{48,99}Cr_{29}Sc_3Rh_{0,01}$	80	24	$Ce_{40}Cr_{59,95}Pd_{0,05}$	47	54
$Ce_{32,3}Ti_{32,25}Cr_{32,3}Hf_3Rh_{0,05}$	72	26	$Ce_{40}Cr_{59,99}Re_{0,01}$	41	16
$Ce_{19}Ti_{48,99}Cr_{29}Gd_3Re_{0,01}$	75	23	$Ce_{40}Cr_{59,95}Re_{0,05}$	68	30
$Ce_{19}Ti_{48,99}Cr_{29}Gd_3Ag_{0,01}$	87	24	$Ce_{40}Cr_{59,95}Rh_{0,05}$	40	14
$Ce_{19}Ti_{48,99}Cr_{29}Si_3Ru_{0,01}$	67	18	$Ti_{62,45}Cr_{37,5}Pt_{0,05}$	49	10
$Ce_{19}Ti_{48,99}Cr_{29}Tm_3Re_{0,01}$	73	18	$Ti_{52,5}Cr_{27,5}Tm_{20}$	40	9
$Ce_{32,3}Ti_{32,29}Cr_{32,3}Hf_3Pd_{0,01}$	74	51	$Ti_{52,5}Cr_{27,5}Mg_{20}$	22	7
$Ce_{32,3}Ti_{32,29}Cr_{32,3}Hf_3Ru_{0,01}$	76	33	$Ti_{52,5}Cr_{27,5}Hf_{20}$	44	2
$Ce_{19}Ti_{48,99}Cr_{29}Gd_3Rh_{0,01}$	79	20	$Ti_{52,5}Cr_{27,5}Sr_{20}$	25	3
$Ce_{20}Ti_{49,95}Cr_{30}Ru_{0,05}$	68	26	$Ti_{52,5}Cr_{27,5}Ce_{20}$	37	14
$Ce_{20}Ti_{49,99}Cr_{30}Ru_{0,01}$	78	24	$Ti_{52,5}Cr_{27,5}Mn_{20}$	41	19
$Ce_{20}Ti_{49,95}Cr_{30}Ir_{0,05}$	77	20	$Ti_{59,5}Cr_{37,5}Dy_3$	28	0

Table 2-23 Conversion of C_3H_8 and CO oxidation at 350°C of active hits of fifth generation

In the case of library 16 hits, it was found that the catalysts were completely selective and only marginal improvement in the activity was found when TiCr catalyst was doped with 20% Hf plotted in figure 2-40c. Remaining hits activities tested conventionally of 5th generation are tabulated in table 2-23.

3 Experimental

This section contains the experimental part of all generations regarding the catalyst synthesis by high throughput and conventional ways, followed by test set up and experimental procedures.

3.1 High throughput library synthesis

The catalyst libraries were synthesised with the selected sol-gel recipe by the library design software Plattenbau [139, 140]. The software calculates the optimised pipetting list based on recipes and reagents which in turn controls the complete operation of the pipetting robot (Lissy, Zinsser Analytic) for the volume transfer from precursor stock solutions to the corresponding 2ml GC vials array containing 50 vessels, which were placed in the roboter work space to get the final mixed catalyst sol. The catalyst sols were stirred in an orbital shaker [Titramax, Heidolph] to get homogeneous solutions. The solutions were dried and calcined to attain complete mixed metal oxide catalysts. The metal nitrates (Al, Ag, Ca, Ce, Cd, Co, Cr, Cu, Dy, Er, Eu, Fe, Ga, Gd, Ho, In, K, La, Li, Lu, Mg, Mn, Na, Nd, Ni, Sc, Sm, Tb, Tm, Y, Yb, Zn and Zr), alkoxides (Bi, Ge, Mo, Si, Ta, Ti and V), chlorides (Ba, Cs, Hf, Ir, Nb, Re, Rh, Ru, Sb, Sn, Sr, Te and W), Bromides (Au and Pt), acid (B and Se), acetates (Pd, Rb) were used as precursors of 0,1M stock solutions dissolved in different solvents such as methanol, 2-propanol, water and n-propanol. Base metal oxide stock solutions were about 0,587M. Each catalyst was prepared in about 300 µmole amounts. Catalysts are described in terms of metal ions with mol% as subscripts which represent the expected concentration of catalyst sols. For example $Ni_{60}Co_{40}O_x$ means 60 mol% of Ni and 40 mol% of Co with O_x as unknown oxidation states of mixed metal oxides. The preparation of catalyst libraries were followed by two methods.

3.1.1 Ethylene glycol method

The sol-gel recipe used to synthesise catalysts based on this method for libraries (2, 3, 4, 5 and 6) and explained elsewhere in [60, 148, 149]. The general recipe is as follows.

a. A: b. B: d. D: 20 EG: 40 H_2O: 4 HNO_3

A, B and C = Ce, Co, Cu, Fe and Ni dissolved in Ethylene glycol
a, b and c = varies from 0 to 100 mol% in steps of 5 mol%
D = 48 dopants listed in each library synthesis of chapter 2 with 3 mol%

For example, synthesis of $Ni_{60}Co_{37}Sr_3$ was done by pipetting 240 µl of 0,587M $NiNO_3.6H_2O$ and 148 µl of 0,587M $CoNO_3.6H_2O$ solutions dissolved in ethylene glycol and water mixtures (66/34,v/v). Then 90 µl of 0,1 M $SrCl_2.6H_2O$ dissolved in methanol were added. Finally, 33 µl of ethylene glycol–water mixture and 83 µl of 65wt% HNO_3 were added. After completion of pipetting steps of one GC rack, the samples were stirred in the orbital shaker (Titramax 100, Heidolph) for about 1h. After stirring, the catalyst was dried and calcined under static air. The calcination program is as follows.

$$25°C \xrightarrow{6°C/h} 80°C\ (12h) \xrightarrow{6°C/h} 105°C\ (60h) \xrightarrow{10°C/h} 400°C\ (5h) \xrightarrow{114°C/h} 25°C.$$

3.1.2 Propionic acid method

The catalysts of library 9 to 16 were prepared by this method [150]. The general recipe of this method is as follows.

aA: b. B: c. C: 3 KB (4-hydroxy 4-methyl 2-pentanone): 0,02 CH_3CH_2COOH

A, B and C = Ce, Cr, and Ti* dissolved in methanol (* indicates Ti dissolved in mixture of small amount of HNO_3 and methanol)
a, b and c = varies from 0 to 100 mol% in steps of 10 mol%

For example the preparation of $Ce_{20}Ti_{50}Cr_{30}$ was performed by pipetting 102 µl of 0,587M $Ce(NO_3)_3.6H_2O$ in methanol, 256 µl of 0,587M $Ti(OiPr)_4$ in methanol and HNO_3 (65wt%), 153 µl of 0,587 M $Cr(NO_3)_3.9H_2O$ in methanol and 112 µl of 8,06M complexing agent mixed with propionic acid is added. Care should be taken while preparing titanium precursors. The weight ratio of HNO_3 to titanium-iso-propoxide is 0,06 to 1. Both acid and titanium were weighed in separate beakers. Then slowly titanium-iso-propoxide was added to the HNO_3 containing beaker under continuous stirring. Finally methanol was added and stirred for about 20 minutes. Similarly propionic acid was mixed with complexing agent because of the very low volume of acid to be pipetted by the robot. After all the pipetting steps for one GC rack were completed, the catalyst sols were stirred in an orbital shaker for 1h. Later racks were dried at 40°C for 5 days to obtain a gel. Finally, the racks were heated from room temperature to 400°C at a heating rate of 20°C/h under static air conditions. At this temperature the catalysts were calcined for 5h and cooled down again at the rate of 120°C/h to room temperature.

The catalysts calcined by both methods were ground into fine powders using a spatula and filled into the wells of the slate plate library containing 206 wells.

3.2 High throughput screening of catalyst libraries

Emissivity corrected infrared thermography (ec-IRT) was used for the parallel investigation of the catalyst libraries. Measurement and working principles were explained in detail previously [141, 142]. The experimental set up of ec-IRT is shown in figure 3-1.

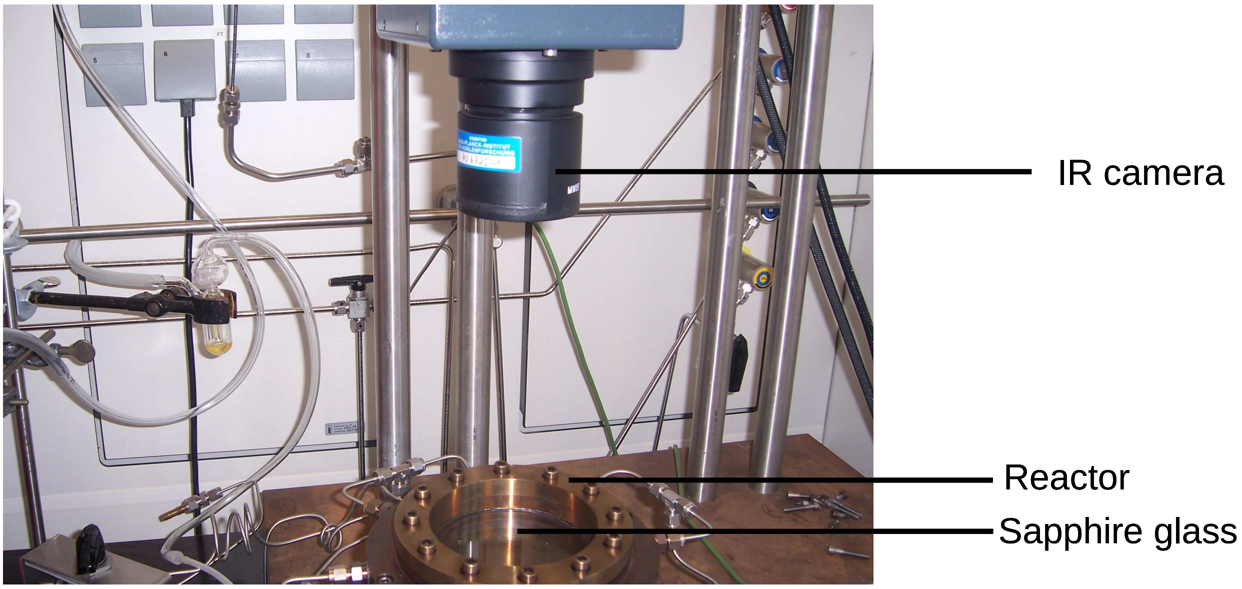

Figure 3-1: IR thermography experimental set up.

The setup consists of reactor made of steel with a large opening where the library is placed for measurement. The reactor has a heating plate beneath the reaction chamber and the library is covered by a sapphire glass which allows direct recording of temperature changes at the catalyst surface through IR radiation. The isothermal temperature distribution is achieved in the reactor by means of thermocouple and a controller [Jumo Dtron 16.1]. The heat of reaction is measured in parallel by using an IR camera. It consists of PtSi detector of 640 x 480 pixel from

Thermosensorik. The required feed gas for the reaction was supplied to the reactor unit with the help of a mass flow controller [MKS]. Feed gases of required composition flows over the library filled with 206 catalysts, placed in a closed tight gas phase reactor. In between reactor unit and mass flow controllers, magnetic valves were installed which act as controller and allow the gas to pass through the reaction unit when the corresponding valve is opened.

The reaction gases were fed into the reactor by 8 drilled holes on the upper part in the radial direction and product gases leaves the reactor unit through central hole in the library. The product gas leaving the reactor enters the steam trap to condense water molecules and then through C_3H_8, CO and CO_2 infrared sensors [GfG].

ec-IRT experiment is carried out as following.

- Placing the library in the reactor, covering with sapphire glass and well tightly screwed to avoid any leakage.
- Start pre-treatment using synthetic air with 50 ml/min at 350°C (250°C in first generation) for 1h.
- Six point calibration using calibration gas ($CO_2/O_2/N_2$ = 15,8/10/74,2 vol%) with 50 ml/min from -4°C to +6°C around the desired reaction temperature.
- Background image taken as a reference image.
- Start propane oxidation with feed flow of 50 ml/min ($C_3H_8/CO_2/O_2/N_2$ = 4/15,8/10/70,2) for 1h.
- Flushing of the reactor using calibration gas for 30 minutes.
- Start CO oxidation with feed flow of 50 ml/min ($CO/CO_2/O_2/N_2$ = 5,45/15,8/10/68,75 vol%) for 1h.
- Purging the reactor and cooling down to room temperature.

It should be noted that propane and CO feed concentration was 2 and 10,9 vol% in the first generation testing of libraries. All processes including, gas dosing, temperature control and IR camera control were automated by using the IR- Testrig software [140].

3.3 Conventional catalyst synthesis

Conventional catalyst syntheses were carried out by up-scaling of potential hits from the ecIRT screening from 8 Mmoles to 300 Mmoles. An example of Ce_5Co_{95} based on Ethylene glycol method is as follows. About 6,81 ml of 0,587M $Ce(NO_3)_3.6H_2O$ and 12,95 ml of 0,587M $CoNO_3.6H_2O$ were prepared by using ethylene glycol/water mixtures (66/34, v/v). Both precursors were mixed together and stirred along with the drop wise addition of 2,23 ml of 65wt% HNO_3 to complete the catalyst synthesis. Further prepared catalyst sols were stirred for 1h at 500 rpm using a Heidolph Stirmax followed by calcination step shown below.

$$25°C \xrightarrow{6°C/h} 80°C\ (12h) \xrightarrow{6°C/h} 105°C\ (60h) \xrightarrow{10°C/h} 400°C\ (5h) \xrightarrow{114°C/h} 25°C.$$

Similarly $Ce_{20}Ti_{50}Cr_{30}$ catalyst based on propionic acid route is synthesised as follows. About 2,72 ml of 0,587M $Ce(NO_3)_3.6H_2O$ and 4,09 ml of 0,587M $Cr(NO_3)_3.9H_2O$ is prepared separately by using methanol as solvent and well mixed by stirring for few minutes. Then Ti precursor $(Ti(OCH(CH_3)_2)_4$ of 0,587M has to be prepared. For this initially about 1,14g of titanium-iso-propoxide is mixed in a beaker containing 0,07g of 65wt% HNO_3 covered with parafilm and stirred about 15 minutes. Further 6,81 ml of methanol is added into the mixture and stirred for again 15 minutes with a covered parafilm over the beaker. Then 2,97 ml of complexing agent (4-hydroxy,4-methyl,2-pentanone) are placed in a fresh empty beaker (50 ml) and stirred well. During stirring the prepared Ce, Ti and Cr precursor solutions are added slowly in sequence respectively. Then 12 µl of propionic acid is added, covered with parafilm and stirred for 1h. The stirred sols were dried for 5 days at 40°C, which is enough time to gel. Then the obtained gel is heated from room temperature to 400°C at a heating rate of 20°C/h under static air conditions and then calcined for 5h at 400°C. Finally the calcined catalyst is cooled at a cooling rate of 120°C/h to room temperature. The cooled catalyst is ground to a fine powder. The cooled catalyst by both conventional methods is screened for the particle size range of 100-200 µm is obtained by sieving.

3.4 Preparation of pure Ti catalyst

3.4.1 TiO_2 recipe 2

This method follows the dissertation of Lettmann [146] for preparing a Ti_{100} catalyst. This method is employed to see whether there is a possibility of improving specific surfaces of the catalyst. The recipe is as follows.

x $Ti(O\text{-}nBu)_4$: 0,23 (x) HCl : 0,84 (x) H_2O : 1,54 ml n-Butanol

Recipe can be rewritten as

32,5 MmolesTi$(O\text{-}nBu)_4$: 0,7368 g (37% HCl) : 0,027 g H_2O : 50,05 ml n-butanol

Initially 11g of Ti precursors were dissolved in 50,05 ml of n-butanol in a 100ml polypropylene beaker and stirred for about 30 minutes. Similarly 0,7368g of 37% HCl was mixed with 0,027g of H_2O and well stirred. Then HCl-H_2O mixture was added to the Ti precursor solution. The resulting sol containing beaker was covered with a parafilm and stirred until the formation of gel and the duration of gel formation is indefinite. Then parafilm is removed and the gel is allowed for drying at room temperature in the exhaust until the gel shrinks. After drying, the catalyst was calcined from room temperature to 65°C at a heating rate of 0,5°C/min and kept at this temperature for 3h. Then it was heated to 250°C at 0,5°C/min and kept at 250°C for 3h. Finally, the catalyst was cooled to room temperature at a cooling rate of 2°C/min.

3.4.2 TiO_2 recipe 3

This is another method employed to improve the specific surface area of a Ti_{100} catalyst. The catalyst synthesis procedure follows as recipe described in dissertation of Klein [145].

x $Ti(OPr)_4$: 3(x)$C_6H_{12}O_2$: 65(x) ^iPrOH : (x)H_2O : 0,06(x)HCl

Recipe can be rewritten by taking basis as 10 Mmoles of catalyst

10 Mmoles $Ti(OPr)_4$: 30 Mmoles $C_6H_{12}O_2$: 650 Mmoles H_2O : 0,6 Mmoles HCl

Initially 3,72 ml of 4-hydroxy, 4-methyl, 2-pentanone is added in the 100 ml beaker. About 2,842g of titanium iso-propoxide is added into the beaker. Then the beaker is covered with parafilm and stirred for about 15 minutes. Then 30 ml of iso-propanol is added into the beaker containing mixture and stirred again for 30 minutes. Simultaneously, in another beaker remaining 19,7 ml iso-propanol, 0,179 ml of H_2O and 0,05 ml of HCl (12N) is added and stirred shortly to get mixed and added into 100 ml beaker containing mixture. The catalyst solution is stirred continuously at room temperature inside the hood until the formation of gel. The gel formed is further aged and dried inside the hood at room temperature without parafilm.

When the gel is dried completely, then the gel is heated to 65°C from room temperature at a heating rate of 30°C/h and kept at this temperature for 5h. Then with the same heating rate, catalyst is heated again to 250°C and kept for 5h. Finally, catalyst temperature is cooled down to room temperature at a cooling rate of 120°C/h.

Catalysts prepared conventionally by all methods ground to fine powders and screened. About 100 – 200 micrometres particles are used for conventional testing.

3.5 Conventional testing of catalysts

Potential hits of all libraries were tested conventionally for the reliable verification of the performance of the catalyst. The conventional experimental set up is shown below in figure 3-2.

Figure 3-2: Conventional experimental setup.

The reaction gas consists of mixture of C_3H_8, CO, CO_2 and N_2 with 4, 21,8, 31,6 and rest N_2 in vol%, but without O_2. The reaction gas is premixed and combined with synthetic air before entering the reactor unit. The ratio of reaction gas to synthetic air was 1:1 to obtain desired reactor feed concentrations (C_3H_8/CO/CO_2/O_2/N_2 = 2/10,9/15,8/10/61,3 vol%) and the flow is controlled by mass flow controllers [Fa. Bronkhorst]. The reaction gas mixture has two possibilities of flow direction. One way is, it can flow through a bypass and another way is through the reactor. The reactor is made of glass tube of 50 cm long and inner diameter of 0,5 cm. Inside the reactor approximately at the centre, frits are placed to hold the catalyst. Thermocouple is inserted into the catalyst bed and temperature is controlled with a help of temperature controller unit. Reactor and bypass exits were entering the steam trap to remove water molecules by using ice. After condensation, gas enters the gas analysis sensors [Fa. GFG]. C_3H_8, CO and CO_2 sensors are used for analysis. Sensors capabilities are for C_3H_8 from 0 to 5 vol%, CO from 0 to 15% and CO_2 from 0 to 25 vol%. Conventional experiments are performed based on the following sequence.

- About 20 mg of catalyst (100-200 µm) and 100 mg of γ-alumina (100-200 µm) were mixed together and filled in the glass reactor.
- Synthetic air (50 ml/min) was passed through the bypass to allow calibration of the infrared sensors for C_3H_8, CO and CO_2.
- Then synthetic air with the same flow rate was passed through the reactor and the temperature is gradually increased to 350°C and the catalyst was pre-treated at this temperature for about 1h.
- Reactor was cooled down to 150°C under a continuous flow of synthetic air.
- Then reactor feed gas composition (25 ml/min of reaction gas and 25 ml/min synthetic air) was controlled again through the bypass.
- Now feed gas flow switched to reactor unit and measurements were carried out at temperatures of 150, 170, 200, 230, 250, 270, 300, 330 and 350°C.
- At each temperature, duration of 20 minutes is allowed for stability of the reaction.
- Concentrations from mini computer and corresponding time were noted for each temperature at start and end of the reaction, which is further used in analysis for conversion and selectivity of the reaction in the excel file.
- After measurements, reaction gas is passed once again through bypass to confirm concentrations of feed flow and compared with bypass before the reaction.
- Then reactor is cooled and purged with N_2.

3.6 Catalyst characterisation

3.6.1 X-ray diffraction

Powder X-ray diffraction studies were performed by a Huber G670 Guinier camera using Cu Kα1 radiation (λ = 1,54056 A°). Lattice parameter refinement was done by full pattern Rietveld refinement with the program TOPAS [151] using the fundamental parameter approach [152]. For the analysis of structure catalysts in powder form were coated in the selotape slat of the sample holder and measurements were carried out with the help of K. Stöwe.

3.6.2 Specific surface area measurements

The surface areas of the catalysts were measured by nitrogen physisorption (Sorptomatic 1990, Carlo Erba). The adsorption desorption measurements were obtained at liquid N_2 temperature of -196°C. Prior to the measurement, the catalysts were heated to 200°C under high vacuum in the N_2 atmosphere, kept for about 2h and cooled. Specific surface areas were measured by BET method and pore distributions using BJH method. All surface areas measurements were carried out with the help of C. Thome.

4 Summary and conclusions

The main objective of our research is to find new noble metal free catalysts for selective combustion of propane in the presence of CO. Due to stringent emission standards and adverse health effects such as respiratory illness and high odour, hydrocarbon combustion has paid major attention. High throughput workflow strategies are adopted in finding out new catalysts, since it is more facile and accelerate the catalyst search process. The work flows in the development of new catalyst libraries based on variation and selection. Catalyst materials were synthesised using highly composition tolerant sol-gel recipes with the help of experimental design software Plattenbau and associated pipetting robots.

Catalytic performance of high throughput libraries were tested using emissivity corrected infrared thermography (ec-IRT) which allows parallel testing of catalysts. Initially first generation libraries were tested in the real exhaust gas atmosphere of both C_3H_8 and CO in the feed. Visualising the relative heats of reaction using ec-IRT, it was difficult to identify which catalysts are selective for C_3H_8 or CO oxidation reaction. Therefore ec-IRT experiments were carried out under C_3H_8 and CO atmospheres separately. Over 2000 catalysts were tested in a high throughput fashion.

Among generation 1, $Ni_{60}Co_{40}$, Ce_5Co_{95}, $Fe_{20}Co_{80}$, $Cu_{20}C0_{70}Ni_{10}$ and $Ce_{30}Co_{60}Fe_{10}$ were found as best hits from high throughput screening and tested conventionally in the real exhaust gas atmospheres (both C_3H_8 and CO in the feed). Those catalysts show high propane conversion and unselective. Hence catalyst development is needful to fulfil our requirements. Among second generation, $Ce_{33,3}Ti_{33,3}Cr_{33,3}$ was found to be the only active and selective catalyst for C_3H_8 oxidation and verified conventionally. In generation 3 which are based on the composition spreads and doping of CeTiCr elements, the $Ce_{20}Ti_{50}Cr_{30}$ as highly active catalyst and $Ce_{10}Ti_{80}Cr_{10}$ as a highly selective catalyst found. Further optimisation of catalysts in generation 4 found that $Ce_{19}Ti_{49}Cr_{29}D_3$ (D = Sc, Si, Gd and Tm) were found best catalysts with very high activity and selectivity towards C_3H_8 combustion.

Then the effect of feed gas compositions ($C_3H_8/CO/CO_2/O_2/N_2$ = 2/10,9/15,8/10/61,3 vol%) over $Ce_{19}Ti_{49}Cr_{29}Sc_3$ catalyst (one of the best catalyst resulted out of fourth generation) is tested. In this study six different experiments based on six different feed conditions such as absence of CO_2, absence of CO, absence of C_3H_8, 5 vol%, 10 vol% O_2 (reference concentration) and 15 vol% O_2 were conducted. It influences the following. In the absence of CO_2 in the feed, the overall C_3H_8 conversion is not affected at high temperatures of about 350°C, but at low temperatures say 300°C, C_3H_8 conversion is approximately 14% higher in the presence of CO_2. Absence of CO in the feed shows that C_3H_8 conversion is slightly increased of 2% and 0,7 vol% of CO is produced. This CO formation could be due to the partial oxidation of C_3H_8 or reduction of C_3H_8 with CO_2 is still unknown. Then in the absence of C_3H_8 in the feed shows that CO conversion is increased approximately 6% at 350°C. Therefore presence of C_3H_8 in the feed, blocks the active sites for CO and C_3H_8 is preferentially oxidised. The effect of O_2 concentration in the feed was tested by two different O_2 concentrations of 5 and 15 vol% and compared with reference concentration of 10 vol%. It was found that reducing the half amount of O_2 from 10 to 5 vol%, reduces the C_3H_8 conversion also into half. With increase in O_2 content to 15 vol% achieves very high C_3H_8 conversion of 97% at the expense of selectivity and inferred that the C_3H_8 conversion as the function of O_2 concentration in the feed.

In other study to gain insight into the nature of catalytic contributions of three metal ions in $Ce_{20}Ti_{50}Cr_{30}$ catalyst, the individual oxides Ce_{100}, Ti_{100} and Cr_{100} and binary oxides of all combinations based on ternary material prepared as $Ce_{28,6}Ti_{71,4}$, $Ce_{40}Cr_{60}$ and $Ti_{62,5}Cr_{37,5}$ were investigated. It was found that Ce_{100} is slightly active and unselective. Ti_{100} is completely inactive for both oxidations and followed by Cr_{100} which is slightly active for propane oxidation at high temperatures of 350°C and shows the origin of hydrocarbon selectivity. On the other hand specific surface areas of Ti_{100} and Cr_{100} are comparatively lesser than Ce_{100} catalyst. Hence reduction of calcination temperatures of the catalyst and new synthesis methods were performed to get comparable surface areas with respect to Ce_{100} catalyst. As a result of those new adoptions, it was found that Cr_{100} is highly active and unselective for C_3H_8 oxidation and Ti_{100} achieves 11% of CO conversion and completely inactive for C_3H_8 oxidation. Interestingly in binary oxides $Ti_{62,5}Cr_{37,5}$ was found as the best performing active and completely selective catalyst for propane combustion. $Ce_{40}Cr_{60}$ is active but less selective and $Ce_{28,6}Ti_{71,4}$ is completely inactive.

The work flow is continued for fine tuning of CeCr and TiCr catalysts and some best hits of fourth generation. Finally $Ce_{19}Ti_{48,99}Cr_{29}Gd_3Ag_{0,01}$ as very active catalyst and $Ti_{62,5}Cr_{37,5}$ as completely selective catalyst for selective hydrocarbon combustion.

Through the random design of experiments we reached the goal of our project and improved catalytic performance from former to latter generations. Thus this shows the good reproducibility of high throughput technology in conventional testing and it is capable to use as a versatile tool for new catalyst development.

Zusammenfassung und Ausblick

Das wichtigste Ziel unserer Forschung ist es, neue Edelmetall-freie Katalysatoren für die selektive Verbrennung von Propan in Anwesenheit von CO zu finden. Bei der Suche nach neuen Katalysatoren wurde eine Hochdurchsatz-Strategie durchlaufen, da es problemlos möglich ist den Suchprozess nach Katalysatoren durch automatisierte Synthese und eine große Anzahl an Proben schneller erfolgreich abzuschließen. Hochdurchsatz-Strategien werden bei der Entwicklung von Katalysatoren-Bibliotheken eingesetzt, die auf Variation und Selektion basieren. Katalysatoren-Materialien werden synthetisiert durch Benutzung von gegenüber der Zusammensetzung toleranten Sol-Gel Rezepten und mit der Hilfe von der Software Plattenbau in Verbindung mit Pipettier-Robotern.

Katalytische Aktivität der Bibliotheken wurde unter Verwendung der emmisivitätskorrigierten-Infrarotthermographie (ec-IRT) getestet, welche die parallele Prüfung verschiedener Katalysatoren erlaubt. Anfangs wurde die erste Generations-Bibliotheken in der realen Abgasatmosphäre geprüft, d.h. in Anwesenheit von C_3H_8 und CO Gas. Mittels Visualisierung der relativen Wärme der Reaktion mit ec-IRT fiel es schwer herauszufinden welche Katalysatoren in der Bibliothek selektiv für die C_3H_8 oder CO Oxidations-Reaktion sind. Daher wurden ec-IRT Experimente unter C_3H_8 und CO-Atmosphären separat durchgeführt. Über 2000 Katalysatoren wurden unter Verwendung der beschriebenen Hochdurchsatz-Techniken getestet.

Unter der Generation 1, wurden $Ni_{60}Co_{40}$, Ce_5Co_{95}, $Fe_{20}Co_{80}$, $Cu_{20}C0_{70}Ni_{10}$ und $Ce_{30}Co_{60}Fe_{10}$ als beste Treffer von Hochdurchsatz-Screening Experimenten gefunden und in der konventionellen Anlage in einer realen Abgasatmosphären (beide C_3H_8 und CO) gestestet. Diese Katalysatoren zeigten einen hohen Propan Umsatz, aber eine schlechte Selektivität. Daher ist eine Katalysatorentwicklung nötig, um unsere Anforderungen zu erfüllen. In der zweiten Generation stellte sich heraus, dass $Ce_{33,3}Ti_{33,3}Cr_{33,3}$ der Einzige aktive und selektive Katalysator für die C_3H_8 Oxidation ist. Die Ergebnisse wurden im konventionellen Test bestätigt.. In der Generation 3, die aus der Variation und Dotierung der Elemente CeTiCr beruht, zeigte sich $Ce_{20}Ti_{50}Cr_{30}$ als hochaktiver und $Ce_{10}Ti_{80}Cr_{10}$ als hochselektiver Katalysator. Weitere Optimierung von Katalysatoren in der Generation 4 zeigten, dass $Ce_{19}Ti_{49}Cr_{29}D_3$ (D = Sc, Si, Gd und Tm) die besten Katalysatoren, mit sehr hoher Aktivität und Selektivität, für die C_3H_8 Verbrennung sind.

Der Einfluss der Zisammensetzung des Reaktiongases ($C_3H_8/CO/CO_2/O_2/N_2$ = 2/10,9/15,8/10/61,3 vol%) auf dem $Ce_{19}Ti_{49}Cr_{29}Sc_3$ Katalysator (einer der besten Katalysator der vierten Generation) wurde getestet. In dieser Studie wurden sechs verschiedene Experimente mit sechs verschiedenen Zusammensetzungen durchgeführt, wie die Abwesenheit von CO_2, Abwesenheit von CO, Abwesenheit von C_3H_8, 5 vol% O_2, 10 vol% O_2 (Referenz-Konzentration) und 15 vol% O_2. Folgendes stellte sich heraus: in Abwesenheit von CO_2 in der Zufuhr, ist der C_3H_8 Umsatz bei hohen Temperaturen von etwa 350°C nicht betroffen, aber bei niedrigen Temperaturen, etwa 300 °C, ist ca. 14% CO_2 anwesend. Zudem, zeigte die Abwesenheit von CO in der Zufuhr, dass der C_3H_8 Umsatz sich auf 2% erhöht und 0,7 Vol% CO wird produziert. Diese CO Bildung könnte durch die partielle Oxidation von C_3H_8 oder Reduktion des C_3H_8 mit CO_2 entstehen, was noch unklar ist. In Abwesenheit von C_3H_8 in der Zufuhr zeigt sich, dass der CO Umsatz sich um ca. 6% bei 350°C erhöht. Daraus folgt, dass die Anwesenheit von C_3H_8 in der Zufuhr das aktive Zentrum für CO blockiert und die C_3H_8 Oxidation bevorzugt wird. Die Wirkung der O_2 Konzentration in der Zufuhr wurde durch zwei verschiedene O_2-Konzentrationen von jeweils 5 vol.% und 15 vol.% getestet und mit der Referenz Konzentration von 10 vol% verglichen. Es stellte sich heraus, dass die Verringerung der O_2 Konzentration von 10 vol% auf 5 vol%, den C_3H_8 Umsatz um die Hälfte vermindert. Mit der Zunahme des Sauerstoffgehalts auf 15 vol% wird ein sehr hoher Umsatz, 97%, von C_3H_8 auf Kosten der Selektivität erreicht, welches die C_3H_8 Umsatz als Funktion der Sauerstoff-Konzentration in der Zufuhr zur Folge hat.

In anderen Studien, wurde das Wesen der katalytischen Beiträge der drei Metall-Ionen im $Ce_{20}Ti_{50}Cr_{30}$ Katalysator, die Monoxide Ce_{100}, Ti_{100} und Cr_{100} und binären Oxide aller Kombinationen auf ternären Material wie $Ce_{28,6}Ti_{71,4}$, $Ce_{40}Cr_{60}$ und $Ti_{62,5}Cr_{37,5}$ vorbereitet und untersucht. Es wurde festgestellt, dass Ce_{100} leicht aktiv ist und unselektiv. Ti_{100} ist völlig untätig für beide Oxidationen, gefolgt von Cr_{100}, welches etwas für Propanoxidation bei hohen Temperaturen von 350°C aktiv ist, und zeigt den Ursprung der Kohlenwasserstoff-Selektivität. Auf der anderen Seite sind spezifische Oberflächen von Ti_{100} und Cr_{100} im Vergleich zu Ce_{100} Katalysatoren sehr geringer. Daher wurden die Kalzinierungstemperaturen gesenkt und neue Synthesemethoden wurden aufgenommen, um vergleichbare Oberflächen zum Ce_{100} Katalysator zu erhalten. Als Folge dieser neuen Optimierungen, wurde festgestellt, dass Cr_{100} sehr aktiv, aber wenig selektiv für die C_3H_8 Oxidation ist. Ti_{100} erreichte 11% des CO Umsatzes und ist nicht aktiv für die C_3H_8 Oxidation. Interessanterweise, stellte sich heraus, dass für die binären Oxide

$Ti_{62,5}Cr_{37,5}$ das beste Ergebnis für die Propan Verbrennung liefert in Hinsicht auf Aktivität und Selektivität. $Ce_{40}Cr_{60}$ ist aktiv, aber weniger selektiv. $Ce_{28,6}Ti_{71,4}$ zeigte keine Aktivität.

Der Arbeitsfluss wurde für die weitere Optimierung von CeCr und TiCr Katalysatoren fortgesetzt und es gab einige gute Treffer. Schließlich wurde $Ce_{19}Ti_{48,99}Cr_{29}Gd_3Ag_{0,01}$ als sehr aktiver Katalysator und $Ti_{62,5}Cr_{37,5}$ als völlig selektiver Katalysator für die selektive Kohlenwasserstoff Verbrennung ermittelt.

Durch den zufälligen Entwurf von Experimenten erreichten wir das Ziel unseres Projektes und konnten somit die katalytische Leistung effektiv von den Anfangsgenerationen zu den Endgenerationen verbessern. So wurde auf diese Art die gute Reproduzierbarkeit der Hochdurchsatz-Technologie in der herkömmlichen Prüfung bewiesen. Diese Technologie ist geeignet für die schnelle und erfolgreiche Suche nach neuen Katalysatoren.

5 References

[1] Y. Yazawa, N.Takagi, H.Yoshida, S.I.Komai, A. Satsuma, T. Tanaka, S. Yoshida, T. Hattori, Appl. Catal. A 233 (2002) 103.

[2] M. Skoglundh, E. Fridell, Topics in catalysis 28 (2004) 79.

[3] J. Calvert, J. Heywood, R. Sawyer and J. Seinfeld, Science 261 (1993) 37.

[4] R. Heck and R. Farrauto, Appl. Catal. A 221 (2001) 443.

[5] D. Lafyatis, G. Ansell, S. Bennett, J. Frost, P. Millington, R. Rajaram M. Skoglundh and E. Fridell, A. Walker and T. Ballinger, Appl. Catal. B 18 (1998) 123.

[6] J. Kaspar, P. Fornasiero and N. Hickey, Catal. Today 77 (2003) 419.

[7] D. Bosteels and R. Searles, Plat. Met. Rev. 46 (2002) 27.

[8] R. Farrauto and R. Heck, Catal. Today 51 (1999) 351.

[9] Götz Veser, Murtaza Ziauddin, D. Lanny Schmidt, Catal. Today 47 (1999) 219.

[10] F. Cavani, F. Trifiro, Appl. Catal. A 88 (1992) 115.

[11] D. L. Trimm, Appl. Catal. 7 (1983) 249.

[12] K. Arnby, J. Assiks, P. A. Carlsson, A. Palmqvist, M. Skoglundh, J. Catal. 233 (2005) 176.

[13] http://en.wikipedia.org/wiki/European_emission_standards.

[14] K. Otto, J. M. Andino, C. L. Parks, J. Catal. 131 (1991) 243.

[15] C. P. Hubbard, K. Otto, H. S. Gandhi, K. Y. S. Ng, J. Catal. 139 (1993) 268.

[16] A. F. Lee, K. Wilson, R. M. Lambert, C. P. Hubbard, R. G. Hurley, R. W. McCabe, H. S. Gandhi; J. Catal. 184 (1999) 491.

[17] L. Kiwi-Minsker, I. Yuranov, E. Slavinskaia, V. Zaikovskii, A. Renken, Catal. Today 59 (2000) 61.

[18] C.Kokkofitis, G. Karagiannakis, S. Zisekas, M. Stoukides, J. Catal. 234 (2005) 476.

[19] V. R. Choudhary, S. Banerjeee, S. G. Pataskar, Proc. Indian Acad. Sci. (Chem. Sci), 115, (2003) 287.

[20] T. F. Garetto, E. Rincon, C. R. Apesteguia, Appl. Catal. B 48 (2004) 167.

[21] H. Yoshida, Y. Yazawa, T. Hattori, Catal. Today 87 (2003) 19.

[22] Y. Yazawa, H. Yoshida, T. Hattori, Appl. Catal. A 237 (2002) 139.

[23] A. Ishikawa, S. Komai, A.Satsuma, T. Hattori, Y. Murakami, Appl. Catal. A 110 (1994) 61.

[24] R. Burch, E. Halpin, M. Hayes, K. Ruth, J. A. Sullivan 47 (1999) Appl. Catal. B 19 (1998) 199.

[25] C. P. Hubbard, K. Otto, H. S. Gandhi, K. Y. S. Ng, J. Catal. 144 (1993) 484.

[26] H. Wu, L. Liu, S. Yang, Appl. Catal. A 211(2001) 159.

[27]] Y. Yazawa, H. Yoshida, S. Komai, T. Hattori, Appl. Catal. A 233 (2002) 113.

[28] A. Hinz, M. Skoglundh, E. Fridell and A. Anderson, J. Catal. 201 (2001) 247.

[29] T. Huizinga, J. V. Grondelle, R. Prinz, Appl. Catal. 10 (1984) 199.

[30] Y. Li, J. N. Armor, Appl. Catal. B 3 (1994) 275.

[31] C. P. Hubbard, K. Otto, H. S. Gandhi, K. Y. S. Ng, J. Catal. 144 (1993) 484.

[32] U. Rodermerck, D. Wolf, O. V. Buyevskaya, P. Claus, S. Senkan, M. Baerns, Chem. Eng. J. 82 (2001) 3.

[33] J. J. Spivey, Catal. 8 (1989) 157.

[34] M. F. M. Zwinkels, S. G. Järas, P. G. Menon, Catal. Rev. Sci. Eng. 35 (1993) 319.

[35] Y. Marooka, Y. Morikawa, A. Ozaki, J. Catal. 7 (1967) 23.

[36] T. Seiyama, Catal. Rev. Sci. Eng. 34 (1992) 281.

[37] A. Kalantar Neyestanaki, N. Kumar, L. E. Lindfors, Appl. Catal. B Environmental 7 (1995) 95.

[38] R. D. Waters, J. J. Weimer, J. E. Smith, Catal. Lett. 30 (1995) 181.

[39] Y. F. Yu Yao, Ind. Eng. Chem . Prod. Res. Dev. 19 (1980) 293.

[40] A. O’ Malley, B. K. Hodnett, Catal. Today 54 (1999) 31.

[41] A. Schlangen, G. W. Neuhaus, M. Madani, W. F. Maier, J. Prakt. Chem. 334 (1992) 465

[42] G. Buchsa, M. Daturi, E. Finocchio, V. Lorenzelli, G. Ramis, R. J. Willey, Catal. Today 33 (1997) 239.

[43] Y. Yazawa, H. Yoshida, N. Takagi, S. Komai, A.Satsuma, T. Hattori, Applied Catal. B 19 (1998)261.

[44] Y. Yazawa, H. Yoshida, N. Takagi, S. Komai, A.Satsuma, T. Hattori, J. Catal. 187 (1999) 15.

[45] Y. Yazawa, H. Yoshida, N. Takagi, N. Kagi, S. Komai, A.Satsuma, Y. Murakami, T. Hattori, Stud. Surf. Sci. Catal. 130 (2000) 2189.

[46] P. Artizzu, E. Garbowski, M. Primet, Y. Brulle, J. Saint-Just, Catal. Today 47 (1999) 83.

[47] J. J. Spivey, Ind. Eng. Chem. Res. 26 (1987) 2165.

[48] V. D. Sokolovskii, Catal. Rev. Sci. Eng. 32 (1990) 1.

[49] I. Yuranov, N. Dunand, L. Kiwi-Minisker, A.Renken, Appl. Catal. B 36 (2002) 183.

[50] M. O’ Connell, A. K. Normann, C. F. Hüttermann, M. A. Morris, Catal. Today 47 (1999) 123.

[51] A. Törncrona, M. Sköglundh, P. Thormählen, E. Fridell, E. Jobson, Appl. Catal. B 14 (1997) 131.

[52] J. J. Spivey, J. B. Butt, Catal. Today 11 (1992) 465.

[53] Guoqing Guan, R. Zapf, G. Kolb, Y. Men, V. Hessel, H. Loewe, J. Ye, R. Zentel Chem. Commun. 2007, 260.

[54] Jin-Young Luo, Ming Meng, Yu-Qing Zha and Li-Hong Guo, J. Phys.Chem.C 112 (2008) 8694.

[55] S. T. Daniells, A. R. Overweg, M. Makkee, J. A. Moulijn, J. Catal. 230 (2005) 52.

[56] M. C. Kung, R. J. Davis, H. H. Kung, J. Phys. Chem C 111 (2007) 11767.

[57] W. Liu, M. J. Flytzani – Stephanopoulus, J. Catal. 153 (1995) 304.

[58] P. Thormählen, M. Skoglundh, E. Fridell, B. J. Andersson, J. Catal. 188 (1999) 300.

[59] J. W. Saalfrank, W. F. Maier, Angew. Chem. Int. Ed. 43 (2004) 2028.

[60] M. Krämer, T. Schmidt, K. Stöwe, W. F. Maier. Appl. Catal. A. 302 (2006) 257

[61] Y. Zhang-Steenwinkel, L. M. Van der Zande, H. L. Castricum, A. Bliek, R. W. Van der Brink, G. D. Elzinga, Top. Catal. 30/31 (2004) 257.

[62] Y. Zhang-Steenwinkel, H. L. Castricum, J. Beckers, E. Eiser, A. Bliek, J. Catal. 221 (2004) 523.

[63] Y. Zhang-Steenwinkel, J. Beckers, A. Bliek, App. Catal. A 235 (2002) 79.

[64] J. Beckers, G. Rothenberg, Chem. Phys. Chem. 6 (2005) 223.

[65] S. Simino, A. Di Benedetto, R. Pirone, G. Russo, Catal. Today 83 (2003) 33.

[66] T. Maillet, C. Solleau, J. Barbier, D. Duprez, Appl. Catal. B 14 (1997) 85.

[67] J. A. Wang, M. A. Valenzuela, S. Castillo, J. Salmones, M. Poren-Pineda J. Sol-Gel. Sci. Tech. 26 (2003) 879.

[68] David A. Ward, Edmond I. Ko, Ind. Eng. Chem. Res. 34 (1995) 421.

[69] Larry L. Hench, Jon K. West, Chem. Rev. 90 (1990) 33.

[70] G. Frenzer, W. F. Maier, Annu. Rev. Mater.Sci. 36 (2006) 281.

[71] T. J. Barton, L. M. Bull, W. G. Klemperer, D. A. Loy, B. Mcenaney, Chem. Mater. 11 (1999) 2633.

[72] J. M. Thomas, Angew. Chem. Int. Ed. 38 (24) 1999 3588.

[73] H. H. Kung, E. I. Ko, Chem. Eng. J. 64 (1996) 203.

[74] Y. M. Fahmy, J. Saudi, Chem. Soc. 4 (2000) 225.

[75] J. Livage, Curr. Opin. Solid State Mater. Sci. 2 (1997) 132.

[76] R. C. Mehrota, J. Non-Cryst. Solids 145 (1992) 1.

[77] H. Schmidt, J. Non-Cryst. Solids 100 (1988) 51.

[78] R. J. P. Corriu, D. Leclercq, Angew. Chem. Int. Ed. 35 (1996) 1420.

[79] Richard D. Gonzalez, Tessie Lopez, Ricardo Gomez, Cat. Today 35 (1997) 293.

[80] K. Haas-Santo, M. Fichtner, K. Schuber, Appl. Catal. A 220 (2001) 79.

[81] J. Klein, W. F. Maier, Chem. Mater. 11 (1999) 2584.

[82] J. Klein, C. Letmann, W. F. Maier, J. Non-Cryst. Solids 282 (2001) 203.

[83] S. Klein, W. F. Maier, Angew. Chem. Int. Ed. 35 (1996) 2230.

[84] http://www.psrc.usm.edu/mauritz/solgel.html.

[85] Do Kyoung Kim, PhD Thesis, Universität des Saarlandes 2006

[86] C. J. Brinker G. W. Scherer, Sol-Gel Science; The Physics and Chemistry of Sol-Gel Processing, Academic Press, New York, (1990).

[87] J. J. Hanak, J. Mater. Sci. 5 (1970) 964

[88] N. E. Olong, PhD Thesis, Universität des Saarlandes 2008

[89] Ken D. Schimizu, Mark L. Snapper, Amir H. Hoveyda, Chem. Eur. J 4 (1998) 1885.

[90] W. F. Maier, K. Stöwe, S. Sieg, Angew. Chem. Int. Ed. 46 (2007) 6016.

[91] Guido Kirsten, W. F. Maier, Applied surface science 223 (2004) 87.

[92] B. Jandeleit, D. J. Schaefer, T. S. Powers, H. W. Turner, W. H. Weinberg, Angew. Chem. Int. Ed. 38 (1999) 2532.

[93] J. Scheidtmann, P. A. Weiß, W. F. Maier, Appl. Catal. A 222 (2001) 79.

[94] R. Potyrailo, W. F. Maier, Combinatorial and High Throughput Discovery and Optimization of Catalysts and Materials, Taylor and Francis, Boca Raton, FL, 2007.

[95] O. Trapp, J. Chromatography A 1184 (2008) 160.

[96] B. Jandeleit, D.J. Schaefer, T. S. Powers, H. W. Turner, W. H. Weinberg, Angew. Chem. Int. Ed. 38 (1999) 2494.

[97] Selim Senkan, Angew. Chem. Int. Ed. 40 (2001) 312.

[98] A. Mittasch, Adv. Catal. 2 (1950) 81.

[99] P. Cong, R. D. Doolen, Q. Fan, D. M. Giaquinta, S. Guan, E. W. Mcfarland, D. M. Poojary, K. Self, H. W. Turner, W. H. Weinberg, Angew. Chem. 111 (1999) 508; Angew. Chem. Int. Ed. 38 (1999) 484.

[100] N. Katada, M. Niwa, Chem. Vap. Dep. 2 (1996) 125.

[101] T. Miyao, I. Shishikura, M. Matsuoka, M. Nagai, Chem. Lett. 121 (1996) 561.

[102] M. B. Kizling, S. G. Jaras, Appl. Catal. A 147 (1996) 1.

[103] G. P. Vossokov, P. S. Pirgov, Appl. Catal. A 168 (1998) 229.

[104] Y. J. Kim, K. Gao, G. A. Chambers, Surf. Sci. 371 (1997) 358.

[105] A. A. Gorbunov, W. Pompe, A. Sewing, S. V. Gapanov, A. D. Akhsakhalyan, I. G. Zabrodin, I. A. Kaskow, E. B. Klyenkow, A. P. Mozorov, N. N. Salashcenko, R. Dietsch, H. Mai, S. Vollmar, Appl. Surf. Sci. (1996) 649.

[106] R. E. Russo, X. L. Mao, D. L. Perry, Chem. Tech. 12 (1994) 14.

[107] S. Marshall, Res. Dev. 40 (1998) 32.

[108] E. Reddington, A. Sapienza, B. Guraou, R. Viswanathan, S. Sarangapani, E. S. Smotkin, T. E. Mallouk, Science 280 (1998) 1735.

[109] C. Hoffman, A. Wolf, F. Schüth, Angew. Chem. 111 (1999) 2971.

[110] W. F. Maier, J. Martens, S. Klein, J. Heilmans, R. Parton, K. Vercruysse, P. Jacobs, Angew. Chem. Int. Ed. 35 (1996) 180.

[111] J. N. Cawse, Acc. Chem. Res. 34 (2001) 213.

[112] A. C. Cooper, L. H. McAlexander, D. –H. Lee, M. T. Torres, R. H. Crabtree, J. Am. Chem. Soc. 120 (1998) 9971; R. H. Crabtree, Chem. Tech 29 (1999) 231.

[113] F. C. Moates, M. Somani, M. Annamalai, J.T. Richardson, D. Luss, R. C. Wilson, Ind. Eng. Chem. Res. 34 (1996) 4801.

[114] A. Holzwarth, P. W. Schmidt, W. F. Maier, Angew. Chem. 110 (1998) 2788; Angew. Chem. Int. Ed. 37 (1998) 2644.

[115] H. Su, E. S. Yeung, J. Am. Chem. Soc. 122 (2000) 7422.

[116] S. Senkan, Nature 394 (1998) 350.

[117] P. Cong, A. Dehestani, R. Doolean, D. M. Giaquinta, S. Guan, V. Markov, D. Poojary, K. Self, H. W. Turner, W. H. Weinberg, Proc. Natl Acad. Sci. USA 96 (1999) 11077

[118] R. Vijay, R. Hendershot, W. B. Rogers, B. J. Feist, C. M. Snively, J. Lauterbach, Cat. Comm. 6 (2005) 167

[119] R. Vijay, C. M. Snively, J. Lauterbach, J. Catal. 243 (2006) 368.

[120] Y. Yamada, T. Kobayashi, J. Japan Petroleum Inst. 49 (2006) 157.

[121] A. R. Cornolly, J. D. Sutherland, Angew. Chem. 112 (2000) 4438; Angew. Chem. Int. Ed. 39 (2000) 4268.

[122] M. Orschell, J. Klein, H. W. Schmidt, W. F. Maier, Angew. Chem. Int. Ed. 38 (1999) 2791.

[123] P. Claus, D. Hönicke, T. Zeck, Cat. Today 76 (2001) 319.

[124] P. Claus, M. Lucas, Appl. Catal. A 254 (2003) 35.

[125] C. Mirodatos, Y. Schurmann, C. Hayayud, A. Holzwarth, D. Farusseng, T. Richter, European Patent (2003) 1293772.

[126] C. Hoffman, H. W. Schmidt, F. Schüth, J. Catal.. 198 (2001) 348.

[127] O. Lavastre, I. Illitchev, G. Jegou, P. H. Dixneuf, J. Am. Chem. Soc. 124 (2002) 5278.

[128] A. Corma, J. M. Serra, P. Serna, E. Argente, S. Valero, V. Botti, J. Catal. 229 (2005) 513.

[129] Y. Yamada, A. Ueda, Z. Zhao, T. Maekawa, K. Suzuki, T. Tkada, T. Kobayashi, Cat. Today, 67 (2001) 379.

[130] U. Rodermerck, P. Ignaszewski, M. Lucas, P. Claus, M. Baerns, Chem. Ing. Tech. 71 (1999) 872

[131] L. Vegvari, A. Tomposb, S. Göbölos, J. Margitfalvi, Cat. Today 81 (2003) 517.

[132] J. Klein, T. Zech, J. N. Newsam, S. A. Schunk, Appl. Catal. A 254 (2003) 121.

[133] L. Weber, S. Wallbaum, C. Broger, K. Gubernator, Angew. Chem. 107 (1995) 2452; Angew. Chem. Int. Ed. 34 (1995) 2280.

[134] J. Singh, M. A. Ator, E. P. Jaeger, M. P. Allen, D. A. Whipple, J. E. Soloweij, S. Choudhary, A. M. Treasurywala, J. Am. Chem. Soc. 118 (1996) 1669.

[135] D. Wolf, O. Buyevskaya, M. Baerns, Appl. Catal. A 200 (2000) 63.

[136] J. M. Serra, A. Chica, A. Corma, Appl. Catal. A 239 (2003) 35.

[137] Y. Yamada, A. Ueda, I. Nakagawa, T. Kobayashi, Res. Chem. Intermed 28 (2002) 397.

[138] C. Klanner, D. Farrusseng, L. Baumes, C. Miradatos, F. Schüth, QSAR Comb. Sci. 22 (2003) 729.

[139] J. Scheidtmann, J. W. Saalfrank, W. F. Maier, Stud. Surf. Sci. Catal. 145 (2003) 13.

[140] J. Scheidtmann, PhD thesis, Universität des Sarrlandes, 2003.

[141] A. Holzwarth and W. F. Maier, Platinum Metals Rev., 44 (2000) 16.

[142] G. Kirsten and W. F. Maier, High-Throughput Screening in Chemical Catalysis, (2004) 175.

[143] S. Sieg, PhD Thesis, Universität des Saarlandes, 2007.

[144] S. Sieg, B. Stutz, T. Schmidt, F. Hamprecht, W. F. Maier, J. Mol. Model 12 (2006) 611.

[145] J. Klein, PhD thesis, Universität des Saarlandes 2001.

[146] C. Letmann, PhD Thesis, Universität des Saarlandes 2005.

[147] A. Trovarelli, Catal. Rev. Sci.Eng. 38 (1996) 439.

[148] C. C. Chen, M. M. Nasarallah, H. U. Anderson, J. Electrochem. Soc. 140 (1993)3555.

[149] M. Krämer, M. Duisberg, K. Stöwe, W.F. Maier, J. Catal. 251 (2007) 410.

[150] D. K. Kim, W. F. Maier, J. Catal. 238 (2006) 142.

[151] TOPAS, Version 2.1, Bruker AXS, Karlsruhe

[152] R. W. Cheary, A. A. Coelho, J. Appl. Cryst.25 (1992) 109.

6 Appendix

6.1 Nomenclatures

ANN	Artificial neural networks
BET	Brunauer, Emmet and Teller method
BJH	Barret, Joyner and Halenda method
°C	Degree centigrade
D	Dopant
DOE	Design of experiment
ec-IRT	Emissivity corrected infrared thermography
EG	Ethylene glycol
EPA	Environmental protection agency
g	gram
GA	Genetic algorithms
GC	Gas chromatography
h	Hour
HC	Hydrocarbons
HPLC	High pressure liquid chromatography
HT	High throughput
IR	Infrared
°K	Degree kelvin
KB	Complexing agent
LIFI	Laser induced fluorescence imaging
MFC	Mass flow controller
MEMS	Micro electro mechanical systems
µl	Microliter
µm	Micrometer
µmole	Micromole
mg	Milligram
min	Minute
Mol%	Mole percent
MS	Mass spectrometry

MSC	Multi sampling concept
NO_x	Nitrogen oxides
PM	Particulate matter
PTD	Photothermal deflection
REMPI	Resonance enhanced multiphoton ionisation
rpm	Revolution per minute
s	Seconds
SULEV	Super low emission vehicles
TEOS	Tetraethoxysilane
TMOS	Tetramethoxysilane
Θ	Theta
Vol%	Volume percent
Wt%	Weight percent
XRD	X-ray diffractometry
ZEV	Zero emission vehicles

6.2 List of chemicals used

Chemical	**Supplier**	**Chemical**	**Supplier**
$AgNO_3$	ABCR	$Mo[OCH(CH_3)_2]_5$	Alfa Aesar
$Al(NO_3)_3 . 9 H_2O$	Alfa Aesar	$NaNO_3$	Merck
$AuCl_3$	Degussa	$NbCl_5$	Alfa Aesar
$BaCl_2$	Unknown	$Nd(NO_3)_3 . 6 H_2O$	Aldrich
$Bi[OOCCH(C_2H_5)C_4H_9]_3$	Stem	$Ni(NO_3)_2 . 6 H_2O$	Merck
$Ca(NO_3)_2 . 4 H_2O$	Merck	$Pd(CH_3COO)_2$	Unknown
$Cd(NO_3)_2 . 4 H_2O$	Fluka	$PtBr_4$	Alfa Aesar
$Ce(NO_3)_3 . 6 H_2O$	Fluka	$Rb[CH_3COCHCOCH_3]$	Aldrich
CeO_2	Aldrich	$ReCl_5$	Aldrich
$Co(NO_3)_2 . 6 H_2O$	Merck	$RhCl_3 . 3 H_2O$	Aldrich
$Cr(NO_3)_2 . 6 H_2O$	Riedel	$RuCl_3 . x H_2O$	Aldrich
Cr_2O_3	ABCR	$SbCl_3$	J. T. Baker
CsCl	Unknown	$Sc(NO_3)_3 . 5 H_2O$	Alfa Aesar
$Cu(NO_3)_2 . 3 H_2O$	Fluka	Se Säure	Aldrich
$Dy(NO_3)_3 . 5 H_2O$	Aldrich	$Si(OC_2H_5)_4$	Acros Organics
$Er(NO_3)_3 . 5 H_2O$	Aldrich	$Sm(NO_3)_3 . 6 H_2O$	Aldrich
$Eu(NO_3)_3 . 6 H_2O$	Strem	$SnCl_2 . 2 H_2O$	Aldrich
$Fe(NO_3)_3 . 9 H_2O$	Riedel	$SrCl_2 . 6 H_2O$	Merck
$Ga(NO_3)_3 . x H_2O$	Aldrich	$Ta(OC_2H_5)_5$	ABCR
$Gd(NO_3)_3 . 6 H_2O$	Aldrich	$Tb(NO_3)_3 . x H_2O$	Alfa Aesar
$Ge[OCH(CH_3)_2]_4$	Aldrich	$TeCl_4$	Aldrich
$HfCl_4$	Aldrich	$Ti[OCH(CH_3)_2]_4$	ABCR
$Ho(NO_3)_3 . 5 H_2O$	Strem	TiO_2	Aldrich
$In(NO_3)_3 . 5 H_2O$	Chempur	$Ti(O\text{-}nBu)_4$	Alfa Aesar
$IrCl_4 . H_2O$	Johnson Matthey	$Tm(NO_3)_3 . 6 H_2O$	ABCR
KNO_3	ABCR	$VO[OCH(CH_3)_2]_3$	ABCR
$La(NO_3)_3 . 6 H_2O$	Fluka	WCl_6	Fluka
$LiNO_3$	Fluka	$Y(NO_3)_3 . 6 H_2O$	Aldrich
$Lu(NO_3)_3 . x H_2O$	Aldrich	$Yb(NO_3)_3 . x H_2O$	ABCR
$Mg(NO_3)_2 . 4 H_2O$	Merck	$Zn(NO_3)_2 . 6 H_2O$	Avocado
$Mn(NO_3)_2 . 4H_2O$	Merck	$ZrO(NO_3)_2 . x H_2O$	Alfa Aesar

Chemical	Supplier	Chemical	Supplier
4-Hydroxy-4-methyl-2-pentanone	ABCR	Iso-propanol	Unknown
Ethylene glycol	Alfa Aesar	n-Butanol	Stem
HCl (37%)	Merck	Propionic acid	Merck
HNO_3 (65%)	Degussa		

Table 6-1 List of chemicals used

6.3 Equipment and software used

Description	**Classification**	**Manufacturer**
Pipetting robot	Lissy	Zinsser Analytic
Orbital shaker	Titramax 100	Heidolph Instrument
Muffle furnace	Controller S27	Nabertherm
Muffle furnace		Carbolite
Muffle furnace		Carbolite
Physisorption equipment	Carlo Erba Sorptomatic 1990	Fision Instruments
X-ray measurement	G670	Huber Guinier
Infrared camera	PtSi 640 x 480, PtSi 256 x 256	Thermosensorik
Infrared reactor		Uni des Saarlandes
Magnetic valve		Herion
Magnetic valve controller unit		Uni des Saarlandes
Mass flow controller	Mass-Flo	MKS Instruments, Bronkhorst Hi-Tec
Mass flow controller unit		MKS Instuments, Bronkhorst Hi-Tec
Temperature controller	dTron 16.1, dicon-401	Jumo
Gas measurement computer	GMA 300	GfG
CO_2 gas transmitter	IR 24	GfG
CO gas transmitter	IR 24	GfG
C_3H_8 gas transmitter	IR 24	GfG
Multimeter	VC 140	Voltcraft
Robot software	Zinsser REDI	Zinsser Analytic
Software	Plattenbau	J. Scheidtmann
IR camera software	IR Testrig	J. Scheidtmann
Gas measurement computer software	GMAPC Interface v 3.50	GfG

Table 6-2 **List of equipment and software used**

6.4 Library filling plan

The figure 6-1 shows the library filling plan of all libraries. x and y corresponds to the respective position of the catalyst (molar ratios of different metal components).

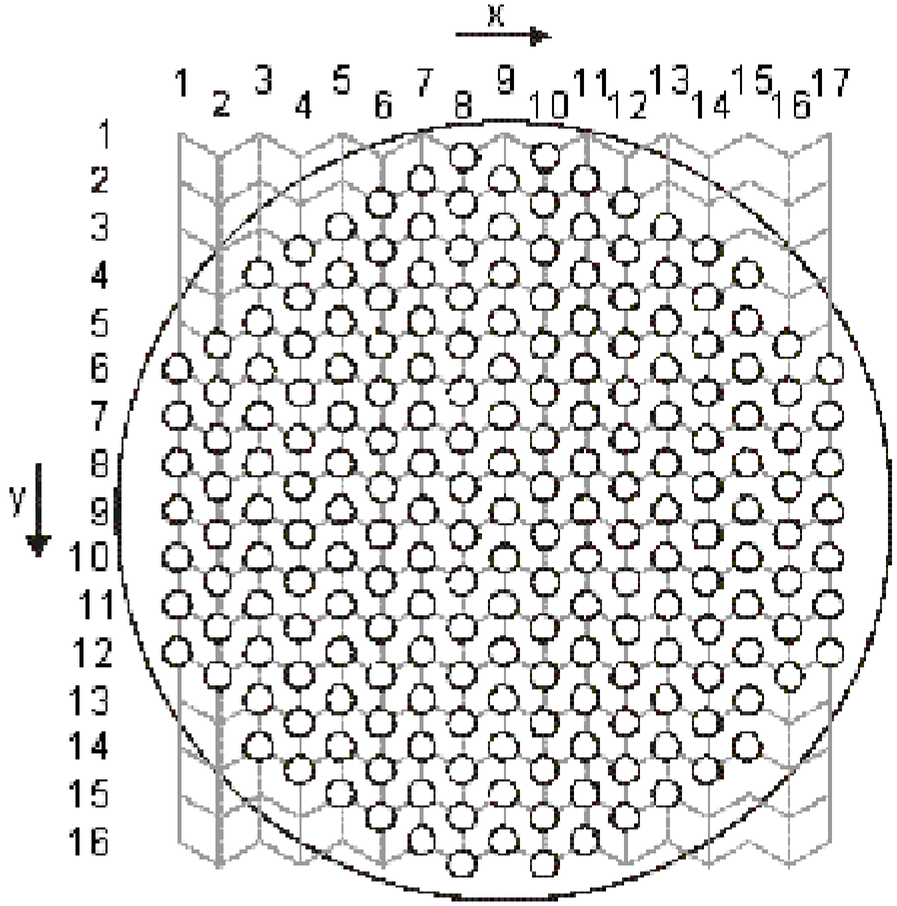

Figure 6-1: Library filling plan

X	Y	Catalyst	X	Y	Catalyst	X	Y	Catalyst
1	6	$W_{33,3}Ce_{33,3}Ti_{33,3}$	5	14	Blank	9	4	Blank
1	7	Blank	5	15	$W_{33,3}Ce_{33,3}V_{33,3}$	9	5	$Mn_{33,3}Sm_{33,3}Ti_{33,3}$
1	8	$Hf_{33,3}Ce_{33,3}Mn_{33,3}$	6	2	$Ce_{50}Hf_{50}$	9	6	$W_{33,3}Hf_{33,3}Ti_{33,3}$
1	9	$Cu_{33,3}Fe_{33,3}Ce_{33,3}$	6	3	$Zr_{33,3}Mn_{33,3}Sm_{33,3}$	9	7	$Ni_{33,3}Ce_{33,3}V_{33,3}$
1	10	$W_{33,3}Ni_{33,3}V_{33,3}$	6	4	$Ti_{50}Hf_{50}$	9	8	$Ni_{50}Hf_{50}$
1	11	$Ce_{50}Sm_{50}$	6	5	$Cr_{33,3}Zr_{33,3}Sm_{33,3}$	9	9	Blank
1	12	$Fe_{33,3}Ce_{33,3}Sm_{33,3}$	6	6	$W_{33,3}Ni_{33,3}Cr_{33,3}$	9	10	Blank
2	5	$Ti_{50}Cr_{50}$	6	7	$Hf_{33,3}Ni_{33,3}Ti_{33,3}$	9	11	$Hf_{33,3}Ni_{33,3}Sm_{33,3}$
2	6	$Ni_{33,3}Cr_{33,3}V_{33,3}$	6	8	$Cr_{33,3}Ce_{33,3}Mn_{33,3}$	9	12	$Cr_{33,3}Ce_{33,3}Sm_{33,3}$
2	7	$Mn_{50}Hf_{50}$	6	9	$W_{33,3}Cr_{33,3}Ce_{33,3}$	9	13	$Hf_{33,3}Ni_{33,3}Ce_{33,3}$
2	8	$Zr_{33,3}Sm_{33,3}Ti_{33,3}$	6	10	$Hf_{33,3}Cr_{33,3}V_{33,3}$	9	14	$W_{33,3}Hf_{33,3}Sm_{33,3}$
2	9	$Hf_{33,3}Ni_{33,3}Zr_{33,3}$	6	11	$Ce_{33,3}Mn_{33,3}Ti_{33,3}$	9	15	$Hf_{33,3}V_{33,3}Sm_{33,3}$
2	10	$Cr_{33,3}Mn_{33,3}Sm_{33,3}$	6	12	$Sm_{50}Hf_{50}$	9	16	$Ce_{99}Rh_{1}$
2	11	Blank	6	13	$Cr_{33,3}V_{33,3}Mn_{33,3}$	10	1	$Hf_{33,3}Cr_{33,3}Ce_{33,3}$
2	12	$W_{33,3}Hf_{33,3}V_{33,3}$	6	14	Blank	10	2	$Cr_{33,3}Ce_{33,3}Ti_{33,3}$
3	4	$W_{33,3}Zr_{33,3}Mn_{33,3}$	6	15	$Hf_{33,3}Zr_{33,3}Mn_{33,3}$	10	3	$Hf_{33,3}Ni_{33,3}V_{33,3}$
3	5	$Ni_{33,3}Ce_{33,3}Sm_{33,3}$	7	2	Blank	10	4	$Ni_{33,3}V_{33,3}Sm_{33,3}$
3	6	Blank	7	3	$W_{33,3}Hf_{33,3}Zr_{33,3}$	10	5	$Hf_{33,3}Zr_{33,3}Ce_{33,3}$
3	7	$Hf_{33,3}Cr_{33,3}Ti_{33,3}$	7	4	$Zr_{33,3}Ce_{33,3}Mn_{33,3}$	10	6	$W_{50}Zr_{50}$
3	8	Blank	7	5	$Ni_{33,3}Zr_{33,3}Ce_{33,3}$	10	7	$Hf_{33,3}Ce_{33,3}V_{33,3}$
3	9	$W_{33,3}Mn_{33,3}Sm_{33,3}$	7	6	$Ni_{33,3}Zr_{33,3}Mn_{33,3}$	10	8	Blank
3	10	Blank	7	7	$Co_{40}Ce_{60}$	10	9	$Zr_{50}Hf_{50}$
3	11	$Hf_{33,3}Zr_{33,3}Sm_{33,3}$	7	8	$Hf_{33,3}Cr_{33,3}Sm_{33,3}$	10	10	$Ni_{97}Na_{3}$
3	12	$Zr_{33,3}V_{33,3}Mn_{33,3}$	7	9	$Ti_{50}Mn_{50}$	10	11	$W_{33,3}Ni_{33,3}Ti_{33,3}$
3	13	$Cr_{50}W_{50}$	7	10	Blank	10	12	$Ce_{50}Mn_{50}$
3	14	$Ni_{15}Ce_{85}$	7	11	$W_{33,3}Hf_{33,3}Ni_{33,3}$	10	13	$V_{50}Hf_{50}$
4	3	$Cr_{50}Sm_{50}$	7	12	$Ni_{33,3}Cr_{33,3}Sm_{33,3}$	10	14	$Ni_{33,3}Cr_{33,3}Ce_{33,3}$
4	4	$Ni_{95}Fe_{5}$	7	13	$Ce_{33,3}V_{33,3}Ti_{33,3}$	10	15	$Mn_{50}V_{50}$
4	5	$Hf_{33,3}Ni_{33,3}Cr_{33,3}$	7	14	$Ni_{50}Zr_{50}$	10	16	$Ni_{33,3}Zr_{33,3}Ti_{33,3}$
4	6	$W_{33,3}Ni_{33,3}Mn_{33,3}$	7	15	$W_{33,3}Cr_{33,3}Mn_{33,3}$	11	2	$Ce_{50}Zr_{50}$
4	7	$Zr_{33,3}V_{33,3}Sm_{33,3}$	7	16	$W_{33,3}Sm_{33,3}Ti_{33,3}$	11	3	$Hf_{33,3}Mn_{33,3}Sm_{33,3}$
4	8	$V_{50}Sm_{50}$	8	1	$Cr_{33,3}Zr_{33,3}Ti_{33,3}$	11	4	$Ce_{33,3}V_{33,3}Sm_{33,3}$
4	9	$W_{50}V_{50}$	8	2	$Ni_{33,3}Ce_{33,3}Mn_{33,3}$	11	5	Blank
4	10	Blank	8	3	$Ce_{33,3}Sm_{33,3}Ti_{33,3}$	11	6	$Mn_{50}Zr_{50}$
4	11	$W_{33,3}V_{33,3}Sm_{33,3}$	8	4	$Zr_{50}V_{50}$	11	7	$Ce_{33,3}Mn_{33,3}Sm_{33,3}$
4	12	$Hf_{33,3}Sm_{33,3}Ti_{33,3}$	8	5	$W_{33,3}Mn_{33,3}Ti_{33,3}$	11	8	Blank
4	13	$Ni_{33,3}V_{33,3}Ti_{33,3}$	8	6	$Ce_{50}Ti_{50}$	11	9	$W_{33,3}V_{33,3}Mn_{33,3}$
4	14	$Ti_{50}Sm_{50}$	8	7	$W_{33,3}Zr_{33,3}Ti_{33,3}$	11	10	$Ce_{33,3}V_{33,3}Mn_{33,3}$
5	3	$Ni_{70}Ce_{30}$	8	8	Blank	11	11	$Hf_{33,3}V_{33,3}Ti_{33,3}$
5	4	$Cr_{33,3}V_{33,3}Sm_{33,3}$	8	9	Blank	11	12	$Cr_{33,3}Ce_{33,3}V_{33,3}$
5	5	$W_{33,3}Cr_{33,3}Ti_{33,3}$	8	10	$Cr_{50}Zr_{50}$	11	13	Blank
5	6	$Ce_{50}Ni_{50}$	8	11	Blank	11	14	Blank
5	7	$Hf_{33,3}V_{33,3}Mn_{33,3}$	8	12	$W_{50}Hf_{50}$	11	15	$W_{33,3}V_{33,3}Ti_{33,3}$
5	8	$Ni_{50}Cr_{50}$	8	13	$Ni_{33,3}Cr_{33,3}Zr_{33,3}$	11	16	$Zr_{33,3}Mn_{33,3}Ti_{33,3}$
5	9	Blank	8	14	Blank	12	2	$W_{33,3}Cr_{33,3}V_{33,3}$
5	10	$Ni_{33,3}Sm_{33,3}Ti_{33,3}$	8	15	$V_{33,3}Mn_{33,3}Ti_{33,3}$	12	3	$W_{33,3}Ni_{33,3}Ce_{33,3}$
5	11	$Mn_{50}Cr_{50}$	8	16	$Ni_{50}V_{50}$	12	4	$Ni_{50}Sm_{50}$
5	12	Blank	9	2	$Cr_{50}V_{50}$	12	5	$W_{33,3}Zr_{33,3}Ce_{33,3}$
5	13	$Ce_{50}W_{50}$	9	3	Blank	12	6	$Cr_{33,3}Sm_{33,3}Ti_{33,3}$

X	Y	Catalyst	X	Y	Catalyst	X	Y	Catalyst
12	7	$Ti_{50}Zr_{50}$	13	14	$Cr_{33,3}Zr_{33,3}Ce_{33,3}$	15	10	$Cu_{50}Ce_{50}$
12	8	$Zr_{33,3}V_{33,3}Ti_{33,3}$	13	15	$Ni_{70}Ce_{30}$	15	11	$Hf_{33,3}Zr_{33,3}Ti_{33,3}$
12	9	$Mn_{50}W_{50}$	14	3	$Hf_{33,3}Ni_{33,3}Mn_{33,3}$	15	12	$Cr_{33,3}V_{33,3}Ti_{33,3}$
12	10	$W_{33,3}Ni_{33,3}Zr_{33,3}$	14	4	$Ti_{50}V_{50}$	15	13	$Ce_{50}V_{50}$
12	11	$Ti_{50}W_{50}$	14	5	$Hf_{33,3}Zr_{33,3}V_{33,3}$	15	14	$W_{33,3}Cr_{33,3}Sm_{33,3}$
12	12	$Zr_{33,3}Ce_{33,3}Sm_{33,3}$	14	6	$W_{33,3}Hf_{33,3}Mn_{33,3}$	16	5	$Hf_{33,3}Mn_{33,3}Ti_{33,3}$
12	13	$W_{33,3}Zr_{33,3}V_{33,3}$	14	7	Blank	16	6	$Ce_{50}Cr_{50}$
12	14	$Hf_{33,3}Cr_{33,3}Mn_{33,3}$	14	8	$Ni_{33,3}V_{33,3}Mn_{33,3}$	16	7	$W_{50}Sm_{50}$
12	15	$W_{33,3}Hf_{33,3}Cr_{33,3}$	14	9	Blank	16	8	$W_{33,3}Ce_{33,3}Mn_{33,3}$
13	3	Blank	14	10	$Zr_{50}Sm_{50}$	16	9	$Mn_{50}Sm_{50}$
13	4	$Ni_{33,3}Mn_{33,3}Ti_{33,3}$	14	11	Blank	16	10	$V_{33,3}Mn_{33,3}Sm_{33,3}$
13	5	$Zr_{33,3}Ce_{33,3}Ti_{33,3}$	14	12	$W_{33,3}Zr_{33,3}Sm_{33,3}$	16	11	$W_{33,3}Hf_{33,3}Ce_{33,3}$
13	6	$Hf_{33,3}Ce_{33,3}Ti_{33,3}$	14	13	$Ni_{33,3}Ce_{33,3}Ti_{33,3}$	16	12	$Hf_{33,3}Cr_{33,3}Zr_{33,3}$
13	7	$Cr_{33,3}Zr_{33,3}V_{33,3}$	14	14	$Cr_{50}Hf_{50}$	17	6	$W_{33,3}Ce_{33,3}Sm_{33,3}$
13	8	$V_{33,3}Sm_{33,3}Ti_{33,3}$	15	4	$Ni_{33,3}Zr_{33,3}Sm_{33,3}$	17	7	$W_{33,3}Cr_{33,3}Zr_{33,3}$
13	9	Blank	15	5	$Cr_{33,3}Mn_{33,3}Ti_{33,3}$	17	8	$Ni_{33,3}Cr_{33,3}Mn_{33,3}$
13	10	$Cr_{33,3}Zr_{33,3}Mn_{33,3}$	15	6	Blank	17	9	$Zr_{33,3}Ce_{33,3}V_{33,3}$
13	11	$Ni_{33,3}Cr_{33,3}Ti_{33,3}$	15	7	$Ni_{33,3}Mn_{33,3}Sm_{33,3}$	17	10	Blank
13	12	$Ni_{33,3}Zr_{33,3}V_{33,3}$	15	8	$Ni_{50}W_{50}$	17	11	$Ti_{50}Ni_{50}$
13	13	$Ni_{50}Mn_{50}$	15	9	$Al_{99}Rh_1$	17	12	$Hf_{33,3}Ce_{33,3}Sm_{33,3}$

Table 6-3 Library 01 filling plan

X	**Y**	**Catalyst**	**X**	**Y**	**Catalyst**	**X**	**Y**	**Catalyst**
1	6	$Ce_{5}Co_{95}$	5	14	$Ce_{60}Fe_{40}$	9	4	$Cu_{15}Fe_{85}$
1	7	$Ce_{10}Co_{90}$	5	15	$Ce_{65}Fe_{35}$	9	5	$Cu_{20}Fe_{80}$
1	8	$Ce_{15}Co_{85}$	6	2	$Ce_{70}Fe_{30}$	9	6	$Cu_{25}Fe_{75}$
1	9	$Ce_{20}Co_{80}$	6	3	$Ce_{75}Fe_{25}$	9	7	$Cu_{30}Fe_{70}$
1	10	$Ce_{25}Co_{75}$	6	4	$Ce_{80}Fe_{20}$	9	8	$Cu_{35}Fe_{65}$
1	11	$Ce_{30}Co_{70}$	6	5	$Ce_{85}Fe_{15}$	9	9	Blank
1	12	$Ce_{35}Co_{65}$	6	6	$Ce_{90}Fe_{10}$	9	10	$Cu_{40}Fe_{60}$
2	5	$Ce_{40}Co_{60}$	6	7	$Ce_{95}Fe_{5}$	9	11	$Cu_{45}Fe_{55}$
2	6	$Ce_{45}Co_{55}$	6	8	$Ce_{5}Ni_{95}$	9	12	$Cu_{50}Fe_{50}$
2	7	$Ce_{50}Co_{50}$	6	9	$Ce_{10}Ni_{90}$	9	13	$Cu_{55}Fe_{45}$
2	8	$Ce_{55}Co_{45}$	6	10	$Ce_{15}Ni_{85}$	9	14	$Cu_{60}Fe_{40}$
2	9	$Ce_{60}Co_{40}$	6	11	$Ce_{20}Ni_{80}$	9	15	$Cu_{65}Fe_{35}$
2	10	$Ce_{65}Co_{35}$	6	12	$Ce_{25}Ni_{75}$	9	16	$Cu_{70}Fe_{30}$
2	11	$Ce_{70}Co_{30}$	6	13	$Ce_{30}Ni_{70}$	10	1	$Cu_{75}Fe_{25}$
2	12	$Ce_{75}Co_{25}$	6	14	$Ce_{35}Ni_{65}$	10	2	$Cu_{80}Fe_{20}$
3	4	$Ce_{80}Co_{20}$	6	15	$Ce_{40}Ni_{60}$	10	3	$Cu_{85}Fe_{15}$
3	5	$Ce_{85}Co_{15}$	7	2	$Ce_{45}Ni_{55}$	10	4	$Cu_{90}Fe_{10}$
3	6	$Ce_{90}Co_{10}$	7	3	$Ce_{50}Ni_{50}$	10	5	$Cu_{95}Fe_{5}$
3	7	$Ce_{95}Co_{5}$	7	4	$Ce_{55}Ni_{45}$	10	6	$Fe_{5}Co_{95}$
3	8	$Ce_{5}Cu_{95}$	7	5	$Ce_{60}Ni_{40}$	10	7	$Fe_{10}Co_{90}$
3	9	$Ce_{10}Cu_{90}$	7	6	$Ce_{65}Ni_{35}$	10	8	$Fe_{15}Co_{85}$
3	10	$Ce_{15}Cu_{85}$	7	7	$Ce_{70}Ni_{30}$	10	9	$Fe_{20}Co_{80}$
3	11	$Ce_{20}Cu_{80}$	7	8	$Ce_{75}Ni_{25}$	10	10	$Fe_{25}Co_{75}$
3	12	$Ce_{25}Cu_{75}$	7	9	$Ce_{80}Ni_{20}$	10	11	$Fe_{30}Co_{70}$
3	13	$Ce_{30}Cu_{70}$	7	10	$Ce_{85}Ni_{15}$	10	12	$Fe_{35}Co_{65}$
3	14	$Ce_{35}Cu_{65}$	7	11	$Ce_{90}Ni_{10}$	10	13	$Fe_{40}Co_{60}$
4	3	$Ce_{40}Cu_{60}$	7	12	$Ce_{95}Ni_{5}$	10	14	$Fe_{45}Co_{55}$
4	4	$Ce_{45}Cu_{55}$	7	13	$Cu_{5}Co_{95}$	10	15	$Fe_{50}Co_{50}$
4	5	$Ce_{50}Cu_{50}$	7	14	$Cu_{10}Co_{90}$	10	16	$Fe_{55}Co_{45}$
4	6	$Ce_{55}Cu_{45}$	7	15	$Cu_{15}Co_{85}$	11	2	$Fe_{60}Co_{40}$
4	7	$Ce_{60}Cu_{40}$	7	16	$Cu_{20}Co_{80}$	11	3	$Fe_{65}Co_{35}$
4	8	$Ce_{65}Cu_{35}$	8	1	$Cu_{25}Co_{75}$	11	4	$Fe_{70}Co_{30}$
4	9	$Ce_{70}Cu_{30}$	8	2	$Cu_{30}Co_{70}$	11	5	$Fe_{75}Co_{25}$
4	10	$Ce_{75}Cu_{25}$	8	3	$Cu_{35}Co_{65}$	11	6	$Fe_{80}Co_{20}$
4	11	$Ce_{80}Cu_{20}$	8	4	$Cu_{40}Co_{60}$	11	7	$Fe_{85}Co_{15}$
4	12	$Ce_{85}Cu_{15}$	8	5	$Cu_{45}Co_{55}$	11	8	$Fe_{90}Co_{10}$
4	13	$Ce_{90}Cu_{10}$	8	6	$Cu_{50}Co_{50}$	11	9	$Fe_{95}Co_{5}$
4	14	$Ce_{95}Cu_{5}$	8	7	$Cu_{55}Co_{45}$	11	10	$Ni_{5}Co_{95}$
5	3	$Ce_{5}Fe_{95}$	8	8	$Cu_{60}Co_{40}$	11	11	$Ni_{10}Co_{90}$
5	4	$Ce_{10}Fe_{90}$	8	9	$Cu_{65}Co_{35}$	11	12	$Ni_{15}Co_{85}$
5	5	$Ce_{15}Fe_{85}$	8	10	$Cu_{70}Co_{30}$	11	13	$Ni_{20}Co_{80}$
5	6	$Ce_{20}Fe_{80}$	8	11	$Cu_{75}Co_{25}$	11	14	$Ni_{25}Co_{75}$
5	7	$Ce_{25}Fe_{75}$	8	12	$Cu_{80}Co_{20}$	11	15	$Ni_{30}Co_{70}$
5	8	$Ce_{30}Fe_{70}$	8	13	$Cu_{85}Co_{15}$	11	16	$Ni_{35}Co_{65}$
5	9	$Ce_{35}Fe_{65}$	8	14	$Cu_{90}Co_{10}$	12	2	$Ni_{40}Co_{60}$
5	10	$Ce_{40}Fe_{60}$	8	15	$Cu_{95}Co_{5}$	12	3	$Ni_{45}Co_{55}$
5	11	$Ce_{45}Fe_{55}$	8	16	Blank	12	4	$Ni_{50}Co_{50}$
5	12	$Ce_{50}Fe_{50}$	9	2	$Cu_{5}Fe_{95}$	12	5	$Ni_{55}Co_{45}$
5	13	$Ce_{55}Fe_{45}$	9	3	$Cu_{10}Fe_{90}$	12	6	$Ni_{60}Co_{40}$

X	Y	Catalyst	X	Y	Catalyst	X	Y	Catalyst
12	7	$Ni_{65}Co_{35}$	13	14	$Ni_{70}Cu_{30}$	15	10	$Ni_{75}Fe_{25}$
12	8	$Ni_{70}Co_{30}$	13	15	$Ni_{75}Cu_{25}$	15	11	Blank
12	9	$Ni_{75}Co_{25}$	14	3	$Ni_{80}Cu_{20}$	15	12	$Ni_{80}Fe_{20}$
12	10	$Ni_{80}Co_{20}$	14	4	$Ni_{85}Cu_{15}$	15	13	$Ni_{85}Fe_{15}$
12	11	$Ni_{85}Co_{15}$	14	5	$Ni_{90}Cu_{10}$	15	14	$Ni_{90}Fe_{10}$
12	12	$Ni_{90}Co_{10}$	14	6	$Ni_{95}Cu_{5}$	16	5	$Ni_{95}Fe_{5}$
12	13	$Ni_{95}Co_{5}$	14	7	$Ni_{5}Fe_{95}$	16	6	Ce_{100}
12	14	$Ni_{5}Cu_{95}$	14	8	$Ni_{10}Fe_{90}$	16	7	Cu_{100}
12	15	$Ni_{10}Cu_{90}$	14	9	$Ni_{15}Fe_{85}$	16	8	Fe_{100}
13	3	$Ni_{15}Cu_{85}$	14	10	$Ni_{20}Fe_{80}$	16	9	Ni_{100}
13	4	$Ni_{20}Cu_{80}$	14	11	$Ni_{25}Fe_{75}$	16	10	Co_{100}
13	5	$Ni_{25}Cu_{75}$	14	12	$Ni_{30}Fe_{70}$	16	11	Blank
13	6	$Ni_{30}Cu_{70}$	14	13	$Ni_{35}Fe_{65}$	16	12	Blank
13	7	$Ni_{35}Cu_{65}$	14	14	$Ni_{40}Fe_{60}$	17	6	Blank
13	8	$Ni_{40}Cu_{60}$	15	4	$Ni_{45}Fe_{55}$	17	7	Blank
13	9	$Ni_{45}Cu_{55}$	15	5	$Ni_{50}Fe_{50}$	17	8	Blank
13	10	$Ni_{50}Cu_{50}$	15	6	$Ni_{55}Fe_{45}$	17	9	Blank
13	11	$Ni_{55}Cu_{45}$	15	7	$Ni_{60}Fe_{40}$	17	10	Blank
13	12	$Ni_{60}Cu_{40}$	15	8	$Ni_{65}Fe_{35}$	17	11	Blank
13	13	$Ni_{65}Cu_{35}$	15	9	$Ni_{70}Fe_{30}$	17	12	Blank

Table 6-4 Library 02 filling plan

X	**Y**	**Catalyst**	**X**	**Y**	**Catalyst**	**X**	**Y**	**Catalyst**
1	6	$Ce_{10}Cu_{10}Fe_{80}$	5	14	$Ce_{20}Cu_{40}Co_{40}$	9	4	$Ce_{40}Co_{40}Ni_{20}$
1	7	$Ce_{10}Cu_{20}Fe_{70}$	5	15	$Ce_{20}Cu_{50}Co_{30}$	9	5	$Ce_{40}Co_{50}Ni_{10}$
1	8	$Ce_{10}Cu_{30}Fe_{60}$	6	2	$Ce_{20}Cu_{60}Co_{20}$	9	6	$Ce_{50}Co_{10}Ni_{40}$
1	9	$Ce_{10}Cu_{40}Fe_{50}$	6	3	$Ce_{20}Cu_{70}Co_{10}$	9	7	$Ce_{50}Co_{20}Ni_{30}$
1	10	$Ce_{10}Cu_{50}Fe_{40}$	6	4	$Ce_{30}Cu_{10}Co_{60}$	9	8	$Ce_{50}Co_{30}Ni_{20}$
1	11	$Ce_{10}Cu_{60}Fe_{30}$	6	5	$Ce_{30}Cu_{20}Co_{50}$	9	9	Blank
1	12	$Ce_{10}Cu_{70}Fe_{20}$	6	6	$Ce_{30}Cu_{30}Co_{40}$	9	10	$Ce_{50}Co_{40}Ni_{10}$
2	5	$Ce_{10}Cu_{80}Fe_{10}$	6	7	$Ce_{30}Cu_{40}Co_{30}$	9	11	$Ce_{60}Co_{10}Ni_{30}$
2	6	$Ce_{20}Cu_{10}Fe_{70}$	6	8	$Ce_{30}Cu_{50}Co_{20}$	9	12	$Ce_{60}Co_{20}Ni_{20}$
2	7	$Ce_{20}Cu_{20}Fe_{60}$	6	9	$Ce_{30}Cu_{60}Co_{10}$	9	13	$Ce_{60}Co_{30}Ni_{10}$
2	8	$Ce_{20}Cu_{30}Fe_{50}$	6	10	$Ce_{40}Cu_{10}Co_{50}$	9	14	$Ce_{70}Co_{10}Ni_{20}$
2	9	$Ce_{20}Cu_{40}Fe_{40}$	6	11	$Ce_{40}Cu_{20}Co_{40}$	9	15	$Ce_{70}Co_{20}Ni_{10}$
2	10	$Ce_{20}Cu_{50}Fe_{30}$	6	12	$Ce_{40}Cu_{30}Co_{30}$	9	16	$Ce_{80}Co_{10}Ni_{10}$
2	11	$Ce_{20}Cu_{60}Fe_{20}$	6	13	$Ce_{40}Cu_{40}Co_{20}$	10	1	$Ce_{10}Co_{10}Fe_{80}$
2	12	$Ce_{20}Cu_{70}Fe_{10}$	6	14	$Ce_{40}Cu_{50}Co_{10}$	10	2	$Ce_{10}Co_{20}Fe_{70}$
3	4	$Ce_{30}Cu_{10}Fe_{60}$	6	15	$Ce_{50}Cu_{10}Co_{40}$	10	3	$Ce_{10}Co_{30}Fe_{60}$
3	5	$Ce_{30}Cu_{20}Fe_{50}$	7	2	$Ce_{50}Cu_{20}Co_{30}$	10	4	$Ce_{10}Co_{40}Fe_{50}$
3	6	$Ce_{30}Cu_{30}Fe_{40}$	7	3	$Ce_{50}Cu_{30}Co_{20}$	10	5	$Ce_{10}Co_{50}Fe_{40}$
3	7	$Ce_{30}Cu_{40}Fe_{30}$	7	4	$Ce_{50}Cu_{40}Co_{10}$	10	6	$Ce_{10}Co_{60}Fe_{30}$
3	8	$Ce_{30}Cu_{50}Fe_{20}$	7	5	$Ce_{60}Cu_{10}Co_{30}$	10	7	$Ce_{10}Co_{70}Fe_{20}$
3	9	$Ce_{30}Cu_{60}Fe_{10}$	7	6	$Ce_{60}Cu_{20}Co_{20}$	10	8	$Ce_{10}Co_{80}Fe_{10}$
3	10	$Ce_{40}Cu_{10}Fe_{50}$	7	7	$Ce_{60}Cu_{30}Co_{10}$	10	9	$Ce_{20}Co_{10}Fe_{70}$
3	11	$Ce_{40}Cu_{20}Fe_{40}$	7	8	$Ce_{70}Cu_{10}Co_{20}$	10	10	$Ce_{20}Co_{20}Fe_{60}$
3	12	$Ce_{40}Cu_{30}Fe_{30}$	7	9	$Ce_{70}Cu_{20}Co_{10}$	10	11	$Ce_{20}Co_{30}Fe_{50}$
3	13	$Ce_{40}Cu_{40}Fe_{20}$	7	10	$Ce_{80}Cu_{10}Co_{10}$	10	12	$Ce_{20}Co_{40}Fe_{40}$
3	14	$Ce_{40}Cu_{50}Fe_{10}$	7	11	$Ce_{10}Co_{10}Ni_{80}$	10	13	$Ce_{20}Co_{50}Fe_{30}$
4	3	$Ce_{50}Cu_{10}Fe_{40}$	7	12	$Ce_{10}Co_{20}Ni_{70}$	10	14	$Ce_{20}Co_{60}Fe_{20}$
4	4	$Ce_{50}Cu_{20}Fe_{30}$	7	13	$Ce_{10}Co_{30}Ni_{60}$	10	15	$Ce_{20}Co_{70}Fe_{10}$
4	5	$Ce_{50}Cu_{30}Fe_{20}$	7	14	$Ce_{10}Co_{40}Ni_{50}$	10	16	$Ce_{30}Co_{10}Fe_{60}$
4	6	$Ce_{50}Cu_{40}Fe_{10}$	7	15	$Ce_{10}Co_{50}Ni_{40}$	11	2	$Ce_{30}Co_{20}Fe_{50}$
4	7	$Ce_{60}Cu_{10}Fe_{30}$	7	16	$Ce_{10}Co_{60}Ni_{30}$	11	3	$Ce_{30}Co_{30}Fe_{40}$
4	8	$Ce_{60}Cu_{20}Fe_{20}$	8	1	$Ce_{10}Co_{70}Ni_{20}$	11	4	$Ce_{30}Co_{40}Fe_{30}$
4	9	$Ce_{60}Cu_{30}Fe_{10}$	8	2	$Ce_{10}Co_{80}Ni_{10}$	11	5	$Ce_{30}Co_{50}Fe_{20}$
4	10	$Ce_{70}Cu_{10}Fe_{20}$	8	3	$Ce_{20}Co_{10}Ni_{70}$	11	6	$Ce_{30}Co_{60}Fe_{10}$
4	11	$Ce_{70}Cu_{20}Fe_{10}$	8	4	$Ce_{20}Co_{20}Ni_{60}$	11	7	$Ce_{40}Co_{10}Fe_{50}$
4	12	$Ce_{80}Cu_{10}Fe_{10}$	8	5	$Ce_{20}Co_{30}Ni_{50}$	11	8	$Ce_{40}Co_{20}Fe_{40}$
4	13	Blank	8	6	$Ce_{20}Co_{40}Ni_{40}$	11	9	$Ce_{40}Co_{30}Fe_{30}$
4	14	Blank	8	7	$Ce_{20}Co_{50}Ni_{30}$	11	10	$Ce_{40}Co_{40}Fe_{20}$
5	3	$Ce_{10}Cu_{10}Co_{80}$	8	8	$Ce_{20}Co_{60}Ni_{20}$	11	11	$Ce_{40}Co_{50}Fe_{10}$
5	4	$Ce_{10}Cu_{20}Co_{70}$	8	9	$Ce_{20}Co_{70}Ni_{10}$	11	12	$Ce_{50}Co_{10}Fe_{40}$
5	5	$Ce_{10}Cu_{30}Co_{60}$	8	10	$Ce_{30}Co_{10}Ni_{60}$	11	13	$Ce_{50}Co_{20}Fe_{30}$
5	6	$Ce_{10}Cu_{40}Co_{50}$	8	11	$Ce_{30}Co_{20}Ni_{50}$	11	14	$Ce_{50}Co_{30}Fe_{20}$
5	7	$Ce_{10}Cu_{50}Co_{40}$	8	12	$Ce_{30}Co_{30}Ni_{40}$	11	15	$Ce_{50}Co_{40}Fe_{10}$
5	8	$Ce_{10}Cu_{60}Co_{30}$	8	13	$Ce_{30}Co_{40}Ni_{30}$	11	16	$Ce_{60}Co_{10}Fe_{30}$
5	9	$Ce_{10}Cu_{70}Co_{20}$	8	14	$Ce_{30}Co_{50}Ni_{20}$	12	2	$Ce_{60}Co_{20}Fe_{20}$
5	10	$Ce_{10}Cu_{80}Co_{10}$	8	15	$Ce_{30}Co_{60}Ni_{10}$	12	3	$Ce_{60}Co_{30}Fe_{10}$
5	11	$Ce_{20}Cu_{10}Co_{70}$	8	16	$Ce_{40}Co_{10}Ni_{50}$	12	4	$Ce_{70}Co_{10}Fe_{20}$
5	12	$Ce_{20}Cu_{20}Co_{60}$	9	2	$Ce_{40}Co_{20}Ni_{40}$	12	5	$Ce_{70}Co_{20}Fe_{10}$
5	13	$Ce_{20}Cu_{30}Co_{50}$	9	3	$Ce_{40}Co_{30}Ni_{30}$	12	6	$Ce_{80}Co_{10}Fe_{10}$

X	Y	Catalyst	X	Y	Catalyst	X	Y	Catalyst
12	7	$Ce_{10}Cu_{10}Ni_{80}$	13	14	Blank	15	10	Blank
12	8	$Ce_{10}Cu_{20}Ni_{70}$	13	15	Blank	15	11	Blank
12	9	$Ce_{10}Cu_{30}Ni_{60}$	14	3	$Ce_{30}Cu_{60}Ni_{10}$	15	12	Blank
12	10	$Ce_{10}Cu_{40}Ni_{50}$	14	4	$Ce_{40}Cu_{10}Ni_{50}$	15	13	Blank
12	11	$Ce_{10}Cu_{50}Ni_{40}$	14	5	$Ce_{40}Cu_{20}Ni_{40}$	15	14	Blank
12	12	$Ce_{10}Cu_{60}Ni_{30}$	14	6	$Ce_{40}Cu_{30}Ni_{30}$	16	5	Blank
12	13	$Ce_{10}Cu_{70}Ni_{20}$	14	7	$Ce_{40}Cu_{40}Ni_{20}$	16	6	Blank
12	14	$Ce_{10}Cu_{80}Ni_{10}$	14	8	$Ce_{40}Cu_{50}Ni_{10}$	16	7	Blank
12	15	$Ce_{20}Cu_{10}Ni_{70}$	14	9	$Ce_{50}Cu_{10}Ni_{40}$	16	8	Blank
13	3	$Ce_{20}Cu_{20}Ni_{60}$	14	10	$Ce_{50}Cu_{20}Ni_{30}$	16	9	Blank
13	4	$Ce_{20}Cu_{30}Ni_{50}$	14	11	$Ce_{50}Cu_{30}Ni_{20}$	16	10	Blank
13	5	$Ce_{20}Cu_{40}Ni_{40}$	14	12	$Ce_{50}Cu_{40}Ni_{10}$	16	11	Blank
13	6	$Ce_{20}Cu_{50}Ni_{30}$	14	13	$Ce_{60}Cu_{10}Ni_{30}$	16	12	Blank
13	7	$Ce_{20}Cu_{60}Ni_{20}$	14	14	$Ce_{60}Cu_{20}Ni_{20}$	17	6	Blank
13	8	$Ce_{20}Cu_{70}Ni_{10}$	15	4	$Ce_{60}Cu_{30}Ni_{10}$	17	7	Blank
13	9	$Ce_{30}Cu_{10}Ni_{60}$	15	5	$Ce_{70}Cu_{10}Ni_{20}$	17	8	Blank
13	10	$Ce_{30}Cu_{20}Ni_{50}$	15	6	$Ce_{70}Cu_{20}Ni_{10}$	17	9	Blank
13	11	$Ce_{30}Cu_{30}Ni_{40}$	15	7	$Ce_{80}Cu_{10}Ni_{10}$	17	10	Blank
13	12	$Ce_{30}Cu_{40}Ni_{30}$	15	8	Blank	17	11	Blank
13	13	$Ce_{30}Cu_{50}Ni_{20}$	15	9	Blank	17	12	Blank

Table 6-5 Library 03 filling plan

X	Y	Catalyst	X	Y	Catalyst	X	Y	Catalyst
1	6	$Ce_{10}Ni_{10}Fe_{80}$	5	14	$Cu_{20}Co_{60}Fe_{20}$	9	4	$Cu_{50}Co_{10}Ni_{40}$
1	7	$Ce_{10}Ni_{20}Fe_{70}$	5	15	$Cu_{20}Co_{70}Fe_{10}$	9	5	$Cu_{50}Co_{20}Ni_{30}$
1	8	$Ce_{10}Ni_{30}Fe_{60}$	6	2	$Cu_{30}Co_{10}Fe_{60}$	9	6	$Cu_{50}Co_{30}Ni_{20}$
1	9	$Ce_{10}Ni_{40}Fe_{50}$	6	3	$Cu_{30}Co_{20}Fe_{50}$	9	7	$Cu_{50}Co_{40}Ni_{10}$
1	10	$Ce_{10}Ni_{50}Fe_{40}$	6	4	$Cu_{30}Co_{30}Fe_{40}$	9	8	$Cu_{60}Co_{10}Ni_{30}$
1	11	$Ce_{10}Ni_{60}Fe_{30}$	6	5	$Cu_{30}Co_{40}Fe_{30}$	9	9	Blank
1	12	$Ce_{10}Ni_{70}Fe_{20}$	6	6	$Cu_{30}Co_{50}Fe_{20}$	9	10	$Cu_{60}Co_{20}Ni_{20}$
2	5	$Ce_{10}Ni_{80}Fe_{10}$	6	7	$Cu_{30}Co_{60}Fe_{10}$	9	11	$Cu_{60}Co_{30}Ni_{10}$
2	6	$Ce_{20}Ni_{10}Fe_{70}$	6	8	$Cu_{40}Co_{10}Fe_{50}$	9	12	$Cu_{70}Co_{10}Ni_{20}$
2	7	$Ce_{20}Ni_{20}Fe_{60}$	6	9	$Cu_{40}Co_{20}Fe_{40}$	9	13	$Cu_{70}Co_{20}Ni_{10}$
2	8	$Ce_{20}Ni_{30}Fe_{50}$	6	10	$Cu_{40}Co_{30}Fe_{30}$	9	14	$Cu_{80}Co_{10}Ni_{10}$
2	9	$Ce_{20}Ni_{40}Fe_{40}$	6	11	$Cu_{40}Co_{40}Fe_{20}$	9	15	$Fe_{10}Co_{10}Ni_{80}$
2	10	$Ce_{20}Ni_{50}Fe_{30}$	6	12	$Cu_{40}Co_{50}Fe_{10}$	9	16	$Fe_{10}Co_{20}Ni_{70}$
2	11	$Ce_{20}Ni_{60}Fe_{20}$	6	13	$Cu_{50}Co_{10}Fe_{40}$	10	1	$Fe_{10}Co_{30}Ni_{60}$
2	12	$Ce_{20}Ni_{70}Fe_{10}$	6	14	$Cu_{50}Co_{20}Fe_{30}$	10	2	$Fe_{10}Co_{40}Ni_{50}$
3	4	$Ce_{30}Ni_{10}Fe_{60}$	6	15	$Cu_{50}Co_{30}Fe_{20}$	10	3	$Fe_{10}Co_{50}Ni_{40}$
3	5	$Ce_{30}Ni_{20}Fe_{50}$	7	2	$Cu_{50}Co_{40}Fe_{10}$	10	4	$Fe_{10}Co_{60}Ni_{30}$
3	6	$Ce_{30}Ni_{30}Fe_{40}$	7	3	$Cu_{60}Co_{10}Fe_{30}$	10	5	$Fe_{10}Co_{70}Ni_{20}$
3	7	$Ce_{30}Ni_{40}Fe_{30}$	7	4	$Cu_{60}Co_{20}Fe_{20}$	10	6	$Fe_{10}Co_{80}Ni_{10}$
3	8	$Ce_{30}Ni_{50}Fe_{20}$	7	5	$Cu_{60}Co_{30}Fe_{10}$	10	7	$Fe_{20}Co_{10}Ni_{70}$
3	9	$Ce_{30}Ni_{60}Fe_{10}$	7	6	$Cu_{70}Co_{10}Fe_{20}$	10	8	$Fe_{20}Co_{20}Ni_{60}$
3	10	$Ce_{40}Ni_{10}Fe_{50}$	7	7	$Cu_{70}Co_{20}Fe_{10}$	10	9	$Fe_{20}Co_{30}Ni_{50}$
3	11	$Ce_{40}Ni_{20}Fe_{40}$	7	8	$Cu_{80}Co_{10}Fe_{10}$	10	10	$Fe_{20}Co_{40}Ni_{40}$
3	12	$Ce_{40}Ni_{30}Fe_{30}$	7	9	$Cu_{10}Co_{10}Ni_{80}$	10	11	$Fe_{20}Co_{50}Ni_{30}$
3	13	$Ce_{40}Ni_{40}Fe_{20}$	7	10	$Cu_{10}Co_{20}Ni_{70}$	10	12	$Fe_{20}Co_{60}Ni_{20}$
3	14	$Ce_{40}Ni_{50}Fe_{10}$	7	11	$Cu_{10}Co_{30}Ni_{60}$	10	13	$Fe_{20}Co_{70}Ni_{10}$
4	3	$Ce_{50}Ni_{10}Fe_{40}$	7	12	$Cu_{10}Co_{40}Ni_{50}$	10	14	$Fe_{30}Co_{10}Ni_{60}$
4	4	$Ce_{50}Ni_{20}Fe_{30}$	7	13	$Cu_{10}Co_{50}Ni_{40}$	10	15	$Fe_{30}Co_{20}Ni_{50}$
4	5	$Ce_{50}Ni_{30}Fe_{20}$	7	14	$Cu_{10}Co_{60}Ni_{30}$	10	16	$Fe_{30}Co_{30}Ni_{40}$
4	6	$Ce_{50}Ni_{40}Fe_{10}$	7	15	$Cu_{10}Co_{70}Ni_{20}$	11	2	$Fe_{30}Co_{40}Ni_{30}$
4	7	$Ce_{60}Ni_{10}Fe_{30}$	7	16	$Cu_{10}Co_{80}Ni_{10}$	11	3	$Fe_{30}Co_{50}Ni_{20}$
4	8	$Ce_{60}Ni_{20}Fe_{20}$	8	1	$Cu_{20}Co_{10}Ni_{70}$	11	4	$Fe_{30}Co_{60}Ni_{10}$
4	9	$Ce_{60}Ni_{30}Fe_{10}$	8	2	$Cu_{20}Co_{20}Ni_{60}$	11	5	$Fe_{40}Co_{10}Ni_{50}$
4	10	$Ce_{70}Ni_{10}Fe_{20}$	8	3	$Cu_{20}Co_{30}Ni_{50}$	11	6	$Fe_{40}Co_{20}Ni_{40}$
4	11	$Ce_{70}Ni_{20}Fe_{10}$	8	4	$Cu_{20}Co_{40}Ni_{40}$	11	7	$Fe_{40}Co_{30}Ni_{30}$
4	12	$Ce_{80}Ni_{10}Fe_{10}$	8	5	$Cu_{20}Co_{50}Ni_{30}$	11	8	$Fe_{40}Co_{40}Ni_{20}$
4	13	$Cu_{10}Co_{10}Fe_{80}$	8	6	$Cu_{20}Co_{60}Ni_{20}$	11	9	$Fe_{40}Co_{50}Ni_{10}$
4	14	$Cu_{10}Co_{20}Fe_{70}$	8	7	$Cu_{20}Co_{70}Ni_{10}$	11	10	$Fe_{50}Co_{10}Ni_{40}$
5	3	$Cu_{10}Co_{30}Fe_{60}$	8	8	$Cu_{30}Co_{10}Ni_{60}$	11	11	$Fe_{50}Co_{20}Ni_{30}$
5	4	$Cu_{10}Co_{40}Fe_{50}$	8	9	$Cu_{30}Co_{20}Ni_{50}$	11	12	$Fe_{50}Co_{30}Ni_{20}$
5	5	$Cu_{10}Co_{50}Fe_{40}$	8	10	$Cu_{30}Co_{30}Ni_{40}$	11	13	$Fe_{50}Co_{40}Ni_{10}$
5	6	$Cu_{10}Co_{60}Fe_{30}$	8	11	$Cu_{30}Co_{40}Ni_{30}$	11	14	$Fe_{60}Co_{10}Ni_{30}$
5	7	$Cu_{10}Co_{70}Fe_{20}$	8	12	$Cu_{30}Co_{50}Ni_{20}$	11	15	$Fe_{60}Co_{20}Ni_{20}$
5	8	$Cu_{10}Co_{80}Fe_{10}$	8	13	$Cu_{30}Co_{60}Ni_{10}$	11	16	$Fe_{60}Co_{30}Ni_{10}$
5	9	$Cu_{20}Co_{10}Fe_{70}$	8	14	$Cu_{40}Co_{10}Ni_{50}$	12	2	$Fe_{70}Co_{10}Ni_{20}$
5	10	$Cu_{20}Co_{20}Fe_{60}$	8	15	$Cu_{40}Co_{20}Ni_{40}$	12	3	$Fe_{70}Co_{20}Ni_{10}$
5	11	$Cu_{20}Co_{30}Fe_{50}$	8	16	$Cu_{40}Co_{30}Ni_{30}$	12	4	$Fe_{80}Co_{10}Ni_{10}$
5	12	$Cu_{20}Co_{40}Fe_{40}$	9	2	$Cu_{40}Co_{40}Ni_{20}$	12	5	$Fe_{10}Cu_{10}Ni_{80}$
5	13	$Cu_{20}Co_{50}Fe_{30}$	9	3	$Cu_{40}Co_{50}Ni_{10}$	12	6	$Fe_{10}Cu_{20}Ni_{70}$

X	Y	Catalyst	X	Y	Catalyst	X	Y	Catalyst
12	7	$Fe_{10}Cu_{30}Ni_{60}$	13	14	$Fe_{40}Cu_{20}Ni_{40}$	15	10	Blank
12	8	$Fe_{10}Cu_{40}Ni_{50}$	13	15	$Fe_{40}Cu_{30}Ni_{30}$	15	11	Blank
12	9	$Fe_{10}Cu_{50}Ni_{40}$	14	3	$Fe_{40}Cu_{40}Ni_{20}$	15	12	Blank
12	10	$Fe_{10}Cu_{60}Ni_{30}$	14	4	$Fe_{40}Cu_{50}Ni_{10}$	15	13	Blank
12	11	$Fe_{10}Cu_{70}Ni_{20}$	14	5	$Fe_{50}Cu_{10}Ni_{40}$	15	14	Blank
12	12	$Fe_{10}Cu_{80}Ni_{10}$	14	6	$Fe_{50}Cu_{20}Ni_{30}$	16	5	Blank
12	13	$Fe_{20}Cu_{10}Ni_{70}$	14	7	$Fe_{50}Cu_{30}Ni_{20}$	16	6	Blank
12	14	$Fe_{20}Cu_{20}Ni_{60}$	14	8	$Fe_{50}Cu_{40}Ni_{10}$	16	7	Blank
12	15	$Fe_{20}Cu_{30}Ni_{50}$	14	9	$Fe_{60}Cu_{10}Ni_{30}$	16	8	Blank
13	3	$Fe_{20}Cu_{40}Ni_{40}$	14	10	$Fe_{60}Cu_{20}Ni_{20}$	16	9	Blank
13	4	$Fe_{20}Cu_{50}Ni_{30}$	14	11	$Fe_{60}Cu_{30}Ni_{10}$	16	10	Blank
13	5	$Fe_{20}Cu_{60}Ni_{20}$	14	12	$Fe_{70}Cu_{10}Ni_{20}$	16	11	Blank
13	6	$Fe_{20}Cu_{70}Ni_{10}$	14	13	$Fe_{70}Cu_{20}Ni_{10}$	16	12	Blank
13	7	$Fe_{30}Cu_{10}Ni_{60}$	14	14	$Fe_{80}Cu_{10}Ni_{10}$	17	6	Blank
13	8	$Fe_{30}Cu_{20}Ni_{50}$	15	4	Blank	17	7	Blank
13	9	$Fe_{30}Cu_{30}Ni_{40}$	15	5	Blank	17	8	Blank
13	10	$Fe_{30}Cu_{40}Ni_{30}$	15	6	Blank	17	9	Blank
13	11	$Fe_{30}Cu_{50}Ni_{20}$	15	7	Blank	17	10	Blank
13	12	$Fe_{30}Cu_{60}Ni_{10}$	15	8	Blank	17	11	Blank
13	13	$Fe_{40}Cu_{10}Ni_{50}$	15	9	Blank	17	12	Blank

Table 6-6 **Library 04 filling plan**

X	**Y**	**Catalyst**	**X**	**Y**	**Catalyst**	**X**	**Y**	**Catalyst**
1	6	Blank	5	14	$Ce_5Co_{92}W_3$	9	4	$Fe_{20}Co_{77}W_3$
1	7	Blank	5	15	$Ce_5Co_{92}V_3$	9	5	$Fe_{20}Co_{77}V_3$
1	8	Blank	6	2	$Ce_5Co_{92}Ti_3$	9	6	$Fe_{20}Co_{77}Ti_3$
1	9	Blank	6	3	$Ce_5Co_{92}Te_3$	9	7	$Fe_{20}Co_{77}Te_3$
1	10	Blank	6	4	$Ce_5Co_{92}Ba_3$	9	8	$Fe_{20}Co_{77}Ba_3$
1	11	Blank	6	5	$Ce_5Co_{92}Tm_3$	9	9	Blank
1	12	Blank	6	6	$Ce_5Co_{92}Ta_3$	9	10	$Fe_{20}Co_{77}Tm_3$
2	5	$Ce_5Co_{92}Al_3$	6	7	Blank	9	11	$Fe_{20}Co_{77}Ta_3$
2	6	$Ce_5Co_{92}B_3$	6	8	$Fe_{20}Co_{77}Al_3$	9	12	$Ni_{60}Co_{37}Al_3$
2	7	$Ce_5Co_{92}Cd_3$	6	9	$Fe_{20}Co_{77}B_3$	9	13	$Ni_{60}Co_{37}B_3$
2	8	$Ce_5Co_{92}Cr_3$	6	10	$Fe_{20}Co_{77}Cd_3$	9	14	$Ni_{60}Co_{37}Cd_3$
2	9	$Ce_5Co_{92}Dy_3$	6	11	$Fe_{20}Co_{77}Cr_3$	9	15	$Ni_{60}Co_{37}Cr_3$
2	10	$Ce_5Co_{92}Er_3$	6	12	$Fe_{20}Co_{77}Dy_3$	9	16	$Ni_{60}Co_{37}Dy_3$
2	11	$Ce_5Co_{92}Gd_3$	6	13	$Fe_{20}Co_{77}Er_3$	10	1	$Ni_{60}Co_{37}Er_3$
2	12	Blank	6	14	$Fe_{20}Co_{77}Gd_3$	10	2	$Ni_{60}Co_{37}Gd_3$
3	4	$Ce_5Co_{92}Ho_3$	6	15	$Fe_{20}Co_{77}Ho_3$	10	3	$Ni_{60}Co_{37}Ho_3$
3	5	$Ce_5Co_{92}Ca_3$	7	2	$Fe_{20}Co_{77}Ca_3$	10	4	$Ni_{60}Co_{37}Ca_3$
3	6	$Ce_5Co_{92}Sr_3$	7	3	$Fe_{20}Co_{77}Sr_3$	10	5	$Ni_{60}Co_{37}Sr_3$
3	7	$Ce_5Co_{92}La_3$	7	4	$Fe_{20}Co_{77}La_3$	10	6	$Ni_{60}Co_{37}La_3$
3	8	$Ce_5Co_{92}Li_3$	7	5	$Fe_{20}Co_{77}Li_3$	10	7	$Ni_{60}Co_{37}Li_3$
3	9	$Ce_5Co_{92}Lu_3$	7	6	$Fe_{20}Co_{77}Lu_3$	10	8	$Ni_{60}Co_{37}Lu_3$
3	10	$Ce_5Co_{92}Mg_3$	7	7	$Fe_{20}Co_{77}Mg_3$	10	9	$Ni_{60}Co_{37}Mg_3$
3	11	$Ce_5Co_{92}Mn_3$	7	8	$Fe_{20}Co_{77}Mn_3$	10	10	$Ni_{60}Co_{37}Mn_3$
3	12	$Ce_5Co_{92}Nd_3$	7	9	$Fe_{20}Co_{77}Nd_3$	10	11	$Ni_{60}Co_{37}Nd_3$
3	13	$Ce_5Co_{92}Sm_3$	7	10	$Fe_{20}Co_{77}Sm_3$	10	12	$Ni_{60}Co_{37}Sm_3$
3	14	$Ce_5Co_{92}Se_3$	7	11	$Fe_{20}Co_{77}Se_3$	10	13	$Ni_{60}Co_{37}Se_3$
4	3	$Ce_5Co_{92}Y_3$	7	12	$Fe_{20}Co_{77}Y_3$	10	14	$Ni_{60}Co_{37}Y_3$
4	4	$Ce_5Co_{92}Zn_3$	7	13	$Fe_{20}Co_{77}Zn_3$	10	15	$Ni_{60}Co_{37}Zn_3$
4	5	$Ce_5Co_{92}Sn_3$	7	14	$Fe_{20}Co_{77}Sn_3$	10	16	$Ni_{60}Co_{37}Sn_3$
4	6	$Ce_5Co_{92}Eu_3$	7	15	$Fe_{20}Co_{77}Eu_3$	11	2	$Ni_{60}Co_{37}Eu_3$
4	7	$Ce_5Co_{92}Sb_3$	7	16	$Fe_{20}Co_{77}Sb_3$	11	3	$Ni_{60}Co_{37}Sb_3$
4	8	$Ce_5Co_{92}Cs_3$	8	1	$Fe_{20}Co_{77}Cs_3$	11	4	$Ni_{60}Co_{37}Cs_3$
4	9	$Ce_5Co_{92}Fe_3$	8	2	$Fe_{20}Co_{77}Fe_3$	11	5	$Ni_{60}Co_{37}Fe_3$
4	10	$Ce_5Co_{92}Ga_3$	8	3	$Fe_{20}Co_{77}Ga_3$	11	6	$Ni_{60}Co_{37}Ga_3$
4	11	$Ce_5Co_{92}Ge_3$	8	4	$Fe_{20}Co_{77}Ge_3$	11	7	$Ni_{60}Co_{37}Ge_3$
4	12	$Ce_5Co_{92}Hf_3$	8	5	$Fe_{20}Co_{77}Hf_3$	11	8	$Ni_{60}Co_{37}Hf_3$
4	13	$Ce_5Co_{92}In_3$	8	6	$Fe_{20}Co_{77}In_3$	11	9	$Ni_{60}Co_{37}In_3$
4	14	$Ce_5Co_{92}Cu_3$	8	7	$Fe_{20}Co_{77}Cu_3$	11	10	$Ni_{60}Co_{37}Cu_3$
5	3	$Ce_5Co_{92}Na_3$	8	8	$Fe_{20}Co_{77}Na_3$	11	11	$Ni_{60}Co_{37}Na_3$
5	4	$Ce_5Co_{92}Si_3$	8	9	$Fe_{20}Co_{77}Si_3$	11	12	$Ni_{60}Co_{37}Si_3$
5	5	$Ce_5Co_{92}Tb_3$	8	10	$Fe_{20}Co_{77}Tb_3$	11	13	$Ni_{60}Co_{37}Tb_3$
5	6	$Ce_5Co_{92}Yb_3$	8	11	$Fe_{20}Co_{77}Yb_3$	11	14	$Ni_{60}Co_{37}Yb_3$
5	7	$Ce_5Co_{92}Zr_3$	8	12	$Fe_{20}Co_{77}Zr_3$	11	15	$Ni_{60}Co_{37}Zr_3$
5	8	$Ce_5Co_{92}K_3$	8	13	$Fe_{20}Co_{77}K_3$	11	16	$Ni_{60}Co_{37}K_3$
5	9	$Ce_5Co_{92}Bi_3$	8	14	$Fe_{20}Co_{77}Bi_3$	12	2	$Ni_{60}Co_{37}Bi_3$
5	10	$Ce_5Co_{92}Mo_3$	8	15	$Fe_{20}Co_{77}Mo_3$	12	3	$Ni_{60}Co_{37}Mo_3$
5	11	$Ce_5Co_{92}Nb_3$	8	16	$Fe_{20}Co_{77}Nb_3$	12	4	$Ni_{60}Co_{37}Nb_3$
5	12	$Ce_5Co_{92}Rb_3$	9	2	$Fe_{20}Co_{77}Rb_3$	12	5	$Ni_{60}Co_{37}Rb_3$
5	13	$Ce_5Co_{92}Sc_3$	9	3	$Fe_{20}Co_{77}Sc_3$	12	6	$Ni_{60}Co_{37}Sc_3$

X	Y	Catalyst	X	Y	Catalyst	X	Y	Catalyst
12	7	$Ni_{60}Co_{37}W_3$	13	14	Blank	15	10	Blank
12	8	$Ni_{60}Co_{37}V_3$	13	15	Blank	15	11	Blank
12	9	$Ni_{60}Co_{37}Ti_3$	14	3	Blank	15	12	Blank
12	10	$Ni_{60}Co_{37}Te_3$	14	4	Blank	15	13	Blank
12	11	$Ni_{60}Co_{37}Ba_3$	14	5	Blank	15	14	Blank
12	12	$Ni_{60}Co_{37}Tm_3$	14	6	Blank	16	5	Blank
12	13	$Ni_{60}Co_{37}Ta_3$	14	7	Blank	16	6	Blank
12	14	Blank	14	8	Blank	16	7	Blank
12	15	Blank	14	9	Blank	16	8	Blank
13	3	Ce_5Co_{95}	14	10	Blank	16	9	Blank
13	4	$Fe_{20}Co_{80}$	14	11	Blank	16	10	Blank
13	5	$Ni_{60}Co_{40}$	14	12	Blank	16	11	Blank
13	6	$Pt/Rh/Al_2O_3$	14	13	Blank	16	12	Blank
13	7	Blank	14	14	Blank	17	6	Blank
13	8	Blank	15	4	Blank	17	7	Blank
13	9	Blank	15	5	Blank	17	8	Blank
13	10	Blank	15	6	Blank	17	9	Blank
13	11	Blank	15	7	Blank	17	10	Blank
13	12	Blank	15	8	Blank	17	11	Blank
13	13	Blank	15	9	Blank	17	12	Blank

Table 6-7 Library 05 filling plan

X	**Y**	**Catalyst**	**X**	**Y**	**Catalyst**	**X**	**Y**	**Catalyst**
1	6	Blank	5	14	$Cu_{20}Co_{67}Ni_{10}Cs_3$	9	4	Blank
1	7	Blank	5	15	$Cu_{20}Co_{67}Ni_{10}Fe_3$	9	5	Blank
1	8	Blank	6	2	$Cu_{20}Co_{67}Ni_{10}Ga_3$	9	6	Blank
1	9	Blank	6	3	$Cu_{20}Co_{67}Ni_{10}Ge_3$	9	7	Blank
1	10	Blank	6	4	$Cu_{20}Co_{67}Ni_{10}Hf_3$	9	8	Blank
1	11	Blank	6	5	$Cu_{20}Co_{67}Ni_{10}In_3$	9	9	Blank
1	12	Blank	6	6	$Cu_{20}Co_{67}Ni_{10}Cu_3$	9	10	Blank
2	5	Blank	6	7	$Cu_{20}Co_{67}Ni_{10}Na_3$	9	11	Blank
2	6	Blank	6	8	$Cu_{20}Co_{67}Ni_{10}Si_3$	9	12	Blank
2	7	Blank	6	9	$Cu_{20}Co_{67}Ni_{10}Tb_3$	9	13	Blank
2	8	Blank	6	10	$Cu_{20}Co_{67}Ni_{10}Yb_3$	9	14	Blank
2	9	Blank	6	11	$Cu_{20}Co_{67}Ni_{10}Zr_3$	9	15	Blank
2	10	Blank	6	12	$Cu_{20}Co_{67}Ni_{10}K_3$	9	16	Blank
2	11	Blank	6	13	$Cu_{20}Co_{67}Ni_{10}Bi_3$	10	1	Blank
2	12	Blank	6	14	$Cu_{20}Co_{67}Ni_{10}Mo_3$	10	2	Blank
3	4	Blank	6	15	$Cu_{20}Co_{67}Ni_{10}Nb_3$	10	3	Blank
3	5	Blank	7	2	$Cu_{20}Co_{67}Ni_{10}Rb_3$	10	4	Blank
3	6	Blank	7	3	$Cu_{20}Co_{67}Ni_{10}Sc_3$	10	5	Blank
3	7	Blank	7	4	$Cu_{20}Co_{67}Ni_{10}W_3$	10	6	Blank
3	8	Blank	7	5	$Cu_{20}Co_{67}Ni_{10}V_3$	10	7	Blank
3	9	Blank	7	6	$Cu_{20}Co_{67}Ni_{10}Ti_3$	10	8	Blank
3	10	Blank	7	7	$Cu_{20}Co_{67}Ni_{10}Te_3$	10	9	Blank
3	11	Blank	7	8	$Cu_{20}Co_{67}Ni_{10}Ba_3$	10	10	Blank
3	12	Blank	7	9	$Cu_{20}Co_{67}Ni_{10}Tm_3$	10	11	Blank
3	13	Blank	7	10	$Cu_{20}Co_{67}Ni_{10}Ta_3$	10	12	Blank
3	14	Blank	7	11	Blank	10	13	Blank
4	3	$Cu_{20}Co_{67}Ni_{10}Al_3$	7	12	Blank	10	14	Blank
4	4	$Cu_{20}Co_{67}Ni_{10}B_3$	7	13	Blank	10	15	Blank
4	5	$Cu_{20}Co_{67}Ni_{10}Cd_3$	7	14	Blank	10	16	Blank
4	6	$Cu_{20}Co_{67}Ni_{10}Cr_3$	7	15	Blank	11	2	$Ce_{30}Co_{57}Fe_{10}Al_3$
4	7	$Cu_{20}Co_{67}Ni_{10}Dy_3$	7	16	Blank	11	3	$Ce_{30}Co_{57}Fe_{10}B_3$
4	8	$Cu_{20}Co_{67}Ni_{10}Er_3$	8	1	Blank	11	4	$Ce_{30}Co_{57}Fe_{10}Cd_3$
4	9	$Cu_{20}Co_{67}Ni_{10}Gd_3$	8	2	Blank	11	5	$Ce_{30}Co_{57}Fe_{10}Cr_3$
4	10	$Cu_{20}Co_{67}Ni_{10}Ho_3$	8	3	Blank	11	6	$Ce_{30}Co_{57}Fe_{10}Dy_3$
4	11	$Cu_{20}Co_{67}Ni_{10}Ca_3$	8	4	Blank	11	7	$Ce_{30}Co_{57}Fe_{10}Er_3$
4	12	$Cu_{20}Co_{67}Ni_{10}Sr_3$	8	5	Blank	11	8	$Ce_{30}Co_{57}Fe_{10}Gd_3$
4	13	$Cu_{20}Co_{67}Ni_{10}La_3$	8	6	Blank	11	9	$Ce_{30}Co_{57}Fe_{10}Ho_3$
4	14	$Cu_{20}Co_{67}Ni_{10}Li_3$	8	7	Blank	11	10	$Ce_{30}Co_{57}Fe_{10}Ca_3$
5	3	$Cu_{20}Co_{67}Ni_{10}Lu_3$	8	8	Blank	11	11	$Ce_{30}Co_{57}Fe_{10}Sr_3$
5	4	$Cu_{20}Co_{67}Ni_{10}Mg_3$	8	9	Blank	11	12	$Ce_{30}Co_{57}Fe_{10}La_3$
5	5	$Cu_{20}Co_{67}Ni_{10}Mn_3$	8	10	Blank	11	13	$Ce_{30}Co_{57}Fe_{10}Li_3$
5	6	$Cu_{20}Co_{67}Ni_{10}Nd_3$	8	11	Blank	11	14	$Ce_{30}Co_{57}Fe_{10}Lu_3$
5	7	$Cu_{20}Co_{67}Ni_{10}Sm_3$	8	12	Blank	11	15	$Ce_{30}Co_{57}Fe_{10}Mg_3$
5	8	$Cu_{20}Co_{67}Ni_{10}Se_3$	8	13	Blank	11	16	$Ce_{30}Co_{57}Fe_{10}Mn_3$
5	9	$Cu_{20}Co_{67}Ni_{10}Y_3$	8	14	Blank	12	2	$Ce_{30}Co_{57}Fe_{10}Nd_3$
5	10	$Cu_{20}Co_{67}Ni_{10}Zn_3$	8	15	Blank	12	3	$Ce_{30}Co_{57}Fe_{10}Sm_3$
5	11	$Cu_{20}Co_{67}Ni_{10}Sn_3$	8	16	Blank	12	4	$Ce_{30}Co_{57}Fe_{10}Se_3$
5	12	$Cu_{20}Co_{67}Ni_{10}Eu_3$	9	2	Blank	12	5	$Ce_{30}Co_{57}Fe_{10}Y_3$
5	13	$Cu_{20}Co_{67}Ni_{10}Sb_3$	9	3	Blank	12	6	$Ce_{30}Co_{57}Fe_{10}Zn_3$

X	Y	Catalyst	X	Y	Catalyst	X	Y	Catalyst
12	7	$Ce_{30}Co_{57}Fe_{10}Sn_3$	13	14	$Ce_{30}Co_{57}Fe_{10}Sc_3$	15	10	Blank
12	8	$Ce_{30}Co_{57}Fe_{10}Eu_3$	13	15	$Ce_{30}Co_{57}Fe_{10}W_3$	15	11	Blank
12	9	$Ce_{30}Co_{57}Fe_{10}Sb_3$	14	3	$Ce_{30}Co_{57}Fe_{10}V_3$	15	12	Blank
12	10	$Ce_{30}Co_{57}Fe_{10}Cs_3$	14	4	$Ce_{30}Co_{57}Fe_{10}Ti_3$	15	13	Blank
12	11	$Ce_{30}Co_{57}Fe_{10}Fe_3$	14	5	$Ce_{30}Co_{57}Fe_{10}Te_3$	15	14	Blank
12	12	$Ce_{30}Co_{57}Fe_{10}Ga_3$	14	6	$Ce_{30}Co_{57}Fe_{10}Ba_3$	16	5	Blank
12	13	$Ce_{30}Co_{57}Fe_{10}Ge_3$	14	7	$Ce_{30}Co_{57}Fe_{10}Tm_3$	16	6	Blank
12	14	$Ce_{30}Co_{57}Fe_{10}Hf_3$	14	8	$Ce_{30}Co_{57}Fe_{10}Ta_3$	16	7	Blank
12	15	$Ce_{30}Co_{57}Fe_{10}In_3$	14	9	Blank	16	8	Blank
13	3	$Ce_{30}Co_{57}Fe_{10}Cu_3$	14	10	$Cu_{20}Co_{70}Ni_{10}$	16	9	Blank
13	4	$Ce_{30}Co_{57}Fe_{10}Na_3$	14	11	$Ce_{30}Co_{60}Fe_{10}$	16	10	Blank
13	5	$Ce_{30}Co_{57}Fe_{10}Si_3$	14	12	$Pt/Rh/Al_2O_3$	16	11	Blank
13	6	$Ce_{30}Co_{57}Fe_{10}Tb_3$	14	13	Blank	16	12	Blank
13	7	$Ce_{30}Co_{57}Fe_{10}Yb_3$	14	14	Blank	17	6	Blank
13	8	$Ce_{30}Co_{57}Fe_{10}Zr_3$	15	4	Blank	17	7	Blank
13	9	$Ce_{30}Co_{57}Fe_{10}K_3$	15	5	Blank	17	8	Blank
13	10	$Ce_{30}Co_{57}Fe_{10}Bi_3$	15	6	Blank	17	9	Blank
13	11	$Ce_{30}Co_{57}Fe_{10}Mo_3$	15	7	Blank	17	10	Blank
13	12	$Ce_{30}Co_{57}Fe_{10}Nb_3$	15	8	Blank	17	11	Blank
13	13	$Ce_{30}Co_{57}Fe_{10}Rb_3$	15	9	Blank	17	12	Blank

Table 6-8 Library 06 filling plan

X	**Y**	**Catalyst**	**X**	**Y**	**Catalyst**	**X**	**Y**	**Catalyst**
1	6	Blank	5	14	$Cu_{10}Fe_{80}Ce_{10}$	9	4	$Cu_{90}Fe_{10}$
1	7	Blank	5	15	$Cu_{70}Fe_{10}Ce_{20}$	9	5	$Cu_{10}Ce_{90}$
1	8	Blank	6	2	$Cu_{40}Fe_{30}Ce_{30}$	9	6	$Cu_{10}Fe_{10}Ce_{80}$
1	9	Blank	6	3	$Cu_{30}Fe_{60}Ce_{10}$	9	7	$Cu_{40}Fe_{20}Ce_{40}$
1	10	Blank	6	4	$Cu_{30}Ce_{70}$	9	8	$Cu_{50}Ce_{50}$
1	11	Blank	6	5	$Cu_{20}Fe_{60}Ce_{20}$	9	9	Blank
1	12	Blank	6	6	$Cu_{50}Fe_{20}Ce_{30}$	9	10	$Fe_{90}Ce_{10}$
2	5	Blank	6	7	$Cu_{10}Fe_{70}Ce_{20}$	9	11	Ce_{100}
2	6	Blank	6	8	$Cu_{20}Fe_{30}Ce_{50}$	9	12	$Cu_{80}Ce_{20}$
2	7	Blank	6	9	$Fe_{60}Ce_{40}$	9	13	$Cu_{80}Fe_{20}$
2	8	Blank	6	10	$Cu_{10}Fe_{50}Ce_{40}$	9	14	$Cu_{40}Fe_{60}$
2	9	Blank	6	11	$Cu_{30}Fe_{40}Ce_{30}$	9	15	$Cu_{70}Fe_{20}Ce_{10}$
2	10	Blank	6	12	$Cu_{10}Fe_{30}Ce_{60}$	9	16	$Cu_{70}Ce_{30}$
2	11	Blank	6	13	$Cu_{90}Ce_{10}$	10	1	$Cu_{60}Fe_{20}Ce_{20}$
2	12	Blank	6	14	$Cu_{20}Fe_{20}Ce_{60}$	10	2	$Cu_{50}Fe_{10}Ce_{40}$
3	4	Blank	6	15	$Cu_{10}Fe_{90}$	10	3	$Fe_{70}Ce_{30}$
3	5	Blank	7	2	$Cu_{60}Fe_{40}$	10	4	Blank
3	6	Blank	7	3	$Cu_{50}Fe_{50}$	10	5	Blank
3	7	Blank	7	4	$Cu_{10}Fe_{40}Ce_{50}$	10	6	$Co_{10}Mn_{70}Ce_{20}$
3	8	Blank	7	5	$Cu_{30}Fe_{30}Ce_{40}$	10	7	$Co_{80}Mn_{10}Ce_{10}$
3	9	Blank	7	6	$Fe_{10}Ce_{90}$	10	8	$Mn_{80}Ce_{20}$
3	10	Blank	7	7	$Cu_{30}Fe_{10}Ce_{60}$	10	9	$Co_{40}Ce_{60}$
3	11	Blank	7	8	$Fe_{30}Ce_{70}$	10	10	$Co_{10}Mn_{80}Ce_{10}$
3	12	Blank	7	9	$Cu_{20}Ce_{80}$	10	11	$Co_{10}Mn_{30}Ce_{60}$
3	13	Blank	7	10	$Fe_{20}Ce_{80}$	10	12	$Co_{10}Mn_{10}Ce_{80}$
3	14	Blank	7	11	$Cu_{30}Fe_{70}$	10	13	$Co_{50}Mn_{10}Ce_{40}$
4	3	$Ni_{95}Fe_{5}$	7	12	$Cu_{20}Fe_{80}$	10	14	$Co_{40}Mn_{30}Ce_{30}$
4	4	$Cu_{33,3}Fe_{33,3}Ce_{33,3}$	7	13	Cu_{100}	10	15	$Co_{70}Mn_{10}Ce_{20}$
4	5	$Co_{40}Ce_{60}$	7	14	$Cu_{50}Fe_{40}Ce_{10}$	10	16	$Mn_{40}Ce_{60}$
4	6	$Cu_{50}Ce_{50}$	7	15	$Cu_{30}Fe_{20}Ce_{50}$	11	2	$Co_{20}Mn_{70}Ce_{10}$
4	7	Blank	7	16	$Cu_{50}Fe_{30}Ce_{20}$	11	3	$Co_{60}Mn_{40}$
4	8	Blank	8	1	$Cu_{60}Fe_{10}Ce_{30}$	11	4	$Co_{90}Ce_{10}$
4	9	Blank	8	2	$Cu_{60}Fe_{30}Ce_{10}$	11	5	$Co_{50}Mn_{40}Ce_{10}$
4	10	Blank	8	3	$Cu_{20}Fe_{70}Ce_{10}$	11	6	$Co_{60}Ce_{40}$
4	11	Blank	8	4	$Cu_{70}Fe_{30}$	11	7	$Co_{20}Mn_{20}Ce_{60}$
4	12	Blank	8	5	Fe_{100}	11	8	$Co_{30}Ce_{70}$
4	13	Blank	8	6	$Fe_{80}Ce_{20}$	11	9	$Co_{70}Ce_{30}$
4	14	Blank	8	7	$Cu_{10}Fe_{60}Ce_{30}$	11	10	$Mn_{20}Ce_{80}$
5	3	Blank	8	8	$Cu_{40}Fe_{40}Ce_{20}$	11	11	$Co_{50}Mn_{50}$
5	4	$Ni_{70}Ce_{30}$	8	9	$Cu_{30}Fe_{50}Ce_{20}$	11	12	$Co_{60}Mn_{30}Ce_{10}$
5	5	$Ni_{15}Ce_{85}$	8	10	$Cu_{40}Ce_{60}$	11	13	$Co_{30}Mn_{20}Ce_{50}$
5	6	$Ni_{95}Y_{5}$	8	11	$Fe_{50}Ce_{50}$	11	14	$Co_{20}Mn_{10}Ce_{70}$
5	7	$Ce_{99}Rh_{1}$	8	12	$Cu_{20}Fe_{10}Ce_{70}$	11	15	$Co_{40}Mn_{20}Ce_{40}$
5	8	Blank	8	13	$Cu_{20}Fe_{40}Ce_{40}$	11	16	$Co_{10}Mn_{40}Ce_{50}$
5	9	Blank	8	14	$Cu_{10}Fe_{20}Ce_{70}$	12	2	Mn_{100}
5	10	Blank	8	15	$Cu_{40}Fe_{50}Ce_{10}$	12	3	Co_{100}
5	11	$Ni_{97}Na_{3}$	8	16	$Cu_{60}Ce_{40}$	12	4	$Co_{50}Mn_{20}Ce_{30}$
5	12	Blank	9	2	$Cu_{40}Fe_{10}Ce_{50}$	12	5	$Co_{10}Mn_{50}Ce_{40}$
5	13	$Fe_{40}Ce_{60}$	9	3	$Cu_{20}Fe_{50}Ce_{30}$	12	6	$Co_{20}Ce_{80}$

X	Y	Catalyst	X	Y	Catalyst	X	Y	Catalyst
12	7	$Mn_{70}Ce_{30}$	13	14	$Co_{70}Mn_{30}$	15	10	$Ni_{93}Y_7$
12	8	$Co_{10}Mn_{90}$	13	15	$Co_{20}Mn_{30}Ce_{50}$	15	11	$Ni_{94}Y_6$
12	9	$Co_{80}Mn_{20}$	14	3	$Co_{50}Mn_{30}Ce_{20}$	15	12	$Ni_{95}Y_5$
12	10	$Co_{20}Mn_{80}$	14	4	$Co_{50}Ce_{50}$	15	13	$Ni_{96}Y_4$
12	11	$Co_{80}Ce_{20}$	14	5	$Co_{70}Mn_{20}Ce_{10}$	15	14	$Ni_{97}Y_3$
12	12	$Co_{10}Mn_{60}Ce_{30}$	14	6	$Co_{40}Mn_{10}Ce_{50}$	16	5	$Ni_{98}Y_2$
12	13	$Co_{40}Mn_{60}$	14	7	$Co_{30}Mn_{60}Ce_{10}$	16	6	$Ni_{99}Y_1$
12	14	$Co_{30}Mn_{30}Ce_{40}$	14	8	$Co_{20}Mn_{60}Ce_{20}$	16	7	Ni_{100}
12	15	$Co_{20}Mn_{50}Ce_{30}$	14	9	$Mn_{60}Ce_{40}$	16	8	$Ni_{92}La_7Re_1$
13	3	$Co_{30}Mn_{10}Ce_{60}$	14	10	$Co_{30}Mn_{70}$	16	9	$Ni_{96}La_3Re_1$
13	4	$Co_{20}Mn_{40}Ce_{40}$	14	11	Ce_{100}	16	10	$Ni_{94}La_5Re_1$
13	5	$Mn_{50}Ce_{50}$	14	12	$Co_{40}Mn_{40}Ce_{20}$	16	11	$Ni_{97}La_2Re_1$
13	6	$Mn_{90}Ce_{10}$	14	13	$Co_{90}Mn_{10}$	16	12	$Ni_{91}La_8Re_1$
13	7	$Co_{60}Mn_{20}Ce_{20}$	14	14	$Co_{30}Mn_{40}Ce_{30}$	17	6	$Ni_{90}La_9Re_1$
13	8	$Co_{30}Mn_{50}Ce_{20}$	15	4	$Co_{40}Mn_{50}Ce_{10}$	17	7	$Ni_{98}La_1Re_1$
13	9	$Mn_{10}Ce_{90}$	15	5	Blank	17	8	$Ni_{89}La_{10}Re_1$
13	10	$Co_{10}Mn_{20}Ce_{70}$	15	6	$Ni_{15}Ce_{85}$	17	9	$Ni_{95}La_4Re_1$
13	11	$Mn_{30}Ce_{70}$	15	7	$Ni_{90}Y_{10}$	17	10	$Ni_{99}Re_1$
13	12	$Co_{60}Mn_{10}Ce_{30}$	15	8	$Ni_{91}Y_9$	17	11	$Ni_{93}La_6Re_1$
13	13	$Co_{10}Ce_{90}$	15	9	$Ni_{92}Y_8$	17	12	Blank

Table 6-9 Library 07 filling plan

X	Y	Catalyst	X	Y	Catalyst	X	Y	Catalyst
1	6	$Cu_{50}Co_{50}$	5	14	Blank	9	4	$Co_{33,3}Cr_{33,3}La_{33,3}$
1	7	$Cu_{50}Mn_{50}$	5	15	Blank	9	5	$Co_{33,3}Cr_{33,3}Ti_{33,3}$
1	8	$Cu_{50}Cr_{50}$	6	2	$Cu_{33,3}Co_{33,3}Mn_{33,3}$	9	6	$Co_{33,3}Fe_{33,3}Ce_{33,3}$
1	9	$Cu_{50}Fe_{50}$	6	3	$Cu_{33,3}Co_{33,3}Cr_{33,3}$	9	7	$Co_{33,3}Fe_{33,3}V_{33,3}$
1	10	$Cu_{50}Ce_{50}$	6	4	$Cu_{33,3}Co_{33,3}Fe_{33,3}$	9	8	$Co_{33,3}Fe_{33,3}Mo_{33,3}$
1	11	$Cu_{50}V_{50}$	6	5	$Cu_{33,3}Co_{33,3}Ce_{33,3}$	9	9	Blank
1	12	$Cu_{50}Mo_{50}$	6	6	$Cu_{33,3}Co_{33,3}V_{33,3}$	9	10	$Co_{33,3}Fe_{33,3}Ti_{33,3}$
2	5	$Cu_{50}La_{50}$	6	7	$Cu_{33,3}Co_{33,3}Mo_{33,3}$	9	11	$Co_{33,3}Ce_{33,3}V_{33,3}$
2	6	$Cu_{50}Ti_{50}$	6	8	$Cu_{33,3}Co_{33,3}La_{33,3}$	9	12	$Co_{33,3}Ce_{33,3}Mo_{33,3}$
2	7	$Co_{50}Mn_{50}$	6	9	$Cu_{33,3}Co_{33,3}Ti_{33,3}$	9	13	$Co_{33,3}Ce_{33,3}La_{33,3}$
2	8	$Co_{50}Cr_{50}$	6	10	$Cu_{33,3}Mn_{33,3}Cr_{33,3}$	9	14	$Co_{33,3}Ce_{33,3}Ti_{33,3}$
2	9	$Co_{50}Fe_{50}$	6	11	$Cu_{33,3}Mn_{33,3}Fe_{33,3}$	9	15	$Co_{33,3}V_{33,3}Mo_{33,3}$
2	10	$Co_{50}Ce_{50}$	6	12	$Cu_{33,3}Mn_{33,3}Ce_{33,3}$	9	16	$Co_{33,3}V_{33,3}La_{33,3}$
2	11	$Co_{50}V_{50}$	6	13	$Cu_{33,3}Mn_{33,3}V_{33,3}$	10	1	$Co_{33,3}V_{33,3}Ti_{33,3}$
2	12	$Co_{50}Mo_{50}$	6	14	$Cu_{33,3}Mn_{33,3}Mo_{33,3}$	10	2	$Co_{33,3}Mo_{33,3}La_{33,3}$
3	4	$Co_{50}La_{50}$	6	15	$Cu_{33,3}Mn_{33,3}La_{33,3}$	10	3	$Co_{33,3}Mo_{33,3}Ti_{33,3}$
3	5	$Co_{50}Ti_{50}$	7	2	$Cu_{33,3}Mn_{33,3}Ti_{33,3}$	10	4	$Co_{33,3}La_{33,3}Ti_{33,3}$
3	6	$Mn_{50}Cr_{50}$	7	3	$Cu_{33,3}Cr_{33,3}Fe_{33,3}$	10	5	$Mn_{33,3}Cr_{33,3}Fe_{33,3}$
3	7	$Mn_{50}Fe_{50}$	7	4	$Cu_{33,3}Cr_{33,3}Ce_{33,3}$	10	6	$Mn_{33,3}Cr_{33,3}Ce_{33,3}$
3	8	$Mn_{50}Ce_{50}$	7	5	$Cu_{33,3}Cr_{33,3}V_{33,3}$	10	7	$Mn_{33,3}Cr_{33,3}V_{33,3}$
3	9	$Mn_{50}V_{50}$	7	6	$Cu_{33,3}Cr_{33,3}Mo_{33,3}$	10	8	$Mn_{33,3}Cr_{33,3}Mo_{33,3}$
3	10	$Mn_{50}Mo_{50}$	7	7	$Cu_{33,3}Cr_{33,3}La_{33,3}$	10	9	$Mn_{33,3}Cr_{33,3}La_{33,3}$
3	11	$Mn_{50}La_{50}$	7	8	$Cu_{33,3}Cr_{33,3}Ti_{33,3}$	10	10	$Mn_{33,3}Cr_{33,3}Ti_{33,3}$
3	12	$Mn_{50}Ti_{50}$	7	9	$Cu_{33,3}Fe_{33,3}Ce_{33,3}$	10	11	$Mn_{33,3}Fe_{33,3}Ce_{33,3}$
3	13	$Cr_{50}Fe_{50}$	7	10	$Cu_{33,3}Fe_{33,3}V_{33,3}$	10	12	$Mn_{33,3}Fe_{33,3}V_{33,3}$
3	14	$Cr_{50}Ce_{50}$	7	11	$Cu_{33,3}Fe_{33,3}Mo_{33,3}$	10	13	$Mn_{33,3}Fe_{33,3}Mo_{33,3}$
4	3	$Cr_{50}V_{50}$	7	12	$Cu_{33,3}Fe_{33,3}La_{33,3}$	10	14	$Mn_{33,3}Fe_{33,3}La_{33,3}$
4	4	$Cr_{50}Mo_{50}$	7	13	$Cu_{33,3}Fe_{33,3}Ti_{33,3}$	10	15	$Mn_{33,3}Fe_{33,3}Ti_{33,3}$
4	5	$Cr_{50}La_{50}$	7	14	$Cu_{33,3}Ce_{33,3}V_{33,3}$	10	16	$Mn_{33,3}Ce_{33,3}V_{33,3}$
4	6	$Cr_{50}Ti_{50}$	7	15	$Cu_{33,3}Ce_{33,3}Mo_{33,3}$	11	2	$Mn_{33,3}Ce_{33,3}Mo_{33,3}$
4	7	$Fe_{50}Ce_{50}$	7	16	$Cu_{33,3}Ce_{33,3}La_{33,3}$	11	3	$Mn_{33,3}Ce_{33,3}La_{33,3}$
4	8	$Fe_{50}V_{50}$	8	1	$Cu_{33,3}Ce_{33,3}Ti_{33,3}$	11	4	$Mn_{33,3}Ce_{33,3}Ti_{33,3}$
4	9	$Fe_{50}Mo_{50}$	8	2	$Cu_{33,3}V_{33,3}Mo_{33,3}$	11	5	$Mn_{33,3}V_{33,3}Mo_{33,3}$
4	10	$Fe_{50}La_{50}$	8	3	$Cu_{33,3}V_{33,3}La_{33,3}$	11	6	$Mn_{33,3}V_{33,3}La_{33,3}$
4	11	$Fe_{50}Ti_{50}$	8	4	$Cu_{33,3}V_{33,3}Ti_{33,3}$	11	7	$Mn_{33,3}V_{33,3}Ti_{33,3}$
4	12	$Ce_{50}V_{50}$	8	5	$Cu_{33,3}Mo_{33,3}La_{33,3}$	11	8	$Mn_{33,3}Mo_{33,3}La_{33,3}$
4	13	$Ce_{50}Mo_{50}$	8	6	$Cu_{33,3}Mo_{33,3}Ti_{33,3}$	11	9	$Mn_{33,3}Mo_{33,3}Ti_{33,3}$
4	14	$Ce_{50}La_{50}$	8	7	$Cu_{33,3}La_{33,3}Ti_{33,3}$	11	10	$Mn_{33,3}La_{33,3}Ti_{33,3}$
5	3	$Ce_{50}Ti_{50}$	8	8	$Co_{33,3}Mn_{33,3}Cr_{33,3}$	11	11	$Cr_{33,3}Fe_{33,3}Ce_{33,3}$
5	4	$V_{50}Mo_{50}$	8	9	$Co_{33,3}Mn_{33,3}Fe_{33,3}$	11	12	$Cr_{33,3}Fe_{33,3}V_{33,3}$
5	5	$V_{50}La_{50}$	8	10	$Co_{33,3}Mn_{33,3}Ce_{33,3}$	11	13	$Cr_{33,3}Fe_{33,3}Mo_{33,3}$
5	6	$V_{50}Ti_{50}$	8	11	$Co_{33,3}Mn_{33,3}V_{33,3}$	11	14	$Cr_{33,3}Fe_{33,3}La_{33,3}$
5	7	$Mo_{50}La_{50}$	8	12	$Co_{33,3}Mn_{33,3}Mo_{33,3}$	11	15	$Cr_{33,3}Fe_{33,3}Ti_{33,3}$
5	8	$Mo_{50}Ti_{50}$	8	13	$Co_{33,3}Mn_{33,3}La_{33,3}$	11	16	$Cr_{33,3}Ce_{33,3}V_{33,3}$
5	9	$La_{50}Ti_{50}$	8	14	$Co_{33,3}Mn_{33,3}Ti_{33,3}$	12	2	$Cr_{33,3}Ce_{33,3}Mo_{33,3}$
5	10	Blank	8	15	$Co_{33,3}Cr_{33,3}Fe_{33,3}$	12	3	$Cr_{33,3}Ce_{33,3}La_{33,3}$
5	11	Blank	8	16	$Co_{33,3}Cr_{33,3}Ce_{33,3}$	12	4	$Cr_{33,3}Ce_{33,3}Ti_{33,3}$
5	12	Blank	9	2	$Co_{33,3}Cr_{33,3}V_{33,3}$	12	5	$Cr_{33,3}V_{33,3}Mo_{33,3}$
5	13	Blank	9	3	$Co_{33,3}Cr_{33,3}Mo_{33,3}$	12	6	$Cr_{33,3}V_{33,3}La_{33,3}$

X	Y	Catalyst	X	Y	Catalyst	X	Y	Catalyst
12	7	$Cr_{33,3}V_{33,3}Ti_{33,3}$	13	14	$V_{33,3}Mo_{33,3}La_{33,3}$	15	10	Blank
12	8	$Cr_{33,3}Mo_{33,3}La_{33,3}$	13	15	$V_{33,3}Mo_{33,3}Ti_{33,3}$	15	11	Blank
12	9	$Cr_{33,3}Mo_{33,3}Ti_{33,3}$	14	3	$V_{33,3}La_{33,3}Ti_{33,3}$	15	12	Blank
12	10	$Cr_{33,3}La_{33,3}Ti_{33,3}$	14	4	$Mo_{33,3}La_{33,3}Ti_{33,3}$	15	13	Blank
12	11	$Fe_{33,3}Ce_{33,3}V_{33,3}$	14	5	Blank	15	14	Blank
12	12	$Fe_{33,3}Ce_{33,3}Mo_{33,3}$	14	6	$Co_{20}Cu_{50}Mn_{30}$	16	5	Blank
12	13	$Fe_{33,3}Ce_{33,3}La_{33,3}$	14	7	Blank	16	6	Blank
12	14	$Fe_{33,3}Ce_{33,3}Ti_{33,3}$	14	8	$Co_{20}Mn_{80}$	16	7	Blank
12	15	$Fe_{33,3}V_{33,3}Mo_{33,3}$	14	9	Blank	16	8	Blank
13	3	$Fe_{33,3}V_{33,3}La_{33,3}$	14	10	Blank	16	9	Blank
13	4	$Fe_{33,3}V_{33,3}Ti_{33,3}$	14	11	Blank	16	10	Blank
13	5	$Fe_{33,3}Mo_{33,3}La_{33,3}$	14	12	Blank	16	11	Blank
13	6	$Fe_{33,3}Mo_{33,3}Ti_{33,3}$	14	13	Blank	16	12	Blank
13	7	$Fe_{33,3}La_{33,3}Ti_{33,3}$	14	14	Blank	17	6	Blank
13	8	$Ce_{33,3}V_{33,3}Mo_{33,3}$	15	4	Blank	17	7	Blank
13	9	$Ce_{33,3}V_{33,3}La_{33,3}$	15	5	Blank	17	8	Blank
13	10	$Ce_{33,3}V_{33,3}Ti_{33,3}$	15	6	Blank	17	9	Blank
13	11	$Ce_{33,3}Mo_{33,3}La_{33,3}$	15	7	Blank	17	10	Blank
13	12	$Ce_{33,3}Mo_{33,3}Ti_{33,3}$	15	8	Blank	17	11	Blank
13	13	$Ce_{33,3}La_{33,3}Ti_{33,3}$	15	9	Blank	17	12	Blank

Table 6-10 Library 08 filling plan

X	Y	Catalyst	X	Y	Catalyst	X	Y	Catalyst
1	6	$Ce_{10}Co_{90}$	5	14	Blank	9	4	$Co_{50}Cu_{50}$
1	7	Blank	5	15	$Ce_{10}Mo_{90}$	9	5	Blank
1	8	$Ce_{50}Co_{50}$	6	2	Blank	9	6	$Co_{90}Cu_{10}$
1	9	Blank	6	3	Blank	9	7	Blank
1	10	$Ce_{90}Co_{10}$	6	4	$Cu_{10}Ti_{90}$	9	8	$Co_{10}Fe_{90}$
1	11	Blank	6	5	Blank	9	9	Blank
1	12	$Ce_{10}Cr_{90}$	6	6	$Fe_{10}Mn_{90}$	9	10	$Co_{50}Fe_{50}$
2	5	Blank	6	7	Blank	9	11	$Cr_{10}Mo_{90}$
2	6	Blank	6	8	Blank	9	12	$Co_{90}Fe_{10}$
2	7	$Cu_{10}Mo_{90}$	6	9	Blank	9	13	Blank
2	8	Blank	6	10	Blank	9	14	$Co_{10}Mn_{90}$
2	9	Blank	6	11	Blank	9	15	Blank
2	10	$Mn_{90}Mo_{10}$	6	12	Blank	9	16	$Co_{50}Mn_{50}$
2	11	Blank	6	13	Blank	10	1	Blank
2	12	Blank	6	14	$Fe_{10}Mo_{90}$	10	2	Blank
3	4	Blank	6	15	Blank	10	3	$Fe_{90}Mn_{10}$
3	5	$Ce_{50}Cr_{50}$	7	2	$Ce_{50}Mo_{50}$	10	4	Blank
3	6	Blank	7	3	Blank	10	5	Blank
3	7	$Ce_{90}Cr_{10}$	7	4	$Ce_{90}Mo_{10}$	10	6	$Fe_{50}Mn_{50}$
3	8	Blank	7	5	Blank	10	7	Blank
3	9	$Ce_{10}Cu_{90}$	7	6	$Ce_{10}Ti_{90}$	10	8	Blank
3	10	Blank	7	7	Blank	10	9	Blank
3	11	$Ce_{50}Cu_{50}$	7	8	$Ce_{50}Ti_{50}$	10	10	$Cu_{90}Mn_{10}$
3	12	Blank	7	9	Blank	10	11	Blank
3	13	$Ce_{90}Cu_{10}$	7	10	$Ce_{90}Ti_{10}$	10	12	Blank
3	14	Blank	7	11	$Fe_{10}Ti_{90}$	10	13	Blank
4	3	Blank	7	12	$Co_{10}Cr_{90}$	10	14	$Mn_{50}Mo_{50}$
4	4	Blank	7	13	Blank	10	15	Blank
4	5	Blank	7	14	$Co_{50}Cr_{50}$	10	16	Blank
4	6	Blank	7	15	Blank	11	2	$Co_{90}Fe_{10}$
4	7	Blank	7	16	$Co_{90}Cr_{10}$	11	3	Blank
4	8	Blank	8	1	Blank	11	4	$Co_{10}Mo_{90}$
4	9	Blank	8	2	Blank	11	5	$Cu_{50}Ti_{50}$
4	10	Blank	8	3	Blank	11	6	$Co_{50}Mo_{50}$
4	11	$Fe_{90}Mo_{10}$	8	4	Blank	11	7	Blank
4	12	Blank	8	5	Blank	11	8	$Co_{90}Mo_{10}$
4	13	Blank	8	6	Blank	11	9	Blank
4	14	$Mo_{10}Ti_{90}$	8	7	Blank	11	10	$Co_{10}Ti_{90}$
5	3	$Ce_{10}Fe_{90}$	8	8	$Cu_{10}Mn_{90}$	11	11	Blank
5	4	Blank	8	9	Blank	11	12	$Co_{50}Ti_{50}$
5	5	$Ce_{50}Fe_{50}$	8	10	Blank	11	13	$Cu_{90}Mo_{10}$
5	6	$Mn_{90}Ti_{10}$	8	11	Blank	11	14	$Co_{90}Ti_{10}$
5	7	$Ce_{90}Fe_{10}$	8	12	Blank	11	15	Blank
5	8	$Cu_{50}Mn_{50}$	8	13	Blank	11	16	$Cr_{10}Cu_{90}$
5	9	$Ce_{10}Mn_{90}$	8	14	$Mn_{10}Mo_{90}$	12	2	Blank
5	10	Blank	8	15	Blank	12	3	$Mn_{10}Ti_{90}$
5	11	$Ce_{50}Mn_{50}$	8	16	Blank	12	4	Blank
5	12	Blank	9	2	$Co_{10}Cu_{90}$	12	5	Blank
5	13	$Ce_{90}Mn_{10}$	9	3	Blank	12	6	$Fe_{90}Ti_{10}$

X	Y	Catalyst	X	Y	Catalyst	X	Y	Catalyst
12	7	Blank	13	14	Blank	15	10	$Cr_{90}Mo_{10}$
12	8	Blank	13	15	$Cr_{50}Mn_{50}$	15	11	$Cu_{90}Ti_{10}$
12	9	Blank	14	3	Blank	15	12	$Cr_{10}Ti_{90}$
12	10	Blank	14	4	Blank	15	13	Blank
12	11	Blank	14	5	$Fe_{50}Mo_{50}$	15	14	$Cr_{50}Ti_{50}$
12	12	Blank	14	6	Blank	16	5	Blank
12	13	$Pt/Rh/Al_2O_3$	14	7	Blank	16	6	Blank
12	14	Blank	14	8	$Fe_{50}Ti_{50}$	16	7	Blank
12	15	Blank	14	9	Blank	16	8	Blank
13	3	$Mn_{50}Ti_{50}$	14	10	Blank	16	9	$Cu_{50}Mo_{50}$
13	4	Blank	14	11	Blank	16	10	Blank
13	5	$Cr_{90}Cu_{10}$	14	12	Blank	16	11	Blank
13	6	Blank	14	13	Blank	16	12	Blank
13	7	$Cr_{10}Fe_{90}$	14	14	Blank	17	6	$Cr_{90}Ti_{10}$
13	8	Blank	15	4	$Cr_{90}Mn_{10}$	17	7	Blank
13	9	$Cr_{50}Fe_{50}$	15	5	Blank	17	8	$Cu_{10}Fe_{90}$
13	10	$Cr_{50}Cu_{50}$	15	6	Blank	17	9	Blank
13	11	$Cr_{90}Fe_{10}$	15	7	$Mo_{90}Ti_{10}$	17	10	$Cu_{50}Fe_{50}$
13	12	$Mo_{50}Ti_{50}$	15	8	$Cr_{50}Mo_{50}$	17	11	Blank
13	13	$Cr_{10}Mn_{90}$	15	9	Blank	17	12	$Cu_{90}Fe_{10}$

Table 6-11 Library 09 filling plan

X	Y	Catalyst	X	Y	Catalyst	X	Y	Catalyst
1	6	$Ce_{32,3}Ti_{32,3}Cr_{32,3}Al_3$	5	14	$Ti_{30}Cr_{70}$	9	4	$Ce_{60}Ti_{10}Cr_{30}$
1	7	$Ce_{32,3}Ti_{32,3}Cr_{32,3}B_3$	5	15	$Ti_{40}Cr_{60}$	9	5	$Ce_{60}Ti_{20}Cr_{20}$
1	8	$Ce_{32,3}Ti_{32,3}Cr_{32,3}Dy_3$	6	2	$Ti_{50}Cr_{50}$	9	6	$Ce_{60}Ti_{30}Cr_{10}$
1	9	$Ce_{32,3}Ti_{32,3}Cr_{32,3}Er_3$	6	3	$Ti_{60}Cr_{40}$	9	7	$Ce_{60}Ti_{40}$
1	10	$Ce_{32,3}Ti_{32,3}Cr_{32,3}Gd_3$	6	4	$Ti_{70}Cr_{30}$	9	8	$Ce_{70}Cr_{30}$
1	11	$Ce_{32,3}Ti_{32,3}Cr_{32,3}Ho_3$	6	5	$Ti_{80}Cr_{20}$	9	9	$Ce_{70}Ti_{10}Cr_{20}$
1	12	$Ce_{32,3}Ti_{32,3}Cr_{32,3}Ca_3$	6	6	$Ti_{90}Cr_{10}$	9	10	Blank
2	5	$Ce_{32,3}Ti_{32,3}Cr_{32,3}Sr_3$	6	7	Ti_{100}	9	11	$Ce_{70}Ti_{20}Cr_{10}$
2	6	$Ce_{32,3}Ti_{32,3}Cr_{32,3}La_3$	6	8	$Ce_{10}Cr_{90}$	9	12	$Ce_{70}Ti_{30}$
2	7	$Ce_{32,3}Ti_{32,3}Cr_{32,3}Li_3$	6	9	$Ce_{10}Ti_{10}Cr_{80}$	9	13	$Ce_{80}Cr_{20}$
2	8	$Ce_{32,3}Ti_{32,3}Cr_{32,3}Lu_3$	6	10	$Ce_{10}Ti_{20}Cr_{70}$	9	14	$Ce_{80}Ti_{10}Cr_{10}$
2	9	$Ce_{32,3}Ti_{32,3}Cr_{32,3}Mg_3$	6	11	$Ce_{10}Ti_{30}Cr_{60}$	9	15	$Ce_{80}Ti_{20}$
2	10	$Ce_{32,3}Ti_{32,3}Cr_{32,3}Mn_3$	6	12	$Ce_{10}Ti_{40}Cr_{50}$	9	16	$Ce_{90}Cr_{10}$
2	11	$Ce_{32,3}Ti_{32,3}Cr_{32,3}Nd_3$	6	13	$Ce_{10}Ti_{50}Cr_{40}$	10	1	$Ce_{90}Ti_{10}$
2	12	$Ce_{32,3}Ti_{32,3}Cr_{32,3}Sm_3$	6	14	$Ce_{10}Ti_{60}Cr_{30}$	10	2	Ce_{100}
3	4	$Ce_{32,3}Ti_{32,3}Cr_{32,3}Se_3$	6	15	$Ce_{10}Ti_{70}Cr_{20}$	10	3	$Ce_{33,3}Ti_{33,3}Cr_{33,3}$
3	5	$Ce_{32,3}Ti_{32,3}Cr_{32,3}Y_3$	7	2	$Ce_{10}Ti_{80}Cr_{10}$	10	4	Cr_{100}
3	6	$Ce_{32,3}Ti_{32,3}Cr_{32,3}Zn_3$	7	3	$Ce_{10}Ti_{90}$	10	5	$Mn_{10}Cr_{90}$
3	7	$Ce_{32,3}Ti_{32,3}Cr_{32,3}Sn_3$	7	4	$Ce_{20}Cr_{80}$	10	6	$Mn_{20}Cr_{80}$
3	8	$Ce_{32,3}Ti_{32,3}Cr_{32,3}Eu_3$	7	5	$Ce_{20}Ti_{10}Cr_{70}$	10	7	$Mn_{30}Cr_{70}$
3	9	$Ce_{32,3}Ti_{32,3}Cr_{32,3}Sb_3$	7	6	$Ce_{20}Ti_{20}Cr_{60}$	10	8	$Mn_{40}Cr_{60}$
3	10	$Ce_{32,3}Ti_{32,3}Cr_{32,3}Cs_3$	7	7	$Ce_{20}Ti_{30}Cr_{50}$	10	9	$Mn_{50}Cr_{50}$
3	11	$Ce_{32,3}Ti_{32,3}Cr_{32,3}Fe_3$	7	8	$Ce_{20}Ti_{40}Cr_{40}$	10	10	$Mn_{60}Cr_{40}$
3	12	$Ce_{32,3}Ti_{32,3}Cr_{32,3}Ga_3$	7	9	$Ce_{20}Ti_{50}Cr_{30}$	10	11	$Mn_{70}Cr_{30}$
3	13	$Ce_{32,3}Ti_{32,3}Cr_{32,3}Ge_3$	7	10	$Ce_{20}Ti_{60}Cr_{20}$	10	12	$Mn_{80}Cr_{20}$
3	14	$Ce_{32,3}Ti_{32,3}Cr_{32,3}Hf_3$	7	11	$Ce_{20}Ti_{70}Cr_{10}$	10	13	$Mn_{90}Cr_{10}$
4	3	$Ce_{32,3}Ti_{32,3}Cr_{32,3}In_3$	7	12	$Ce_{20}Ti_{80}$	10	14	Mn_{100}
4	4	$Ce_{32,3}Ti_{32,3}Cr_{32,3}Cu_3$	7	13	$Ce_{30}Cr_{70}$	10	15	Co_{100}
4	5	$Ce_{32,3}Ti_{32,3}Cr_{32,3}Na_3$	7	14	$Ce_{30}Ti_{10}Cr_{60}$	10	16	$Mn_{10}Co_{90}$
4	6	$Ce_{32,3}Ti_{32,3}Cr_{32,3}Si_3$	7	15	$Ce_{30}Ti_{20}Cr_{50}$	11	2	$Mn_{20}Co_{80}$
4	7	$Ce_{32,3}Ti_{32,3}Cr_{32,3}Tb_3$	7	16	$Ce_{30}Ti_{30}Cr_{40}$	11	3	$Mn_{30}Co_{70}$
4	8	$Ce_{32,3}Ti_{32,3}Cr_{32,3}Yb_3$	8	1	$Ce_{30}Ti_{40}Cr_{30}$	11	4	$Mn_{40}Co_{60}$
4	9	$Ce_{32,3}Ti_{32,3}Cr_{32,3}Zr_3$	8	2	$Ce_{30}Ti_{50}Cr_{20}$	11	5	$Mn_{50}Co_{50}$
4	10	$Ce_{32,3}Ti_{32,3}Cr_{32,3}K_3$	8	3	$Ce_{30}Ti_{60}Cr_{10}$	11	6	$Mn_{60}Co_{40}$
4	11	$Ce_{32,3}Ti_{32,3}Cr_{32,3}Bi_3$	8	4	$Ce_{30}Ti_{70}$	11	7	$Mn_{70}Co_{30}$
4	12	$Ce_{32,3}Ti_{32,3}Cr_{32,3}Mo_3$	8	5	$Ce_{40}Cr_{60}$	11	8	$Mn_{80}Co_{20}$
4	13	$Ce_{32,3}Ti_{32,3}Cr_{32,3}Nb_3$	8	6	$Ce_{40}Ti_{10}Cr_{50}$	11	9	$Mn_{90}Co_{10}$
4	14	$Ce_{32,3}Ti_{32,3}Cr_{32,3}Rb_3$	8	7	$Ce_{40}Ti_{20}Cr_{40}$	11	10	$Co_{10}Cr_{90}$
5	3	$Ce_{32,3}Ti_{32,3}Cr_{32,3}Sc_3$	8	8	$Ce_{40}Ti_{30}Cr_{30}$	11	11	$Co_{20}Cr_{80}$
5	4	$Ce_{32,3}Ti_{32,3}Cr_{32,3}W_3$	8	9	$Ce_{40}Ti_{40}Cr_{20}$	11	12	$Co_{30}Cr_{70}$
5	5	$Ce_{32,3}Ti_{32,3}Cr_{32,3}V_3$	8	10	$Ce_{40}Ti_{50}Cr_{10}$	11	13	$Co_{40}Cr_{60}$
5	6	$Ce_{32,3}Ti_{32,3}Cr_{32,3}Te_3$	8	11	$Ce_{40}Ti_{60}$	11	14	$Co_{50}Cr_{50}$
5	7	$Ce_{32,3}Ti_{32,3}Cr_{32,3}Ba_3$	8	12	$Ce_{50}Cr_{50}$	11	15	$Co_{60}Cr_{40}$
5	8	$Ce_{32,3}Ti_{32,3}Cr_{32,3}Tm_3$	8	13	$Ce_{50}Ti_{10}Cr_{40}$	11	16	$Co_{70}Cr_{30}$
5	9	$Ce_{32,3}Ti_{32,3}Cr_{32,3}Ta_3$	8	14	$Ce_{50}Ti_{20}Cr_{30}$	12	2	$Co_{80}Cr_{20}$
5	10	$Ce_{32,3}Ti_{32,3}Cr_{32,3}Co_3$	8	15	$Ce_{50}Ti_{30}Cr_{20}$	12	3	$Co_{90}Cr_{10}$
5	11	Cr_{100}	8	16	$Ce_{50}Ti_{40}Cr_{10}$	12	4	$Mn_{10}Co_{10}Cr_{80}$
5	12	$Ti_{10}Cr_{90}$	9	2	$Ce_{50}Ti_{50}$	12	5	$Mn_{10}Co_{20}Cr_{70}$
5	13	$Ti_{20}Cr_{80}$	9	3	$Ce_{60}Cr_{40}$	12	6	$Mn_{10}Co_{30}Cr_{60}$

X	Y	Catalyst	X	Y	Catalyst	X	Y	Catalyst
12	7	$Mn_{10}Co_{40}Cr_{50}$	13	14	$Mn_{40}Co_{30}Cr_{30}$	15	10	$Pt/Rh/Al_2O_3$
12	8	$Mn_{10}Co_{50}Cr_{40}$	13	15	$Mn_{40}Co_{40}Cr_{20}$	15	11	Blank
12	9	$Mn_{10}Co_{60}Cr_{30}$	14	3	$Mn_{40}Co_{50}Cr_{10}$	15	12	Blank
12	10	$Mn_{10}Co_{70}Cr_{20}$	14	4	$Mn_{50}Co_{10}Cr_{40}$	15	13	Blank
12	11	$Mn_{10}Co_{80}Cr_{10}$	14	5	$Mn_{50}Co_{20}Cr_{30}$	15	14	Blank
12	12	$Mn_{20}Co_{10}Cr_{70}$	14	6	$Mn_{50}Co_{30}Cr_{20}$	16	5	Blank
12	13	$Mn_{20}Co_{20}Cr_{60}$	14	7	$Mn_{50}Co_{40}Cr_{10}$	16	6	Blank
12	14	$Mn_{20}Co_{30}Cr_{50}$	14	8	$Mn_{60}Co_{10}Cr_{30}$	16	7	Blank
12	15	$Mn_{20}Co_{40}Cr_{40}$	14	9	$Mn_{60}Co_{20}Cr_{20}$	16	8	Blank
13	3	$Mn_{20}Co_{50}Cr_{30}$	14	10	$Mn_{60}Co_{30}Cr_{10}$	16	9	Blank
13	4	$Mn_{20}Co_{60}Cr_{20}$	14	11	$Mn_{70}Co_{10}Cr_{20}$	16	10	Blank
13	5	$Mn_{20}Co_{70}Cr_{10}$	14	12	$Mn_{70}Co_{20}Cr_{10}$	16	11	Blank
13	6	$Mn_{30}Co_{10}Cr_{60}$	14	13	$Mn_{80}Co_{10}Cr_{10}$	16	12	Blank
13	7	$Mn_{30}Co_{20}Cr_{50}$	14	14	$Mn_{33,3}Co_{33,3}Cr_{33,3}$	17	6	Blank
13	8	$Mn_{30}Co_{30}Cr_{40}$	15	4	$Ce_{33,3}Ti_{33,3}Cr_{33,3}$	17	7	Blank
13	9	$Mn_{30}Co_{40}Cr_{30}$	15	5	Blank	17	8	Blank
13	10	$Mn_{30}Co_{50}Cr_{20}$	15	6	Blank	17	9	Blank
13	11	$Mn_{30}Co_{60}Cr_{10}$	15	7	Blank	17	10	Blank
13	12	$Mn_{40}Co_{10}Cr_{50}$	15	8	Blank	17	11	Blank
13	13	$Mn_{40}Co_{20}Cr_{40}$	15	9	Blank	17	12	Blank

Table 6-12 Library 10 filling plan

X	**Y**	**Catalyst**	**X**	**Y**	**Catalyst**	**X**	**Y**	**Catalyst**
1	6	$Ce_9Ti_{79}Cr_9Al_3$	5	14	$Cr_{20}Fe_{80}$	9	4	Blank
1	7	$Ce_9Ti_{79}Cr_9B_3$	5	15	$Cr_{30}Fe_{70}$	9	5	Blank
1	8	$Ce_9Ti_{79}Cr_9Dy_3$	6	2	$Cr_{40}Fe_{60}$	9	6	Blank
1	9	$Ce_9Ti_{79}Cr_9Er_3$	6	3	$Cr_{50}Fe_{50}$	9	7	$Cr_{87}Fe_{10}Zn_3$
1	10	$Ce_9Ti_{79}Cr_9Gd_3$	6	4	$Cr_{60}Fe_{40}$	9	8	$Cr_{87}Fe_{10}Zr_3$
1	11	$Ce_9Ti_{79}CrHo_3$	6	5	$Cr_{70}Fe_{30}$	9	9	Blank
1	12	$Ce_9Ti_{79}Cr_9Ca_3$	6	6	$Cr_{80}Fe_{20}$	9	10	$Cr_{87}Fe_{10}Ce_3$
2	5	$Ce_9Ti_{79}Cr_9Sr_3$	6	7	$Cr_{90}Fe_{10}$	9	11	$Cr_{87}Fe_{10}Ti_3$
2	6	$Ce_9Ti_{79}Cr_9La_3$	6	8	Cr_{100}	9	12	$Ce_{19}Ti_{49}Cr_{29}V_3$
2	7	$Ce_9Ti_{79}Cr_9Li_3$	6	9	$Cr_{87}Fe_{10}Al_3$	9	13	$Ce_{18,33}Ti_{48,33}Cr_{28,33}V_5$
2	8	$Ce_9Ti_{79}Cr_9Lu_3$	6	10	$Cr_{87}Fe_{10}Ba_3$	9	14	$Ce_{17,67}Ti_{47,67}Cr_{27,67}V_7$
2	9	$Ce_9Ti_{79}Cr_9Mg_3$	6	11	$Cr_{87}Fe_{10}Bi_3$	9	15	$Ce_{17}Ti_{47}Cr_{27}V_9$
2	10	$Ce_9Ti_{79}Cr_9Mn_3$	6	12	$Cr_{87}Fe_{10}B_3$	9	16	$Ce_{19}Ti_{49}Cr_{29}Sc_3$
2	11	$Ce_9Ti_{79}Cr_9Nd_3$	6	13	$Cr_{87}Fe_{10}Ca_3$	10	1	$Ce_{18,33}Ti_{48,33}Cr_{28,33}Sc_5$
2	12	$Ce_9Ti_{79}Cr_9Sm_3$	6	14	$Cr_{87}Fe_{10}Co_3$	10	2	$Ce_{17,67}Ti_{47,67}Cr_{27,67}Sc_7$
3	4	$Ce_9Ti_{79}Cr_9Se_3$	6	15	$Cr_{87}Fe_{10}Cs_3$	10	3	$Ce_{17}Ti_{47}Cr_{27}Sc_9$
3	5	$Ce_9Ti_{79}Cr_9Y_3$	7	2	$Cr_{87}Fe_{10}Cu_3$	10	4	$Ce_{19}Ti_{49}Cr_{29}Hf_3$
3	6	$Ce_9Ti_{79}Cr_9Zn_3$	7	3	$Cr_{87}Fe_{10}Dy_3$	10	5	$Ce_{18,33}Ti_{48,33}Cr_{28,33}Hf_5$
3	7	$Ce_9Ti_{79}Cr_9Sn_3$	7	4	$Cr_{87}Fe_{10}Er_3$	10	6	$Ce_{17,67}Ti_{47,67}Cr_{27,67}Hf_7$
3	8	$Ce_9Ti_{79}Cr_9Eu_3$	7	5	$Cr_{87}Fe_{10}Eu_3$	10	7	$Ce_{17}Ti_{47}Cr_{27}Hf_9$
3	9	$Ce_9Ti_{79}Cr_9Sb_3$	7	6	$Cr_{87}Fe_{10}Ga_3$	10	8	$Ce_{19}Ti_{49}Cr_{29}In_3$
3	10	$Ce_9Ti_{79}Cr_9Cs_3$	7	7	$Cr_{87}Fe_{10}Gd_3$	10	9	$Ce_{18,33}Ti_{48,33}Cr_{28,33}In_5$
3	11	$Ce_9Ti_{79}Cr_9Fe_3$	7	8	$Cr_{87}Fe_{10}Ge_3$	10	10	$Ce_{17,67}Ti_{47,67}Cr_{27,67}In_7$
3	12	$Ce_9Ti_{79}Cr_9Ga_3$	7	9	$Cr_{87}Fe_{10}Hf_3$	10	11	$Ce_{17}Ti_{47}Cr_{27}In_9$
3	13	$Ce_9Ti_{79}Cr_9Ge_3$	7	10	$Cr_{87}Fe_{10}Ho_3$	10	12	$Ce_{19,8}Ti_{49,8}Cr_{29,8}Ag_{0,5}$
3	14	$Ce_9Ti_{79}Cr_9Hf_3$	7	11	$Cr_{87}Fe_{10}In_3$	10	13	$Ce_{19,8}Ti_{49,8}Cr_{29,8}Au_{0,5}$
4	3	$Ce_9Ti_{79}Cr_9In_3$	7	12	$Cr_{87}Fe_{10}K_3$	10	14	$Ce_{19,8}Ti_{49,8}Cr_{29,8}Ir_{0,5}$
4	4	$Ce_9Ti_{79}Cr_9Cu_3$	7	13	$Cr_{87}Fe_{10}La_3$	10	15	$Ce_{19,8}Ti_{49,8}Cr_{29,8}Pd_{0,5}$
4	5	$Ce_9Ti_{79}Cr_9Na_3$	7	14	$Cr_{87}Fe_{10}Li_3$	10	16	$Ce_{19,8}Ti_{49,8}Cr_{29,8}Pt_{0,5}$
4	6	$Ce_9Ti_{79}Cr_9Si_3$	7	15	$Cr_{87}Fe_{10}Lu_3$	11	2	$Ce_{19,8}Ti_{49,8}Cr_{29,8}Re_{0,5}$
4	7	$Ce_9Ti_{79}Cr_9Tb_3$	7	16	$Cr_{87}Fe_{10}Mg_3$	11	3	$Ce_{19,8}Ti_{49,8}Cr_{29,8}Rh_{0,5}$
4	8	$Ce_9Ti_{79}Cr_9Yb_3$	8	1	$Cr_{87}Fe_{10}Mn_3$	11	4	$Ce_{19,8}Ti_{49,8}Cr_{29,8}Ru_{0,5}$
4	9	$Ce_9Ti_{79}Cr_9Zr_3$	8	2	$Cr_{87}Fe_{10}Mo_3$	11	5	Blank
4	10	$Ce_9Ti_{79}Cr_9K_3$	8	3	$Cr_{87}Fe_{10}Na_3$	11	6	Blank
4	11	$Ce_9Ti_{79}Cr_9Bi_3$	8	4	$Cr_{87}Fe_{10}Nb_3$	11	7	Blank
4	12	$Ce_9Ti_{79}Cr_9Mo_3$	8	5	$Cr_{87}Fe_{10}Nd_3$	11	8	Blank
4	13	$Ce_9Ti_{79}Cr_9Nb_3$	8	6	$Cr_{87}Fe_{10}Rb_3$	11	9	Blank
4	14	$Ce_9Ti_{79}Cr_9Rb_3$	8	7	$Cr_{87}Fe_{10}Sb_3$	11	10	Blank
5	3	$Ce_9Ti_{79}Cr_9Sc_3$	8	8	$Cr_{87}Fe_{10}Sc_3$	11	11	Blank
5	4	$Ce_9Ti_{79}Cr_9W_3$	8	9	$Cr_{87}Fe_{10}Se_3$	11	12	Blank
5	5	$Ce_9Ti_{79}Cr_9V_3$	8	10	$Cr_{87}Fe_{10}Si_3$	11	13	$Ce_{20}Ti_{49,5}Cr_{30}Ag_{0,5}$
5	6	$Ce_9Ti_{79}Cr_9Te_3$	8	11	$Cr_{87}Fe_{10}Sm_3$	11	14	$Ce_{20}Ti_{49,5}Cr_{30}Au_{0,5}$
5	7	$Ce_9Ti_{79}Cr_9Ba_3$	8	12	$Cr_{87}Fe_{10}Sn_3$	11	15	$Ce_{20}Ti_{49,5}Cr_{30}Ir_{0,5}$
5	8	$Ce_9Ti_{79}Cr_9Tm_3$	8	13	$Cr_{87}Fe_{10}Sr_3$	11	16	$Ce_{20}Ti_{49,5}Cr_{30}Pd_{0,5}$
5	9	$Ce_9Ti_{79}Cr_9Ta_3$	8	14	$Cr_{87}Fe_{10}Ta_3$	12	2	$Ce_{20}Ti_{49,5}Cr_{30}Pt_{0,5}$
5	10	$Ce_9Ti_{79}Cr_9Co_3$	8	15	$Cr_{87}Fe_{10}Tb_3$	12	3	$Ce_{20}Ti_{49,5}Cr_{30}Re_{0,5}$
5	11	$Ce_{10}Ti_{80}Cr_{10}$	8	16	$Cr_{87}Fe_{10}Te_3$	12	4	$Ce_{20}Ti_{49,5}Cr_{30}Rh_{0,5}$
5	12	Fe_{100}	9	2	$Cr_{87}Fe_{10}Tm_3$	12	5	$Ce_{20}Ti_{49,5}Cr_{30}Rh_{0,5}$
5	13	$Cr_{10}Fe_{90}$	9	3	$Cr_{87}Fe_{10}V_3$	12	6	Blank

X	Y	Catalyst	X	Y	Catalyst	X	Y	Catalyst
12	7	Blank	13	13	Blank	15	10	Blank
12	8	Blank	13	14	Blank	15	11	Blank
12	9	Blank	14	3	Blank	15	12	Blank
12	10	Blank	14	4	Blank	15	13	Blank
12	11	Blank	14	5	Blank	15	14	Blank
12	12	Blank	14	6	Blank	16	5	Blank
12	13	Blank	14	7	Blank	16	6	Blank
12	14	Blank	14	8	Blank	16	7	Blank
12	15	Blank	14	9	Blank	16	8	Blank
13	3	$Ce_{33,3}Ti_{33,3}Cr_{33,3}$	14	10	Blank	16	9	Blank
13	4	$Pt/Rh/Al_2O_3$	14	11	Blank	16	10	Blank
13	5	$Ce_{20}Ti_{50}Cr_{30}$	14	12	Blank	16	11	Blank
13	6	Blank	14	13	Blank	16	12	Blank
13	7	Blank	14	14	Blank	17	6	Blank
13	8	Blank	15	4	Blank	17	7	Blank
13	9	Blank	15	5	Blank	17	8	Blank
13	10	Blank	15	6	Blank	17	9	Blank
13	11	Blank	15	7	Blank	17	10	Blank
13	12	Blank	15	8	Blank	17	11	Blank
13	13	Blank	15	9	Blank	17	12	Blank

Table 6-13 Library 11 and 12 filling plan

X	Y	Catalyst	X	Y	Catalyst	X	Y	Catalyst
1	6	$Ce_{32,3}Ti_{32,3}Cr_{32,3}V_3$	5	14	Blank	9	4	$Ce_{20}Ti_{49}Cr_{30}Ir_1$
1	7	Blank	5	15	$Ce_{19,7}Ti_{49,7}Cr_{29,7}Ag_1$	9	5	Blank
1	8	$Ce_{32,3}Ti_{32,3}Cr_{32,3}Sc_3$	6	2	Blank	9	6	$Ce_{20}Ti_{49}Cr_{30}Pd_1$
1	9	Blank	6	3	$Ce_{19}Ti_{49}Cr_{29}Lu_3$	9	7	Blank
1	10	$Ce_{32,3}Ti_{32,3}Cr_{32,3}Hf_3$	6	4	Blank	9	8	$Ce_{20}Ti_{49}Cr_{30}Pt_1$
1	11	Blank	6	5	$Ce_{19}Ti_{49}Cr_{29}Mg_3$	9	9	Blank
1	12	$Ce_{32,3}Ti_{32,3}Cr_{32,3}In_3$	6	6	Blank	9	10	$Ce_{20}Ti_{49}Cr_{30}Re_1$
2	5	$Ce_{19}Ti_{49}Cr_{29}Al_3$	6	7	$Ce_{19}Ti_{49}Cr_{29}Mn_3$	9	11	Blank
2	6	Blank	6	8	Blank	9	12	$Ce_{20}Ti_{49}Cr_{30}Rh_1$
2	7	$Ce_{19}Ti_{49}Cr_{29}B_3$	6	9	$Ce_{19}Ti_{49}Cr_{29}Nd_3$	9	13	Blank
2	8	Blank	6	10	Blank	9	14	$Ce_{20}Ti_{49}Cr_{30}Ru_1$
2	9	$Ce_{19}Ti_{49}Cr_{29}Dy_3$	6	11	$Ce_{19}Ti_{49}Cr_{29}Sm_3$	9	15	Blank
2	10	Blank	6	12	Blank	9	16	$Ce_{33,13}Ti_{33,13}Cr_{33,13}Ag_{0,5}$
2	11	$Ce_{19}Ti_{49}Cr_{29}Er_3$	6	13	$Ce_{19}Ti_{49}Cr_{29}Se_3$	10	1	$Ce_{19}Ti_{49}Cr_{29}Hf_3$
2	12	Blank	6	14	Blank	10	2	Blank
3	4	$Ce_{31,63}Ti_{31,63}Cr_{31,63}V_5$	6	15	$Ce_{19}Ti_{49}Cr_{29}Y_3$	10	3	$Ce_{19}Ti_{49}Cr_{29}In_3$
3	5	Blank	7	2	$Ce_{19,7}Ti_{49,7}Cr_{29,7}Au_1$	10	4	Blank
3	6	$Ce_{31,63}Ti_{31,63}Cr_{31,63}Sc_5$	7	3	Blank	10	5	$Ce_{19}Ti_{49}Cr_{29}Cu_3$
3	7	Blank	7	4	$Ce_{19,7}Ti_{49,7}Cr_{29,7}Ir_1$	10	6	Blank
3	8	$Ce_{31,63}Ti_{31,63}Cr_{31,63}Hf_5$	7	5	Blank	10	7	$Ce_{19}Ti_{49}Cr_{29}Na_3$
3	9	Blank	7	6	$Ce_{19,7}Ti_{49,7}Cr_{29,7}Pd_1$	10	8	Blank
3	10	$Ce_{31,63}Ti_{31,63}Cr_{31,63}In_5$	7	7	Blank	10	9	$Ce_{19}Ti_{49}Cr_{29}Si_3$
3	11	Blank	7	8	$Ce_{19,7}Ti_{49,7}Cr_{29,7}Pt_1$	10	10	Blank
3	12	$Ce_{30,97}Ti_{30,97}Cr_{30,97}V_7$	7	9	Blank	10	11	$Ce_{19}Ti_{49}Cr_{29}Tb_3$
3	13	Blank	7	10	$Ce_{19,7}Ti_{49,7}Cr_{29,7}Re_1$	10	12	Blank
3	14	$Ce_{30,97}Ti_{30,97}Cr_{30,97}Sc_7$	7	11	Blank	10	13	$Ce_{19}Ti_{49}Cr_{29}Yb_3$
4	3	$Ce_{19}Ti_{49}Cr_{29}Gd_3$	7	12	$Ce_{19,7}Ti_{49,7}Cr_{29,7}Rh_1$	10	14	Blank
4	4	Blank	7	13	Blank	10	15	$Ce_{19}Ti_{49}Cr_{29}Zr_3$
4	5	$Ce_{19}Ti_{49}Cr_{29}Ho_3$	7	14	$Ce_{19,7}Ti_{49,7}Cr_{29,7}Ru_1$	10	16	Blank
4	6	Blank	7	15	Blank	11	2	$Ce_{33,13}Ti_{33,13}Cr_{33,13}Au_{0,5}$
4	7	$Ce_{19}Ti_{49}Cr_{29}Ca_3$	7	16	$Ce_{20}Ti_{49}Cr_{30}Ag_1$	11	3	Blank
4	8	Blank	8	1	$Ce_{19}Ti_{49}Cr_{29}Zn_3$	11	4	$Ce_{33,13}Ti_{33,13}Cr_{33,13}Ir_{0,5}$
4	9	$Ce_{19}Ti_{49}Cr_{29}Sr_3$	8	2	Blank	11	5	Blank
4	10	Blank	8	3	$Ce_{19}Ti_{49}Cr_{29}Sn_3$	11	6	$Ce_{33,13}Ti_{33,13}Cr_{33,13}Pd_{0,5}$
4	11	$Ce_{19}Ti_{49}Cr_{29}La_3$	8	4	Blank	11	7	Blank
4	12	Blank	8	5	$Ce_{19}Ti_{49}Cr_{29}Eu_3$	11	8	$Ce_{33,13}Ti_{33,13}Cr_{33,13}Pt_{0,5}$
4	13	$Ce_{19}Ti_{49}Cr_{29}Li_3$	8	6	Blank	11	9	Blank
4	14	Blank	8	7	$Ce_{19}Ti_{49}Cr_{29}Sb_3$	11	10	$Ce_{33,13}Ti_{33,13}Cr_{33,13}Re_{0,5}$
5	3	$Ce_{30,97}Ti_{30,97}Cr_{30,97}Hf_7$	8	8	Blank	11	11	Blank
5	4	Blank	8	9	$Ce_{19}Ti_{49}Cr_{29}Cs_3$	11	12	$Ce_{33,13}Ti_{33,13}Cr_{33,13}Rh_{0,5}$
5	5	$Ce_{30,97}Ti_{30,97}Cr_{30,97}In_7$	8	10	Blank	11	13	Blank
5	6	Blank	8	11	$Ce_{19}Ti_{49}Cr_{29}Fe_3$	11	14	$Ce_{33,13}Ti_{33,13}Cr_{33,13}Ru_{0,5}$
5	7	$Ce_{30,3}Ti_{30,3}Cr_{30,3}V_9$	8	12	Blank	11	15	Blank
5	8	Blank	8	13	$Ce_{19}Ti_{49}Cr_{29}Ga_3$	11	16	$Ce_{32,97}Ti_{32,97}Cr_{32,97}Ag_1$
5	9	$Ce_{30,3}Ti_{30,3}Cr_{30,3}Sc_9$	8	14	Blank	12	2	Blank
5	10	Blank	8	15	$Ce_{19}Ti_{49}Cr_{29}Ge_3$	12	3	$Ce_{19}Ti_{49}Cr_{29}K_3$
5	11	$Ce_{30,3}Ti_{30,3}Cr_{30,3}Hf_9$	8	16	Blank	12	4	Blank
5	12	Blank	9	2	$Ce_{20}Ti_{49}Cr_{30}Au_1$	12	5	$Ce_{19}Ti_{49}Cr_{29}Bi_3$
5	13	$Ce_{30,3}Ti_{30,3}Cr_{30,3}In_9$	9	3	Blank	12	6	Blank

X	Y	Catalyst	X	Y	Catalyst	X	Y	Catalyst
12	7	$Ce_{19}Ti_{49}Cr_{29}Mo_{3}$	13	14	Blank	15	10	Blank
12	8	Blank	13	15	$Ce_{32,97}Ti_{32,97}Cr_{32,97}Ru_{1}$	15	11	Blank
12	9	$Ce_{19}Ti_{49}Cr_{29}Nb_{3}$	14	3	$Ce_{19}Ti_{49}Cr_{29}V_{3}$	15	12	Blank
12	10	Blank	14	4	Blank	15	13	Blank
12	11	$Ce_{19}Ti_{49}Cr_{29}Rb_{3}$	14	5	$Ce_{19}Ti_{49}Cr_{29}Te_{3}$	15	14	Blank
12	12	Blank	14	6	Blank	16	5	Blank
12	13	$Ce_{19}Ti_{49}Cr_{29}Sc_{3}$	14	7	$Ce_{19}Ti_{49}Cr_{29}Ba_{3}$	16	6	Blank
12	14	Blank	14	8	Blank	16	7	Blank
12	15	$Ce_{19}Ti_{49}Cr_{29}W_{3}$	14	9	$Ce_{19}Ti_{49}Cr_{29}Tm_{3}$	16	8	Blank
13	3	$Ce_{32,97}Ti_{32,97}Cr_{32,97}Au_{1}$	14	10	Blank	16	9	Blank
13	4	Blank	14	11	$Ce_{19}Ti_{49}Cr_{29}Ta_{3}$	16	10	Blank
13	5	$Ce_{32,97}Ti_{32,97}Cr_{32,97}Ir_{1}$	14	12	Blank	16	11	Blank
13	6	Blank	14	13	$Ce_{19}Ti_{49}Cr_{29}Co_{3}$	16	12	Blank
13	7	$Ce_{32,97}Ti_{32,97}Cr_{32,97}Pd_{1}$	14	14	$Ce_{19}Ti_{49}Cr_{29}Ag_{3}$	17	6	Blank
13	8	Blank	15	4	$Ce_{33,3}Ti_{33,3}Cr_{33,3}$	17	7	Blank
13	9	$Ce_{32,97}Ti_{32,97}Cr_{32,97}Pt_{1}$	15	5	Blank	17	8	Blank
13	10	Blank	15	6	$Pt/Rh/Al_{2}O_{3}$	17	9	Blank
13	11	$Ce_{32,97}Ti_{32,97}Cr_{32,97}Re_{1}$	15	7	Blank	17	10	Blank
13	12	Blank	15	8	$Ce_{20}Ti_{50}Cr_{30}$	17	11	Blank
13	13	$Ce_{32,97}Ti_{32,97}Cr_{32,97}Rh_{1}$	15	9	Blank	17	12	Blank

Table 6-14 Library 13 filling plan

X	**Y**	**Catalyst**	**X**	**Y**	**Catalyst**	**X**	**Y**	**Catalyst**
1	6	$Ce_{32,3}Ti_{32,25}Cr_{32,3}V_{3}Au_{0,05}$	5	14	$Ce_{32,3}Ti_{32,25}Cr_{32,3}In_{3}Ir_{0,05}$	9	4	$Ce_{32,3}Ti_{32,25}Cr_{32,3}Hf_{3}Pt_{0,05}$
1	7	$Ce_{32,3}Ti_{32,25}Cr_{32,3}In_{3}Au_{0,05}$	5	15	$Ce_{32,3}Ti_{32,25}Cr_{32,3}Hf_{3}Ir_{0,05}$	9	5	$Ce_{32,3}Ti_{32,25}Cr_{32,3}Sc_{3}Pt_{0,05}$
1	8	$Ce_{32,3}Ti_{32,25}Cr_{32,3}Hf_{3}Au_{0,05}$	6	2	$Ce_{32,3}Ti_{32,25}Cr_{32,3}Sc_{3}Ir_{0,05}$	9	6	$Ce_{33,3}Ti_{33,25}Cr_{33,3}Pt_{0,05}$
1	9	$Ce_{32,3}Ti_{32,25}Cr_{32,3}Sc_{3}Au_{0,05}$	6	3	$Ce_{33,3}Ti_{33,25}Cr_{33,3}Ir_{0,05}$	9	7	$Ce_{19}Ti_{48,95}Cr_{29}Tm_{3}Pt_{0,05}$
1	10	$Ce_{33,3}Ti_{33,25}Cr_{33,3}Au_{0,05}$	6	4	$Ce_{19}Ti_{48,95}Cr_{29}Tm_{3}Ir_{0,05}$	9	8	$Ce_{19}Ti_{48,95}Cr_{29}Gd_{3}Pt_{0,05}$
1	11	$Ce_{19}Ti_{48,95}Cr_{29}Tm_{3}Au_{0,05}$	6	5	$Ce_{19}Ti_{48,95}Cr_{29}Gd_{3}Ir_{0,05}$	9	9	Blank
1	12	$Ce_{19}Ti_{48,95}Cr_{29}Gd_{3}Au_{0,05}$	6	6	$Ce_{19}Ti_{48,95}Cr_{29}Sc_{3}Ir_{0,05}$	9	10	$Ce_{19}Ti_{48,95}Cr_{29}Sc_{3}Pt_{0,05}$
2	5	$Ce_{19}Ti_{48,95}Cr_{29}Sc_{3}Au_{0,05}$	6	7	$Ce_{19}Ti_{48,95}Cr_{29}Si_{3}Ir_{0,05}$	9	11	$Ce_{19}Ti_{48,95}Cr_{29}Si_{3}Pt_{0,05}$
2	6	$Ce_{19}Ti_{48,95}Cr_{29}Si_{3}Au_{0,05}$	6	8	$Ce_{20}Ti_{49,95}Cr_{30}Ir_{0,05}$	9	12	$Ce_{20}Ti_{49,95}Cr_{30}Pt_{0,05}$
2	7	$Ce_{20}Ti_{49,95}Cr_{30}Au_{0,05}$	6	9	$Ce_{9}Ti_{78,95}Cr_{9}Bi_{3}Ir_{0,05}$	9	13	$Ce_{9}Ti_{78,95}Cr_{9}Bi_{3}Pt_{0,05}$
2	8	$Ce_{9}Ti_{78,95}Cr_{9}Bi_{3}Au_{0,05}$	6	10	$Ce_{9}Ti_{78,95}Cr_{9}Mg_{3}Ir_{0,05}$	9	14	$Ce_{9}Ti_{78,95}Cr_{9}Mg_{3}Pt_{0,05}$
2	9	$Ce_{9}Ti_{78,95}Cr_{9}Mg_{3}Au_{0,05}$	6	11	$Ce_{32,3}Ti_{32,29}Cr_{32,3}V_{3}Ir_{0,01}$	9	15	$Ce_{32,3}Ti_{32,29}Cr_{32,3}V_{3}Pt_{0,01}$
2	10	$Ce_{32,3}Ti_{32,29}Cr_{32,3}V_{3}Au_{0,01}$	6	12	$Ce_{32,3}Ti_{32,29}Cr_{32,3}In_{3}Ir_{0,01}$	9	16	$Ce_{32,3}Ti_{32,29}Cr_{32,3}In_{3}Pt_{0,01}$
2	11	$Ce_{32,3}Ti_{32,29}Cr_{32,3}In_{3}Au_{0,01}$	6	13	$Ce_{32,3}Ti_{32,29}Cr_{32,3}Hf_{3}Ir_{0,01}$	10	1	$Ce_{32,3}Ti_{32,29}Cr_{32,3}Hf_{3}Pt_{0,01}$
2	12	$Ce_{32,3}Ti_{32,29}Cr_{32,3}Hf_{3}Au_{0,01}$	6	14	$Ce_{32,3}Ti_{32,29}Cr_{32,3}Sc_{3}Ir_{0,01}$	10	2	$Ce_{32,3}Ti_{32,29}Cr_{32,3}Sc_{3}Pt_{0,01}$
3	4	$Ce_{32,3}Ti_{32,29}Cr_{32,3}Sc_{3}Au_{0,01}$	6	15	$Ce_{33,3}Ti_{33,29}Cr_{33,3}Ir_{0,01}$	10	3	$Ce_{33,3}Ti_{33,29}Cr_{33,3}Pt_{0,01}$
3	5	$Ce_{33,3}Ti_{33,29}Cr_{33,3}Au_{0,01}$	7	2	$Ce_{19}Ti_{48,99}Cr_{29}Tm_{3}Ir_{0,01}$	10	4	$Ce_{19}Ti_{48,99}Cr_{29}Tm_{3}Pt_{0,01}$
3	6	$Ce_{19}Ti_{48,99}Cr_{29}Tm_{3}Au_{0,01}$	7	3	$Ce_{19}Ti_{48,99}Cr_{29}Gd_{3}Ir_{0,01}$	10	5	$Ce_{19}Ti_{48,99}Cr_{29}Gd_{3}Pt_{0,01}$
3	7	$Ce_{19}Ti_{48,99}Cr_{29}Gd_{3}Au_{0,01}$	7	4	$Ce_{19}Ti_{48,99}Cr_{29}Sc_{3}Ir_{0,01}$	10	6	$Ce_{19}Ti_{48,99}Cr_{29}Sc_{3}Pt_{0,01}$
3	8	$Ce_{19}Ti_{48,99}Cr_{29}Sc_{3}Au_{0,01}$	7	5	$Ce_{19}Ti_{48,99}Cr_{29}Si_{3}Ir_{0,01}$	10	7	$Ce_{19}Ti_{48,99}Cr_{29}Si_{3}Pt_{0,01}$
3	9	$Ce_{19}Ti_{48,99}Cr_{29}Si_{3}Au_{0,01}$	7	6	$Ce_{20}Ti_{49,99}Cr_{30}Ir_{0,01}$	10	8	$Ce_{20}Ti_{49,99}Cr_{30}Pt_{0,01}$
3	10	$Ce_{20}Ti_{49,99}Cr_{30}Au_{0,01}$	7	7	$Ce_{9}Ti_{78,99}Cr_{9}Bi_{3}Ir_{0,01}$	10	9	$Ce_{9}Ti_{78,99}Cr_{9}Bi_{3}Pt_{0,01}$
3	11	$Ce_{9}Ti_{78,99}Cr_{9}Bi_{3}Au_{0,01}$	7	8	$Ce_{9}Ti_{78,99}Cr_{9}Mg_{3}Ir_{0,01}$	10	10	$Ce_{9}Ti_{78,99}Cr_{9}Mg_{3}Pt_{0,01}$
3	12	$Ce_{9}Ti_{78,99}Cr_{9}Mg_{3}Au_{0,01}$	7	9	$Ce_{32,3}Ti_{32,25}Cr_{32,3}V_{3}Pd_{0,05}$	10	11	$Ce_{32,3}Ti_{32,25}Cr_{32,3}V_{3}Re_{0,05}$
3	13	$Ce_{32,3}Ti_{32,25}Cr_{32,3}V_{3}Ag_{0,05}$	7	10	$Ce_{32,3}Ti_{32,25}Cr_{32,3}In_{3}Pd_{0,05}$	10	12	$Ce_{32,3}Ti_{32,25}Cr_{32,3}In_{3}Re_{0,05}$
3	14	$Ce_{32,3}Ti_{32,25}Cr_{32,3}In_{3}Ag_{0,05}$	7	11	$Ce_{32,3}Ti_{32,25}Cr_{32,3}Hf_{3}Pd_{0,05}$	10	13	$Ce_{32,3}Ti_{32,25}Cr_{32,3}Hf_{3}Re_{0,05}$
4	3	$Ce_{32,3}Ti_{32,25}Cr_{32,3}Hf_{3}Ag_{0,05}$	7	12	$Ce_{32,3}Ti_{32,25}Cr_{32,3}Sc_{3}Pd_{0,05}$	10	14	$Ce_{32,3}Ti_{32,25}Cr_{32,3}Sc_{3}Re_{0,05}$
4	4	$Ce_{32,3}Ti_{32,25}Cr_{32,3}Sc_{3}Ag_{0,05}$	7	13	$Ce_{33,3}Ti_{33,25}Cr_{33,3}Pd_{0,05}$	10	15	$Ce_{33,3}Ti_{33,25}Cr_{33,3}Re_{0,05}$
4	5	$Ce_{33,3}Ti_{33,25}Cr_{33,3}Ag_{0,05}$	7	14	$Ce_{19}Ti_{48,95}Cr_{29}Tm_{3}Pd_{0,05}$	10	16	$Ce_{19}Ti_{48,95}Cr_{29}Tm_{3}Re_{0,05}$
4	6	$Ce_{19}Ti_{48,95}Cr_{29}Tm_{3}Ag_{0,05}$	7	15	$Ce_{19}Ti_{48,95}Cr_{29}Gd_{3}Pd_{0,05}$	11	2	$Ce_{19}Ti_{48,95}Cr_{29}Gd_{3}Re_{0,05}$
4	7	$Ce_{19}Ti_{48,95}Cr_{29}Gd_{3}Ag_{0,05}$	7	16	$Ce_{19}Ti_{48,95}Cr_{29}Sc_{3}Pd_{0,05}$	11	3	$Ce_{19}Ti_{48,95}Cr_{29}Sc_{3}Re_{0,05}$
4	8	$Ce_{19}Ti_{48,95}Cr_{29}Sc_{3}Ag_{0,05}$	8	1	$Ce_{19}Ti_{48,95}Cr_{29}Si_{3}Pd_{0,05}$	11	4	$Ce_{19}Ti_{48,95}Cr_{29}Si_{3}Re_{0,05}$
4	9	$Ce_{19}Ti_{48,95}Cr_{29}Si_{3}Ag_{0,05}$	8	2	$Ce_{20}Ti_{49,95}Cr_{30}Pd_{0,05}$	11	5	$Ce_{20}Ti_{49,95}Cr_{30}Re_{0,05}$
4	10	$Ce_{20}Ti_{49,95}Cr_{30}Ag_{0,05}$	8	3	$Ce_{9}Ti_{78,95}Cr_{9}Bi_{3}Pd_{0,05}$	11	6	$Ce_{9}Ti_{78,95}Cr_{9}Bi_{3}Re_{0,05}$
4	11	$Ce_{9}Ti_{78,95}Cr_{9}Bi_{3}Ag_{0,05}$	8	4	$Ce_{9}Ti_{78,95}Cr_{9}Mg_{3}Pd_{0,05}$	11	7	$Ce_{9}Ti_{78,95}Cr_{9}Mg_{3}Re_{0,05}$
4	12	$Ce_{9}Ti_{78,95}Cr_{9}Mg_{3}Ag_{0,05}$	8	5	$Ce_{32,3}Ti_{32,29}Cr_{32,3}V_{3}Pd_{0,01}$	11	8	$Ce_{32,3}Ti_{32,29}Cr_{32,3}V_{3}Re_{0,01}$
4	13	$Ce_{32,3}Ti_{32,29}Cr_{32,3}V_{3}Ag_{0,01}$	8	6	$Ce_{32,3}Ti_{32,29}Cr_{32,3}In_{3}Pd_{0,01}$	11	9	$Ce_{32,3}Ti_{32,29}Cr_{32,3}In_{3}Re_{0,01}$
4	14	$Ce_{32,3}Ti_{32,29}Cr_{32,3}In_{3}Ag_{0,01}$	8	7	$Ce_{32,3}Ti_{32,29}Cr_{32,3}Hf_{3}Pd_{0,01}$	11	10	$Ce_{32,3}Ti_{32,29}Cr_{32,3}Hf_{3}Re_{0,01}$
5	3	$Ce_{32,3}Ti_{32,29}Cr_{32,3}Hf_{3}Ag_{0,01}$	8	8	$Ce_{32,3}Ti_{32,29}Cr_{32,3}Sc_{3}Pd_{0,01}$	11	11	$Ce_{32,3}Ti_{32,29}Cr_{32,3}Sc_{3}Re_{0,01}$
5	4	$Ce_{32,3}Ti_{32,29}Cr_{32,3}Sc_{3}Ag_{0,01}$	8	9	$Ce_{33,3}Ti_{33,29}Cr_{33,3}Pd_{0,01}$	11	12	$Ce_{33,3}Ti_{33,29}Cr_{33,3}Re_{0,01}$
5	5	$Ce_{33,3}Ti_{33,29}Cr_{33,3}Ag_{0,01}$	8	10	$Ce_{19}Ti_{48,99}Cr_{29}Tm_{3}Pd_{0,01}$	11	13	$Ce_{19}Ti_{48,99}Cr_{29}Tm_{3}Re_{0,01}$
5	6	$Ce_{19}Ti_{48,99}Cr_{29}Tm_{3}Ag_{0,01}$	8	11	$Ce_{19}Ti_{48,99}Cr_{29}Gd_{3}Pd_{0,01}$	11	14	$Ce_{19}Ti_{48,99}Cr_{29}Gd_{3}Re_{0,01}$
5	7	$Ce_{19}Ti_{48,99}Cr_{29}Gd_{3}Ag_{0,01}$	8	12	$Ce_{19}Ti_{48,99}Cr_{29}Sc_{3}Pd_{0,01}$	11	15	$Ce_{19}Ti_{48,99}Cr_{29}Sc_{3}Re_{0,01}$
5	8	$Ce_{19}Ti_{48,99}Cr_{29}Sc_{3}Ag_{0,01}$	8	13	$Ce_{19}Ti_{48,99}Cr_{29}Si_{3}Pd_{0,01}$	11	16	$Ce_{19}Ti_{48,99}Cr_{29}Si_{3}Re_{0,01}$
5	9	$Ce_{19}Ti_{48,99}Cr_{29}Si_{3}Ag_{0,01}$	8	14	$Ce_{20}Ti_{49,99}Cr_{30}Pd_{0,01}$	12	2	$Ce_{20}Ti_{49,99}Cr_{30}Re_{0,01}$
5	10	$Ce_{20}Ti_{49,99}Cr_{30}Ag_{0,01}$	8	15	$Ce_{9}Ti_{78,99}Cr_{9}Bi_{3}Pd_{0,01}$	12	3	$Ce_{9}Ti_{78,99}Cr_{9}Bi_{3}Re_{0,01}$
5	11	$Ce_{9}Ti_{78,99}Cr_{9}Bi_{3}Ag_{0,01}$	8	16	$Ce_{9}Ti_{78,99}Cr_{9}Mg_{3}Pd_{0,01}$	12	4	$Ce_{9}Ti_{78,99}Cr_{9}Mg_{3}Re_{0,01}$
5	12	$Ce_{9}Ti_{78,99}Cr_{9}Mg_{3}Ag_{0,01}$	9	2	$Ce_{32,3}Ti_{32,25}Cr_{32,3}V_{3}Pt_{0,05}$	12	5	$Ce_{32,3}Ti_{32,25}Cr_{32,3}V_{3}Rh_{0,05}$
5	13	$Ce_{32,3}Ti_{32,25}Cr_{32,3}V_{3}Ir_{0,05}$	9	3	$Ce_{32,3}Ti_{32,25}Cr_{32,3}In_{3}Pt_{0,05}$	12	6	$Ce_{32,3}Ti_{32,25}Cr_{32,3}In_{3}Rh_{0,05}$

X	Y	Catalyst	X	Y	Catalyst	X	Y	Catalyst
12	7	$Ce_{32,3}Ti_{32,25}Cr_{32,3}Hf_{3}Rh_{0,05}$	13	14	$Ce_{9}Ti_{78,99}Cr_{9}Bi_{3}Rh_{0,01}$	15	10	$Ce_{19}Ti_{48,99}Cr_{29}Gd_{3}Ru_{0,01}$
12	8	$Ce_{32,3}Ti_{32,25}Cr_{32,3}Sc_{3}Rh_{0,05}$	13	15	$Ce_{9}Ti_{78,99}Cr_{9}Mg_{3}Rh_{0,01}$	15	11	$Ce_{19}Ti_{48,99}Cr_{29}Sc_{3}Ru_{0,01}$
12	9	$Ce_{33,3}Ti_{33,25}Cr_{33,3}Rh_{0,05}$	14	3	$Ce_{32,3}Ti_{32,25}Cr_{32,3}V_{3}Ru_{0,05}$	15	12	$Ce_{19}Ti_{48,99}Cr_{29}Si_{3}Ru_{0,01}$
12	10	$Ce_{19}Ti_{48,95}Cr_{29}Tm_{3}Rh_{0,05}$	14	4	$Ce_{32,3}Ti_{32,25}Cr_{32,3}In_{3}Ru_{0,05}$	15	13	$Ce_{20}Ti_{49,99}Cr_{30}Ru_{0,01}$
12	11	$Ce_{19}Ti_{48,95}Cr_{29}Gd_{3}Rh_{0,05}$	14	5	$Ce_{32,3}Ti_{32,25}Cr_{32,3}Hf_{3}Ru_{0,05}$	15	14	$Ce_{9}Ti_{78,99}Cr_{9}Bi_{3}Ru_{0,01}$
12	12	$Ce_{19}Ti_{48,95}Cr_{29}Sc_{3}Rh_{0,05}$	14	6	$Ce_{32,3}Ti_{32,25}Cr_{32,3}Sc_{3}Ru_{0,05}$	16	5	$Ce_{9}Ti_{78,99}Cr_{9}Mg_{3}Ru_{0,01}$
12	13	$Ce_{19}Ti_{48,95}Cr_{29}Si_{3}Rh_{0,05}$	14	7	$Ce_{33,3}Ti_{33,25}Cr_{33,3}Ru_{0,05}$	16	6	$Ce_{33,3}Ti_{33,3}Cr_{33,3}$
12	14	$Ce_{20}Ti_{49,95}Cr_{30}Rh_{0,05}$	14	8	$Ce_{19}Ti_{48,95}Cr_{29}Tm_{3}Ru_{0,05}$	16	7	$Ce_{20}Ti_{50}Cr_{30}$
12	15	$Ce_{9}Ti_{78,95}Cr_{9}Bi_{3}Rh_{0,05}$	14	9	$Ce_{19}Ti_{48,95}Cr_{29}Gd_{3}Ru_{0,05}$	16	8	$Ce_{32,3}Ti_{32,3}Cr_{32,3}V_{3}$
13	3	$Ce_{9}Ti_{78,95}Cr_{9}Mg_{3}Rh_{0,05}$	14	10	$Ce_{19}Ti_{48,95}Cr_{29}Sc_{3}Ru_{0,05}$	16	9	$Ce_{32,3}Ti_{32,3}Cr_{32,3}In_{3}$
13	4	$Ce_{32,3}Ti_{32,29}Cr_{32,3}V_{3}Rh_{0,01}$	14	11	$Ce_{19}Ti_{48,95}Cr_{29}Si_{3}Ru_{0,05}$	16	10	$Ce_{32,3}Ti_{32,3}Cr_{32,3}Hf_{3}$
13	5	$Ce_{32,3}Ti_{32,29}Cr_{32,3}In_{3}Rh_{0,01}$	14	12	$Ce_{20}Ti_{49,95}Cr_{30}Ru_{0,05}$	16	11	$Ce_{32,3}Ti_{32,3}Cr_{32,3}Sc_{3}$
13	6	$Ce_{32,3}Ti_{32,29}Cr_{32,3}Hf_{3}Rh_{0,01}$	14	13	$Ce_{9}Ti_{78,95}Cr_{9}Bi_{3}Ru_{0,05}$	16	12	$Ce_{9}Ti_{79}Cr_{9}Bi_{3}$
13	7	$Ce_{32,3}Ti_{32,29}Cr_{32,3}Sc_{3}Rh_{0,01}$	14	14	$Ce_{9}Ti_{78,95}Cr_{9}Mg_{3}Ru_{0,05}$	17	6	$Ce_{9}Ti_{79}Cr_{9}Mg_{3}$
13	8	$Ce_{33,3}Ti_{33,29}Cr_{33,3}Rh_{0,01}$	15	4	$Ce_{32,3}Ti_{32,29}Cr_{32,3}V_{3}Ru_{0,01}$	17	7	$Ce_{19}Ti_{49}Cr_{29}Tm_{3}$
13	9	$Ce_{19}Ti_{48,99}Cr_{29}Tm_{3}Rh_{0,01}$	15	5	$Ce_{32,3}Ti_{32,29}Cr_{32,3}In_{3}Ru_{0,01}$	17	8	$Ce_{19}Ti_{49}Cr_{29}Gd_{3}$
13	10	$Ce_{19}Ti_{48,99}Cr_{29}Gd_{3}Rh_{0,01}$	15	6	$Ce_{32,3}Ti_{32,29}Cr_{32,3}Hf_{3}Ru_{0,01}$	17	9	$Ce_{19}Ti_{49}Cr_{29}Sc_{3}$
13	11	$Ce_{19}Ti_{48,99}Cr_{29}Sc_{3}Rh_{0,01}$	15	7	$Ce_{32,3}Ti_{32,29}Cr_{32,3}Sc_{3}Ru_{0,01}$	17	10	$Ce_{19}Ti_{49}Cr_{29}Si_{3}$
13	12	$Ce_{19}Ti_{48,99}Cr_{29}Si_{3}Rh_{0,01}$	15	8	$Ce_{33,3}Ti_{33,29}Cr_{33,3}Ru_{0,01}$	17	11	$Pt/Rh/Al_{2}O_{3}$
13	13	$Ce_{20}Ti_{49,99}Cr_{30}Rh_{0,01}$	15	9	$Ce_{19}Ti_{48,99}Cr_{29}Tm_{3}Ru_{0,01}$	17	12	Blank

Table 6-15 Library 14 filling plan

X	**Y**	**Catalyst**	**X**	**Y**	**Catalyst**	**X**	**Y**	**Catalyst**
1	6	$Ce_{40}Cr_{59,99}Au_{0,01}$	5	14	Blank	9	4	$Ti_{62,45}Cr_{37,5}Ir_{0,05}$
1	7	Blank	5	15	$Ti_{62,49}Cr_{37,5}Au_{0,01}$	9	5	Blank
1	8	$Ce_{40}Cr_{59,99}Ag_{0,01}$	6	2	Blank	9	6	$Ti_{62,45}Cr_{37,5}Pd_{0,05}$
1	9	Blank	6	3	Blank	9	7	Blank
1	10	$Ce_{40}Cr_{59,99}Ir_{0,01}$	6	4	Blank	9	8	$Ti_{62,45}Cr_{37,5}Pt_{0,05}$
1	11	Blank	6	5	Blank	9	9	Blank
1	12	$Ce_{40}Cr_{59,99}Pd_{0,01}$	6	6	Blank	9	10	$Ti_{62,45}Cr_{37,5}Re_{0,05}$
2	5	Blank	6	7	Blank	9	11	Blank
2	6	Blank	6	8	Blank	9	12	$Ti_{62,45}Cr_{37,5}Rh_{0,05}$
2	7	Blank	6	9	Blank	9	13	Blank
2	8	Blank	6	10	Blank	9	14	$Ti_{62,45}Cr_{37,5}Ru_{0,05}$
2	9	Blank	6	11	Blank	9	15	Blank
2	10	Blank	6	12	Blank	9	16	Blank
2	11	Blank	6	13	Blank	10	1	Blank
2	12	Blank	6	14	Blank	10	2	Blank
3	4	$Ce_{40}Cr_{59,99}Pt_{0,01}$	6	15	Blank	10	3	Blank
3	5	Blank	7	2	$Ti_{62,49}Cr_{37,5}Ag_{0,01}$	10	4	Blank
3	6	$Ce_{40}Cr_{59,99}Re_{0,01}$	7	3	Blank	10	5	Blank
3	7	Blank	7	4	$Ti_{62,49}Cr_{37,5}Ir_{0,01}$	10	6	Blank
3	8	$Ce_{40}Cr_{59,99}Rh_{0,01}$	7	5	Blank	10	7	Blank
3	9	Blank	7	6	$Ti_{62,49}Cr_{37,5}Pd_{0,01}$	10	8	Blank
3	10	$Ce_{40}Cr_{59,99}Ru_{0,01}$	7	7	Blank	10	9	Blank
3	11	Blank	7	8	$Ti_{62,49}Cr_{37,5}Pt_{0,01}$	10	10	Blank
3	12	$Ce_{40}Cr_{59,95}Au_{0,05}$	7	9	Blank	10	11	Blank
3	13	Blank	7	10	$Ti_{62,49}Cr_{37,5}Re_{0,01}$	10	12	Blank
3	14	$Ce_{40}Cr_{59,95}Ag_{0,05}$	7	11	Blank	10	13	Blank
4	3	Blank	7	12	$Ti_{62,49}Cr_{37,5}Rh_{0,01}$	10	14	Blank
4	4	Blank	7	13	Blank	10	15	Blank
4	5	Blank	7	14	$Ti_{62,49}Cr_{37,5}Ru_{0,01}$	10	16	Blank
4	6	Blank	7	15	Blank	11	2	Blank
4	7	Blank	7	16	$Ti_{62,45}Cr_{37,5}Au_{0,05}$	11	3	Blank
4	8	Blank	8	1	Blank	11	4	Blank
4	9	Blank	8	2	Blank	11	5	Blank
4	10	Blank	8	3	Blank	11	6	Blank
4	11	Blank	8	4	Blank	11	7	Blank
4	12	Blank	8	5	Blank	11	8	Blank
4	13	Blank	8	6	Blank	11	9	Blank
4	14	Blank	8	7	Blank	11	10	Blank
5	3	$Ce_{40}Cr_{59,95}Ir_{0,05}$	8	8	Blank	11	11	Blank
5	4	Blank	8	9	Blank	11	12	Blank
5	5	$Ce_{40}Cr_{59,95}Pd_{0,05}$	8	10	Blank	11	13	Blank
5	6	Blank	8	11	Blank	11	14	Blank
5	7	$Ce_{40}Cr_{59,95}Pt_{0,05}$	8	12	Blank	11	15	Blank
5	8	Blank	8	13	Blank	11	16	Blank
5	9	$Ce_{40}Cr_{59,95}Re_{0,05}$	8	14	Blank	12	2	Blank
5	10	Blank	8	15	Blank	12	3	Blank
5	11	$Ce_{40}Cr_{59,95}Rh_{0,05}$	8	16	Blank	12	4	Blank
5	12	Blank	9	2	$Ti_{62,45}Cr_{37,5}Ag_{0,05}$	12	5	Blank
5	13	$Ce_{40}Cr_{59,95}Ru_{0,05}$	9	3	Blank	12	6	Blank

X	Y	Catalyst	X	Y	Catalyst	X	Y	Catalyst
12	7	Blank	13	14	Blank	15	10	Blank
12	8	Blank	13	15	Blank	15	11	Blank
12	9	Blank	14	3	Blank	15	12	Blank
12	10	Blank	14	4	Blank	15	13	Blank
12	11	Blank	14	5	Blank	15	14	Blank
12	12	Blank	14	6	Blank	16	5	Blank
12	13	Blank	14	7	Blank	16	6	Blank
12	14	Blank	14	8	Blank	16	7	Blank
12	15	Blank	14	9	Blank	16	8	Blank
13	3	Blank	14	10	Blank	16	9	Blank
13	4	Blank	14	11	Blank	16	10	Blank
13	5	Blank	14	12	Blank	16	11	Blank
13	6	Blank	14	13	Blank	16	12	Blank
13	7	Blank	14	14	Blank	17	6	Blank
13	8	Blank	15	4	Blank	17	7	$Ce_{19}Ti_{49}Cr_{29}Sc_3$
13	9	Blank	15	5	$Ce_{40}Cr_{60}$	17	8	Blank
13	10	Blank	15	6	Blank	17	9	$Ce_{20}Ti_{50}Cr_{30}$
13	11	Blank	15	7	$Ti_{62,5}Cr_{37,5}$	17	10	Blank
13	12	Blank	15	8	Blank	17	11	$Pt/Rh/Al_2O_3$
13	13	Blank	15	9	Blank	17	12	Blank

Table 6-16 Library 15 filling plan

X	Y	Catalyst	X	Y	Catalyst	X	Y	Catalyst
1	6	$Ti_{42,5}Cr_{37,5}Al_{20}$	5	14	Blank	9	4	$Ti_{62,5}Cr_{17,5}Se_{20}$
1	7	Blank	5	15	$Ti_{62,5}Cr_{17,5}Al_{20}$	9	5	Blank
1	8	$Ti_{42,5}Cr_{37,5}Bi_{20}$	6	2	Blank	9	6	$Ti_{62,5}Cr_{17,5}Si_{20}$
1	9	Blank	6	3	$Ti_{59,5}Cr_{37,5}V_{3}$	9	7	Blank
1	10	$Ti_{42,5}Cr_{37,5}Ce_{20}$	6	4	Blank	9	8	$Ti_{62,5}Cr_{17,5}Sr_{20}$
1	11	Blank	6	5	Blank	9	9	Blank
1	12	$Ti_{42,5}Cr_{37,5}Dy_{20}$	6	6	$Ti_{59,5}Cr_{37,5}Zn_{3}$	9	10	$Ti_{62,5}Cr_{17,5}Tm_{20}$
2	5	Blank	6	7	Blank	9	11	Blank
2	6	$Ti_{59,5}Cr_{37,5}Mg_{3}$	6	8	Blank	9	12	$Ti_{62,5}Cr_{17,5}V_{20}$
2	7	Blank	6	9	Blank	9	13	Blank
2	8	Blank	6	10	Blank	9	14	$Ti_{62,5}Cr_{17,5}Zn_{20}$
2	9	$Ti_{59,5}Cr_{37,5}Mn_{3}$	6	11	Blank	9	15	Blank
2	10	Blank	6	12	Blank	9	16	$Ti_{52,5}Cr_{27,5}Al_{20}$
2	11	Blank	6	13	Blank	10	1	Blank
2	12	$Ti_{59,5}Cr_{37,5}Sc_{3}$	6	14	Blank	10	2	Blank
3	4	$Ti_{42,5}Cr_{37,5}Gd_{20}$	6	15	Blank	10	3	Blank
3	5	Blank	7	2	$Ti_{62,5}Cr_{17,5}Bi_{20}$	10	4	Blank
3	6	$Ti_{42,5}Cr_{37,5}Hf_{20}$	7	3	Blank	10	5	Blank
3	7	Blank	7	4	$Ti_{62,5}Cr_{17,5}Ce_{20}$	10	6	Blank
3	8	$Ti_{42,5}Cr_{37,5}In_{20}$	7	5	Blank	10	7	Blank
3	9	Blank	7	6	$Ti_{62,5}Cr_{17,5}Dy_{20}$	10	8	Blank
3	10	$Ti_{42,5}Cr_{37,5}Mg_{20}$	7	7	Blank	10	9	Blank
3	11	Blank	7	8	$Ti_{62,5}Cr_{17,5}Gd_{20}$	10	10	Blank
3	12	$Ti_{42,5}Cr_{37,5}Mn_{20}$	7	9	Blank	10	11	Blank
3	13	Blank	7	10	$Ti_{62,5}Cr_{17,5}Hf_{20}$	10	12	Blank
3	14	$Ti_{42,5}Cr_{37,5}Sc_{20}$	7	11	Blank	10	13	Blank
4	3	Blank	7	12	$Ti_{62,5}Cr_{17,5}In_{20}$	10	14	Blank
4	4	$Ti_{59,5}Cr_{37,5}Se_{3}$	7	13	Blank	10	15	Blank
4	5	Blank	7	14	$Ti_{62,5}Cr_{17,5}Mg_{20}$	10	16	Blank
4	6	Blank	7	15	Blank	11	2	$Ti_{52,5}Cr_{27,5}Bi_{20}$
4	7	$Ti_{59,5}Cr_{37,5}Si_{3}$	7	16	$Ti_{62,5}Cr_{17,5}Mn_{20}$	11	3	Blank
4	8	Blank	8	1	Blank	11	4	$Ti_{52,5}Cr_{27,5}Ce_{20}$
4	9	Blank	8	2	Blank	11	5	Blank
4	10	$Ti_{59,5}Cr_{37,5}Sr_{3}$	8	3	Blank	11	6	$Ti_{52,5}Cr_{27,5}Dy_{20}$
4	11	Blank	8	4	Blank	11	7	Blank
4	12	Blank	8	5	Blank	11	8	$Ti_{52,5}Cr_{27,5}Gd_{20}$
4	13	$Ti_{59,5}Cr_{37,5}Tm_{3}$	8	6	Blank	11	9	Blank
4	14	Blank	8	7	Blank	11	10	$Ti_{52,5}Cr_{27,5}Hf_{20}$
5	3	$Ti_{42,5}Cr_{37,5}Se_{20}$	8	8	Blank	11	11	Blank
5	4	Blank	8	9	Blank	11	12	$Ti_{52,5}Cr_{27,5}In_{20}$
5	5	$Ti_{42,5}Cr_{37,5}Si_{20}$	8	10	Blank	11	13	Blank
5	6	Blank	8	11	Blank	11	14	$Ti_{52,5}Cr_{27,5}Mg_{20}$
5	7	$Ti_{42,5}Cr_{37,5}Sr_{20}$	8	12	Blank	11	15	Blank
5	8	Blank	8	13	Blank	11	16	$Ti_{52,5}Cr_{27,5}Mn_{20}$
5	9	$Ti_{42,5}Cr_{37,5}Tm_{20}$	8	14	Blank	12	2	Blank
5	10	Blank	8	15	Blank	12	3	Blank
5	11	$Ti_{42,5}Cr_{37,5}V_{20}$	8	16	Blank	12	4	Blank
5	12	Blank	9	2	$Ti_{62,5}Cr_{17,5}Sc_{20}$	12	5	Blank
5	13	$Ti_{42,5}Cr_{37,5}Zn_{20}$	9	3	Blank	12	6	Blank

X	Y	Catalyst	X	Y	Catalyst	X	Y	Catalyst
12	7	Blank	13	14	Blank	15	10	$Ti_{59,5}Cr_{37,5}Dy_3$
12	8	Blank	13	15	Blank	15	11	Blank
12	9	Blank	14	3	Blank	15	12	$Ti_{59,5}Cr_{37,5}Gd_3$
12	10	Blank	14	4	Blank	15	13	Blank
12	11	Blank	14	5	Blank	15	14	$Ti_{59,5}Cr_{37,5}Hf_3$
12	12	Blank	14	6	Blank	16	5	Blank
12	13	Blank	14	7	Blank	16	6	Blank
12	14	Blank	14	8	Blank	16	7	Blank
12	15	Blank	14	9	Blank	16	8	Blank
13	3	$Ti_{52,5}Cr_{27,5}Sc_{20}$	14	10	Blank	16	9	Blank
13	4	Blank	14	11	Blank	16	10	Blank
13	5	$Ti_{52,5}Cr_{27,5}Se_{20}$	14	12	Blank	16	11	Blank
13	6	Blank	14	13	Blank	16	12	Blank
13	7	$Ti_{52,5}Cr_{27,5}Si_{20}$	14	14	Blank	17	6	$Ti_{59,5}Cr_{37,5}In_3$
13	8	Blank	15	4	$Ti_{59,5}Cr_{37,5}Al_3$	17	7	Blank
13	9	$Ti_{52,5}Cr_{27,5}Sr_{20}$	15	5	Blank	17	8	$Pt/Rh/Al_2O_3$
13	10	Blank	15	6	$Ti_{59,5}Cr_{37,5}Bi_3$	17	9	Blank
13	11	$Ti_{52,5}Cr_{27,5}Tm_{20}$	15	7	Blank	17	10	$Ce_{20}Ti_{50}Cr_{30}$
13	12	Blank	15	8	$Ti_{59,5}Cr_{37,5}Ce_3$	17	11	Blank
13	13	$Ti_{52,5}Cr_{27,5}V_{20}$	15	9	Blank	17	12	$Ti_{62,5}Cr_{37,5}$

Table 6-17 Library 16 filling plan